

Ochraceocephala foeniculi gen. et sp. nov., a new pathogen causing crown rot of fennel in Italy

Dalia Aiello¹, Alessandro Vitale¹, Giancarlo Polizzi¹, Hermann Voglmayr^{2,3}

1 Dipartimento di Agricoltura, Alimentazione e Ambiente, sezione Patologia Vegetale, University of Catania, Via S. Sofia 100, 95123 Catania, Italy **2** Institute of Forest Entomology, Forest Pathology and Forest Protection, Department of Forest and Soil Sciences, BOKU - University of Natural Resources and Life Sciences, Franz Schwachhöfer Haus, Peter-Jordan-Straße 82/I, 1190 Vienna, Austria **3** Division of Systematic and Evolutionary Botany, Department of Botany and Biodiversity Research, University of Vienna, Rennweg 14, 1030 Wien, Austria

Corresponding author: Dalia Aiello (dalia.aiello@unict.it)

Academic editor: N. Wijayawardene | Received 12 November 2019 | Accepted 17 January 2020 | Published 30 March 2020

Citation: Aiello D, Vitale A, Polizzi G, Voglmayr H (2020) *Ochraceocephala foeniculi* gen. et sp. nov., a new pathogen causing crown rot of fennel in Italy. MycoKeys 66: 1–22. <https://doi.org/10.3897/mycokeys.66.48389>

Abstract

A new disease of fennel is described from Sicily (southern Italy). Surveys of the disease and sampling were conducted during spring 2017 and 2018 in Adrano and Bronte municipalities (Catania province) where this crop is widely cultivated. Isolations from the margin of symptomatic tissues resulted in fungal colonies with the same morphology. Pathogenicity tests with one isolate of the fungus on 6-month-old plants of fennel reproduced similar symptoms to those observed in nature. Inoculation experiments to assess the susceptibility of six different fennel cultivars to infection by the pathogen showed that the cultivars ‘Narciso’, ‘Apollo’, and ‘Pompeo’ were more susceptible than ‘Aurelio’, ‘Archimede’, and ‘Pegaso’. Phylogenetic analyses based on a matrix of the internal transcribed spacer (ITS), the large subunit (LSU), and the small subunit (SSU) rDNA regions revealed that the isolates represent a new genus and species within the Leptosphaeriaceae, which is here described as *Ochraceocephala foeniculi* gen. et sp. nov. This study improves the understanding of this new fennel disease, but further studies are needed for planning effective disease management strategies. According to the results of the phylogenetic analyses, *Subplenodomus iridicola* is transferred to the genus *Alloleptosphaeria* and *Acicuseptoria rumicis* to *Paraleptosphaeria*.

Keywords

Fungal disease, Leptosphaeriaceae, pathogenicity, susceptibility

Introduction

Fennel (*Foeniculum vulgare* Mill.), native in arid and semi-arid regions of southern Europe and the Mediterranean area, is used as a vegetable, herb, and seed spice in the food, pharmaceutical, cosmetic, and healthcare industries. Italy is the leading world producer of fennel (around 85% of the world production), with 20,035 ha of area cultivated and a total production of 537,444 tons. Fennel represents an important crop widely cultivated in Sicily (southern Italy) with 1,620 ha harvested and a production of 35,930 tons (ISTAT 2018). Several diseases caused by fungi have been reported from this crop throughout the world (Table 1). Amongst soilborne diseases, brown rot and wilt caused by *Phytophthora megasperma* and crown rot caused by *Didymella glomerata* (syn. *Phoma glomerata*) were reported in Italy (Cacciola et al. 2006; Lahoz et al. 2007).

In 2017, a new disease was first observed on fennel in a farm of Adrano area (Catania province, eastern Sicily, Italy). The disease symptoms were necrotic lesions on the crown, root, and stem of fennel plants. Disease incidence initially was about 5% on ‘Apollo’ cultivar. However, in 2018 different surveys conducted in the same area showed a high increase of the incidence on three different cultivars with yield losses of about 20–30%. The aims of the present study were to identify the causal agent obtained from symptomatic fennel plants, using morphological characteristics and DNA sequence analyses, to evaluate the pathogenicity of one representative isolate and to evaluate the susceptibility of different cultivars of fennel to the newly described disease.

Materials and methods

Collection of samples and fungal isolates

In order to identify the causal agent of the fennel disease, 30 samples were collected during several surveys in Adrano and Bronte area (Catania province, eastern Sicily). Pieces of tissue obtained from different parts of fennel plants (crown, root, and stem) were surface disinfected for 1 min in 1.5% sodium hypochlorite solution, rinsed in sterile water, placed on potato dextrose agar (3.9% PDA, Oxoid, Basingstoke, UK) amended with 100 mg/L of streptomycin sulfate (Sigma-Aldrich, USA) to prevent bacteria growth, and then incubated at 25 ± 1 °C for seven days. Fungal colonies consistently grown from symptomatic tissues were subcultured on new PDA plates. Subsequently, single-spore isolates were obtained from these pure cultures and stored at -20 °C in sterile 15% glycerol solution. The fungal isolates were provisionally identified by cultural and morphological characteristics, and they were deposited in the culture collection of the Department of Agriculture, Food and Environment, University of Catania. One representative isolate (Di3A-F1; ex holotype culture) was deposited at the Westerdijk Fungal Biodiversity Institute (CBS), Utrecht, the Netherlands. The holotype specimen of the new pathogen species was deposited in

Table 1. Main diseases caused by fungal pathogens on fennel.

Disease	Fungal pathogen	Reference
Collar rot	<i>Sclerotium rolfsii</i>	Khare et al. 2014
Damping off and Root rot	<i>Pythium</i> spp.	Khare et al. 2014; Koike et al. 2015
Vascular wilt	<i>Fusarium oxysporum</i>	Shaker and Alhamadany 2015
Vascular wilt	<i>Verticillium dahliae</i>	Ghoneem et al. 2009
Root and Foot rot	<i>Rhizoctonia solani</i>	Shaker and Alhamadany 2015
Brown rot and Wilt	<i>Phytophthora megasperma</i>	Cacciola et al. 2006
Stem rot	<i>Sclerotinia sclerotiorum</i>	Choi et al. 2016
Blight and Leaf spot	<i>Alternaria alternata</i>	D'Amico et al. 2008
Blight and Leaf spot	<i>Ascochyta foeniculina</i>	Khare et al. 2014
Blight and Leaf spot	<i>Fusoidiella anethi</i>	Taubenrauch et al. 2008
	syn. <i>Cercospora foeniculi</i>	
	<i>Cercosporidium punctum</i>	
	<i>Mycosphaerella anethi</i>	
	<i>M. foeniculi</i>	
	<i>Passalora kirchneri</i>	
	<i>P. puncta</i>	
	<i>Ramularia foeniculi</i>	
Umbel browning and Stem necrosis	<i>Diaporthe angelicae</i>	Rodeva and Gabler 2011
Downy mildew	<i>Plasmopara mei-foeniculi</i>	Khare et al. 2014
	syn. <i>P. nivea</i> sensu lato	
Powdery mildew	<i>Leveillula languinosa</i>	Khare et al. 2014
Powdery mildew	<i>Erysiphe heraclei</i>	Choi et al. 2015
Leaf spot	<i>Leptosphaeria purpurea</i>	Odstrčilová et al. 2002
Leaf spot	<i>Subplenodomus apiicola</i>	Odstrčilová et al. 2002
	syn. <i>Phoma apiicola</i>	
Leaf spot and blight	<i>Phoma herbarum</i>	Shaker and Alhamadany 2015
Crown rot	<i>Didymella glomerata</i>	Lahoz et al. 2007
	syn. <i>Phoma glomerata</i>	

the fungarium of the Department of Botany and Biodiversity Research, University of Vienna (WU).

Morphology

For culture characteristics, cultures were grown on 2% (w/v) malt extract agar (MEA, VWR) and on corn meal agar (CMA, Sigma-Aldrich) supplemented with 2% w/v dextrose (CMD). Colony diameters and morphologies were determined after seven days of incubation at room temperature (22 ± 1 °C) and daylight.

Microscopic observations were made in tap water. Methods of microscopy included stereomicroscopy using a Nikon SMZ 1500 equipped with a Nikon DS-U2 digital camera, and Nomarski differential interference contrast (DIC) using a Zeiss Axio Imager.A1 compound microscope equipped with a Zeiss AxioCam 506 colour digital camera. Images and data were gathered using the NIS-Elements D v. 3.22.15 or Zeiss ZEN Blue Edition software packages. Measurements are reported as maxima and minima in parentheses and the range representing the mean plus and minus the standard deviation of a number of measurements given in parentheses.

DNA extraction and PCR amplification

The extraction of genomic DNA from pure cultures was performed by using the Wizard Genomic DNA Purification Kit (Promega Corporation, WI, USA). Partial regions of six loci (ITS, LSU, and SSU rDNA, *RPB2*, *TEF1*, *TUB2*) were amplified; for details on the primers and annealing temperatures used for PCR and sequencing, see Table 2. The PCR products were sequenced in both directions by Macrogen Inc. (South Korea) or at the Department of Botany and Biodiversity Research, University of Vienna using the ABI PRISM Big Dye Terminator Cycle Sequencing Ready Reaction Kit v. 3.1 (Applied Biosystems, Warrington, UK) and an automated DNA sequencer (3730xl Genetic Analyser, Applied Biosystems). The DNA sequences generated were assembled with Lasergene SeqMan Pro (DNASTAR, Madison, USA). Sequences generated during the present study were uploaded to Genbank (Table 3).

Phylogenetic analysis

According to the results of BLAST searches in GenBank, the newly generated ITS, LSU, and SSU rDNA sequences of the fennel pathogen were aligned with selected sequences of Leptosphaeriaceae from Gruyter et al. (2013) and complemented with a few recent additions from GenBank. The familial and generic concept of Leptosphaeriaceae implemented here follows the molecular phylogenetic studies of Gruyter et al. (2013), Ariyawansa et al. (2015), and Phookamsak et al. (2019). Due to insufficient *RPB2*, *TEF1*, and *TUB2* sequence data available in Genbank for the study group, the sequences of these markers could not be included in phylogenetic analyses, but they were deposited in GenBank (Table 3). A combined SSU-ITS-LSU rDNA matrix was produced for phylogenetic analyses, with six species of *Coniothyrium* (*C. carteri*, *C. dolichi*, *C. glycines*, *C. multiporum*, *C. telephii*, *C. palmarum*) from Coniothyriaceae added as the outgroup according to the results of the phylogenetic analyses of Gruyter et al. (2013). As the rDNA sequences of the fennel pathogen isolates were (almost) identical (see Results section below), only a single isolate (CBS 145654 = Di3A-F1; ex holotype strain) was included in the final matrix. The GenBank accession numbers of sequences used in the analyses are given in Table 4. Sequence alignments were produced with the server version of MAFFT (<http://mafft.cbrc.jp/alignment/server>), checked and refined using BioEdit v. 7.2.6 (Hall 1999). The combined data matrix contained 3312 characters; i.e. 607 nucleotides of the ITS, 1333 nucleotides of the LSU and 1372 nucleotides of the SSU).

Maximum likelihood (ML) analyses were performed with RAxML (Stamatakis 2006) as implemented in raxmlGUI 1.3 (Silvestro and Michalak 2012), using the ML + rapid bootstrap setting and the GTRGAMMA substitution model with 1000 bootstrap replicates.

Table 2. Primers used to amplify and sequence the nuclear internal transcribed spacer (ITS), large subunit (LSU) and small subunit (SSU) rDNA regions, the RNA polymerase II second largest subunit (*RPB2*) gene, the translation elongation factor 1- α (*TEF1*) gene and the β -tubulin (*TUB2*) gene.

Gene	Primer	Sequence (5'-3')	Direction	Annealing t (°C)	Reference			
ITS	ITS5	GGAAGTAAAAGTCGTAACAAGG	forward	48	White et al. 1990			
	ITS4	TCCTCCGCTTATTGATATGC	reverse					
LSU	LR0R	GTACCCGCTGAACCTAAGC	forward	48	Vilgalys and Hester 1990			
	LR5	TCCTGAGGGAAACTTCG	reverse					
ITS-LSU	V9G	TTAAGTCCCCTGCCCTTTGTIA	forward	55	Hoog and Gerrits van den Ende 1998			
	LR5	TACTTGAAGGAACCCCTTACC	reverse					
	LR2R-A ^z	CAGAGACCGATAGCGCAC	forward					
	LR3 ^z	CCGTGTTTCAAGACGGG	reverse					
	ITS4 ^z	TCCTCCGCTTATTGATATGC	reverse					
	SSU	NS1	GTAGTCATATGCTTGTCTC			forward	48	White et al. 1990
		NS4	CTTCCGTC AATTCCTTTAAG			reverse		
<i>RPB2</i>	RPB2-5F2	GGGGWGWAYCAGAAGAAGGC	forward	52	Sung et al. 2007			
	RPB2-7cR	CCCATRGCTTGYTTRCCCAT	reverse					
<i>TEF1</i>	EF1-728F	CATCGAGAAGTTCGAGAAGG	forward	52	Carbone and Kohn 1999			
	EF1-986R	TACTTGAAGGAACCCCTTACC	reverse					
	EF1-728F	CATCGAGAAGTTCGAGAAGG	forward	55	Carbone and Kohn 1999			
	TEF1-LLE ^{rev}	AACTTGCAGGCAATGTGG	reverse					
	TEF1_INTF ^z	CCGTGAYTTCATCAAGAACATG	forward					
	TEF1_INT2 ^z	CCACTNNGTNGTGTCCATCTTRTT	reverse					
<i>TUB2</i>	T1	AACATGCCGTGAGATTGTAAGT	forward	52	O'Donnell and Cigelnik 1997			
	bt2b	ACCCTCAGTGTAGTGACCCTTGGC	reverse					
					Glass and Donaldson 1995			

^z internal primers used only for sequencing

Maximum parsimony (MP) bootstrap analyses were performed with PAUP v. 4.0a165 (Swofford 2002). All molecular characters were unordered and given equal weight; analyses were performed with gaps treated as missing data; the COLLAPSE command was set to MINBLEN. MP bootstrap analyses were performed with 1000 replicates, using 5 rounds of random sequence addition and subsequent TBR branch swapping (MULTREES option in effect, steepest descent option not in effect) during each bootstrap replicate. In the Results and Discussion, bootstrap values below 70 % are considered low, between 70–90 % medium and above 90 % high.

Pathogenicity test

To determine the ability of the representative isolate Di3A-F1 (CBS 145654) to cause disease symptoms, pathogenicity tests were conducted on 6-month-old plants of fennel grown in a growth chamber. Five plants for each of the three replicates were used. The inoculum, which consisted of a 6-mm-diameter mycelial plug from a 10-day-old culture on PDA, was inserted in four points for each crown and the wounds wrapped

Table 3. Characteristics and accession numbers of isolates collected from fennel plants in Sicily.

Strain ¹	Year	Cultivar	Farm	ITS ²	LSU ²	SSU ²	RPB2 ²	TEF1 ²	TUB2 ²
D13AF1 = CBS 145654*	2017	Apollo	Farm 1	MN516753	MN516774	MN516743	MN520145	MN520149	MN520147
D13AF2	2017	Apollo	Farm 1	MN516754	MN516775	MN516744			
D13AF3	2018	Apollo	Farm 1	MN516755	MN516776	MN516745			
D13AF4	2018	Apollo	Farm 1						
D13AF5	2018	Apollo	Farm 1	MN516756	MN516777	MN516746			
D13AF6	2018	Apollo	Farm 1	MN516757	MN516778	MN516747			
D13AF7	2018	Apollo	Farm 1	MN516758					
D13AF8	2018	Apollo	Farm 1	MN516759					
D13AF9	2018	Apollo	Farm 1	MN516760	MN516779	MN516748			
D13AF10	2018	Apollo	Farm 1	MN516761	MN516780	MN516749	MN520146	MN520150	MN520148
D13AF11	2018	Apollo	Farm 1	MN516762					
D13AF12	2018	Apollo	Farm 1	MN516763					
D13AF13	2018	Apollo	Farm 1	MN516764	MN516781	MN516750			
D13AF14	2018	Apollo	Farm 1	MN516765	MN516782	MN516751			
D13AF15	2018	Apollo	Farm 1	MN516766	MN516783	MN516752			
D13AF16	2018	Apollo	Farm 1	MN516767					
D13AF17	2018	Apollo	Farm 1	MN516768					
D13AF18	2018	Narciso	Farm 2						
D13AF19	2018	Narciso	Farm 2	MN516769					
D13AF20	2018	Narciso	Farm 2	MN516770					
D13AF21	2018	Narciso	Farm 2	MN516771					
D13AF22	2018	Narciso	Farm 2						
D13AF23	2018	Narciso	Farm 2						
D13AF24	2018	Narciso	Farm 2						
D13AF25	2018	Narciso	Farm 2						
D13AF26	2018	Narciso	Farm 3						
D13AF27	2018	Narciso	Farm 3						
D13AF28	2018	Narciso	Farm 3						
D13AF29	2018	Narciso	Farm 4						
D13AF30	2018	Narciso	Farm 4	MN516772					
D13AF31	2018	Narciso	Farm 4						
D13AF32	2018	Aurelio	Farm 5	MN516773					

D13A: Cultures stored at the University of Catania, Italy; CBS: Culture collection of the Westerdijk Fungal Biodiversity Institute, Utrecht, The Netherlands. Isolates in bold were sequenced in the present study. ² ITS: internal transcribed spacer rDNA region, LSU: large subunit rDNA region, SSU: small subunit rDNA region, RPB2: RNA polymerase II second largest subunit gene, TEF1: translation elongation factor 1- α , TUB2: β -tubulin gene. *Ex-type strain.

Table 4. Isolates and accession numbers used in the phylogenetic analyses. Isolate/sequences in bold were isolated/sequenced in the present study.

Taxon	Culture, specimen	Host, substrate	Country	ITS	GenBank accession no	SSU
<i>Alloposphaeria iridicola</i>	CBS 143395	<i>Iris</i> sp. (Iridaceae)	United Kingdom	MH107919	MH107965	
<i>Alloposphaeria italica</i>	MFLUCC 14-934	<i>Clematis vitalba</i> (Ranunculaceae)	Italy	KT454722	KT454714	
<i>Alternaria bidensis</i>	CBS 134021	<i>Bidens sulphurea</i> (Asteraceae)	Brazil	KC609333	KC609341	
<i>Alternaria centaurae-diffusae</i>	MFLUCC 14-0992	<i>Centauria diffusa</i> (Asteraceae)	Russia	KT454723	KT454715	KT454730
<i>Alternaria helianthi</i>	CBS 119672	<i>Helianthus</i> sp. (Asteraceae)	USA	KC609337	KC584368	KC584626
<i>Alternaria trigonospora</i>	MFLU 15-2237	<i>Cirsium</i> sp. (Asteraceae)	Russia	KY674857	KY674858	
<i>Coniothyrium carteri</i>	CBS 105.91	<i>Quercus robur</i> (Fagaceae)	Germany	JF740181	GQ387594	GQ387533
<i>Coniothyrium dolichi</i>	CBS 124140	<i>Dolichos biflorus</i> (Fabaceae)	India	JF740183	GQ387611	GQ387550
<i>Coniothyrium glycines</i>	CBS 124455	<i>Glycine max</i> (Fabaceae)	Zambia	JF740184	GQ387597	GQ387536
<i>Coniothyrium multiporum</i>	CBS 501.91	Unknown	Egypt	JF740186	GU238109	
<i>Coniothyrium palmarium</i>	CBS 400.71	<i>Chamaerops humilis</i> (Arecaceae)	Italy	AY720708	EU754153	EU754054
<i>Coniothyrium telephii</i>	CBS 188.71	Air	Finland	JF740188	GQ387599	GQ387538
<i>Heterosporicola chenopodii</i>	CBS 448.68	<i>Chenopodium album</i> (Chenopodiaceae)	Netherlands	FJ427023	EU754187	EU754088
<i>Heterosporicola dimorphospora</i>	CBS 165.78	<i>Chenopodium quinoa</i> (Chenopodiaceae)	Peru	JF740204	JF740281	JF740099
<i>Leptosphaeria conoidea</i>	CBS 616.75	<i>Lunaria annua</i> (Brassicaceae)	Netherlands	JF740201	JF740279	JF740099
<i>Leptosphaeria dolioalum</i>	CBS 188.71	<i>Urtica dioica</i> (Urticaceae)	Netherlands	JF740205	GQ387576	GQ387515
<i>Leptosphaeria erubunda</i>	CBS 617.75	<i>Solidago</i> sp. (hybrid) (Asteraceae)	Netherlands	JF740216	JF740289	
<i>Leptosphaeria macrocapsa</i>	CBS 640.93	<i>Mercurialis perennis</i> (Euphorbiaceae)	Netherlands	JF740237	JF740304	
<i>Leptosphaeria pedicularis</i>	CBS 126582	<i>Gentiana punicata</i> (Gentianaceae)	Switzerland	JF740223	JF740293	
<i>Leptosphaeria sclerotoides</i>	CBS 144.84	<i>Medicago sativa</i> (Fabaceae)	Canada	JF740192	JF740269	
<i>Leptosphaeria slovacica</i>	CBS 389.80	<i>Balota nigra</i> (Lamiaceae)	Netherlands	JF740247	JF740315	JF740101
<i>Leptosphaeria sydowii</i>	CBS 385.80	<i>Senecio jacobaea</i> (Asteraceae)	UK	JF740244	JF740313	
<i>Leptosphaeria veronicae</i>	CBS 145.84	<i>Veronica chamaedryoides</i> (Scrophulariaceae)	Netherlands	JF740254	JF740320	
<i>Neoleptosphaeria rubefaciens</i>	CBS 387.80	<i>Tilia</i> (x) <i>europaea</i> (Malvaceae)	Netherlands	JF740242	JF740311	
<i>Ochraceocephala foeniculi</i>	D13AF1 = CBS 145654	<i>Foeniculum vulgare</i> (Apiaceae)	Italy	MN516753	MN516774	MN516743
<i>Paraleptosphaeria dryadis</i>	CBS 643.86	<i>Dryas octopetala</i> (Rosaceae)	Switzerland	JF740213	GU301828	
<i>Paraleptosphaeria macrospora</i>	CBS 114198	<i>Rumex domesticus</i> (Chenopodiaceae)	Norway	JF740238	JF740305	
<i>Paraleptosphaeria nitischkei</i>	CBS 306.51	<i>Cirsium spinosissimum</i> (Asteraceae)	Switzerland	JF740239	JF740308	
<i>Paraleptosphaeria orobanchis</i>	CBS 101638	<i>Epifagus virginiana</i> (Orobanchaceae)	USA	JF400230	JF740299	
<i>Paraleptosphaeria padi</i>	MFLU 15-2756	<i>Prunus padus</i> (Rosaceae)	Russia	KY554203	KY554198	KY554201
<i>Paraleptosphaeria pratensis</i>	CBS 114591	<i>Rubus idaeus</i> (Rosaceae)	Sweden	JF740241	JF740310	
<i>Paraleptosphaeria rubi</i>	MFLUCC 14-0211	<i>Rubus</i> sp. (Rosaceae)	Italy	KT454726	KT454718	KT454733

Taxon	Culture, specimen	Host, substrate	Country	GenBank accession no		
				ITS	LSU	SSU
<i>Parataphaearia ramicis</i>	CBS 522.78	<i>Rumex alpinus</i> (Polygonaceae)	France	KF251144	KF251648	
<i>Plenodomus agrinus</i>	CBS 121.89	<i>Eupatorium cannabinum</i> (Asteraceae)	Netherlands	JF740194	JF740271	
<i>Plenodomus agrinus</i>	CBS 126584	<i>Eupatorium cannabinum</i> (Asteraceae)	Netherlands	JF740195	JF740272	
<i>Plenodomus artemisiae</i>	KUMCC 18-0151	<i>Artemisia</i> sp. (Asteraceae)	China	MKS387920	MKS387958	MKS387928
<i>Plenodomus biglobosus</i>	CBS 119951	<i>Brassica napa</i> (Brassicaceae)	Netherlands	JF740198	JF740274	JF740102
<i>Plenodomus biglobosus</i>	CBS 127249	<i>Brassica juncea</i> (Brassicaceae)	France	JF740199	JF740275	
<i>Plenodomus chrysanthemi</i>	CBS 539.63	<i>Chrysanthemum</i> sp. (Asteraceae)	Greece	JF740253	GU238151	GU238230
<i>Plenodomus collinsoniae</i>	CBS 120227	<i>Vitis coignetiae</i> (Vitaceae)	Japan	JF740200	JF740276	
<i>Plenodomus confertus</i>	CBS 375.64	<i>Anacyclus radiatus</i> (Asteraceae)	Spain	AF439459	JF740277	
<i>Plenodomus congestus</i>	CBS 244.64	<i>Erigeron canadensis</i> (Asteraceae)	Spain	AF439460	JF740278	
<i>Plenodomus deqinensis</i>	CGMCC 3.18221	soil	China	KY064027	KY064031	
<i>Plenodomus enteroleucis</i>	CBS 142.84	<i>Catalpa bignonioides</i> (Bignoniaceae)	Netherlands	JF740214	JF740287	
<i>Plenodomus enteroleucis</i>	CBS 831.84	<i>Triticum aestivum</i> (Poaceae)	Germany	JF740215	JF740288	
<i>Plenodomus fallaciosus</i>	CBS 414.62	<i>Satureia montana</i> (Lamiaceae)	France	JF740222	JF740292	
<i>Plenodomus guttulatus</i>	MFLU 15-1876	unidentified dead stem	Germany	KT454721	KT454713	KT454729
<i>Plenodomus hendersoniae</i>	CBS 113702	<i>Salix cinerea</i> (Salicaceae)	Sweden	JF740225	JF740295	
<i>Plenodomus hendersoniae</i>	CBS 139.78	<i>Pyrus malus</i> (Rosaceae)	Netherlands	JF740226	JF740296	
<i>Plenodomus hendersoniae</i>	LTO	<i>Salix appendiculata</i> (Salicaceae)	Austria	MF795790	MF795790	
<i>Plenodomus inflorescens</i>	CBS 143.84	<i>Fraxinus excelsior</i> (Oleaceae)	Netherlands	JF740228	JF740297	
<i>Plenodomus inflorescens</i>	PD 73/1382	<i>Lilium</i> sp. (Liliaceae)	Netherlands	JF740229	JF740298	
<i>Plenodomus libanotis</i>	CBS 113795	<i>Seseli libanotis</i> (Apiaceae)	Sweden	JF740231	JF740300	
<i>Plenodomus lijiangensis</i>	KUMCC 18-0186	dead fern fronds	China	MKS387921	MKS387959	MKS387929
<i>Plenodomus lindquistii</i>	CBS 386.80		former Yugoslavia	JF740232	JF740301	
<i>Plenodomus lindquistii</i>	CBS 381.67	<i>Helianthus annuus</i> (Asteraceae)	Canada	JF740233	JF740302	
<i>Plenodomus lingam</i>	CBS 275.63	<i>Brassica</i> sp. (Brassicaceae)	UK	JF740234	JF740306	JF740103
<i>Plenodomus lingam</i>	CBS 260.94	<i>Brassica oleracea</i> (Brassicaceae)	Netherlands	JF740235	JF740307	
<i>Plenodomus lupini</i>	CBS 248.92	<i>Lupinus mutabilis</i> (Fabaceae)	Peru	JF740236	JF740303	
<i>Plenodomus pimpinellae</i>	CBS 101637	<i>Pimpinella anisum</i> (Apiaceae)	Israel	JF740240	JF740309	
<i>Plenodomus salviae</i>	MFLUCC 13-0219	<i>Salvia glutinosa</i> (Lamiaceae)	Italy	KT454725	KT454717	KT454732
<i>Plenodomus sinensis</i>	MFLU 17-0757	<i>Plukenetia volubilis</i> (Euphorbiaceae)	China	MF072722	MF072718	MF072720
<i>Plenodomus tracheiphilus</i>	CBS 551.93	<i>Citrus limonium</i> (Rutaceae)	Israel	JF740249	JF740317	JF740104
<i>Plenodomus tracheiphilus</i>	CBS 127250	<i>Citrus</i> sp. (Rutaceae)	Italy	JF740250	JF740318	
<i>Plenodomus visci</i>	CBS 122783	<i>Viscum album</i> (Viscaceae)	France	JF740256	EU754195	EU754096
<i>Plenodomus wasabiiae</i>	CBS 120119	<i>Wasabia japonica</i> (Brassicaceae)	Taiwan	JF740257	JF740323	

Taxon	Culture, specimen	Host, substrate	Country	GenBank accession no		
				ITS	LSU	SSU
<i>Plenodomus wasabiae</i>	CBS 120120	<i>Wasabia japonica</i> (Brassicaceae)	Taiwan	JF740258	JF740324	
<i>Pseudoleptophaeria etheridgei</i>	CBS 125980	<i>Populus tremuloides</i> (Salicaceae)	Canada	JF740221	JF740291	
<i>Sphaerellopsis flum</i>	CBS 317.68	<i>Puccinia deschampsiae</i> uredinium, on <i>Deschampsia caespitosa</i>	Germany	KP170657	KP170725	
<i>Sphaerellopsis hakeae</i>	CPC 29566	<i>Hakea</i> sp. (Proteaceae)	Australia	KV173466	KV173555	
<i>Sphaerellopsis ishrnospora</i>	KUN-HKAS 102225	Unidentified twig	China	MK387925	MK387963	MK387934
<i>Sphaerellopsis macroconidioidis</i>	CBS 233.51	<i>Uromyces caryophylli</i> on <i>Dianthus caryophyllus</i>	Italy	KP170658	KP170726	
<i>Sphaerellopsis paraphysata</i>	CPC 21841	<i>Pennisetum</i> sp. (Poaceae)	Brazil	KP170662	KP170729	
<i>Subplenodomus apicola</i>	CBS 285.72	<i>Apium graveolens</i> var. <i>rapaceum</i> (Apiaceae)	Germany	JF740196	GU238040	
<i>Subplenodomus drobojaciensis</i>	CBS 269.92	<i>Eustoma exaltatum</i> (Gentianaceae)	Netherlands	JF740211	JF740285	JF740100
<i>Subplenodomus valerianae</i>	CBS 630.68	<i>Valeriana phu</i> (Valerianaceae)	Netherlands	JF740251	GU238150	
<i>Subplenodomus violicola</i>	CBS 306.68	<i>Viola tricolor</i> (Violaceae)	Netherlands	FJ427083	GU238156	GU238231

with Parafilm to prevent desiccation. Fennel plants inoculated with sterile PDA plugs served as a control. After inoculation, plants were covered with a plastic bag for 48 h and maintained at 25 ± 1 °C and 95% relative humidity (RH) under a 12 h fluorescent light/dark regime. Five days after inoculation the presence of a lesion was evaluated in each inoculation point. To fulfill Koch's postulates, symptomatic tissues taken from the crown of each inoculated plant were plated on PDA and the identity of the fungal isolates was confirmed as described above.

Cultivar susceptibility

To evaluate the susceptibility of six different cultivars of fennel to infection by the pathogen, one experiment was conducted on 1 to 2-month-old seedlings of fennel in a growth chamber. Eight plants for each of three replicates were used. The inoculum, which consisted of a 6-mm-diameter mycelial plug from a 10-day-old culture on PDA, was inserted at the crown of each plant and wrapped with Parafilm to prevent desiccation. Fennel plants inoculated with sterile PDA plugs served as a control. All the replicates were enclosed in plastic bags and maintained at 25 ± 1 °C and 95% relative humidity (RH) under a 12 h fluorescent light/dark regime in a growth chamber until the symptoms were observed. Plant mortality (PM), disease incidence (DI) and symptom severity (SS) were evaluated. Symptom severity was rated using a category scale from 0 to 5, where 0 = healthy plant; 1 = necrotic lesion on crown from 0.1 to 0.2 cm; 2 = from 0.3 to 1 cm; 3 = from 1.1 to 2 cm; 4 = from 2.1 to 3.5 cm; 5 = dead plant. The experiment was performed twice.

Statistical analysis

Data about disease susceptibility of examined fennel cultivars from the repeated experiments were analysed by using the Statistica package software (v. 10; Statsoft Inc., Tulsa, OK, USA). The arithmetic means of PM, DI, and SS were calculated, averaging the values determined for the single replicates of each treatment. Percentage data concerning PM and DI were transformed into the arcsine (\sin^{-1} square rootx) prior to analysis of variance (ANOVA), whereas SS values were not transformed. Initial analyses of PM and DI were performed by calculating F and P values associated to evaluate whether the effects of single factor (cultivar) and cultivar \times trial interactions are significant. In the post hoc analyses, the corresponding mean values of PM and DI were subsequently separated by the Fisher's least significant difference test ($P = 0.05$). Because ordinal scales were adopted for SS data calculation, different nonparametric approaches were used. Kendall's coefficient of concordance (W) was calculated to assess whether the rankings of the SS scores among fennel cultivars are similar within each trial (cultivar \times trial interactions). Since in the susceptibility experiment W was higher than 0.9, the SS scores were at first analysed by using Friedman's nonparametric rank test, and subsequently followed by the all possible pairwise performed with the Wil-

coxon signed-rank at $P < 0.05$. On the other hand, when only the cultivar effects were examined, the Kruskal-Wallis non parametric one-way test was preliminarily applied, calculating χ^2 and P value associated.

Results

Collection of samples and isolates

Symptoms referable to infection (Fig. 1a, b) were detected in five commercial farms surveyed in eastern Sicily, Italy. The disease was observed on 3 different cultivars of fennel (4 to 6-month-old) in open fields. The symptoms consisted of depressed necrotic lesions formed near the soil line and affected crown, root, and stem. The lesion was first light brown with wet appearance, becoming dark brown to black with age and sometimes appearing dry. Under favourable conditions (high humidity), the lesion extended and the infection resulted in a crown and root rot. Fungal colonies representing the new fennel pathogen were consistently obtained from symptomatic tissues. A total of 32 single-spore isolates were collected (Table 3). Preliminary identity of the fungal isolates was based on cultural and morphological characteristics. Among these, 17 isolates were obtained from 'Apollo', 14 from 'Narciso', and one from 'Aurelio' cultivars.

Sequencing

All strains of the new fennel pathogen sequenced had identical LSU, SSU, *RPB2*, *TEFI*, and *TUB2* sequences. Also all ITS sequences were identical, except for a single nucleotide polymorphism (A/G) towards the end of the ITS2 region. All sequences generated during this study were deposited at GenBank; for GenBank accession numbers, see Table 3.

Phylogenetic analyses

Of the 3312 characters included in the phylogenetic analyses, 294 were parsimony informative (222 from the ITS, 62 from the LSU, 10 from the SSU). The best ML tree (lnL = -14211.5558) revealed by RAxML is shown in Figure 2. In the phylogenetic tree, the Leptosphaeriaceae received high (96% ML and MP) support. Within Leptosphaeriaceae, most of the deeper nodes of the tree backbone received low to insignificant support. Highly supported genera include *Alloleptosphaeria*, *Heterosporicola*, *Leptosphaeria* (all three with maximum support) and *Alternariaster* (99% ML and 100% MP), while *Sphaerellopsis* received low (53%) and *Paraleptosphaeria* medium (75%) support only in the ML analyses, and *Plenodomus* and *Subplenodomus* were unsupported. *Subplenodomus iridicola* was not contained within the *Subplenodomus* clade, but sister species to *Alloleptosphaeria italica* with maximum support, and *Aci-*



Figure 1. Symptoms caused by *Ochraceocephala foeniculi* on fennel plants. **a, b** Necrotic lesions and crown rot on ‘Narciso’ cultivar. **c, d** Necrotic lesions and crown rot on ‘Apollo’ cultivar. **e** Symptoms on artificially inoculated seedlings of ‘Pompeo’ cultivar.

cuseptoria rumicis was embedded within the *Paraleptosphaeria* clade, indicating that they are generically misplaced. The new fennel pathogen was placed basal to the *Plenodomus* clade, however, without significant support. Although the new fennel pathogen is closely related to the genus *Plenodomus*, it is morphologically highly distinct. As no suitable described genus is available, a new genus is therefore established here.

Taxonomy

Ochraceocephala Voglmayr & Aiello, gen. nov.

Mycobank No: 833933

Etymology. referring to the ochraceous conidial capitula of the type species.

Conidiophores erect, variable in shape and branching, from unbranched, loosely to densely branched up to several times; branching commonly irregularly verticillate. Phialides arising singly or in irregular whorls, cylindrical, lageniform or ampulliform, producing basipetal conidial chains. Conidia in chains, unicellular, thick-walled.

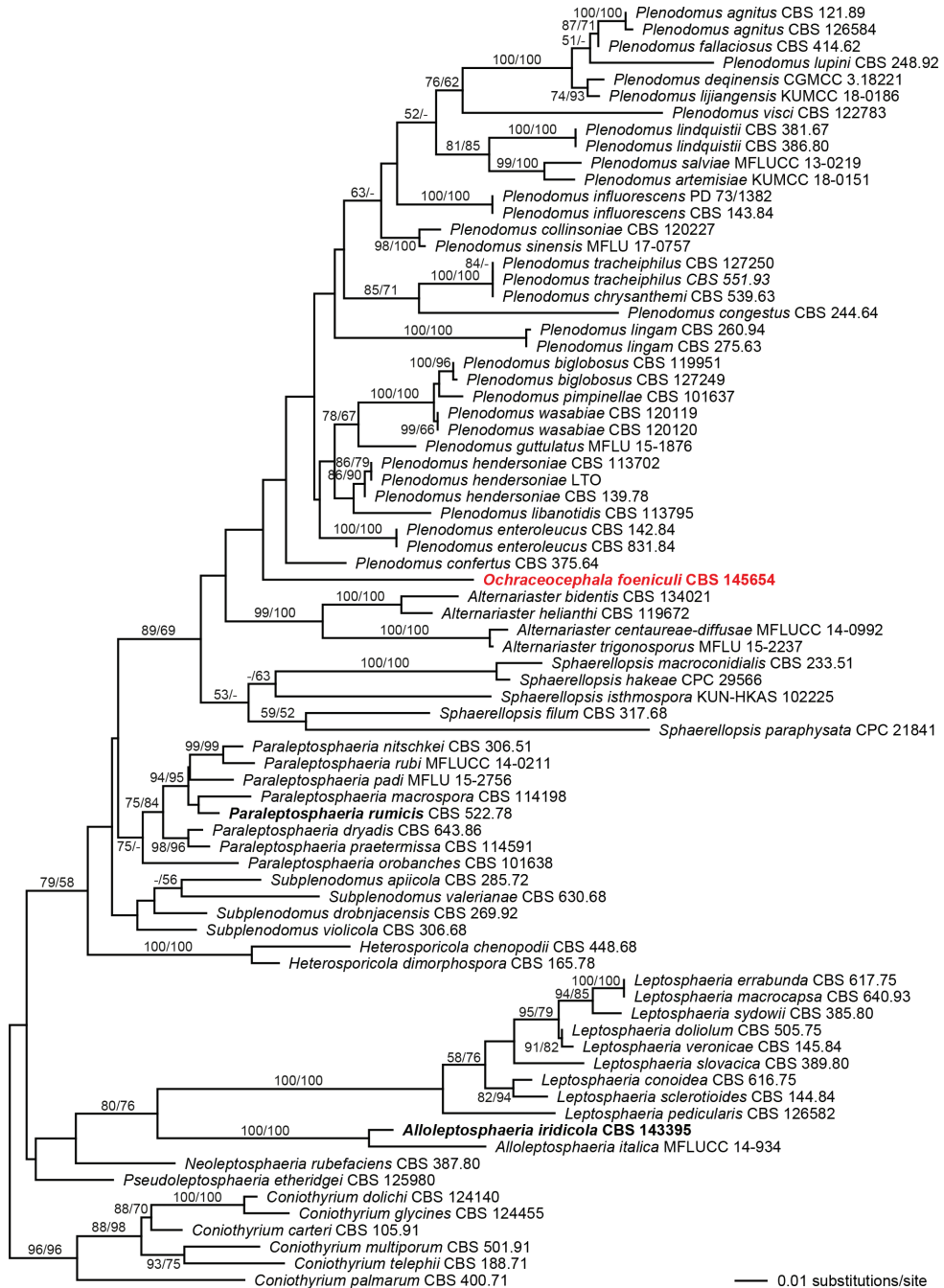


Figure 2. Phylogram of the best ML tree ($-\ln L = 14211.5558$) revealed by RAxML from an analysis of the combined SSU-ITS-LSU matrix of selected Leptosphaeriaceae, showing the phylogenetic position of *Ochraceocephala foeniculi* (bold red). Taxa in bold black denote new combinations proposed here. ML and MP bootstrap support above 50% are given above or below the branches.

Type species. *Ochraceocephala foeniculi* Voglmayr & Aiello.

Notes. *Ochraceocephala* is phylogenetically closely related to *Plenodomus*, from which it deviates substantially in morphology. *Plenodomus* species are characterised by pycnidial phoma-like asexual morphs, and while in two *Plenodomus* species (*P. chrysanthemi*, *P. tracheiphilus*) simple hyphomycetous, phialophora-like synanamorphs have been recorded (Boerema et al. 1994), these are very different from the complex conidiophores of the present fennel pathogen. These morphological differences, the lack of a suitable genus within Leptosphaeriaceae and its phylogenetic position therefore warrants the establishment of a new genus.

***Ochraceocephala foeniculi* Voglmayr & Aiello, sp. nov.**

Mycobank No: 833934

Figure 3

Etymology. referring to its host genus, *Foeniculum* (Apiaceae).

Colonies fast-growing, at room temperature (22 ± 1 °C) on CMD reaching 80 mm after 7 d; on MEA 38 mm after 7 d; with dull white to cream surface, upon conidiation becoming beige to olive yellow from the centre, reverse cream with greyish to dark brown centre; cottony, with abundant surface mycelium; sporulation abundant on aerial hyphae. Aerial hyphae hyaline, 2–6 µm wide. Conidiophores hyaline, produced terminally or laterally on aerial hyphae, variable in shape and branching, unbranched, loosely or densely branched up to two times; branching commonly irregularly verticillate. Phialides arising singly or in whorls of 2–5, (3.8–)5.8–13.5(–21.0) × (2.5–)3.0–4.3(–5.5) µm ($n = 100$), cylindrical, lageniform or ampulliform, often with a distinct collarete, producing basipetal conidial chains; polyphialides rarely present. Conidia (3.2–)3.5–6.0(–8.5) × (2.5–)3.0–4.2(–6.0) µm, l/w (1.0–)1.1–1.5(–2.1) ($n = 155$), hyaline to yellowish, in masses sand to olive yellow, smooth, mostly globose to subglobose, rarely broadly ellipsoid to pip-shaped, thick-walled.

Distribution. Italy (Sicily).

Host and substrate. Pathogenic on crown, roots and stems of living *Foeniculum vulgare*.

Holotype. Italy, Sicily, Catania province, Adrano, May 2017 (WU 40034); ex-holotype culture CBS 145654; ex holotype sequences MN516753 (ITS), MN516774 (LSU), MN516743 (SSU), MN520145 (*RPB2*), MN520149 (*TEFI*), MN520147 (*TUB2*).

***Alloleptosphaeria iridicola* (Crous & Denman) Voglmayr, comb. nov.**

Mycobank No: 833935

Basionym. *Subplenodomus iridicola* Crous & Denman, in Crous, Schumacher, Wingfield, Akulov, Denman, Roux, Braun, Burgess, Carnegie, Váczy, Guatimosim,

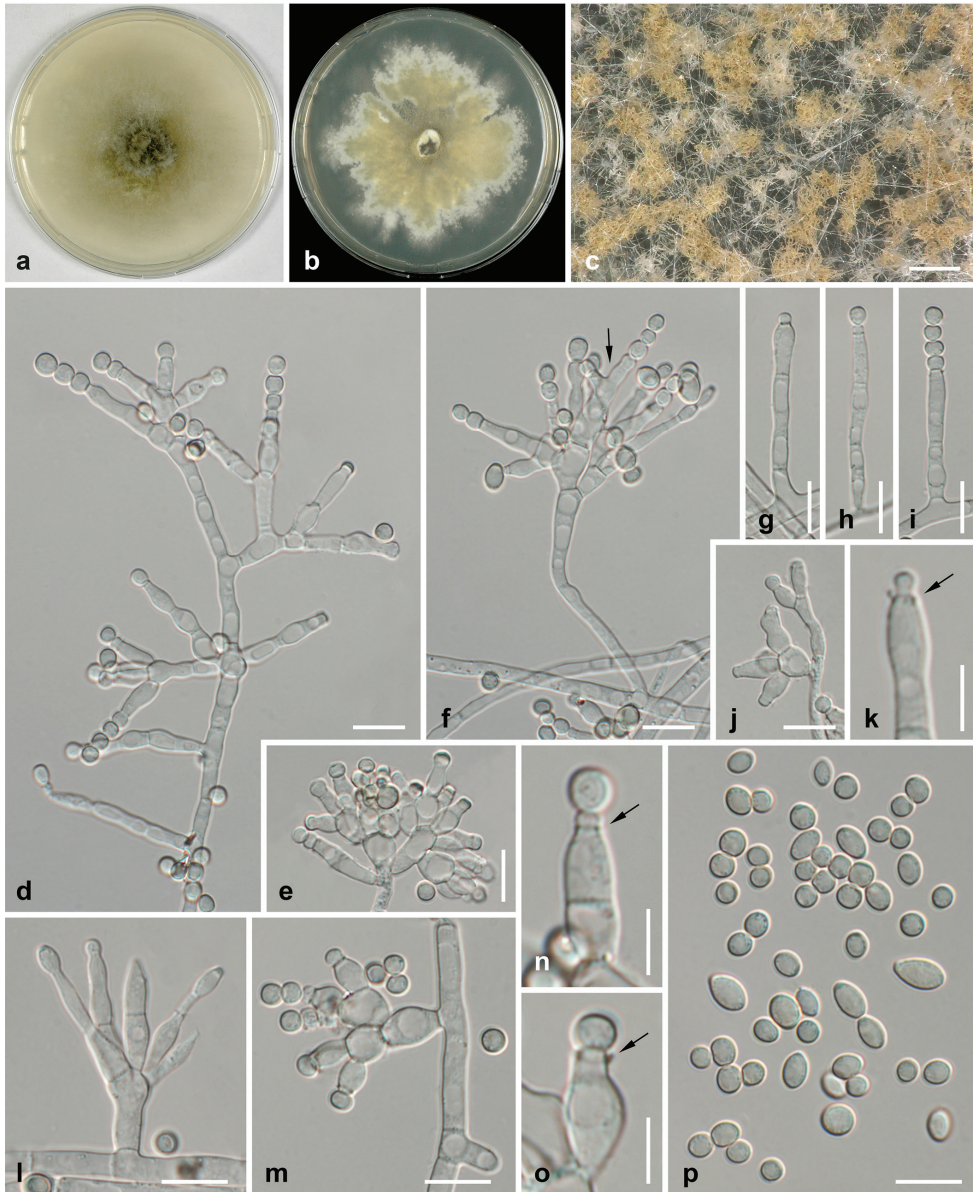


Figure 3. *Ochraceocephala foeniculi*, holotype **a** culture on CMD (7d, 22 °C) **b** culture on MEA (21d, 22 °C) **c** conidiophores on aerial hyphae producing yellowish brown conidial masses in chains **d–j**, **l**, **m** unbranched (**g–i**) and vertically branched (**d–f**, **j**, **l**, **m**) conidiophores (MEA, 21d, 22 °C) with phialides; in **f** with polyphialide (arrow) **k**, **n**, **o** phialides with collarettes (arrows) and young conidia **p** conidia. All microscopic preparations from MEA (21d, 22 °C) and mounted in water. Scale bars: 200 μm (**c**); 10 μm (**d–j**, **l**, **m**, **p**); 5 μm (**k**, **n**, **o**).

Schwartsburd, Barreto, Hernández-Restrepo, Lombard & Groenewald, Fungal Systematics and Evolution 1: 207. 2018.

Notes. In the phylogenetic analyses (Fig. 2) *Subplenodomus iridicola* is placed remote from the other species of *Subplenodomus*, but is sister species to *Alloleptosphaeria italica* with maximum support; *S. iridicola* is therefore transferred to the genus *Alloleptosphaeria*.

***Paraleptosphaeria rumicis* (Quaedvl., Verkley & Crous) Voglmayr, comb. nov.**

Mycobank No: 833936

Basionym. *Acicuseptoria rumicis* Quaedvl., Verkley & Crous, Stud. Mycol. 75: 376 (2013).

Notes. The monotypic genus *Acicuseptoria* was described by Quaedvlieg et al. (2013) as a segregate of the polyphyletic genus *Septoria*, and it was characterised by brown, globose pycnidia with conidiophores reduced to ampulliform conidiogenous cells bearing acicular, hyaline, euseptate conidia. However, its position within the Leptosphaeriaceae remained undetermined as no other representatives of the family were included in their phylogenetic tree (Quaedvlieg et al. 2013: fig. 2). In our phylogenetic analyses (Fig. 2), *Acicuseptoria rumicis* is embedded within the genus *Paraleptosphaeria* and placed in a highly supported subclade that also contains the generic type, *P. nitschkei*. *Acicuseptoria rumicis* is therefore transferred to the genus *Paraleptosphaeria*.

Pathogenicity test

The representative isolate (CBS 145654) was pathogenic to fennel plants, and produced symptoms similar to those observed in open field after five days (Fig. 1e). The pathogen was re-isolated from the artificially inoculated plants, and identified as previously described. No symptoms were observed on control plants.

Cultivar susceptibility

In the experiments on fennel susceptibility there was always a significant effect of the cultivar on all disease parameters (PM, DI and SS) of pathogen infections ($p < 0.0001$). Otherwise, a not significant cultivar \times trial effect ($p > 0.56$) was observed for parametric variables (PM and DI) in this repeated experiment (Table 5). Besides, Kendall's coefficient of concordance was 0.96 for SS data, thus indicating very high concordance between the two trials (Table 5). Therefore, the two trials were combined.

Regarding susceptibility of fennel to this phytopathogenic fungus, a great variability was detected among the tested cultivars eight days after inoculation. Comprehensively, cultivar 'Narciso' was the most susceptible since all disease parameters and

Table 5. ANOVA effects of cultivar and cultivar \times trial interactions on plant mortality, disease incidence and severity of symptoms caused by *Ochraceocephala foeniculi* on inoculated young fennel plants.

Model effect Factor(s)	Parameter								
	Plant mortality (PM) ¹			Disease incidence (DI) ¹			Symptom severity (SS) ²		
	df	<i>F</i>	<i>P</i> value	df	<i>F</i>	<i>P</i> value	χ^2	<i>W</i>	<i>P</i> value
Cultivar	5	70.6286	< 0.0001	5	33.659	< 0.0001	89.2051	...	< 0.0001
Cultivar \times trial	5	0.1273	0.98475 ^{ns}	5	0.789 ^{ns}	0.56797 ^{ns}	...	0.95873	0.0003

¹ *F* test of fixed effects, df = degrees of freedom, and *P* value associated to *F*; ns = not significant. ² The χ^2 value for Kruskal-Wallis one-way analysis of variance test (cultivar) and Friedman two-way analysis of variance (cultivar \times trial), respectively; *W* = Kendall's coefficient of concordance between repeated trials in the experiment.

Table 6. Compared susceptibility to crown and root rot infections of six commercial fennel cultivars.

Cultivar	Plant mortality (PM) ¹	Disease incidence (DI) ¹	Symptom severity (SS) ²
'Narciso'	72.92 \pm 2.08 a	100 a	4.15 \pm 0.10 a
'Apollo'	58.33 \pm 4.17 b	100 a	4.33 \pm 0.17 a
'Pompeo'	45.83 \pm 4.17 b	100 a	3.37 \pm 0.13 b
'Aurelio'	10.42 \pm 2.08 c	100 a	2.56 \pm 0.06 b
'Archimede'	0.00 d	83.33 \pm 4.17 b	1.94 \pm 0.10 c
'Pegaso'	0.00 d	77.08 \pm 2.08 b	1.48 \pm 0.10 d

¹Data derived from repeated experiment. Standard error of the mean = SEM, means are from 24 fennel young plants. Arithmetic means are presented although analysis was performed on angular transformed values. Means followed by different letters within the column are significantly different according to Fisher's least significance differences test ($\alpha = 0.05$). ² Differences among SS (0-to-5 scale) data for each treatment were analysed with Friedman two-way analysis of variance by mean rank scores ($P < 0.001$) followed by all pairwise multiple comparison with Wilcoxon.

its PM value were significantly the highest among the tested cultivars. 'Apollo' was also highly susceptible to infection by the new fennel pathogen, significantly differing only in a slightly lower PM value. 'Pompeo' displayed PM and DI values similar to those recorded for 'Apollo', but its SS score was significantly lower than in the former (Table 6). In decreasing order of susceptibility, 'Aurelio' did not significantly differ from 'Pompeo' for DI and SS values, but its PM caused by the fennel pathogen was strongly reduced. No dead seedlings (PM = 0) were recorded for both 'Archimede' and 'Pegaso', that significantly differed for DI and SS from the other remaining cultivars. Altogether, 'Pegaso' was the least susceptible cultivar to fungal infection since it showed the lowest values of disease severity.

Discussion

In the present study, 32 fungal isolates were recovered from symptomatic fennel plants in Sicily over a 2-year period. Disease symptoms were observed in three farms, and included necrotic lesions and crown and root rot on three different cultivars. The fungal species obtained from symptomatic tissues was identified based on morphological characters and molecular phylogenetic analyses of an ITS-LSU-SSU rDNA matrix, resulting in the description of the fennel pathogen as a new genus and species, *Ochraceocephala foeniculi*.

In the phylogenetic analyses, *O. foeniculi* was revealed as sister group of *Plenodomus*; however, without significant support (Fig. 2). As commonly observed with ITS-LSU-SSU rDNA data, support of many backbone nodes is low or absent, and additional protein-coding markers like *RPB2*, *TEF1* and *TUB2* are necessary for an improved phylogenetic resolution of genera and families in Pleosporales (Voglmayr and Jaklitsch 2017; Jaklitsch et al. 2018). Although we sequenced *RPB2*, *TEF1*, and *TUB2* for *O. foeniculi*, it was currently not feasible to perform multi-gene analyses due to insufficient sequence data for most species of Leptosphaeriaceae, in particular for *Plenodomus*. However, we consider the phylogenetic and morphological evidence conclusive for establishing the new genus *Ochraceocephala*. Also the generic transfer of *Subplenodomus iridicola* to *Alloleptosphaeria* is well substantiated, considering its highly supported phylogenetic position as sister species of *Alloleptosphaeria italica*, remote from the generic type (*S. violicola*) and other species of *Subplenodomus* (Fig. 2). In the phylogenetic analyses of the LSU rDNA matrix of Crous et al. (2018: fig. 1), only few taxa of Leptosphaeriaceae were included, and the phylogenetic position of *S. iridicola* remained inconclusive due to low resolution; however, also in their analyses it was placed remote from the generic type, *S. violicola*. In addition, they did not include its closest relative, *Alloleptosphaeria italica*, although it was mentioned as the closest match of an ITS BLAST search (Crous et al. 2018). No asexual morph is known for *A. italica* (Dayarathne et al. 2015), but the ascomata, asci and ascospores of *A. iridicola* and *A. italica* share many traits. Our phylogenetic analyses also showed that *Acicuseptoria rumicis* should be included within *Paraleptosphaeria* (Fig. 2). Although it was correctly placed within Leptosphaeriaceae by Quaedvlieg et al. (2013), its position within the family remained undetermined as no other representatives of the family were included in their phylogenetic analyses. As for most other species of *Paraleptosphaeria* no asexual morphs are known, no comprehensive morphological comparison can currently be made with *P. rumicis*.

Within Leptosphaeriaceae, *O. foeniculi* is remarkable and unique by its complex hyphomycetous asexual morph composed of branched conidiophores with phialidic conidiation and conidia produced in basipetal chains. Asexual morphs in Leptosphaeriaceae are typically coelomycetous and phoma-like, which is also the case in the closest relative of *Ochraceocephala*, *Plenodomus* (Gruyter et al. 2013). Another genus of Leptosphaeriaceae with a hyphomycetous asexual morph is *Alternariaster*, which, however, differs significantly by tetric conidiogenous cells forming large, brown, septate conidia not produced in chains (Simmons 2007; Alves et al. 2013). Therefore, the unique morphology in combination with an isolated phylogenetic position within Leptosphaeriaceae warrant the establishment of a new genus.

Other fungal species belonging to Leptosphaeriaceae, as well as the closely related Didymellaceae (Odstrčilová et al. 2002; Shaker and Alhamadany 2015) have been reported worldwide in fennel crops. In Italy, crown rot of fennel caused by *Didymella glomerata* (syn. *Phoma glomerata*) was recorded from southern Italy (Lahoz et al. 2007). As confirmed in the pathogenicity tests, *O. foeniculi* caused symptoms on artificially inoculated plants of the same cultivar and, moreover, also on different fennel cultivars

that showed some variability in disease susceptibility. To this regard, it is noteworthy that this study also represents a preliminary evaluation of fennel germplasm according to their susceptibility to this new disease. Although these data should be confirmed by additional investigations, this study might provide very useful information for local farmers and technicians. The determination of the extent of susceptibility to *O. foeniculi* is a starting point for evaluating the tolerance of commercial fennel cultivars to this disease under different agronomic and phytosanitary conditions.

On the basis of the disease incidence and severity observed in the field, we believe that this disease represents a serious threat to fennel crop in Sicily and may become a major problem also to other areas of fennel production if accidentally introduced. Moreover, infected soil could represent an inoculum source for this fungus. Further studies are needed to examine the life cycle of *O. foeniculi* and to ascertain the cardinal temperatures of the fungus for successful infection since this pathogen is well established in this representative fennel production area. This information is required for the setup and timing of sustainable approaches for soil disinfection, including solarization and/or fumigation at low rates, to reduce the level of the primary inoculum in the soil and hence the disease amount, like successfully applied for other soilborne plant pathogens (Vitale et al. 2013; Aiello et al. 2018).

Although not always conclusive, soil disinfestation and host resistance can be considered environmentally friendly means to be included within integrated pest management (IPM) strategies against crown rot caused by *O. foeniculi* in order to minimize the number and intensity of fungicide applications.

Acknowledgements

This research was supported by Research Project 2016–2018 “Monitoraggio, caratterizzazione e controllo sostenibile di microrganismi e artropodi di interesse agrario” WP2-5A722192134.

References

- Aiello D, Vitale A, Alfenas RS, Alfenas AC, Cirvilleri G, Polizzi G (2018) Effects of sublethal rates of dazomet and metam-sodium applied under low-permeability films on *Calonectria microsclerotia* survival. *Plant Disease* 102: 782–789. <https://doi.org/10.1094/PDIS-06-16-0801-RE>
- Alves JL, Woudenberg JH, Duarte LL, Crous PW, Barreto RW (2013) Reappraisal of the genus *Alternariaster* (Dothideomycetes). *Persoonia* 31: 77–85. <https://doi.org/10.3767/003158513X669030>
- Ariyawansa HA, Phukhamsakda C, Thambugala KM, Bulgakov TS, Wanasinghe DN, Perera RH, Mapook A, Camporesi E, Kang JC, Jones EG, Bahkali AH, Jayasiri SC, Hyde KD,

- Liu ZY, Bhat JD (2015) Revision and phylogeny of Leptosphaeriaceae. *Fungal Diversity* 74: 19–51. <https://doi.org/10.1007/s13225-015-0349-2>
- Boerema GH, de Gruyter J, van Kesteren HA (1994) Contributions towards a monograph of *Phoma* (Coelomycetes) – III. 1. Section *Plenodomus*: Taxa often with a *Leptosphaeria* teleomorph. *Persoonia* 15: 431–487.
- Cacciola SO, Pane A, Cooke DEL, Raudino F, Magnano di San Lio G (2006) First report of brown rot and wilt of fennel caused by *Phytophthora megasperma* in Italy. *Plant Disease* 90: 110. <https://doi.org/10.1094/PD-90-0110A>
- Carbone I, Kohn LM (1999) A method for designing primer sets for speciation studies in filamentous ascomycetes. *Mycologia* 91: 553–556. <https://doi.org/10.2307/3761358>
- Choi IY, Hong SH, Cho SE, Park JH, Shin HD (2015) First report of powdery mildew caused by *Erysiphe heraclei* on fennel (*Foeniculum vulgare*) in Korea. *Plant Disease* 99: 1185. <https://doi.org/10.1094/PDIS-02-15-0147-PDN>
- Choi IY, Kim JH, Kim BS, Park MJ, Shin HD (2016) First report of Sclerotinia stem rot of fennel caused by *Sclerotinia sclerotiorum* in Korea. *Plant Disease* 100: 223. <https://doi.org/10.1094/PDIS-05-15-0512-PDN>
- Crous PW, Schumacher RK, Wingfield MJ, Akulov A, Denman S, Roux J, Braun U, Burgess TI, Carnegie AJ, Váczy KZ, Guatimosim E, Schwartsburd PB, Barreto RW, Hernández-Restrepo M, Lombard L, Groenewald JZ (2018) New and interesting fungi. 1. *Fungal Systematics and Evolution* 1: 169–215. <https://doi.org/10.3114/fuse.2018.01.08>
- D'Amico M, Frisullo S, Cirulli M (2008) Endophytic fungi occurring in fennel, lettuce, chicory, and celery-commercial crops in southern Italy. *Mycological Research* 112: 100. <https://doi.org/10.1016/j.mycres.2007.11.007>
- Dayarathne MC, Phookamsak R, Ariyawansa HA, Jones EBG, Camporesi E, Hyde KD (2015) Phylogenetic and morphological appraisal of *Leptosphaeria italica* sp. nov. (Leptosphaeriaceae, Pleosporales) from Italy. *Mycosphere* 6: 634–642. <https://doi.org/10.5943/mycosphere/6/5/13>
- Ghoneem KM, Saber WA, Elwakil MA (2009) Alkaline seed bed an innovative technique for manifesting *Verticillium dahliae* on fennel seeds. *Plant Pathology Journal* 8: 22–26. <https://doi.org/10.3923/ppj.2009.22.26>
- Glass NL, Donaldson GC (1995) Development of primer sets designed for use with the PCR to amplify conserved genes from filamentous ascomycetes. *Applied and Environmental Microbiology* 61: 1323–1330. <https://doi.org/10.1128/AEM.61.4.1323-1330.1995>
- Gruyter Jde, Woudenberg JH, Aveskamp MM, Verkley GJ, Groenewald JZ, Crous PW (2013) Redisposition of phoma-like anamorphs in Pleosporales. *Studies in Mycology* 75: 1–36. <https://doi.org/10.3114/sim0004>
- Hoog GSde, Gerrits van den Ende AHG (1998) Molecular diagnostics of clinical strains of filamentous basidiomycetes. *Mycoses* 41: 183–189. <https://doi.org/10.1111/j.1439-0507.1998.tb00321.x>
- ISTAT (Istituto Nazionale di Statistica) (2018) Ortive: finocchio in pien'aria. <http://dati.istat.it> [Accessed on: 2019-09-16]
- Jaklitsch, WM (2009) European species of *Hypocrea* Part I. The green-spored species. *Studies in Mycology* 63: 1–91. <https://doi.org/10.3114/sim.2009.63.01>

- Jaklitsch WM, Checa J, Blanco MN, Olariaga I, Tello S, Voglmayr H (2018) A preliminary account of the Cucurbitariaceae. *Studies in Mycology* 90: 71–118. <https://doi.org/10.1016/j.simyco.2017.11.002>
- Jaklitsch WM, Komon M, Kubicek CP, Druzhinina IS (2005) *Hypocrea voglmayrii* sp. nov. from the Austrian Alps represents a new phylogenetic clade in *Hypocreales Trichoderma*. *Mycologia* 97: 1365–1378. <https://doi.org/10.1080/15572536.2006.11832743>
- Koike ST, Tompkins DV, Martin F, Ramon ML (2015) First report of *Pythium* root rot of fennel in California caused by *Pythium sulcatum*. *Plant Disease* 99: 1645. <https://doi.org/10.1094/PDIS-03-15-0288-PDN>
- Khare MN, Tiwari SP, Sharma YK (2014) Disease problems in fennel (*Foeniculum vulgare* Mill) and fenugreek (*Trigonella foenum-graceum* L.) cultivation and their management for production of quality pathogen free seeds. *International Journal of Seed Spices* 4: 11–17.
- Lahoz E, Caiazzo R, Fanigliulo A, Comes S, Crescenzi A (2007) *Phoma glomerata* as causal agent of crown rot disease of fennel in southern Italy. *Communications in Agricultural and Applied Biological Sciences* 72: 875–878.
- Liu YL, Whelen S, Hall BD (1999) Phylogenetic relationships among ascomycetes: evidence from an RNA polymerase II subunit. *Molecular Biology and Evolution* 16: 1799–1808. <https://doi.org/10.1093/oxfordjournals.molbev.a026092>
- O'Donnell K, Cigelnik E (1997) Two divergent intragenomic rDNA ITS2 types within a monophyletic lineage of the fungus *Fusarium* are nonorthologous. *Molecular Phylogenetics and Evolution* 7: 103–116. <https://doi.org/10.1006/mpev.1996.0376>
- Odstrčilová L, Ondřej M, Kocourková B, Růžičková G (2002) Monitoring of incidence and determination of fungi on caraway, fennel, coriander and anise, consideration of disease importance and possibility of chemical protection. *Plant Protection Science* 38: 340–343. <https://doi.org/10.17221/10485-PPS>
- Phookamsak R, Hyde KD, Jeewon R, Bhat DJ, Jones EBG, Maharachchikumbura SSN, Raspé O, Karunarathna SC, Wanasinghe DN, Hongsanan S, Doilom M, Tennakoon DS, Machado AR, Firmino AL, Ghosh A, Karunarathna A, Mešić A, Dutta AK, Thongbai B, Devadatha B, Norphanphoun C, Senwanna C, Wei D, Pem Di, Ackah FK, Wang GN, Jiang HB, Madrid H, Lee HB, Goonasekara ID, Manawasinghe IS, Kušan I, Cano J, Gené J, Li J, Das K, Acharya K, Raj KNA, Latha KPD, Chethana KWT, He MQ, Dueñas M, Jadan M, Martín MP, Samarakoon MC, Dayarathne MC, Raza M, Park MS, Telleria MT, Chaiwan N, Matočec N, de Silva NI, Pereira OL, Singh PN, Manimohan P, Uniyal P, Shang QJ, Bhatt RP, Perera RH, Alvarenga RLM, Nogal-Prata S, Singh SK, Vadthananat S, Oh SY, Huang SK, Rana S, Konta S, Paloi S, Jayasiri SC, Jeon SJ, Mehmood T, Gibertoni TB, Nguyen TTT, Singh U, Thiyagaraja V, Sarma VV, Dong W, Yu XD, Lu YZ, Lim YW, Chen Y, Tkalcic Z, Zhang ZF, Luo ZL, Daranagama DA, Thambugala KM, Tibpromma S, Camporesi E, Bulgakov TS, Dissanayake AJ, Senanayake IC, Dai DQ, Tang LZ, Khan S, Zhang H, Promputtha I, Cai L, Chomnunti P, Zhao RL, Lumyong S, Boonmee S, Wen T-C, Mortimer PE, Xu J (2019) Fungal diversity notes 929–1035: taxonomic and phylogenetic contributions on genera and species of fungi. *Fungal Diversity* 95: 1–273. <https://doi.org/10.1007/s13225-019-00421-w>

- Quaedvlieg W, Verkley GJ, Shin HD, Barreto RW, Alfenas AC, Swart WJ, Groenewald JZ, Crous PW (2013) Sizing up *Septoria*. *Studies in Mycology* 75: 307–390. <https://doi.org/10.3114/sim0017>
- Rodeva R, Gabler J (2011) Umbel browning and stem necrosis: a new disease of fennel in Bulgaria. *Journal of Phytopathology* 159: 184–187. <https://doi.org/10.1111/j.1439-0434.2010.01728.x>
- Shaker GA, Alhamadany HS (2015) Isolation and identification of fungi which infect fennel *Foeniculum vulgare* Mill. and its impact as antifungal agent. *Iraq Natural History Research Center and Museum* 13: 31–38.
- Silvestro D, Michalak I (2012) raxmlGUI: a graphical front-end for RAxML. *Organisms Diversity and Evolution* 12: 335–337. <https://doi.org/10.1007/s13127-011-0056-0>
- Simmons EG (2007) *Alternaria: An Identification Manual*. CBS Biodiversity Series 6. Centraalbureau voor Schimmelcultures, Utrecht, Netherlands, 775 pp.
- Stamatakis E (2006) RAxML-VI-HPC: maximum likelihood-based phylogenetic analyses with thousands of taxa and mixed models. *Bioinformatics* 22: 2688–2690. <https://doi.org/10.1093/bioinformatics/btl446>
- Sung GH, Sung JM, Hywel-Jones NL, Spatafora JW (2007) A multi-gene phylogeny of Clavicipitaceae (Ascomycota, Fungi): Identification of localized incongruence using a combinatorial bootstrap. *Molecular Phylogenetics and Evolution* 44: 1204–1223. <https://doi.org/10.1016/j.ympev.2007.03.011>
- Swofford DL (2002) PAUP* 4.0b10: phylogenetic analysis using parsimony (*and other methods). Sinauer Associates, Sunderland, Massachusetts. <https://doi.org/10.1111/j.0014-3820.2002.tb00191.x>
- Taubenrauch K, Gabler J, Hau B (2008) Mykologische Untersuchung von *Mycosphaerella anethi* an Fenchel (*Foeniculum vulgare* Mill.). *Mitteilungen aus dem Julius Kühn-Institut* 417: 387–388.
- Vilgalys R, Hester M (1990) Rapid genetic identification and mapping of enzymatically amplified ribosomal DNA from several *Cryptococcus* species. *Journal of Bacteriology* 172: 4238–4246. <https://doi.org/10.1128/jb.172.8.4238-4246.1990>
- Vitale A, Castello I, D’Emilio A, Mazzarella R, Perrone G, Epifani S, Polizzi G (2013) Short-term effects of soil solarization in suppressing *Calonectria* microsclerotia. *Plant and Soil* 368: 603–617. <https://doi.org/10.1007/s11104-012-1544-5>
- Voglmayr H, Jaklitsch WM (2017) *Corynespora*, *Exosporium* and *Helminthosporium* revisited – new species and generic reclassification. *Studies in Mycology* 87: 43–76. <https://doi.org/10.1016/j.simyco.2017.05.001>
- Voglmayr H, Rossman AY, Castlebury LA, Jaklitsch WM (2012) Multigene phylogeny and taxonomy of the genus *Melanconiella* (Diaporthales). *Fungal Diversity* 57: 1–44. <https://doi.org/10.1007/s13225-012-0175-8>
- White TJ, Bruns TD, Lee SB, Taylor JW (1990) Amplification and direct sequencing of fungal ribosomal RNA genes for phylogenetics. In: Innis MA, Gelfand DH, Sninsky JJ, White TJ (Eds) *PCR Protocols: a Guide to Methods and Applications*. Academic Press, New York, 315–322. <https://doi.org/10.1016/B978-0-12-372180-8.50042-1>

Additions to the genus *Chroogomphus* (Boletales, Gomphidiaceae) from Pakistan

Munazza Kiran¹, Ammara Sattar¹, Khushbakht Zamir¹,
Danny Haelewaters^{2,3}, Abdul Nasir Khalid¹

1 Department of Botany, University of the Punjab, Quaid-e-Azam Campus, Lahore, 54590, Pakistan **2** Department of Botany and Plant Pathology, Purdue University, USA **3** Faculty of Science, University of South Bohemia, Czech Republic

Corresponding author: Ammara Sattar (ammarasattar81@gmail.com)

Academic editor: O. Raspé | Received 30 July 2019 | Accepted 24 January 2020 | Published 30 March 2020

Citation: Kiran M, Sattar A, Zamir K, Haelewaters D, Khalid AN (2020) Additions to the genus *Chroogomphus* (Boletales, Gomphidiaceae) from Pakistan. MycoKeys 66: 23–38. <https://doi.org/10.3897/mycokeys.66.38659>

Abstract

With only three published reports, the genus *Chroogomphus* (Boletales, Gomphidiaceae) is poorly studied in Pakistan. During recent sampling events in Khyber Pakhtunkhwa province, Pakistan, several collections of *Chroogomphus* were made, representing undescribed taxa. Based on morphological and molecular data, two new species are described: *Chroogomphus pakistanicus* and *C. pruinosus*. We present a description and illustrations for both taxa. A molecular phylogenetic reconstruction, based on the internal transcribed spacer (ITS1–5.8S–ITS2) barcode region, shows that *C. pakistanicus* and *C. pruinosus* are placed in two different subgenera of *Chroogomphus* (subg. *Chroogomphus* and subg. *Siccigomphus*, respectively).

Keywords

2 new taxa, Basidiomycota, Boletales, coniferous forests, macrofungi, phylogeny, taxonomy

Introduction

Chroogomphus (Singer) Mill. was initially recognised as a sub-genus of *Gomphidius* Fr. (Singer 1948). It was Miller (1964) who elevated it to genus level. More than 33 taxa are currently recognised worldwide, including species, subspecies and varieties, but the number of accepted species in the genus is ambiguous (Miller and Aime 2001; Miller 2003; Watling 2004; Li et al. 2009; Martín et al. 2016; Razaq et al. 2016; Scambler

et al. 2018). Members of the genus are characterised by ochraceous basidiomata; orange to somewhat ochraceous, decurrent lamellae; a fibrous veil; and grey to black spore deposit. Other useful characters are the pileipellis hyphae (moist to glutinous or viscid) and the stipe base (with hyphae that are amyloid in Melzer's reagent) (Miller 1964; Miller and Aime 2001; Li et al. 2009; Martín et al. 2016).

The genus is currently divided into three subgenera – *Chroogomphus*, *Floccigomphus* (Imai) Niskanen, Scambler, & Liimat. and *Siccigomphus* Niskanen, Scambler, & Liimat. (Scambler et al. 2018). Subg. *Chroogomphus* includes species that have a pileipellis made of repent, gelatinised, narrow hyphae and a shiny pileus surface when dry (Miller and Aime 2001; Scambler et al. 2018). Members of subg. *Floccigomphus* are distinguished by a pileipellis composed of broad, filamentous, non-gelatinised hyphae, an unpolished pileus when dry and amyloid lamellar trama. Species of subg. *Siccigomphus* have inamyloid lamellar trama, smaller basidiospores and non-gelatinised pileipellis hyphae (Scambler et al. 2018).

Chroogomphus species are economically very important because of their ectomycorrhizal association with pines and applications as drugs and food (Agerer 1990, 1991; Miller 1964; Xie et al. 1986; Yu and Liu 2005; Dai and Tolgor 2007). They are found in Europe, America and Asia (Miller 1964; Miller and Aime 2001; Legon and Henrici 2005; Li et al. 2009; Knudsen and Taylor 2012; Scambler et al. 2018). In Pakistan, the genus is underexplored with only three published reports. These are *C. helveticus* (Singer) M.M. Moser, *C. roseolus* Yan C. Li & Zhu L. Yang and *C. rutilus* (Schaeff.) O.K. Mill. (Ahmad et al. 1997; Razaq et al. 2016). Here, we describe two new species of *Chroogomphus* belonging to two different subgenera, based on their morpho-anatomical features and molecular phylogenetic analysis.

Materials and methods

Sampling site

Specimens were collected from the Kumrat valley (35°32'N, 72°13'E, Siddiqui et al. 2013), district Upper Dir, Khyber Pakhtunkhwa, Pakistan. In this area, rainfall reaches 100–255 mm during monsoon season (Wahab 2011). The Panjkora River flows through the dense vegetation of the valley, which includes mixed pine forests. *Abies pindrow* Royle, *Cedrus deodara* (Roxb. ex D. Don) G. Don and *Pinus wallichiana* A.B. Jacks. are the main coniferous species (Shinwari et al. 2006).

Morphological observations

Macro-morphological characters of fresh basidiomata were recorded and colour codes were assigned using Munsell Soil Color Charts (1975). Macro-morphological characters included the size, shape and colour of pileus; colour of gills and mode of attachment to

the stipe; colour of stipe and attachment to the pileus; presence or absence of annular ring and volva. Micro-morphological features were observed using a compound light microscope (MX4300H, Meiji Techno, Japan). For detailed microscopic examination, sections of lamellae, pileipellis and stiptipellis from dried specimens were observed in 5% potassium hydroxide (KOH), Congo red stain and Melzer's reagent. Anatomical features were measured using ScopeImage software version 1.0.0 (BioImager, Maple, Canada). Measurements of basidiospores were made under oil immersion. A minimum of 60 basidiospores, 20 basidia and 20 cystidia were measured. The abbreviations 'n/m/p' indicates number of basidiospores 'n', measured from 'm' basidiomata from 'p' collections. Basidiospores dimensions are given as length × width with extreme values given in parentheses; avQ = average Q of all spores ± standard deviation. Voucher specimens are deposited in LAH (Department of Botany, University of the Punjab, Pakistan).

DNA extraction, PCR amplifications and sequencing

Genomic DNA was extracted from dried tissue employing a modified CTAB protocol (Gardes and Bruns 1993). Amplification of the internal transcribed spacer (ITS, including ITS1, 5.8S and ITS2) barcode region of the nuclear ribosomal DNA was done using the primer pair ITS1F and ITS4 (Gardes and Bruns 1993; White et al. 1990). Polymerase chain reaction (PCR) was performed in a reaction volume of 20 µl containing 10 µl of 2× PCR buffer (Sigma-Aldrich, St. Louis, Missouri), 0.1 µl of each 0.6 nM primer, 8.8 µl of ddH₂O and 1 µl of template DNA under the following cycling parameters: initial denaturation at 94 °C for 1 min; followed by 35 cycles of denaturation at 94 °C for 1 min, annealing at 53 °C for 1 min and extension at 72 °C for 1 min; and a final extension at 72 °C for 8 min. Amplified PCR products were directly sequenced in both directions by Sanger sequencing, using the same primers (Macrogen Inc., South Korea). Consensus sequences were generated using BioEdit software version 7.2.5.0 (Hall 1999) and then blasted against the NCBI GenBank database (<https://blast.ncbi.nlm.nih.gov/>).

Sequence alignment and phylogenetic analysis

We constructed an ITS dataset of our newly generated sequences along with closely related sequences that were downloaded from GenBank (Li et al. 2009; Martín et al. 2016; Scambler et al. 2018). We included species of *Gomphidius* Fr. as outgroup taxa (Scambler et al. 2018). Multiple sequence alignment was done using MUSCLE (Edgar 2004) available from EMBL-EBI (<http://www.ebi.ac.uk/Tools/msa/muscle/>). The final alignment was submitted to TreeBASE under study ID: S24298.

The ITS1, 5.8S and ITS2 loci were extracted from the aligned ITS dataset, allowing the selection of substitution models for each partition. Models were selected using ModelFinder (Kalyaanamoorthy et al. 2017) by considering the corrected Akaike In-

formation Criterion (AICc). Selected models were TNe+G4 (ITS1, -lnL = 4480.541), K2P (5.8S, -lnL = 754.828) and TIM3e+G4 (ITS2, -lnL = 4453.285). Phylogenetic relationships were inferred by Maximum Likelihood (ML) using IQ-TREE (Nguyen et al. 2015) from the command line, under partitioned models (Chernomor et al. 2016). Ultrafast bootstrapping was done with 1000 replicates (Hoang et al. 2017).

A Bayesian Inference (BI) phylogeny was estimated using BEAST version 1.8.4 (Drummond et al. 2012) with an uncorrelated lognormal relaxed clock, allowing for evolutionary rates to vary across branches. We selected a Birth-Death Incomplete Sampling speciation model (Stadler 2009) tree prior and appropriate substitution models as determined by jModelTest2 (Darriba et al. 2012) under AICc. Models were TrNef+G (ITS1, -lnL = 2028.8929), JC (5.8S, -lnL = 320.6928) and TPM3+G (ITS2, -lnL = 1905.6932). Four independent runs were performed from a random starting tree for 40 million generations with a sampling frequency of 4000. The analyses were run from the BEAST on XSEDE tool on the Cipes Science Gateway (Miller et al. 2010). Resulting log files were entered in Tracer (Rambaut et al. 2014) to check trace plots and burn-in values. Effective sample sizes were well over 200 for all sampled parameters for each run and so we selected a standard burn-in of 10%. After the removal of 10% of each run as burn-in, log files and trees files were combined in LogCombiner. TreeAnnotator was used to generate consensus trees (with 0% burn-in) and to infer the Maximum Clade Credibility tree.

Final phylogenetic reconstructions with ML bootstrap values (BS) and BI posterior probabilities (pp) were visualised in FigTree v1.4.3 (<http://tree.bio.ed.ac.uk/software/figtree/>) and edited in Adobe Illustrator version 23.0.6 (San Jose, California).

Results

Phylogenetic analyses

Amplification of the ITS from three basidiomata of *C. pruinosis* resulted in 670 bp sequences (GenBank accession numbers MK509768, MK509769 and MK509770). All of these sequences showed 97% similarity to *C. roseolus* (LT576117, Pakistan) with 100% query coverage. The ITS sequences obtained from two basidiomata of *C. pakistanicus* (MK509771, MK509772) were 650 bp in length and showed 98% similarity to *C. filiformis* Yan C. Li & Zhu L. Yang (EU706324, China) with 95% query coverage.

The ITS1–5.8S–ITS2 dataset included a total of 768 characters for 84 sequences including *Gomphidius* spp. as outgroup taxa (Suppl. material 1: Table S1). Out of 768 characters, 309 were of ITS1, 161 of 5.8S and 298 of ITS2; 121 (ITS1), 8 (5.8S) and 116 (ITS2) characters were parsimony-informative; and 164 (ITS1), 148 (5.8S) and 158 (ITS2) characters were constant. In the phylogenetic analysis of the ITS dataset (Figure 1), three main clades of *Chroogomphus* were recovered, representing the different subgenera: subg. *Floccigomphus* (clade I, maximum support), subg. *Siccigomphus* (clade II, BS = 100%, pp = 0.99) and subg. *Chroogomphus* (clade III, BS = 95%, pp = 0.98). The two isolates of *C. pakistanicus* sp. nov. formed a monophyletic clade

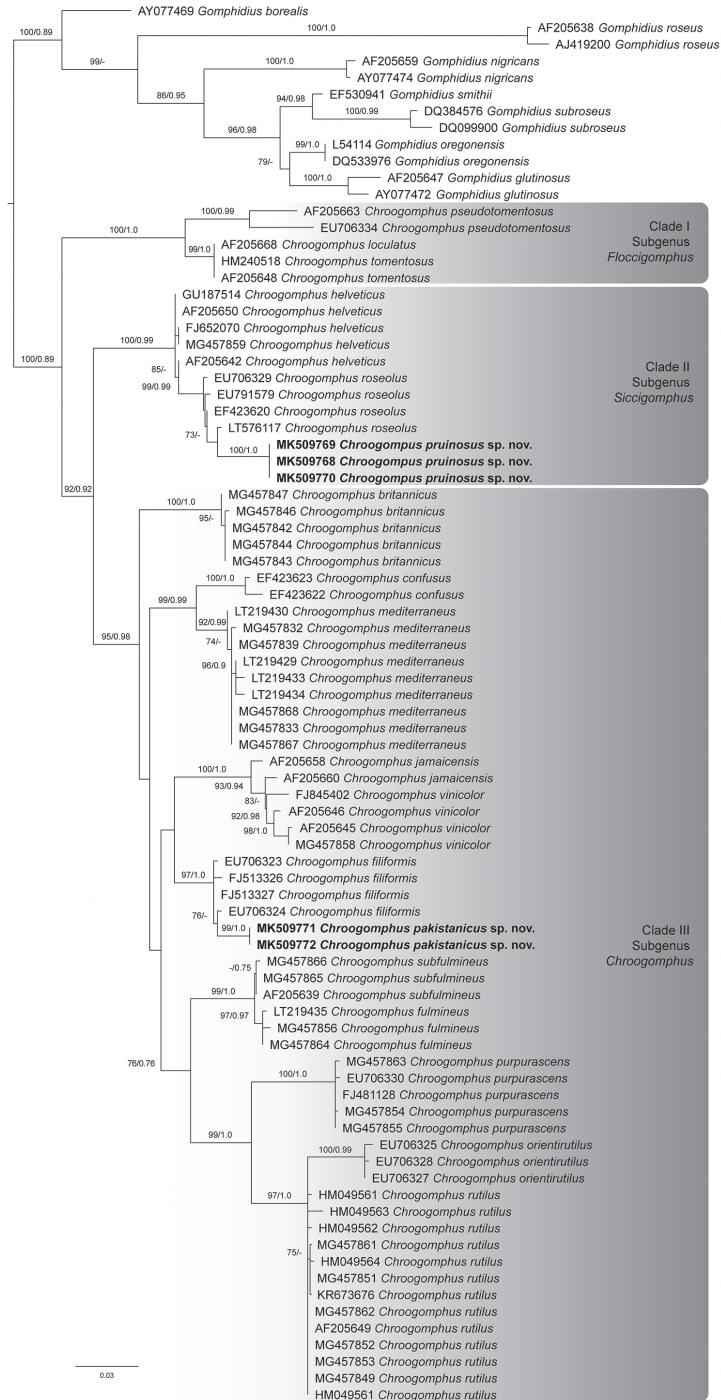


Figure 1. The best-scoring ML tree ($-\ln L = 4385.926$) of the genus *Chroogomphus*, reconstructed from the ITS dataset. ML bootstraps ($> 70\%$) and posterior probabilities (> 0.75) are indicated above or in front of the branch leading to each node. Newly described species are in boldface.

(ML BS = 99%, pp = 1.0) within subg. *Chroogomphus*, sister to *C. filiformis*. Our three collections of *C. pruinus* sp. nov. formed a separate clade with maximum support within subg. *Siccigomphus*, sister to *C. roseolus*.

Taxonomy

Chroogomphus pakistanicus M. Kiran & A.N. Khalid, sp. nov.

MycoBank No: 829715

Figures 2, 3

Diagnosis. Differs from *Chroogomphus filiformis* by the pileus ranging in colour from greyish-yellow brown to dark bluish-grey to orange and by the absence of a pinkish mycelium at the base of the stipe.

Types. Holotype: PAKISTAN, Khyber Pakhtunkhwa province, district Dir (Upper), Kumrat valley, 35°32'N, 72°13'E, 2400 m a.s.l., gregarious on forest floor, 20 Aug 2016, M. Kiran & A.N. Khalid, KM82 (LAH35889), GenBank accession number MK509771 (ITS). **Paratype:** *ibid.*, KM83 (LAH35890), GenBank accession number MK509772 (ITS).

Etymology. Referring to the country where the type collections were collected.

Habitat. On forest floor under mixed conifers.

Description. *Basidiomata* small to medium-sized. *Pileus* 2–5 cm in diameter, secotioid when young, expanding broadly-parabolic to hemispherical towards maturity, radially fibrillose, ranging in colour from greyish-yellow brown (2.5Y,5/2) to dark bluish-grey (5BG,4/1) to orange (5YR,6/6), surface shiny or glistening, smooth, margin inrolled initially becoming straight to slightly seriate when mature. *Lamellae* adnate to slightly decurrent, distant, regular, concolorous to pileus, smooth, entire, lamellulae in two tiers, alternating with lamellae, short. *Stipe* 3–5.5 × 1 cm, central, more or less equal or sometimes enlarged at base, orange (5YR7/8) to reddish-brown (2.5YR4/8), pruinose to fibrillose to squamulose, with pinkish-white mycelium at stipe base, universal and partial veil absent. Odour and taste not recorded.

Basidiospores [60/3/2], (15–)16–19.5(–20.5) × (5.5–)6–7.5(–8) μm, avl × avw = 17.5 × 6.6 μm, Q = (2.1–)2.2–3(–3.5) μm, avQ = 2.56±0.33 μm, oblong to elongate, mono-guttulate to multi-guttulate, pale brown in KOH, apiculus prominent, smooth, dextrinoid. *Basidia* 30–50 × 8–10.5 μm, avl × avw = 40 × 9 μm, hyaline to pale yellow in KOH, clavate to club-shaped. *Lamellar trama* yellowish hyphae in KOH, 5–11 μm, with brownish encrustations, inamyloid and non-dextrinoid. *Pleurocystidia* 75–107 × 17.5–25.5 μm, avl × avw = 91 × 43 μm, clavate to sometimes slightly utriform, pale brown to brown in KOH, encrusted, inamyloid. *Cheilocystidia* similar to pleurocystidia. *Pileipellis* a cutis, pale yellow to brownish KOH, 4–6 μm wide, amyloid, septate, clamped. *Pileal trama* composed of amyloid encrusted hyphae, 4–18 μm, yellowish in KOH. *Stipitipellis* a cutis of 3–9.5 μm wide, pale yellow to pale brown KOH, cylindrical, parallel, septate amyloid hyphae present at the base. Clamp connection present in all tissues.



Figure 2. Basidiomata of *Chroogomphus* spp. **A–E** *Chroogomphus pakistanicus* **A, B** LAH 35889, holotype **C–E** LAH 35890 **F–K** *Chroogomphus pruinosus* **F, G** LAH 35887 **H, I** LAH 35888; **J, K** LAH 35886, holotype. Scale bars: 1 cm.

Notes. *Chroogomphus pakistanicus* can be easily distinguished from the other members in the genus by the unique bluish-grey colour of its pileus. The phylogenetically closest relative, *C. filiformis*, (Figure 1) is discriminated from *C. pakistanicus* based on the

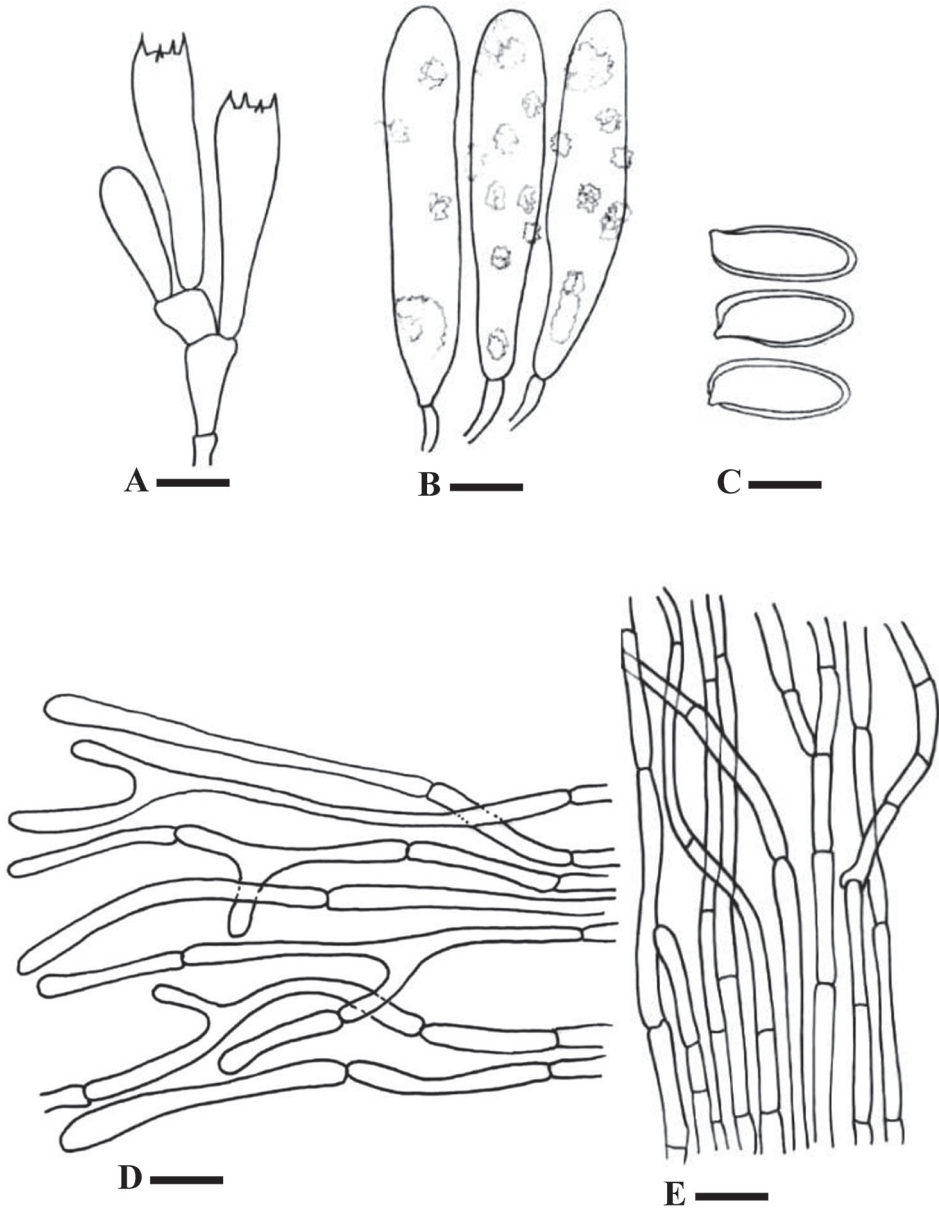


Figure 3. Line drawings of *Chroogomphus pakistanicus*. **A** Basidia **B** Cystidia **C** Basidiospores **D** Pileipellis hyphae **E** Stipitipellis hyphae. Scale bars: 12 μm (**A**), 17.5 μm (**B**), 8.5 μm (**C**), 25 μm (**D**), 30 μm (**E**).

following morphological features: (1) the pileus of *C. pakistanicus* ranges in colour from greyish-yellow brown to dark bluish-grey to orange and has a glistening surface, whereas in *C. filiformis* the pileus is clearly olive grey to pinkish-orange; and (2) the pinkish mycelium at the base of the stipe typical for *C. filiformis* (Li et al. 2009) is absent in *C. pakistanicus*.

Chroogomphus britannicus was included in sect. *Filiformes* by Scambler et al. (2018). In our phylogenetic tree, its position is unresolved within subg. *Chroogomphus*. Morphologically, it can be easily distinguished from the new species. *Chroogomphus britannicus* has larger basidiospores ($20.3 \times 7.1 \mu\text{m}$), amyloid lamellar trama and inamyloid pileal trama (Scambler et al. 2018). The morphology of *Chroogomphus pakistanicus* is similar to *C. mediterraneus*, which can be distinguished by a subconical to convex pileus ranging in colour from grey to olivaceous to brown to red to pink to purplish, in combination with differently shaped cystidia, ranging from cylindrical, subfusiform, subutriform to sometimes subcapitate (Scambler et al. 2018). *Chroogomphus vinicolor* is another species related to *C. pakistanicus*, but the cystidia of *C. vinicolor* are thick-walled ($5\text{--}7.5 \mu\text{m}$) and it has a differently coloured pileus (Miller 1964; Singer and Kuthan 1976). Furthermore, geographically, members of the section *Vinicolores* have thus far only been reported from North America (Scambler et al. 2018). *Chroogomphus jamaicensis* may also be confused with *C. pakistanicus*, but it can be separated from the latter in having different micromorphological characters including thick-walled ($4\text{--}5 \mu\text{m}$) fusiform caulocystidia, which are occasionally amyloid towards the base (Miller 1964).

***Chroogomphus pruinosis* M. Kiran & A.N. Khalid, sp. nov.**

MycoBank No: 829714

Figures 2, 4

Diagnosis. Differs from *Chroogomphus roseolus* by the pileal trama that is inamyloid in Melzer's reagent and by the presence of pileocystidia and caulocystidia.

Types. Holotype: PAKISTAN, Khyber Pakhtunkhwa province, district Upper Dir, Kumrat valley, $35^{\circ}32'N$, $72^{\circ}13'E$, 2400 m a.s.l., solitary or sub-gregarious on moisture rich loamy soil, 20 Aug. 2016, M. Kiran & A.N. Khalid, KM86 (LAH35886), GenBank accession MK509768 (ITS). **Paratypes:** *ibid.*, KM85 (LAH35888), GenBank accession number MK509769 (ITS); *ibid.*, FS12 (LAH35887), GenBank accession number MK509770 (ITS).

Etymology. Referring to the pruinose surface of pileus and stipe.

Habitat. On forest floor under mixed conifers.

Description. *Basidiomata* small to medium-sized, *Pileus* 0.5–3.5 cm in diameter, hemispherical, obtusely conic when young, expanding convex to broadly convex with maturity, margin inrolled initially becoming decurved, surface rough, pruinose, yellowish-orange to reddish-brown (7.5YR8/8–2.5YR4/8). *Lamellae* decurrent, sub-distant to distant, regular, broad up to 0.5 cm, forked near margin, light yellowish-orange (10YR,8/3), gill margins even, smooth, lamellulae in 2 tiers, alternating with lamellae. *Stipe* up to 4 cm long, central, pruinose, yellowish-orange to reddish-brown (7.5YR8/8–2.5YR4/8) in colour, rough, with tawny basal mycelium, more or less equal to broader towards base, universal and partial veil absent. Odour and taste not recorded.

Basidiospores [60/3/3], $(11\text{--})15\text{--}19\text{--}(21) \times (4\text{--})4.5\text{--}8\text{--}(8.5) \mu\text{m}$, $avl \times avw = 16.5 \times 6.5 \mu\text{m}$, $Q = (2.2\text{--})2.3\text{--}3.4\text{--}(3.5)$, $avQ = 2.64 \pm 0.43 \mu\text{m}$, pale yellow to pale

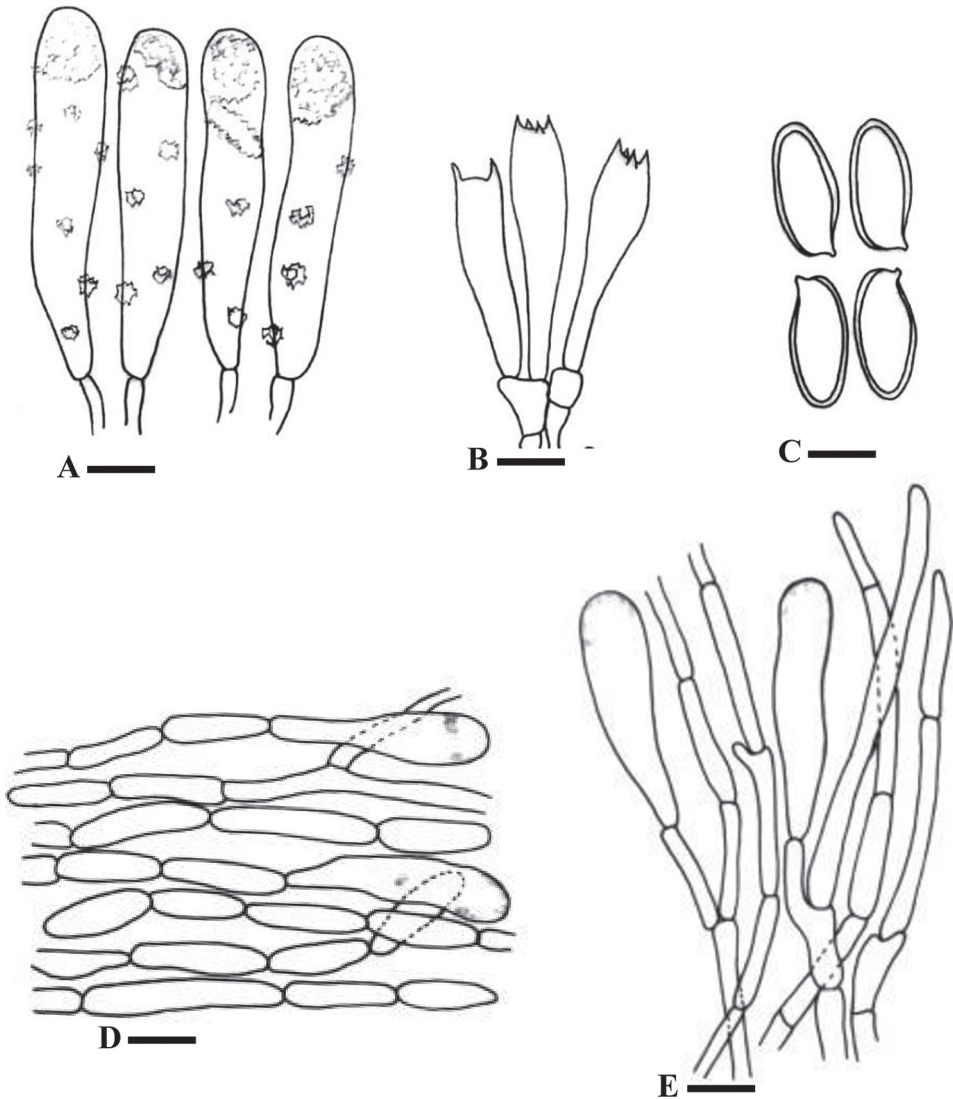


Figure 4. Line drawings of *Chroogomphus pruinosus*. **A** Basidia **B** Cystidia **C** Basidiospores **D** Pileipellis hyphae **E** Stipitipellis hyphae. Scale bars: 17.5 μm (**A**), 12 μm (**B**), 8 μm (**C**), 26.5 μm (**D**), 45 μm (**E**).

grey-brown in KOH, elongate to somewhat ellipsoid, slightly thick-walled, apiculate, dextrinoid, mostly mono-guttulate, germ pore absent. *Basidia* 37–53 \times 7–13 μm , $\text{avl} \times \text{avw} = 41 \times 11 \mu\text{m}$, hyaline in 5% KOH, clavate, clamped at base, four-spored. *Lamellar trama* made up of hyphae, 3–6 μm , yellowish in KOH, encrusted, hyphae inamyloid with no or slightly amyloid encrustations, non-dextrinoid. Pleurocystidia 87–112 \times 15–23 μm , $\text{avl} \times \text{avw} = 93 \times 18 \mu\text{m}$, hyaline with pale yellow walls

in KOH, abundant, encrusted. *Cheilocystidia* similar to pleurocystidia but slightly smaller. *Pileipellis* an ixocutis of radially arranged hyphae, 10–12 µm in diameter, yellow to pale brown in KOH, inamyloid, with thin encrusted walls, cylindrical, septate, clamped. *Pileocystidia* 47–65 × 15–22 µm (avl × avw = 55 × 20 µm), similar to hymenial cystidia, pale yellow to pale brown in KOH. *Pileal trama* composed of yellowish hyphae with brownish encrustation in KOH, 12–20 µm, inamyloid and nondextrenoid. *Stipitipellis* 6–12 µm, pale brown in KOH, inamyloid, straight, cylindrical, smooth and parallel. *Caulocystidia* 37–111.5 × 7–13.6 µm (avl × avw = 76.5 × 10.25 µm), rare, similar to hymenial cystidia.

Notes. *Chroogomphus pruinus* differs from all other members of the genus in having pileocystidia. This new species is phylogenetically most closely related to *C. roseolus*, a species that has been reported from China and Pakistan (Li et al. 2009; Razaq et al. 2016). The macro- and micro-morphology of *C. pruinus* is different from *C. roseolus* in the following characters: *C. pruinus* possesses an obtusely conic to broadly convex, yellowish-orange, pruinose, larger pileus; presence of pileocystidia and caulocystidia in *C. pruinus*; and the pileal and lamellar trama and stipitipellis of *C. pruinus* are inamyloid, whereas those of *C. roseolus* are amyloid or partially amyloid (Li et al. 2009; Razaq et al. 2016). *Chroogomphus helveticus* is another close relative of *C. pruinus* and has also been reported from China and Pakistan (Li et al. 2009; Razaq et al. 2016). However, no herbarium specimens are available for the Pakistani reports of *C. helveticus* (Ahmad et al. 1997) and it is likely that these collections represent *C. roseolus*, as discussed by Razaq et al. (2016). *Chroogomphus roseolus* is an Asian native species, whereas reports of *C. helveticus* have so far only been confirmed in Europe, generally in association with 5-needle pines – mostly *Pinus cembra* (Li et al. 2009), which does not occur in Pakistan. A striking feature of *C. helveticus* is the presence of a pinkish mycelium at the base of the stipe (Li et al. 2009; Razaq et al. 2016; Scambler et al. 2018), which is not observed in *C. pruinus*. *Chroogomphus rutilus* and *C. purpurascens* are morphologically very similar to *C. pruinus*. However, *C. rutilus* has larger basidiomata (20–90 mm) with vinaceous brown or ochraceous-buff to vinaceous red, reddish-brown to purplish, umbonate pileus, buff to yellowish mycelium on the base of the stipe, slightly larger basidiospores (18.0 × 6.2 µm), cylindrical to subfusiform thick walled cystidia and lamellar trama composed of amyloid hyphae (Singer 1949; Miller 1964; Singer and Kuthan 1976; Gerhardt 1984; Breitenbach and Kränzlin 1991; Villarreal and Heykoop 1996; Horak 2005; Li et al. 2009; Scambler et al. 2018). *Chroogomphus purpurascens* is distinguished by a grey to brown then purple pileus that is slightly depressed, an ochraceous stipe, salmon to purple pink mycelium on the base of the stipe, thin-walled cystidia and deeply amyloid pileal trama. Moreover, the species is only known to be in association with *Pinus cembra*, *P. koraiensis* and *P. tabuliformis*, three pine species that are not found in Pakistan (Vassiljeva 1950, 1973; Azbukina 1990; Li et al. 2009). *Chroogomphus tomentosus*, a species that has been reported from Asia (Li et al. 2009), can be distinguished by its larger basidiospores [15–25 × 6–8(9) µm], thick-walled cystidia (2–4 µm) and strongly amyloid lamellar and pileal trama (Miller 1964).

Key to species of *Chroogomphus* reported from Pakistan

- 1 Pileipellis hyphae non-gelatinised.....2
 – Pileipellis hyphae gelatinised.....3 **Subgenus *Chroogomphus***
 2 Lamellar trama amyloid, cystidia thick-walled**Subgenus *Floccigomphus***
 – Lamellar trama inamyloid, cystidia thin-walled....4 **Subgenus *Siccigomphus***
 3 Pileus umbonate, ochraceous to vinaceous, Pileipellis hyphae inamyloid.....
 ***Chroogomphus rutilus***
 – Pileus broadly parabolic, bluish-grey to orange, Pileipellis hyphae amyloid ...
 ***Chroogomphus pakistanicus***
 4 Pileal trama amyloid, pileocystidia and caulocystidia absent.....
 ***Chroogomphus roseolus***
 – Pileal trama inamyloid, pileocystidia and caulocystidia present
 ***Chroogomphus pruinus***

Discussion

Many taxa of fungi have recently been described using an integrative approach, combining morphology, DNA data and ecology (e.g. Aime 2004; Singh et al. 2015; Accioly et al. 2019; Jumbam et al. 2019; Sochorová et al. 2019). This was also shown to be a useful approach in the delimitation of species within *Chroogomphus* (Scambler et al. 2018). The genus can be found throughout the Northern Hemisphere with the exception of only one species, *C. papillatus*, which was reported from the Southern Hemisphere by Raithelhuber (1974). There is morphological and molecular evidence of intercontinental distribution for *C. purpurascens* and *C. rutilus*, which both occur in Europe and Asia (Miller and Aime 2001; Li et al. 2009; Martín et al. 2016; Scambler et al. 2018).

Our phylogenetic tree, obtained from ML and BI analyses (Figure 1), is in accordance with Scambler et al. (2018), with the division of the genus into the subgenera *Chroogomphus*, *Floccigomphus* and *Siccigomphus*. Subg. *Chroogomphus* was further subdivided by Scambler et al. (2018) into four sections – sect. *Chroogomphus*, sect. *Confusi*, sect. *Filiformes* and sect. *Fulminei* – and one informal clade, *Vinicolores*. Two identical sequences of *C. pakistanicus* are nested within subg. *Chroogomphus* sect. *Filiformes* and three identical sequences of *C. pruinus* cluster within subg. *Siccigomphus*. In our phylogeny, sect. *Filiformes* is not monophyletic; the position of *C. britannicus* within subg. *Chroogomphus* is unresolved. The other sections are retrieved as monophyletic in our phylogeny with high support: sect. *Chroogomphus* (with *C. orientirutilus*, *C. purpurascens* and *C. rutilus*), sect. *Confusi* (*C. confusus* and *C. mediterraneus*), sect. *Fulminei* (*C. fulmineus* and *C. subfulmineus*) and the informal *Vinicolores* clade (*C. jamaicensis* and *C. vinicolor*).

The subgenera in our phylogenetic analyses are also supported morphologically. Members of clade II fall in subg. *Siccigomphus* found all over the Northern Hemisphere and are similar in having comparatively smaller basidiospores and inamyloid lamellar

trama. They can be distinguished from the members of clade III, which belong to subg. *Chroogomphus* and have a narrow pileipellis and shiny pileus surface and distributed throughout Eurasia, but not in North America. Clade I represents subg. *Floccigomphus*, with members that are found in North America and Asia, but not in Europe and recognised by non-gelatinised pileipellis hyphae and amyloid lamellar trama.

Based on the distinct and well-supported molecular phylogenetic placement of our Pakistani collections in combination with morphological differences with their closest described relatives, we confirm that they represent two new species in the genus *Chroogomphus*.

Acknowledgements

The authors thank María Paz Martín Esteban (Real Jardín Botánico, Departamento de Micología, Madrid, Spain) for support and critically reviewing early drafts of this manuscript, and Zhu L. Yang (Chinese Academy of Sciences, Kunming Institute of Botany, Key Laboratory of Biodiversity and Biogeography, Kunming, China) for providing helpful suggestions. Sincere thanks to the Higher Education Commission (HEC) in Pakistan for providing partial financial support under the National Research Program for Universities (NRPU: 203383/NRPU/R&D/HEC/14/184).

References

- Accioly T, Sousa JO, Moreau P-A, Lécure C, Silva BDB, Roy M, Gardes M, Baseia IG, Martín MP (2019) Hidden fungal diversity from the Neotropics: *Geastrum hirsutum*, *G. schweinitzii* (Basidiomycota, Geastrales) and their allies. *Plos One* 14: e0211388. <https://doi.org/10.1371/journal.pone.0211388>
- Agerer R (1990) Studies on ectomycorrhizae XXIV. Ectomycorrhizae of *Chroogomphus helveticus* and *C. rutilus* (*Gomphidiaceae*, Basidiomycetes) and their relationship to those of *Suillus* and *Rhizopogon*. *Nova Hedwigia* 50: 1–63. <https://doi.org/10.1127/nova.hedwigia/50/1990/1>
- Agerer R (1991) Studies on ectomycorrhizae XXXIV. Mycorrhizae of *Gomphidius glutinosus* and of *G. roseus* with some remarks on *Gomphidiaceae* (Basidiomycetes). *Nova Hedwigia* 53: 127–170.
- Ahmad S, Iqbal SH, Khalid AN (1997) Fungi of Pakistan. Sultan Ahmad Mycological Society of Pakistan, Department of Botany, University of the Punjab, Quaid-e-Azam campus, Lahore, Pakistan.
- Aime MC (2004) Intercompatibility tests and phylogenetic analysis in the *Crepidotus* Sphaerula group complex: concordance between ICGs and nuclear rDNA sequences highlight phenotypic plasticity within Appalachian species. In: Cripps CL (Ed.) *Fungi in forest ecosystems: systematics, diversity, and ecology*. New York Botanical Gardens, New York, 71–80.

- Breitenbach J, Kränzlin F (1991) Pilze der Schweiz. Band 3 Röhrling und Blätterpilze 1. Teil. Switzerland: Verlag Mykologia, 353 pp.
- Chernomor O, Von Haeseler A, Minh BQ (2016) Terrace aware data structure for phylogenomic inference from supermatrices. *Systematic Biology* 65: 997–1008. <https://doi.org/10.1093/sysbio/syw037>
- Dai YC, Tolgor B (2007) Illustration of Edible and Medicinal Fungi in Northeastern China. Beijing: Science Press, 231 pp. [in Chinese]
- Edgar RC (2004) MUSCLE: multiple sequence alignment with high accuracy and high throughput. *Nucleic Acids Research* 32: 1792–1797. <https://doi.org/10.1093/nar/gkh340>
- Fries EM (1836) *Corpus Florarum provincialium suecicae I. Floram Scanicam*. 349 pp. <https://doi.org/10.5962/bhl.title.47083>
- Gardes M, Bruns TD (1993) ITS primers with enhanced specificity for basidiomycetes – application to the identification of mycorrhizae and rusts. *Molecular Ecology* 2: 113–118. <https://doi.org/10.1111/j.1365-294X.1993.tb00005.x>
- Gerhardt E (1984) Pilze. Band 1: Lamellenpilze, Täublinge, Milchlinge und andere Gruppen mit Lamellen. München: BLV Verlagsgesellschaft, 319 pp.
- Hall TA (1999) BioEdit: a user-friendly biological sequence alignment editor and analysis program for Windows 95/98/NT. *Nucleic Acids Symposium Series* 41: 95–98.
- Hoang DT, Chernomor O, Von Haeseler A, Minh BQ, Vinh LS (2017) UFBoot2: improving the ultrafast bootstrap approximation. *Molecular Biology and Evolution* 35: 518–22. <https://doi.org/10.1093/molbev/msx281>
- Horak E (2005) Röhrlinge und Blätterpilze in Europa. Munich: Spektrum Akademischer Verlag, 557 pp.
- Jumbam B, Haelewaters D, Koch RA, Dentinger BTM, Henkel TW, Aime MC (2019) A new and unusual species of *Hericium* (Basidiomycota: Russulales, Hericiaceae) from the Dja Biosphere Reserve, Cameroon. *Mycological Progress* 18: 1253–1262. <https://doi.org/10.1007/s11557-019-01530-1>
- Kalyaanamoorthy K, Minh BQ, Wong TKF, von Haeseler A, Jermin LS (2017) ModelFinder: Fast model selection for accurate phylogenetic estimates. *Nature Methods* 14: 587–589. <https://doi.org/10.1038/nmeth.4285>
- Knudsen H, Taylor A (2012) *Chroogomphus* (Singer) O.K. Miller and *Gomphidius* Fr. In: Knudsen H, Vesterholt J (Eds) *Funga Nordica*, 2nd edn. Nordsvamp, Copenhagen, 198–199.
- Legon NW, Henrici A (2005) Checklist of the British and Irish Basidiomycota. Kew: Royal Botanic Gardens.
- Li YC, Yang ZL, Tolgor B (2009) Phylogenetic and biogeographic relationships of *Chroogomphus* species as inferred from molecular and morphological data. *Fungal Diversity* 38: 85–104.
- Martín MP, Siquier JL, Salom JC, Telleria MT, Finschow G (2016) Barcoding sequences clearly separate *Chroogomphus mediterraneus* (Gomphidiaceae, Boletales) from *C. rutilus*, and allied species. *Mycoscience* 57: 384–392. <https://doi.org/10.1016/j.myc.2016.06.004>
- Miller OK (1964) Monograph of *Chroogomphus* (Gomphidiaceae). *Mycologia* 56: 526–549. <https://doi.org/10.1080/00275514.1964.12018141>

- Miller OK (2003) The *Gomphidiaceae* revisited: a worldwide perspective. *Mycologia* 95: 176–183. <https://doi.org/10.1080/15572536.2004.11833147>
- Miller OK, Aime MC (2001) Systematics, ecology and world distribution in the genus *Chroogomphus* (*Gomphidiaceae*). In: Misra JK, Horn BW (Eds) *Trichomyces* and other fungal groups. Science Publishers, Enfield, New Hampshire, 315–333.
- Munsell Soil Color Charts (1975) Munsell Color Co., Baltimore, Maryland, USA.
- Nguyen L-T, Schmidt HA, Von Haeseler A, Minh BQ (2015) IQ-TREE: A fast and effective stochastic algorithm for estimating maximum likelihood phylogenies. *Molecular Biology and Evolution* 32: 268–274. <https://doi.org/10.1093/molbev/msu300>
- Raithelhuber J (1974) Hongos de la Provincial de Buenos Aires y de la capital federal. Buenos Aires: J. Raithelhuber.
- Razaq A, Ilyas S, Khalid AN (2016) Molecular identification of Chinese *Chroogomphus roseolus* from Pakistani forests, a mycorrhizal fungus, using ITS-rDNA marker. *Pakistan Journal of Agricultural Sciences* 53: 393–398. <https://doi.org/10.21162/PAKJAS/16.2240>
- Scambler R, Niskanen T, Assyov B, Ainsworth AM, Bellanger JM, Loizides M, Moreau PA, Kirk PM, Liimatainen K (2018) Diversity of *Chroogomphus* (*Gomphidiaceae*, *Boletales*) in Europe, and typification of *C. rutilus*. *IMA Fungus* 9: 271–290.
- Shinwari ZK, Rehman M, Watanabe T, Yoshikawa Y (2006) Medicinal and aromatic plants of Pakistan. A Pictorial Guide. Kohat University of Science and Technology, Pakistan.
- Siddiqui MF, Shaikat SS, Ahmed N, Khan NA, Khan IA (2013) Vegetation-Environment relationship of conifer dominating forests of moist temperate belt of Himalayan and Hindu Kush regions of Pakistan. *Pakistan Journal of Botany* 45(2): 577–592.
- Singer R (1949) The genus *Gomphidius* Fries in North America. *Mycologia* 41: 462–489. <https://doi.org/10.1080/00275514.1949.12017792>
- Singer R, Kuthan J (1976) Notes on *Chroogomphus* (*Gomphidiaceae*). *Česká Mykologie* 30: 81–89.
- Singh G, Dal Grande F, Divakar PK, Otte J, Leavitt SD, Szczepanska K, Crespo A, Rico VJ, Aptroot A, da Silva Cáceres ME, Lumbsch HT, Schmitt I (2015) Coalescent-based species delimitation approach uncovers high cryptic diversity in the cosmopolitan lichen-forming fungal genus *Protoparmelia* (Lecanorales, Ascomycota). *Plos One* 10: e0124625. <https://doi.org/10.1371/journal.pone.0124625>
- Sochorová Z, Döbbeler P, Sochor M, van Rooy J (2019) *Octospora conidiophora* (Pyronemataceae) – a new species from South Africa and the first report of anamorph in bryophilous Pezizales. *MycKeys* 54: 49–76. <https://doi.org/10.3897/mycokeys.54.34571>
- Villarreal M, Heykoop M (1996) *Chroogomphus ochraceus* (Kauffman) O.K. Mill., the correct name for *Chroogomphus fulmineus* (R. Heim) Courtec. *Zeitschrift für Mykologie* 62: 205–212.
- Wahab M (2011) Population dynamics and dendrochronological potential of pine tree species of District Dir Pakistan. Ph.D. dissertation. Department of Botany, Federal Urdu University, Karachi, Pakistan.
- White TJ, Bruns TD, Lee SB, Taylor JW (1990) Analysis of phylogenetic relationships by amplification and direct sequencing of ribosomal RNA genes. In: Innis MA, Gelfand DH,

- Sninsky JJ, White TJ (Eds) PCR Protocols: a guide to methods and applications. Academic Press, San Diego, 315–322. <https://doi.org/10.1016/B978-0-12-372180-8.50042-1>
- Xie ZX, Wang Y, Wang B (1986) Illustration of agarics of Changbai Mountains, China. Jilin Scientific and Technology Press, Changchun, 1–288. [in Chinese]
- Yu FQ, Liu PG (2005) Species diversity of wild edible mushrooms from *Pinus yunnanensis* forests and conservation strategies. Biodiversity Science 13: 58–69. [in Chinese] <https://doi.org/10.1360/biodiv.040129>

Supplementary material I

Table S1. Taxa used in molecular phylogenetic analysis with voucher, country, and ITS GenBank accession number

Authors: Munazza Kiran, Ammara Sattar, Khushbakht Zamir, Danny Haelewaters, Abdul Nasir Khalid

Data type: GenBank accession numbers and associated metadata

Copyright notice: This dataset is made available under the Open Database License (<http://opendatacommons.org/licenses/odbl/1.0/>). The Open Database License (ODbL) is a license agreement intended to allow users to freely share, modify, and use this Dataset while maintaining this same freedom for others, provided that the original source and author(s) are credited.

Link: <https://doi.org/10.3897/mycokeys.66.38659.suppl1>

Studies of Neotropical tree pathogens in *Moniliophthora*: a new species, *M. mayarum*, and new combinations for *Crinipellis ticoi* and *C. brasiliensis*

Nicolás Niveiro^{1,2}, Natalia A. Ramírez^{1,2}, Andrea Michlig^{1,2}, D. Jean Lodge³,
M. Catherine Aime⁴

1 Instituto de Botánica del Nordeste (IBONE), Consejo Nacional de Investigaciones Científicas y Tecnológicas (CONICET). Sargento Cabral 2131, CC 209 Corrientes Capital, CP 3400, Argentina **2** Departamento de Biología, Facultad de Ciencias Exactas y Naturales y Agrimensura, Universidad Nacional del Nordeste. Av. Libertad 5470, Corrientes Capital, CP 3400, Argentina **3** Department of Plant Pathology, University of Georgia, Athens, GA 30606, USA **4** Department of Botany & Plant Pathology, Purdue University, West Lafayette, IN, 47907-2054, USA

Corresponding author: Nicolás Niveiro (niconiveiro@gmail.com); D. Jean Lodge (dlodgester@gmail.com);
M. Catherine Aime (maime@purdue.edu)

Academic editor: D. Schigel | Received 22 November 2019 | Accepted 24 February 2020 | Published 30 March 2020

Citation: Niveiro N, Ramírez NA, Michlig A, Lodge DJ, Aime MC (2020) Studies of Neotropical tree pathogens in *Moniliophthora*: a new species, *M. mayarum*, and new combinations for *Crinipellis ticoi* and *C. brasiliensis*. MycoKeys 66: 39–54. <https://doi.org/10.3897/mycokeys.66.48711>

Abstract

The crinipelloid genera *Crinipellis* and *Moniliophthora* (Agaricales, Marasmiaceae) are characterized by basidiomes that produce long, dextrinoid, hair-like elements on the pileus surface. Historically, most species are believed to be saprotrophic or, rarely, parasitic on plant hosts. The primary morphological diagnostic characters that separate *Crinipellis* and *Moniliophthora* are pliant vs. stiff (*Crinipellis*) stipes and a tendency toward production of reddish pigments (ranging from violet to orange) in the basidiome in *Moniliophthora*. Additionally, most species of *Moniliophthora* appear to have a biotrophic habit, while those of *Crinipellis* are predominantly saprotrophic. Recently, several new neotropical collections prompted a morphological and phylogenetic analysis of this group. Herein, we propose a new species and two new combinations: *Moniliophthora mayarum* **sp. nov.**, described from Belize, is characterized by its larger pileus and narrower basidiospores relative to other related species; *Moniliophthora ticoi* **comb. nov.** (= *Crinipellis ticoi*) is recollected and redescribed from biotrophic collections from northern Argentina; and *M. brasiliensis* **comb. nov.** (= *Crinipellis brasiliensis*), a parasite of *Heteropterys acutifolia*. The addition of these three parasitic species into *Moniliophthora* support a hypothesis of a primarily biotrophic/parasitic habit within this genus.

Keywords

Agaricomycotina, fungal taxonomy, Marasmiineae, plant parasites, tropical fungi

Introduction

The crinipelloid genera *Crinipellis* Pat. and *Moniliophthora* H.C. Evans, Stalpers, Samson & Benny are characterized by basidiomes that produce thick-walled, dextrinoid, hair-like terminal cells on the pileus surface (Kerekes and Desjardin 2009). These belong to the Marasmiaceae in a lineage that includes *Marasmius* Fr. and *Chaetocalathus* Singer (Aime and Phillips-Mora 2005; Antonín 2013). *Crinipellis* and *Moniliophthora* appear to be most speciose in the Neotropics (Singer 1976; Kerekes and Desjardin 2009). Only a few authors have studied these genera in the Neotropics, primarily Singer (1942, 1976), who described 41 neotropical species of *Crinipellis*.

Moniliophthora was described by Evans et al. (1978) as an *incertae sedis*, monotypic genus of basidiomycetes, with *M. roreri* (Cif.) H.C. Evans, Stalpers, Samson and Benny, a parasitic fungus of *T. cacao*, as the type. Aime and Phillips-Mora (2005) used a five-locus analysis to place *M. roreri* within the Marasmiaceae (Agaricales), and included two additional species in *Moniliophthora*: *M.* (= *Crinipellis*) *perniciosa* (Stahel) Aime and Phillips-Mora – also a pathogen of cacao – and an unnamed species known only as an endophyte of the grass *Bouteloua* Lag. The authors speculated that other *Crinipellis* species, especially those currently placed in section *Iopodinae* (Singer) Singer, would be found to belong to *Moniliophthora* (Aime & Phillips-Mora, 2005). Subsequent studies have added an additional five species of mushroom-forming agarics to *Moniliophthora*: *M. aurantiaca* Kropp & Albee-Scott (Kropp and Albee-Scott 2012), *M.* (= *Crinipellis*) *canescens* (Har. Takah.) Kerekes & Desjardin (Kerekes and Desjardin 2009), *M.* (= *Crinipellis*) *conchata* (Har. Takah.) Antonín, Ryoo & Ka (Takahashi 2002), *M. marginata* Kerekes, Desjardin & Vikinesw., and *M.* (= *Crinipellis*) *nigrilineata* (Corner) Desjardin & Kerekes (Kerekes and Desjardin 2009). The primary morphological diagnostic characters that separate *Crinipellis* and *Moniliophthora* are pliant vs. stiff (*Crinipellis*) stipes, and a tendency toward production of pink to orange pigments in the basidiome, that do not change to green or olive when treated with KOH or NaOH (*Moniliophthora*). Additionally, many *Moniliophthora* species appear to have a biotrophic habit, including important pathogens of tropical crops such as cocoa (*Theobroma cacao* L.), while those of *Crinipellis* are primarily saprotrophic.

Recent collecting efforts in northern Argentina and within the Mayan Mountains of Belize included two crinipelloid species. One, an orange fungus fruiting copiously from living roots and trunks of three different species of living trees in Argentina was identified as *Crinipellis ticoi*. The other, an orange fungus fruiting gregariously on a dead root in Belize was determined to represent a new species of *Moniliophthora*. Herein we provide updated descriptions, as well as phylogenetic analyses supporting the placement of these and one other former species of *Crinipellis* within *Moniliophthora* as: *M. ticoi* comb. nov., *M. brasiliensis* comb. nov., and *M. mayarum* sp. nov., bringing the total number of known species of *Moniliophthora* to 11.

Methods

Morphological studies

The specimens studied here were collected in Belize (deposited at BRH and CFMR) and from northern Argentina (deposited at CTES). Specimens were described macroscopically according to Largent (1986). Kornerup and Wanscher (1978) colors are followed by chart numbers and letters in parentheses. Capitalized color names are from Ridgway (1912) as reproduced by Smithe (1975), except for Spectrum Orange which was created by Smithe (1975) to fill a gap. Microscopic characters were examined by light microscopy (LM) on a Leica model CME or an Olympus BH-2. All LM images were made with a Leica EC3 incorporated camera from material mounted in 5% KOH and Phloxine (1%), and Melzer's reagent. The measurements were made directly in the LM or through the photographs taken using the software IMAGEJ (Schneider et al. 2012). Microstructures (length and width of spores, basidia, hyphae, pileipellis) were measured using LM. The following notations were used for spore measurement: \bar{x} = arithmetic mean of the spore length and width, with standard deviation (+/-); Q = quotient of length and width indicated as a range of variation; Q_x = mean of Q values; n = number of spores measured, N = number of analyzed basidiomes. All GPS readings were taken on a Garmin eTrex 10, hand-held unit using WGS84 standard. Herbarium abbreviations follow Index Herbariorum (Thiers 2019) and authors' abbreviations follow Kirk and Ansell (1992).

DNA extraction, amplification, and sequencing

Extraction, amplification and sequencing of the new species at CFMR in Madison, WI followed Lindner and Banik (2009). For the other specimens, DNA was extracted from dried basidiomes using the Promega Wizard Genomic DNA Purification Kit (Promega Corp., Madison, WI, USA). Amplification of the internal transcribed spacer (ITS) and large subunit (28S) of the ribosomal DNA repeat follow the methods of Aime and Phillips-Mora (2005). Sequencing of PCR products was conducted at GeneWiz (South Plainfield, NJ, USA). Sequences were manually edited with Sequencher 5.2.3 (Gene Codes Corp., MI, USA) and confirmed via BLAST queries of the NCBI databases (National Center for Biotechnology Information, Bethesda, MD, USA). Collection data and GenBank accession numbers of the specimens used in this study are detailed in Table 1.

Phylogenetic analysis

Initially, sequences derived for this study were analyzed within a dataset (Aime unpubl.) of 612 published and unpublished Marasmiaceae sequences inclusive of all genera in the family (data not shown). Results from preliminary phylogenetic and blast analyses indicated that the Argentina and Belize material both belong within *Moniliophthora*, as does

Table 1. Origin of sequences used in this study.

Taxon	Coll. #	Country	ITS	LSU	Source
<i>Brunneocorticium coryneocarpon</i>	MCA 5784	Guyana	MG717359	MG717347	Koch et al. (2018)
<i>Chaetocalathus liliputianus</i>	MCA 485	Puerto Rico	AY916682	AY916680	Aime and Phillips-Mora (2005)
<i>Chaetocalathus</i> sp.	MCA 2538	Ecuador	AY916686	AY916684	Aime and Phillips-Mora (2005)
<i>Crinipellis</i> sp.	MCA 2240	Guyana	MG717367	AY916695	Koch et al. (2018) (ITS); Aime and Phillips-Mora (2005) (LSU)
<i>Crinipellis</i> sp.	MCA 1527	Guyana	AY916701	AY916699	Aime and Phillips-Mora (2005)
<i>Marasmius</i> sp.	MCA 1708	Guyana	AY916720	AY916718	Aime and Phillips-Mora (2005)
<i>Marasmius</i> sp.	MCA 7492	Cameroon	MG717368	MG717354	Koch et al. (2018)
<i>Marasmius rotula</i>	PBM2563	USA	DQ182506	DQ457686	Matheny et al. (2006a) (ITS); Matheny et al. (2006b) (LSU)
<i>Moniliophthora aurantiaca</i>	UTC253824 ^T	American Samoa	JN692482	JN692483	Kropp and Albee-Scott (2012)
<i>Moniliophthora brasiliensis</i>	UB2053	Brazil	AY317137	–	Arruda et al. (2005)
<i>Moniliophthora canescens</i>	DED 7518	Malaysia	FJ167668	–	Kerekes and Desjardin (2009)
<i>Moniliophthora mayarum</i>	DJL BZ511 ^T	Belize	MT162718	MT162714	This paper
<i>Moniliophthora pernicioso</i>	MCA 2520	Ecuador	AY916743	AY916742	Aime and Phillips-Mora (2005)
<i>Moniliophthora roreri</i>	MCA 2953	Mexico	DQ222925	DQ222926	Phillips-Mora et al. (2006a)
<i>Moniliophthora roreri</i>	MCA 2954	Belize	DQ222927	DQ222928	Phillips-Mora et al. (2006b)
<i>Moniliophthora</i> sp.	MCA 2500	USA	AY916754	AY916752	Aime and Phillips-Mora (2005)
<i>Moniliophthora</i> sp.	MCA 2501	USA	MT162719	MT162715	This paper
<i>Moniliophthora ticoi</i>	NY00511157 ^T	Bolivia	MT162721	MT162717	This paper
<i>Moniliophthora ticoi</i>	Niveiro 2249	Argentina	MT162720	MT162716	This paper
<i>Tetrapyrgos nigripes</i>	MCA 6925	USA	MG717370	MG717355	Koch et al. (2018)

T = type material

Crinipellis brasiliensis – the sister species to *M. pernicioso* (Arruda et al. 2005). Datasets were then trimmed to include: 1) all species of *Moniliophthora* for which ITS and/or 28S sequence data exist (only ITS data were available for *M. canescens*, *M. aurantiaca*, and *M. brasiliensis*); 2) newly generated sequences of the material from Argentina and Belize and from the type of *C. ticoi*; 3) exemplar sequences from the other related Marasmiaceae genera – *Crinipellis*, *Marasmius*, and *Chaetocalathus* – for context (Aime and Phillips-Mora 2005; Antonín et al. 2014; Koch et al. 2018). Individual datasets for each locus were aligned in GENEIOUS 9.1.5 (Biomatters Ltd., Auckland, NZ) using the MUSCLE algorithm (Edgar 2004). Individual alignments were then concatenated in Geneious, and analyzed by maximum likelihood (RAXML; Stamatakis 2006) methods using the CIPRES Science Gateway (Miller et al. 2010), following the methods of Koch et al. (2018).

Results

Phylogenetic analyses

Based on our Maximum Likelihood (ML) analysis of ITS and 28S rDNA, Marasmiaceae is comprised of two clades, *Marasmius* + *Crinipellis* + *Moniliophthora* +

4–6 μm). Differs from *M. ticoi* by smaller basidiospores (8.0 \pm 1.3 \times 3.8 \pm 0.3 μm vs 12.1 \pm 0.8 \times 5.4 \pm 0.4 μm).

Type. Belize, Stann Creek District, Cockscomb Basin Wildlife Sanctuary, Jaguar Preserve, near Maya Center Community, Rubber Tree Trail, on dead tree roots, possibly *Ceiba pentandra*, 16°42'58.32"N, 88°39'38.88"W, 180 m a.s.l., 16. 11. 2001, D.J.Lodge, K.K.Nakasone, S.Schmeiding, E.Gaitlan BZ-43-Nov-2001, BZ-511 (**Holotype:** CFMR!)

Description. *Pileus* 7–20 mm, convex with an inrolled margin when young, broadly convex with age, some slightly depressed at center, some with a papillate umbo, color Chrome Orange (Plate II, 11, -), with center Scarlet (Plate I, 5, -) to Flame Scarlet (Plate II, 9, -), surface moist or slightly viscid when wet but not gelatinized, smooth, rarely sparsely minutely pubescent on umbo when dry, margin translucent-striate to disc, some sulcate-striate with age. *Lamellae* subdistant, 2 per mm on margin and half-way to margin, adnate or slightly adnexed, 2–4 mm broad, regular, 1 or more lengths of lamellulae inserted, Spectrum Orange with a coral tint, margin even, concolorous. *Stipe* central, 12–27 \times 0.8–1.2 mm, equal or slightly clavate, some flared at apex, pale Spectrum Orange, pale Orange-Yellow (Plate III, 17, f) at apex, surface dry, densely minutely pubescent, dense Warm Buff (Plate XV, 17', d) mycelial pad at base. *Annulus* absent. *Spore-print* not observed, presumably white. *Context* pale orange in pileus and stipe, odor none, taste sweet. KOH and NaOH reactions on pileus surface negative.

Basidiospores on lamellae of two sizes, larger ones 6.5–8.5(–10.5) \times 3.2–4.2 μm , $x = 8.0 \pm 1.3 \times 3.8 \pm 0.3 \mu\text{m}$, $Q = 1.60\text{--}2.65$, $Q_x = 2.02 \pm 0.3$, $n = 14$; smaller spores 4–6 \times 2.4–4.2 μm , $x = 5.2 \pm 0.8 \times 3.3 \pm 0.6 \mu\text{m}$, $Q = 1.25\text{--}1.89$, $Q_x = 1.60 \pm 0.3$, $n = 10$. *Basidia* 4-sterigmate, 14.4–28 \times 4–8 μm , sterigmata up to 6.4 μm long, with basal clamp connections. *Pleurocystidia* absent. *Cheilocystidia* 22–26.5 \times 6–13 μm , of three types: 1) clavate or hyphoid, 2) with 2–3 lobes, 3) clavate with apical digitate appendages or irregular lumps overall. *Hymenophoral trama* regular, hyphae 2.6–5.2 μm diameter, smooth, thin-walled, not dextrinoid, with clamp-connections. *Pileipellis* a cutis of repent, more or less interwoven hyphae, 4–8 μm broad, thin-walled ones occasionally with incrustated rusty pigments, apical segments of some hairs thick-walled and dextrinoid. *Hairs of the pileus surface* setiform, dextrinoid thick-walled part (66–)86–240 \times (4.8–)5.1–8.2 μm , comprised of 1–3 segments dextrinoid, walls (1.4–)2–4 μm thick, hyphae sometimes almost occluded, septa usually with clamp connections but clamp connections absent on the few secondary septations, with obtuse or acute apex. *Hypodermium* of short, broad, thin-walled cells 21.6–24 \times 16–17.5 μm , with basal clamp connections.

Distribution. Known only for the type locality.

Ecology. Gregarious, putatively parasitic on roots of a tree, possibly *Ceiba pentandra* (L.) Gaertn.

Etymology. mayarum – of the Maya people in the region where the fungus was found.

Specimens studied. BELIZE • Stann Creek District, Cockscomb Basin Wildlife Sanctuary, Jaguar Preserve, near Maya Center Community, Rubber Tree Trail, on dead tree roots, possibly *Ceiba pentandra*; 16°42'58.32"N, 88°39'38.88"W, 180 m a.s.l.; 16.XI.2001; D.J.Lodge, K.K.Nakasone, S.Schmeiding, E.Gaitlan BZ-43-Nov-2001, BZ-511 (**Holotype:** CFMR!; **Isotype** BRH!).



Figure 2. Photographs of sister species, *Moniliophthora mayarum* and *M. ticoi*: **A** basidiomes of *M. mayarum* on piece of tree root in Belize (BZ-511) (photo by S. Schmeiding) **B–F** Basidiomes of *M. ticoi* on trunks of *Holocalix balansae* (Fabaceae) and *Pogonopus tubulosus* (Rubiaceae) in Argentina. Scale bars: 10 mm.

Observations. Few previously described *Crinipellis* and *Moniliophthora* species share the striking bright orange coloration of *M. mayarum*. This taxon most closely resembles *M. aurantiaca* Kropp & Albee-Scott described from the South Pacific island of Samoa, *Crinipellis hygrocyboides* (Henn.) Singer (= *Marasmius hygrocyboides* Henn.) described by Hennings from Africa, and *M. ticoi* (Halling) Niveiro, Ramírez, Lodge & Aime described from South America. Our phylogenetic analysis places *M. mayarum* as a sister species to *M. ticoi*—the other Neotropical species in this complex.

The two Neotropical species are more robust, reaching 20 mm in diameter (or more in *M. ticoi*), compared to the two Paleotropical species, 6–11 mm in *C. hygrocyboides* and 3–15 mm in *M. aurantiaca*. Antonín (2007) published a type revision of *C. hygrocyboides* based on study of an isotype that included microscopic meas-

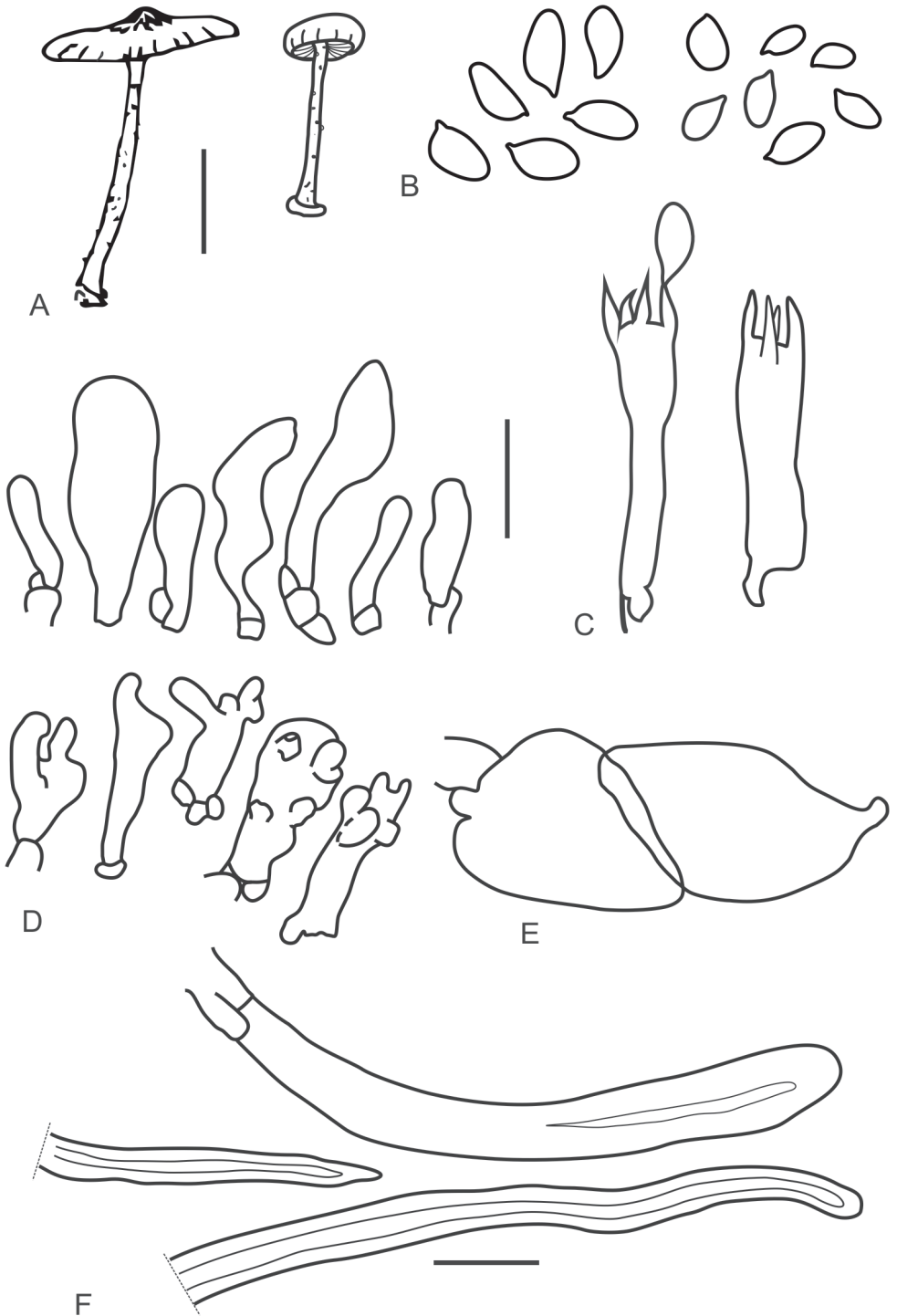


Figure 3. *Moniliophthora mayarum*: **A** basidiomes **B** basidiospores **C** basidium **D** cheilocystidia **E** hypodermium cells **F** pileipellis elements. Scale bars: 10 mm (**A**); 10 μm (**B–F**).

urements and observations of spores and cheilocystidia as neither Hennings (1902) nor Singer (1989) included these details and Halling (1993) reported he could not find spores or cystidia in the type. The spores of *M. mayarum* are distinctly narrower (3.2–4.2 μm) than those of *C. hygrocycoides* [4.5–6(–7) μm]. While Antonín's description of the cheilocystidia in *C. hygrocycoides* notes they are ornamented with apically branched obtuse projections, cheilocystidia shape seems to be highly variable and therefore unreliable for distinguishing species in this group. The basidiospores are longer and broader in both *M. aurantiaca* 7.5–11 \times 4–6, and *M. ticoi* (9.5–)10.5–13.7 \times (3.8–)4.5–6.3 μm , than in *M. mayarum* 6.5–8.5(–10.5) \times 3.2–4.2 μm . Only the larger spores of *M. mayarum* are used in the preceding comparison, and it is not clear why there is a cohort of smaller basidiospores also present. Although, different spore sizes are often observed in the presence of bisporic basidia, lacking clamp-connection and bearing larger spores that are mixed with tetrasporic basidia bearing smaller spores, in repeated examination of the material specifically looking for 2-sterigmate basidia and absence of basal clamps, we observed only 4-sterigmate basidia, and all hymenial elements with clamp-connections. Furthermore, one of the illustrated 4-spored basidia (Fig. 3C), shows a large spore attached to a 4-sterigmate basidium with a basal clamp connection, which negates the hypothesis of a bisterigmate origin for the large spore cohort in *M. mayarum*. Although small spores observed on the hymenium could have been immature and thus smaller, basidiospores of similar size and shape were observed on the pileipellis surface that must have been released from basidia, which indicates they were mature. A similar case occurs in *Crinipellis trinitatis* Dennis. Dennis (1951) in the original description reported smaller basidiospores (5–7 \times 2–4 μm) than the revised description of the type by Pegler (1983) (7–9 \times 4.1–5.1 μm), so there may be something unusual in the phenology of spore production in this group that leads to two size classes of spores depending on when they are formed and released.

New combinations

***Moniliophthora brasiliensis* (Arruda, G.F.Sepúlveda, R.N.G.Miller, M.A.Ferreira & M.S.Felipe) Niveiro, Lodge & Aime, comb. nov.**

Mycobank No: 830320

Genbank No: AY317137

≡ *Crinipellis brasiliensis* Arruda, G.F.Sepúlveda, R.N.G.Miller, M.A.Ferreira & M.S.Felipe, *Mycologia* 97: 1355 (2006). Type: Brazil. Minas Gerais, Itumirim. On dry fan brooms of *Heteropterys acutifolia* A.Dr. Juss., 19 Oct 1999, MCC de Arruda 43 [Holotype: UB (Mycol. Col.) 19198].

Distribution. This species is known from Minas Gerais, Brazil (Arruda et al. 2005).

Observations. *Moniliophthora brasiliensis* is characterized by the light pink to crimson red pileus surface, ellipsoidal basidiospores, 10–14 \times 5–7 μm , and lageniform

cheilocystidia, with a thin apex, $28\text{--}37 \times 10\text{--}16 \mu\text{m}$ in size (Arruda et al. 2005). *Moniliophthora brasiliensis* is a parasite of *Heteropterys acutifolia* (Malpighiaceae). Only ITS sequence data are available for this taxon, which was derived from a dikaryotic basidiome collected from a necrotic broom on *H. acutifolia* (Arruda et al. 2005). *Moniliophthora brasiliensis* is extremely similar to *M. pernicioso* and diagnosis between the two species at present is based solely on differences in ITS sequence data (Arruda et al. 2005).

***Moniliophthora ticoi* (Halling) Niveiro, Ramírez, Lodge & Aime, comb. nov.**

Mycobank No: 830321

Genbank No: ITS: MT162721, MT162720. LSU: MT162717, MT162716.

Figs 2B–F, 4A–D

≡ *Crinipellis ticoi* Halling, Mycotaxon 47: 379 (1993). Type: Bolivia. Beni, Iturralde, S of Rurrenabaque, Rio Tuichi near junction with Rio Beni, “Laguna del Tigre”, $14^{\circ}25'S$, $67^{\circ}30'W$, 14 Apr 1990, R.Halling 6433 (Isotype: NY!).

Description. *Pileus* 7–40(–62) mm, parabolic to convex when young, convex to plane with age, with a shallow umbilicus, surface bright orange (7A8–8A8) with reddish to dark brown center (7C7–7C8), with a narrow light yellowish margin (6A7–6B7 to near 5A6–5A7), dry or moist but not hygrophanous, tomentose or subtomentose in disc, pubescent margin in young specimens, striate disc in young specimens, more marked at the margin, in mature or driest basidiomes with reddish to dark brown sulcate margin (7C8–8C8). *Lamellae* subdistant, 1 per mm, adnexed to narrowly adnate, thick and broad, not intervenose, concolorous with the pileus surface (7A8–6A8); edge entire, concolorous with sides, with 2 tiers lamellulae inserted. *Stipe* 18–68 \times 1–3.5 mm, central, cylindrical, equal or slightly thinner towards the middle, sometimes with a small basal bulb, solid, surface orange to reddish (7A7–7A8) in young specimens, light orange, yellowish orange to creamy yellow (5A6–5A7 to 4A8) and brown (6D8–6D7) toward base in older specimens, densely pubescent at apex when young, then fibrillose-pruinose, dry, insititious. *Annulus* absent, but forming a strongly pubescent zone where the veil is inserted in young specimens. *Spore-print* not observed, presumably white. *Context* pale orange (5A5) in pileus, thin, fleshy in the center and membranous towards the margins, orange white (5A2) in stipe. Odor and taste not tested. KOH and NaOH reactions on pileus surface negative.

Basidiospores (9.5–)10.5–13.7 \times (3.8–)4.5–6.3 μm , $x = 12.1 \pm 0.8 \times 5.4 \pm 0.4 \mu\text{m}$; $Q = 2.11\text{--}2.67$; $Q_x = 2.38 \pm 0.1$; $n = 60$; $N = 2$; oblong to subcylindrical, phaseoliform in side view, thin-walled, smooth, hyaline, inamyloid, without germ-pore. *Basidia* 34.3–58 \times 7.7–8.6 μm , subcylindrical to narrowly clavate, 4-spored. *Pleurocystidia* absent. *Cheilocystidia* 32–43 \times 7–10 μm , subcylindrical to narrowly clavate, inconspicuous, thin-walled, smooth, hyaline. *Hymenophoral trama* subregular, hyphae 40–150 \times 5–12 μm , smooth, thin-walled, with clamp-connections. *Pileipellis* a cutis of repent, more or less interwoven hyphae, 4–15 μm broad, occasionally with

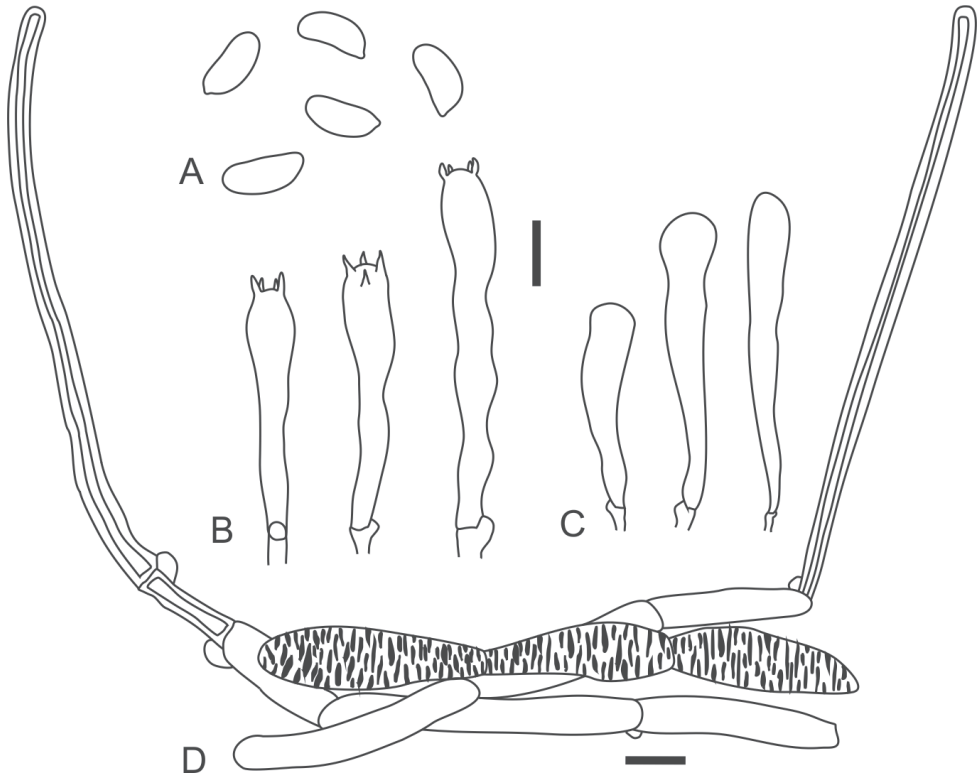


Figure 4. *Moniliophthora ticoi*: **A** spores **B** basidia **C** cheilocystidia **D** pileipellis elements. Scale bars: 10 μ m.

incrusted pigments, covered by clusters of dextrinoid hairs and chains of thin-walled monilioid, inamyloid hyphae. **Hairs of the pileus surface** setiform, scattered on the surface, distributed mainly towards the margin, arising from a pileipellis, 90–560 \times 4.5–9 μ m, dextrinoid, thick-walled, hyphal walls 1.5–3 μ m diam, with basal clamp-connection, occasionally 1 or 2 septate, with obtuse apex. **Stipitipellis** a cutis of repent hyphae, 6–10 μ m broad, with abundant dextrinoid hairs, 40–370 \times 5–10 μ m, setiform, thick-walled, with obtuse apex, basal clamp-connections.

Distribution. This species is known from Bolivia (Halling 1993) and northern Argentina (Yungas and Chaco region).

Ecology. Gregarious. Parasitic on living roots and trunks of *Myrcianthes pungens* (O.Berg) D.Legrand, (Myrtaceae) *Holocalix balansae* Micheli (Fabaceae) and *Pogonopus tubulosus* (A.Rich.) K-Schum (Rubiaceae), in tropical and subtropical forest.

Specimens studied. ARGENTINA • Chaco, 1° de Mayo, Colonia Benitez Educational Reserve, interpretative trail; 27°19'04.12"S, 058°56'59.58"W, 64 m a.s.l.; on Guabiyú (*Myrcianthes pungens* – Myrtaceae) trunk and roots; 21.III.2014; N.Ramírez & N.Niveiro CB 23-65 (CTES). • Ibid., on trunk and roots of Alecrín (*Holocalix balansae* – Fabaceae); 22.III.2016; N.Ramírez & N.Niveiro 103, 105 (CTES). • Jujuy, Ledesma, Calilegua National Park, Guarani trail; 23°45'66.1"S, 064°51'15.0"W,

627 m a.s.l.; on montane forest, on *Pogonopus tubulosus* (Rubiaceae); 24.III.2011; N.Niveiro, E.Albertó, B.Lechner & T.Baroni 2249 (CTES). BOLIVIA • Beni, Iturralde, S of Rurrenabaque, Rio Tuichi near junction with Rio Beni, “Laguna del Tigre”; 14°25'S, 067°30'W; 14.IV.1990; R.Halling 6433 (**Isotype**: NY00511157!).

Observations. This species was described by Halling (1993) from Bolivian specimens. It is characterized by its relatively large, bright orange basidiomes, covered with scattered dextrinoid setiform hairs. The most similar species is *M. mayarum*, which shares morphological characters such as the large basidiomes with bright orange coloration. These two species, however, differ clearly by the smaller spores and by the presence of ornamented cheilocystidia in *M. mayarum*. Another similar species is *M. aurantiaca* from American Samoa (Kroop and Albee-Scott 2012). Both share the orange colored pileus surface with a narrow light yellowish margin. However, they differ in that *M. aurantiaca* has the smaller pileus (3–15 mm broad), smaller basidiospores ($7.5\text{--}11 \times 5\text{--}8 \mu\text{m}$) and numerous cheilocystidia with several irregular apical appendages resembling fingers (Kroop and Albee-Scott 2012). Another similar species is *C. hygrocyboides* (Henn.) Singer from Africa (Singer 1989), however this is a smaller fungus (pileus 6–11 mm broad) with an umbilicate to papillate pileus that is pilose at the margin (Halling 1993). Based on its morphological characters such as the bright orange pileus surface, *C. hygrocyboides* could be included in the genus *Moniliophthora*, but new collections are needed to elucidate its habitat and to obtain sequences and corroborate this hypothesis (currently there are not sequences available for *C. hygrocyboides*).

Other known parasitic Neotropical species are *M. perniciosa*, *C. trinitatis* Dennis and *C. siparunae* Singer. *Moniliophthora perniciosa*, a destructive parasite of *Theobroma cacao*, differs in having smaller basidiomes (pileus up to 25 mm diam) with a red pileus surface and white stipe (Singer 1976; Aime and Phillips-Mora 2005). *Crinipellis trinitatis* has a smaller, red pileus and smaller spores [$5\text{--}7 \times 2\text{--}4 \mu\text{m}$ ss. Dennis (1951) and $7\text{--}9 \times 4\text{--}5 \mu\text{m}$ ss. Pegler (1983)].

Crinipellis siparunae is a widely distributed species that is microscopically similar to *M. ticoi*, especially regarding the range of spore size. However, *C. siparunae* is distinguished by its lilac to brownish lilac pileus surface and by its appendiculate cheilocystidia (Singer 1942, 1976). A taxon thought to be closely related to *C. siparunae*, *C. eggersii* Pat. var. *lilaciceps* Singer and described from Amazonian Ecuador shares unornamented cheilocystidia with *C. ticoi*, but it differs from the latter in having a violet to lilac vs orange pileus, and broader basidiospores $6\text{--}6.5 \times (3.8\text{--})4.5\text{--}6.3 \mu\text{m}$ (Singer 1976; Kerekes and Desjardin 2009). *Crinipellis eggersii* var. *eggersii*, which includes the facultative synonym *Marasmius vinosus* Speg. described from Argentina, has similar spore dimensions (mostly $11\text{--}13 \times 5.5\text{--}6.3 \mu\text{m}$) but differs in having a purple to violet purple pileus and a variety of cheilocystidia shapes (ampullaceous, fusiform, cylindrical or clavate and mostly forked, obtuse or mucronate, sometimes with a subcapitate or capitate apex).

Of the three recent collections in northern Argentina, the specimens of the Yungas forest (Niveiro et al. 2249) closely resemble the original description of *M. ticoi*, with specimens not exceeding 40 mm broad and having a bright red pileus surface (Halling 1993). However, the specimens of the Chaco region differ in having larger basidiomes up to 60 mm broad, and a paler coloration (orange with a yellowish margin), differ-

ences that may be due to the drier weather conditions in the Chaco region. Another important difference observed in the Argentinean specimens is the habitat. Halling (1993) found this species growing on rotten wood, however, the new specimens examined were growing on tree trunks and roots of living trees, confirming a biotrophic habit for this species during at least part of its life history.

Key to striking bright orange *Moniliophthora* and *Crinipellis* species

- 1 Biotrophic habit, on diverse hosts. Pileus more than 20 mm diam. Neotropical distribution..... **2**
- Saprotrophic habit. Pileus less than 20 mm diam. Paleotropical distribution ... **3**
- 2 Spores $8.0 \pm 1.3 \times 3.8 \pm 0.3 \mu\text{m}$, cheilocystidia clavate or hyphoid, or with 2–3 lobes, or clavate with apical digitate appendages or irregular lumps overall *M. mayarum*
- Spores larger, $12.1 \pm 0.8 \times 5.4 \pm 0.4 \mu\text{m}$, cheilocystidia simple, inconspicuous, subcylindrical to narrowly clavate, thin-walled, smooth, hyaline *M. ticoi*
- 3 Stipitipellis covered by short and moderately thick-walled hairs, resembling setae, $52\text{--}85 \times 5\text{--}10 \mu\text{m}$ *M. aurantiaca*
- Stipitipellis covered with larger ($48\text{--}180 \times 12\text{--}18 \mu\text{m}$), cylindrical to clavate, thick-walled (up to $3.0 \mu\text{m}$), slightly dextrinoid hairs *C. hygrocybioides*

Discussion

The addition of these three parasitic species into *Moniliophthora* support a hypothesis of a primarily biotrophic/parasitic habit in this lineage of Marasmiaceae. However, nutritional strategies for several species not studied in the present work remain to be definitively ascertained: *M. aurantiaca* was found on woody debris (Kropp and Albee-Scott 2012); *M. conchata* on dead twigs of the liana *Trachelospermum asiaticum* (Siebold et Zucc.) Nakai. (Takahashi 2002) and on fallen twigs of an unidentified liana (Antonín et al. 2014); *M. canescens* on a dead fallen twig of a broad-leaved tree (the Type specimen) and on undetermined dicotyledonous plants (Kerekes and Desjardin 2009); *M. marginata* on undetermined decaying woody stem (Kerekes and Desjardin 2009); and in *M. nigrilineata* the substrate was not specified (Kerekes and Desjardin 2009).

Purple, violet, and red pigments in the pileus combined with a negative (not greenish) reaction with KOH distinguish *Crinipellis* section *Iopodinae* (Singer 1976), and these characters are shared with the known basidiome-producing species of *Moniliophthora*. Although no recent collections or sequences are available for other species of *Crinipellis* section *Iopodinae*, Kerekes and Desjardin (2009) did show that a specimen identified as *C. aff. iopus* Singer (the type species of *Crinipellis* sect. *Iopodinae*) belonged in *Moniliophthora*, although due to a lack of data they were unable to confirm this placement. The current study adds striking orange pigmentation to the suite of characteristics for *Moniliophthora*, as well as confirming a biotrophic habit for the majority of species.

Acknowledgments

This research was possible thanks to the support of Secretaría General de Ciencia y Técnica, Universidad Nacional del Nordeste (SGCyT-UNNE - PI15-P003) and the Consejo Nacional de Investigaciones Científicas y Técnicas (CONICET) from Argentina (PIP 2014-0714). Collecting in Belize was supported by a National Science Foundation, Biotic Surveys and Inventory Program award to the State University of New York, College at Cortland (DEB0103621) in a joint venture agreement with CFMR at the USDA Forest Service, Forest Products Laboratory. The authors thank the Administración de Parques Nacionales (APN) for collection permits in Argentina, the Belize Forestry Department for collecting permits in Belize, and Dr. Roy Halling for facilitating access to the holotype of *M. ticoi*. The Department of Plant Pathology at the University of Georgia in Athens, GA, USA covered publication costs. The manuscript was improved by suggestions from V. Antonín and an anonymous reviewer.

References

- Aime MC, Phillips-Mora W (2005) The causal agents of witches' broom and frosty pod rot of cacao (chocolate, *Theobroma cacao*) form a new lineage of Marasmiaceae. *Mycologia* 97: 1012–1022. <https://doi.org/10.3852/mycologia.97.5.1012>
- Antonín V (2007) Fungus flora of tropical Africa. Vol. 1. Monograph of *Marasmius*, *Gliocephala*, *Palaeocephala* and *Setulipes* in tropical Africa. Meise Botanical Garden. <https://www.ffa-online.org/ffa1/>
- Antonín V (2013) Fungus flora of tropical Africa. Vol. 3. Monograph of *Crinipellis* and *Chaetocalathus* in tropical Africa. Meise Botanical Garden. <https://www.ffa-online.org/ffa3/>
- Antonín V, Ryoo R, Ka KH, Sou HD (2014) Three new species of *Crinipellis* and one new variety of *Moniliophthora* (Basidiomycota, Marasmiaceae) described from the Republic of Korea. *Phytotaxa* 170: 86–102. <https://doi.org/10.11646/phytotaxa.170.2.2>
- Arruda MCC, Sepuvela GF, Miller RNG, Ferreira MASV, Santiago DVR, Resende MLV, Dianese JC, Felipe MSS (2005) *Crinipellis brasiliensis*, a new species based on morphological and molecular data. *Mycologia* 97: 1378–1361. <https://doi.org/10.3852/mycologia.97.6.1348>
- Dennis RWG (1951) Some Agaricaceae from Trinidad and Venezuela. *Leucosporae: Part 1. Transactions of the British Mycological Society* 34: 411–482. [https://doi.org/10.1016/S0007-1536\(51\)80030-5](https://doi.org/10.1016/S0007-1536(51)80030-5)
- Diaz-Valderrama JR, Aime MC (2016a) The cacao pathogen *Moniliophthora roreri* (Marasmiaceae) possesses a tetrapolar mating system but reproduces clonally. *Heredity* 116: 491–501. <https://doi.org/10.1038/hdy.2016.5>
- Diaz-Valderrama JR, Aime MC (2016b) The cacao pathogen *Moniliophthora roreri* (Marasmiaceae) produces rhexolytic thallic conidia and their size is influenced by nuclear condition. *Mycoscience* 57: 208–216. <https://doi.org/10.1016/j.myc.2016.01.004>
- Edgar RC (2004) MUSCLE: multiple sequence alignment with high accuracy and high throughput. *Nucleic Acids Research* 32: 1792–1797. <https://doi.org/10.1093/nar/gkh340>

- Evans HC, Stalpers JA, Samson RA, Benny GL (1978) On the taxonomy of *Monilia roveri*, an important pathogen of *Theobroma cacao* in South America. *Canadian Journal of Botany* 56(20): 2528–2532. <https://doi.org/10.1139/b78-305>
- Halling R (1993) Two new Crinipellinae (Tricholomataceae: Marasmiaceae) from South America. *Mycotaxon* 47: 379–385.
- Hennings P (1902) Fungi camerunensis novi. III. *Botanische Jahrbücher für Systematik* 30: 39–57.
- Kerekes JF, Desjardin DE (2009) A monograph of the genera *Crinipellis* and *Moniliophthora* from Southeast Asia including molecular phylogeny of the nrITS region. *Fungal Diversity* 37: 101–151.
- Kirk PM, Ansell AE (1992) Authors of fungal names. Index of Fungi supplement. <http://www.indexfungorum.org/AuthorsOfFungalNames.htm>
- Koch RA, Lodge DJ, Sourell S, Nakasone K, McCoy AG, Aime MC (2018) Tying up loose threads: revised taxonomy and phylogeny of an avian-dispersed Neotropical rhizomorph-forming fungus. *Mycological Progress* 17: 989–998. <https://doi.org/10.1007/s11557-018-1411-8>
- Kornerup A, Wanscher JH (1978) *Methuen handbook of colour*. 3rd edn., Eyre Methuen, 1–252.
- Kropp BR, Albee-Scott S (2012) *Moniliophthora aurantiaca* sp. nov., a Polynesian species occurring in littoral forest. *Mycotaxon* 120: 493–503. <https://doi.org/10.5248/120.493>
- Largent DL (1986) *How to identify mushrooms to genus I: macroscopic features*. 3rd edn. Mad River Press, 1–166.
- Lindner DL, Banik MT (2009) Effects of cloning and root-tip size on observations of fungal ITS sequences from *Picea glauca* roots. *Mycologia* 101: 157–165. <https://doi.org/10.3852/08-034>
- Matheny PB, Curtis JM, Hibbett DS (2006a) Assembling the fungal tree of life. NCBI GenBank. <https://www.ncbi.nlm.nih.gov/genbank/> [Accessed 4 June 2018]
- Matheny PB, Curtis JM, Hofstetter V, Aime MC, Moncalvo JM, Ge ZW, Slot JC, Ammirati JF, Baroni TJ, Bougher NL, Hughes KW, Lodge DJ, Kerrigan RW, Seidl MT, Aanen DK, DeNitis M, Daniele GM, Desjardin DE, Kropp BR, Norvell LL, Parker A, Vellinga EC, Vilgalys R, Hibbett DS (2006b) Major clades of Agaricales: a multilocus phylogenetic overview. *Mycologia* 98: 982–995. <https://doi.org/10.1080/15572536.2006.11832627>
- Miller MA, Pfeiffer W, Schwartz T (2010) Creating the CIPRES Science Gateway for inference of large phylogenetic trees. *Proceedings of the Gateway Computing Environments Workshop (GCE)*, New Orleans, LA, 1–8. <https://doi.org/10.1109/GCE.2010.5676129>
- Pegler DN (1983) *Agaric Flora of the Lesser Antilles*. *Kew Bulletin Additional Series* 9: 1–668.
- Phillips-Mora W, Cawich J, Garnett W, Aime MC (2006a) First report of frosty pod rot (moniliasis disease) caused by *Moniliophthora roveri* on cacao in Belize. *Plant Pathology* 55: 584. <https://doi.org/10.1111/j.1365-3059.2006.01378.x>
- Phillips-Mora W, Coutino A, Ortiz CF, Lopez AP, Hernandez J, Aime MC (2006b) First report of *Moniliophthora roveri* causing frosty pod rot (moniliasis disease) of cocoa in Mexico. *Plant Pathology* 55: 584. <https://doi.org/10.1111/j.1365-3059.2006.01418.x>
- Ridgway R (1912) *Standards and color nomenclature*. The author, 1–43.
- Ronquist F, Teslenko M, Van Dermark P, Ayres DL, Darling A, Höhna S, Larget B, Liu L, Suchard MA, Huelsenbeck JP (2012) MrBayes 3.2: efficient Bayesian phylogenetic inference and model choice across a large model space. *Systematic Biology* 61: 539–542.

- Singer R (1942) A monographic study of the genera *Crinipellis* and *Chaetocalathus*. Lilloa 8: 441–533.
- Singer R (1976) Marasmieae (Basidiomycetes – Tricholomataceae). Flora Neotropica 17: 1–347.
- Singer R (1989) New taxa and new combinations of Agaricales (Diagnoses fungorum novorum agaricalium IV). Fieldiana, Botany 21: 1–133. <https://doi.org/10.5962/bhl.title.2537>
- Schneider CA, Rasband WS, Eliceiri KW (2012) NIH Image to ImageJ: 25 years of image analysis. Nature Methods 9(7): 671–675. <https://doi.org/10.1038/nmeth.2089>
- Smithe FB (1975) Naturalists' color guide. The American Museum of Natural History, 1–22.
- Stamatakis A (2006) RAxML-VI-HPC: maximum likelihood-based phylogenetic analyses with thousands of taxa and mixed models. Bioinformatics 22: 2688–2690. <https://doi.org/10.1093/bioinformatics/btl446>
- Takahashi H (2002) Four new species of *Crinipellis* and *Marasmius* in eastern Honshu, Japan. Mycoscience 43: 343–350. <https://doi.org/10.1007/S102670200050>
- Thiers B (2019 – continuously updated) Index Herbariorum: A global directory of public herbaria and associated staff. New York Botanical Garden's Virtual Herbarium. <http://sweetgum.nybg.org/ih/>

A taxonomic revision of the genus *Conidiobolus* (Ancylistaceae, Entomophthorales): four clades including three new genera

Yong Nie^{1,2}, De-Shui Yu¹, Cheng-Fang Wang¹, Xiao-Yong Liu³, Bo Huang¹

1 Anhui Provincial Key Laboratory for Microbial Pest Control, Anhui Agricultural University, Hefei 230036, China **2** School of Civil Engineering and Architecture, Anhui University of Technology, Ma'anshan 243002, China **3** State Key Laboratory of Mycology, Institute of Microbiology, Chinese Academy of Sciences, Beijing 100101, China

Corresponding author: Xiao-Yong Liu (liuxiaoyong@im.ac.cn), Bo Huang (bhuang@ahau.edu.cn)

Academic editor: M. Stadler | Received 14 September 2019 | Accepted 13 March 2020 | Published 30 March 2020

Citation: Nie Y, Yu D-S, Wang C-F, Liu X-Y, Huang B (2020) A taxonomic revision of the genus *Conidiobolus* (Ancylistaceae, Entomophthorales): four clades including three new genera. MycoKeys 66: 55–81. <https://doi.org/10.3897/mycokeys.66.46575>

Abstract

The genus *Conidiobolus* is an important group in entomophthoroid fungi and is considered to be polyphyletic in recent molecular phylogenies. To re-evaluate and delimit this genus, multi-locus phylogenetic analyses were performed using the large and small subunits of nuclear ribosomal DNA (nucLSU and nucSSU), the small subunit of the mitochondrial ribosomal DNA (mtSSU) and the translation elongation factor 1-alpha (EF-1 α). The results indicated that the *Conidiobolus* is not monophyletic, being grouped into a paraphyletic grade with four clades. Consequently, the well-known *Conidiobolus* is revised and three new genera *Capillidium*, *Microconidiobolus* and *Neoconidiobolus* are proposed along with one new record and 22 new combinations. In addition, the genus *Basidiobolus* is found to be basal to the other entomophthoroid taxa and the genus *Batkoa* locates in the *Entomophthoraceae* clade.

Keywords

Zygomycetes, *Entomophthorales*, Morphology, Phylogeny, New taxa

Introduction

More than 250 species of entomophthoroid fungi were isolated from insects, soil and litter throughout the world (Gryganskyi et al. 2013). For a long time, this group has been considered to be polyphyletic (Nagahama et al. 1995; Jensen et al. 1998; James

et al. 2006; Liu and Voigt 2010) and was classified into a subphylum *Entomophthoromycotina* and a pending taxon *Basidiobolus* (Hibbett et al. 2007). However, a recent phylogeny using the multi-gene dataset, 18S rDNA, 28S rDNA, mtSSU and RPB2, indicated that this group formed a monophyletic lineage including *Basidiobolus* and it was consequently reclassified as a new fungal phylum *Entomophthoromycota*. More recently, a phylogenomic analysis (192 clusters of orthologous proteins) has divided traditional zygomycotan into two phyla *Mucoromycota* and *Zoopagomycota* and the entomophthoroid fungi have been re-assigned into the subphylum *Entomophthoromycotina* under the latter phylum (Spatafora et al. 2016). This taxonomic scheme was supported by the phylogeny of mitochondrial genomes (Nie et al. 2019).

Together with other two genera *Ancylistes* and *Macrobotophtora*, the genus *Conidiobolus* belongs to *Ancylistaceae*, *Entomophthorales*, *Entomophthoromycetes*, *Entomophthoromycotina* (Humber 2012). There are six and two accepted species within the *Ancylistes* and *Macrobotophtora*, respectively, while *Conidiobolus*, one of the largest groups in the entomophthoroid fungi, contains 76 names (<http://www.indexfungorum.org/>). The genus *Conidiobolus* is typified by *C. utriculosus* Bref. 1884 and characterised morphologically by simple sporophores, globose to pyriform multinucleate primary conidia, various types of secondary conidia and resting spores (Brefeld 1884; Humber 1997). Up to the 1940s, for half a century, only three more species were reported, *C. minor* Bref., *C. villosus* Martin and *C. brefeldianus* Couch (Brefeld 1884; Martin 1925; Couch 1939). In the 1950s–1960s, 38 *Conidiobolus* species and a variety were isolated from the United States and India (Drechsler 1952, 1953a, b, 1954, 1955a, b, c, 1956, 1957a, b, c, 1960, 1961, 1962, 1965; Srinivasan and Thirumalachar 1961, 1962a, b, 1965, 1967, 1968a, b). Based on a numerical taxonomy, King (1976a, b, 1977) recognised 27 definitive species. Since then, along with some new combinations, 10 more species have been added to *Conidiobolus* (Bałazy et al. 1987; Waters and Callaghan 1989; Bałazy 1993; Huang et al. 2007; Waingankar et al. 2008; Nie et al. 2012, 2016, 2017, 2018). A total of 37 species are currently accepted in this genus (Nie et al. 2018).

Three subgenera – *Capillidium*, *Conidiobolus* and *Delacroixia* – were proposed within the *Conidiobolus*, based on shape of the secondary conidia and, amongst them, the subgenus *Delacroixia* was reduced from generic rank (Ben-Ze'ev and Kenneth 1982). This subgeneric criterion provided a valuable contribution for the taxonomy of the genus *Conidiobolus* (Humber 1989). Since the 1990s, molecular analysis has become an increasingly important tool for fungal taxonomy (Bruns et al. 1991; Taylor et al. 2000). The nuLSU rDNA and EF-1 α regions proved to be distinguishable amongst *Conidiobolus* species (Nie et al. 2012), while nucSSU rDNA indicated the genus *Conidiobolus* might be a polyphyletic group (Jensen et al. 1998). The subgeneric circumscription was not defined because of instability to form a certain type of secondary conidia for each phylogenetic clade (Callaghan et al. 2000; Gryganskyi et al. 2013; Nie et al. 2018). Besides, the phylogenetic relationships amongst species of *Conidiobolus* have not been fully resolved due to the absence of types. The genus *Batkoa*, morphologically similar to *Conidiobolus*, was phylogenetically closely related to *Entomophthoraceae* rather than *Ancylistaceae* (Gryganskyi et al. 2012, 2013).

In the present study, a reclassification of the entomophthoroid fungi, including as many as available *Conidiobolus* types, was constructed based on four loci (nucSSU, nucLSU, EF-1 α and mtSSU) to present the taxonomic delimitation of the genus *Conidiobolus* and to re-evaluate the phylogenetic relationship between *Basidiobolus* and *Batkoa*.

Materials and methods

Isolates and morphology

A total of 26 ex-types of *Conidiobolus* were purchased from the American Type Culture Collection, Manassas, USA (ATCC) and collected from the China General Microbiological Culture Collection Center, Beijing, China (CGMCC) and the Research Center for Entomogenous Fungi of Anhui Agricultural University, Anhui Province, China (RCEF). Dried cultures were deposited in the Herbarium Mycologicum Academiae Sinicae, Beijing, China (HMAS). Morphology was observed with an Olympus BX51 research microscope and photographed by an Olympus DP25 microscope-camera system. Growth diameter on PDA (potato 200 g, dextrose 20 g, agar 20 g, H₂O 1 l), Mycelia, primary conidiophores, primary conidia, microconidia, capilliconidia and resting spores were measured and described with the method of King (1976a).

DNA extraction, PCR amplification and sequencing

Fungal strains were incubated on PDA for 7 d at 21 °C. Total genomic DNA was extracted from the fresh fungal mycelia by using modified CTAB method (Watanabe et al. 2010). Four gene portions from cell nuclei and mitochondria and one protein coding gene were used in this study: the large subunit of nuclear ribosomal RNA genes (nucLSU), the small subunit of nuclear ribosomal RNA genes (nucSSU), the small subunit of mitochondrial ribosomal RNA genes (mtSSU) and the translation elongation factor 1-alpha gene (EF-1 α). The nucLSU region was amplified with the primers LR0R and LR5 (Vilgalys and Hester 1990), the nucSSU region with nucSSU-0021-5' (Gargas and DePriest 1996) and nucSSU-1780-3' (DePriest 1993) and EF-1 α region with the primers EF983 and EF1aZ-1R (<http://www.aftol.org/primers.php>). These PCR reactions have been described by Liu et al. (2005), Jensen et al. (1998) and Nie et al. (2012). The primers used for the mtSSU region were mtSSU1 and mtSSU2R and the PCR reaction was performed using the following cycling parameters: denaturation at 94 °C for 3 min, followed by 35 cycles of denaturation at 94 °C for 1 min, annealing at 52 °C for 1 min, extension at 72 °C for 1 min and finalised with an extra extension at 72 °C for 7 min (Zoller et al. 1999). PCR products were purified and sequenced by Shanghai Genecore Biotechnologies Company (Shanghai, China) with the same primers as relative PCR. The nucleotide sequence data have been deposited in the GenBank (Table 1).

Table I. The species used in phylogenetic analyses.

Species	Strains*	GenBank accession numbers			
		nucSSU	nucLSU	EF-1 α	mtSSU
<i>Allomyces arbusculus</i>	AFTOL 300	AY552524	DQ273806	DQ275334	–
<i>Basidiobolus haptosporus</i>	ARSEF 261	JX242606	JX242586	–	JX242626
<i>B. heterosporus</i>	CBS 311.66	JX242607	JX242587	–	JX242627
<i>B. magnus</i>	CBS 205.64	JX242608	JX242588	–	JX242628
<i>B. meristosporus</i>	CBS 931.73	JX242609	JX242589	–	JX242629
<i>B. microsporus</i>	CBS 130.62 (T)	JX242610	JX242590	–	JX242630
<i>B. ranarum</i>	NRRL 34594	AY635841	DQ273807	DQ275340	EF392490
<i>Batkoa apiculata</i>	ARSEF 3130	DQ177437	EF392404	–	EF392513
<i>B. gigantea</i>	ARSEF 214	JX242611	JX242591	–	JX242631
<i>B. major</i>	ARSEF 2936	EF392559	EF392401	–	EF392511
<i>B. obscurus**</i>	CBS 182.60	JX242614	JX242595	–	JX242635
<i>B. pseudapiculata**</i>	ARSEF 395	EF392557	EF392378	–	EF392508
<i>Coemansia reversa</i>	AFTOL 140	AY546685	AY546689	DQ282615	–
<i>Conidiobolus adiaeretus</i>	ARSEF 451 (T)	–	KC461182	–	–
<i>C. adiaeretus</i>	CGMCC 3.15888	–	MN061284	MN061481	MN061287
<i>C. antarcticus</i>	ARSEF 6913 (T)	–	DQ364207	–	DQ364227
<i>C. bangalorensis</i>	ARSEF 449 (T)	–	DQ364204	–	DQ364225
<i>C. brefeldianus</i>	ARSEF 452 (T)	AF368506	EF392382	–	EF392495
<i>C. chlamydosporus</i>	ATCC 12242 (T)	–	JF816212	JF816234	MK301178
<i>C. coronatus</i>	NRRL 28638	AF113418	AY546691	DQ275337	–
<i>C. coronatus</i>	RCEF 4518	–	JN131537	JN131543	–
<i>C. couchii</i>	ATCC 18152 (T)	–	JN131538	JN131544	MK301179
<i>C. dabieshanensis</i>	CGMCC 3.15763 (T)	–	KY398125	KY402206	MK301180
<i>C. denaesporus</i>	ATCC 12940 (T)	–	JF816215	JF816228	MK301181
<i>C. firmipilleus</i>	ARSEF 6384	JX242612	JX242592	–	JX242632
<i>C. gonimodes</i>	ATCC 14445 (T)	–	JF816221	JF816226	MK301182
<i>C. heterosporus</i>	RCEF 4430	–	JF816225	JF816239	MK301183
<i>C. humicolus</i>	ATCC 28849 (T)	–	JF816220	JF816231	MK301184
<i>C. incongruus</i>	NRRL 28636	AF113419	AF113457	–	–
<i>C. iuxtagenitus</i>	ARSEF 6378 (T)	–	KC788410	–	–
<i>C. iuxtagenitus</i>	RCEF 4445	–	JX946695	JX946700	MK333391
<i>C. khandalensis</i>	ATCC 15162 (T)	–	KX686994	KY402204	MK301185
<i>C. lachnodes</i>	ARSEF 700	–	KC788408	–	–
<i>C. lamprauges</i>	ARSEF 2338	AF296754	DQ364206	–	DQ364226
<i>C. lichenicolus</i>	ATCC 16200 (T)	–	JF816216	JF816232	MK301186
<i>C. lobatus</i>	ATCC 18153 (T)	–	JF816218	JF816233	MK301187
<i>C. marcosporus</i>	ATCC 16578 (T)	–	KY398124	KY402209	MK301188
<i>C. megalotocus</i>	ATCC 28854 (T)	–	MF616383	MF616385	MK301189
<i>C. mirabilis</i>	CGMCC 3.17763 (T)	–	MH282852	MH282853	MK333389
<i>C. mycophagus</i>	ATCC 16201 (T)	–	JX946694	JX946698	MK301190
<i>C. mycophilus</i>	ATCC 16199 (T)	–	KX686995	KY402205	MK301191
<i>C. nodosus</i>	ATCC 16577 (T)	–	JF816217	JF816235	MK333388
<i>C. osmodes</i>	ARSEF 79	AF368510	EF392371	–	DQ364219
<i>C. osmodes</i>	RCEF4447	–	JN131539	JN131545	MK333392
<i>C. pachyzygosporus</i>	CGMCC 3.17764 (T)	–	KP218521	KP218524	MK333390
<i>C. paulus</i>	ARSEF 450 (T)	–	vv	–	–
<i>C. polyspermus</i>	ATCC 14444 (T)	–	MF616382	MF616384	MK301193
<i>C. polytocus</i>	ATCC 12244 (T)	–	JF816213	JF816227	MK301194
<i>C. pumilus</i>	ARSEF 453 (T)	JX242615	EF392383	–	EF392496
<i>C. rhyosporus</i>	ATCC 12588 (T)	–	JN131540	JN131546	MK301195
<i>C. sinensis</i>	RCEF 4952 (T)	–	JF816224	JF816238	MK301196
<i>C. stilbeus</i>	RCEF 5584 (T)	–	KP218522	KP218525	MK301197
<i>C. stromoideus</i>	ATCC 15430 (T)	–	JF816219	JF816229	MK301198

Species	Strains*	GenBank accession numbers			
		nucSSU	nucLSU	EF-1 α	mtSSU
<i>C. terrestris</i>	ATCC 16198 (T)	–	KX752050	KY402208	MK301199
<i>C. thromboides</i>	ATCC 12587 (T)	–	JF816214	JF816230	MK301200
<i>C. thromboides</i>	FSU 785	JX242616	JX242597	–	JX242637
<i>C. thromboides</i>	RCEF 4492	–	JF816223	JF816236	MK333393
<i>C. undulatus</i>	ATCC 12943 (T)	–	JX946693	JX946699	MK301201
<i>Dimargaris bacillispora</i>	AFTOL 136	AB016020	DQ273791	DQ282609	–
<i>Endogone pisiformis</i>	AFTOL 539	DQ322628	DQ273811	DQ282618	–
<i>Entomophaga aulicae</i>	ARSEF 172	EF392542	EF392372	–	EF392487
<i>E. conglomerata</i>	ARSEF 2273	AF368509	–	–	–
<i>E. maimaga</i>	ARSEF 1400	EF392556	EF392395	–	EF392505
<i>Eryniopsis caroliniana</i>	ARSEF 640	EF392552	EF392387	–	EF392500
<i>Entomophthora chromaphidis</i>	ARSEF 1860	AF353725	–	–	–
<i>E. culicis</i>	ARSEF 387	AF368516	–	–	–
<i>E. grandis</i>	ARSEF 6701	–	DQ481229	–	–
<i>E. scatophaga</i>	ARSEF 6704	–	DQ481226	–	–
<i>E. muscae</i>	ARSEF 3074	AY635820	DQ273772	DQ275343	–
<i>E. planconiana</i>	ARSEF 6252	AF353723	GQ285878	–	–
<i>E. schizophorae</i>	ARSEF 5348	AF052402	GQ285883	–	–
<i>E. syrphi</i>	ARSEF 5595	–	DQ481230	–	–
<i>E. tripidium</i>	ARSEF 6518	AF296755	–	–	–
<i>Erynia conica</i>	ARSEF 1439	AF368513	EF392396	–	EF392506
<i>E. ovispora</i>	ARSEF 400	JX242620	JX242601	–	JX242641
<i>E. rhizospora</i>	ARSEF 1441	AF368514	EF392397	–	EF392507
<i>E. sciarae</i>	ARSEF 1870	AF368515	EF392399	–	EF392509
<i>Furia americana</i>	ARSEF 742	EF392554	EF392389	–	–
<i>F. gastropachae</i>	ARSEF 5541	EF392562	EF392407	–	EF392516
<i>F. ithacensis</i>	ARSEF 663	EF392553	EF392388	–	EF392501
<i>F. neopyralidarum</i>	ARSEF 1145	AF368518	EF392394	–	EF392504
<i>F. pieris</i>	ARSEF 781	AF368519	EF392390	–	EF392502
<i>F. virescens</i>	ARSEF 1129	EF392555	EF392393	–	EF392503
<i>Gaertneriomyces semiglobiferus</i>	AFTOL 34	AF164247	DQ273778	DQ275338	–
<i>Macrobotiophthora vermicola</i>	ARSEF 650	AF052400	–	–	–
<i>Massospora cicadina</i>	ARSEF 374	EF392548	EF392377	–	EF392492
<i>Mortierella verticillata</i>	AFTOL 141	AF157145	DQ273794	–	–
<i>Pandora blunckii</i>	ARSEF 217 (T)	JX242621	JX242602	–	–
<i>P. delphacis</i>	ARSEF 459	AF368521	EF392384	–	EF392497
<i>P. dipterigena</i>	ARSEF 397	AF368522	EF392380	–	EF392565
<i>P. kondoiensis</i>	CBS 642.92	JX242622	JX242603	–	JX242642
<i>P. neoaphidis</i>	ARSEF 3240	EF392560	EF392405	–	EF392514
<i>Piptocephalis corymbifera</i>	AFTOL 145	AB016023	AY546690	DQ282619	–
<i>Rhizophagus intraradices</i>	AFTOL 845	DQ322630	FJ461839	DQ282611	–
<i>Rozella allomycis</i>	AFTOL 297	AY635838	DQ273803	DQ275342	–
<i>Schizangiella serpentis</i>	ARSEF 2237	AF368523	EF392428	–	EF392488
<i>Strongwellsea castrans</i>	–	AF052406	–	–	–
<i>Zancudomyces culisetae</i>	AFTOL 29	AF277007	DQ273773	–	–
<i>Zoophthora anglica</i>	ARSEF 396	–	EF392379	–	EF392493
<i>Z. lanceolata</i>	ARSEF 469	EF392550	EF392385	–	EF392498
<i>Z. phalloides</i>	ARSEF 2281	EF392558	EF392400	–	EF392510
<i>Z. radicans</i>	ARSEF 388	JX242624	JX242605	–	JX242644

* AFTOL, Assembling the Fungal Tree of Life; ARSEF, ARS Entomopathogenic Fungus Collection (Ithaca, U.S.A.); ATCC, American Type Culture Collection (Manassas, U.S.A.); CGMCC, China General Microbiological Culture Collection Center (Beijing, China); FSU, Jena Microbial Resource Collection (Friedrich-Schiller-University of Jena, Germany); NRRL, ARS Culture Collection (Peoria, U.S.A.); RCEF, Research Center for Entomogenous Fungi (Hefei, China). T = ex-type.

** *Batkoa* sp. CBS 182.60 was received as *Conidiobolus obscurus*, while *B. pseudapiculata* ARSEF 395 was received as *C. pseudapiculatus*.

Phylogenetic analyses

More available nucLSU, nucSSU, mtSSU and EF-1 α sequences of 14 *Conidiobolus* species and 47 other entomophthoroid fungi were obtained from GenBank. Ten species of *Glomeromycotina*, *Mortierellomycotina*, *Mucoromycotina*, *Kickxellomycotina*, *Zoopagomycotina*, *Blastocladiomycota*, *Chytridiomycota* and *Cryptomycota*, were chosen as outgroups. Alignments were constructed separately for each locus with MUSCLE 3.8.31 (Edgar 2004) and the concatenated matrices were assembled by SequenceMatrix 1.7.8 (Vaidya et al. 2011). The best model for the phylogenetic analysis was selected with Akaike Information Criterion (AIC) by using Modeltest 3.7 (Posada and Crandall 1998). Phylogenetic relationships were inferred using Maximum Likelihood (ML) and Bayesian Inference (BI). The best-scoring ML tree analysis was performed using raxmlGUI 1.5b1 with GTRGAMMA model and 1000 replicates (Silvestro and Michalak 2012). The BI analysis was performed using MrBayes 3.2.2 (Ronquist and Huelsenbeck 2003). Markov Chain Monte Carlo (MCMC) chains ran until the convergences met and the standard deviation fell below 0.01. The first 25% of trees were discarded as burn-in. The combined dataset was deposited at TreeBase (No. S25064). Phylogenetic trees were checked and modified in FigTree 1.4 (Rambaut 2012).

Results

Phylogenetic analyses

The combined dataset contained 4521 characters of nucLSU (1–1326), nucSSU (1327–3424), EF-1 α (3425–4062) and mtSSU (4063–4521) after alignment. With the optimal model GTR+I+G and random starting trees, four Markov chains were run for 7 million generations and every 100th generation was sampled once. ML and BI analyses of the combined dataset resulted in phylogenetic reconstructions with almost similar topologies and the average standard deviation of split frequencies was 0.006721 (BI).

In the ML phylogenetic tree (Figure 1), the *Basidiobolaceae* lineage (88/0.94) is located at the base of the entomophthoroid fungi and is closely related to the *Ancylistaceae* group (56/0.91). The *Batkoa* lineage is grouped within the *Entomophthoraceae* Clade (60/0.89). All *Conidiobolus* lineages are clustered into a paraphyletic grade and therefore cannot be considered congeneric. Moreover, the *Conidiobolus* grade consists of four well supported clades. In detail, there are 7, 10, 16 and 3 species in Clade I (100/1.00), II (77/1.00), III (100/1.00) and IV (99/1.00), respectively.

Taxonomy

In order to provide a more natural taxonomic classification, four genera (*Capillidium*, *Conidiobolus*, *Microconidiobolus* and *Neoconidiobolus*) and their type species (*Ca. heterosporum*, *C. utriculosus*, *M. paulus* and *N. thromboides*) are described here in this paper.

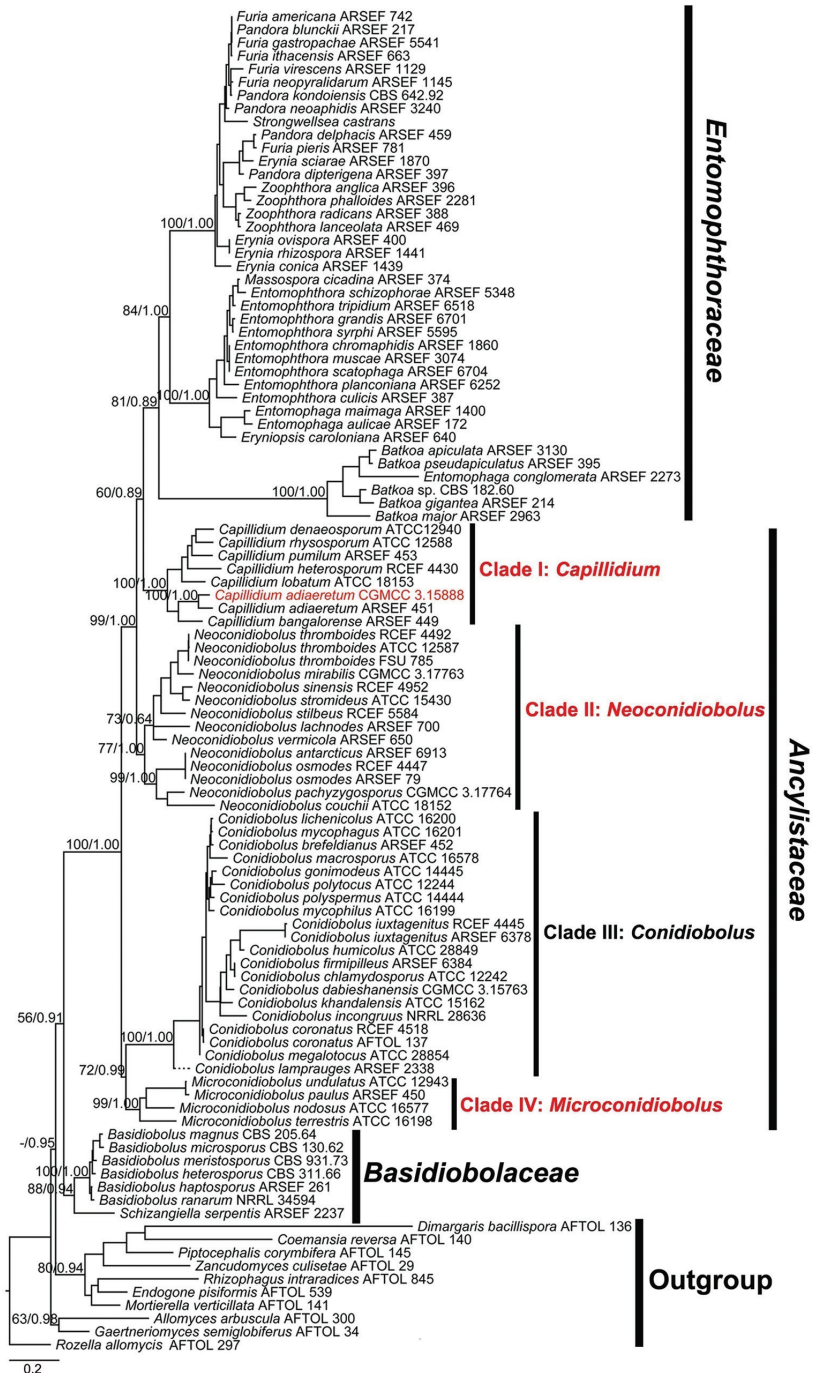


Figure 1. Phylogenetic tree constructed by maximum likelihood analyses of nucLSU, nucSSU, EF-1 α and mtSSU sequences for *Entomophthoromycotina*, with some chytrid and mucoralean fungi as outgroups. Three new genera and one Chinese new record are shown in red. Maximum likelihood bootstrap values ($\geq 50\%$) / Bayesian posterior probabilities (≥ 0.50) of main clades are indicated along branches. Scale bar indicates substitutions per site.

Additionally, a new record *Ca. adiaereturum*, *C. coronatus* and *C. iuxtagenitus* with new isolates from China and *C. khandalensis* being first reported to produce microconidia are illustrated herein.

***Capillidium* B. Huang & Y. Nie, gen. nov.**

MycoBank No: MB831596

Etymology. Referring to unique ellipsoidal secondary conidia (capilliconidia).

Type species. *Capillidium heterosporum* (Drechsler) B. Huang & Y. Nie.

Description. Mycelia colourless. Primary conidiophores simple, bearing a single primary conidia. Primary conidia forcibly discharged multinucleate, colourless, globose, pyriform to obovoid. Two kinds of replicative conidia, the first one is similar and smaller than primary conidia, the second one (capilliconidia) arises from elongate and slender conidiophores. Zygosporangia present or absent, formed in axial alignment with conjugating segments, globose to subglobose, often smooth, sometimes rough, colourless or yellowish.

Notes. *Conidiobolus* subgen. *Capillidium* Ben-Ze'ev & Kenneth was firstly established to include species with capilliconidia (Ben-Ze'ev and Kenneth 1982). In this phylogenetic analysis, all members of the subgenus *Capillidium* grouped with good support (100/1.00) and, therefore, it was raised from subgenus to genus status based on the monophyly, as well as the stability to form ellipsoidal secondary conidia (capilliconidia). In addition to capilliconidia, *C. adiaereturum* also produces microconidia.

***Capillidium heterosporum* (Drechsler) B. Huang & Y. Nie, comb. nov.**

MycoBank No: MB831601

Figure 2

Conidiobolus heterosporus Drechsler, Am. J. Bot. 40: 107 (1953). Basionym.

=*Conidiobolus rugosus* Drechsler, Am. J. Bot. 42: 437 (1955).

Specimens examined. CHINA, Anhui Province, Plant detritus, 8 Nov 2008, *C.F. Wang*, RCEF 4430.

Description. Colonies on PDA at 25 °C after 3 d, white, reaching ca. 21 mm in diameter. Mycelia colourless, 5–9 µm wide. Primary conidiophores, colourless, unbranched and producing a single globose conidium with widening upwards, extending to a length of 30–245 µm into the air, 8–17 µm wide. Primary conidia forcibly discharged, colourless, globose to subglobose, measuring 12–37 µm in greatest length and 11–31 µm in total width, including a basal papilla 1.5–5 µm high and 5–12 µm wide. After discharging on to 2% water-agar, similar and smaller secondary conidia arise from primary conidia, 1–6 ellipsoidal secondary conidia (capilliconidia, 10–20 × 12–38 µm) arise from slender conidiophores (50–250 × 2.5–4 µm). Resting spores not observed.

Notes. The ex-type living culture is ATCC 12941 (United States, Maryland, 18 Mar 1952, Drechsler).

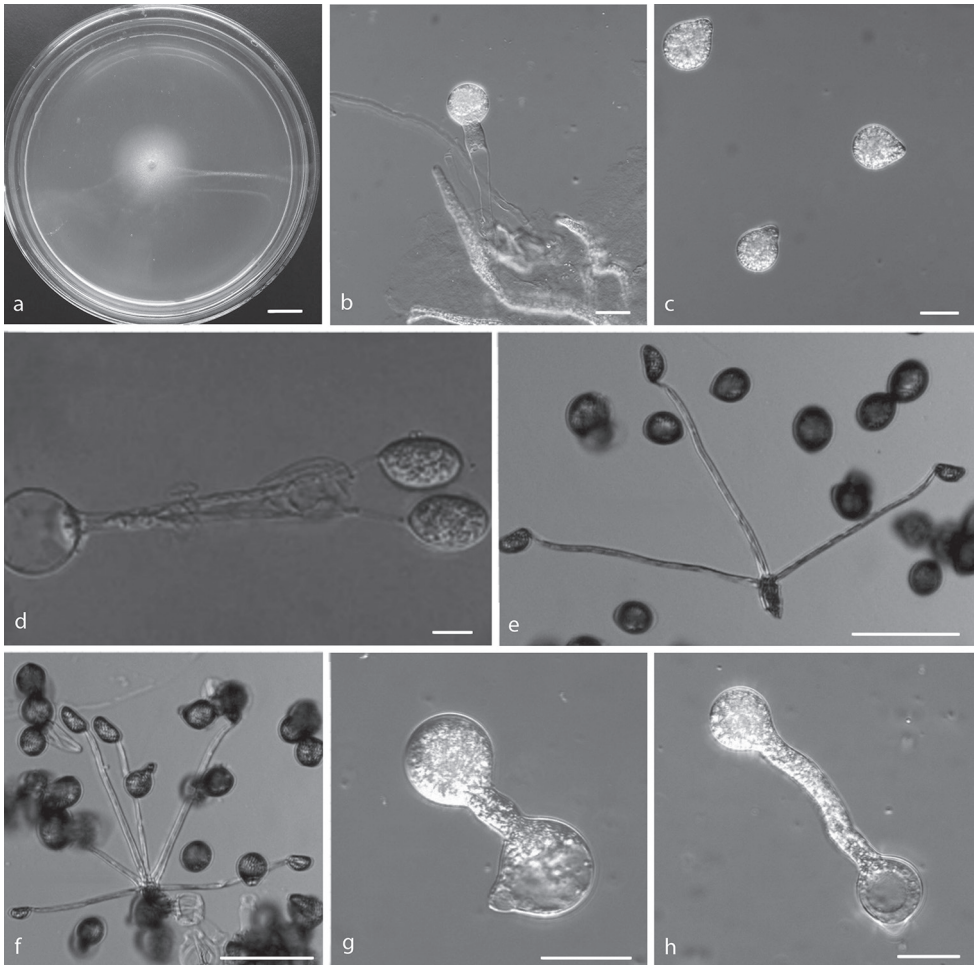


Figure 2. *Capillidium heterosporum* **a** colony on PDA after 3 d at 25 °C **b** primary conidiophores bearing primary conidia **c** primary conidia **d, e, f** ellipsoidal secondary conidia arising from slender conidiophores **g, h** production of secondary conidia. Scale bars: 10 mm (**a**); 20 µm (**b, c, d, g, h**); 100 µm (**e, f**).

***Capillidium adiaeretum* (Drechsler) B. Huang & Y. Nie, comb. nov.**

Mycobank No: MB831602

Figure 3

Conidiobolus adiaeretus Drechsler, J. Wash. Acad. Sci. 43: 42 (1953). Basionym.

Specimens examined. CHINA, Jiangsu Province, Nanjing City, Laoshan Forest Park, 32°5'58"N, 118°35'53"E, Plant detritus, 1 Dec 2018, *Y. Nie and Y. Gao*, HMAS 248358, culture CGMCC 3.15888 (=RCEF 6550).

Description. Colonies on PDA at 25 °C after 3 d, white, reaching ca. 7–10 mm in diameter. Mycelia colourless, 3–4.5 µm wide. Primary conidiophores, colourless, unbranched and producing a single globose conidium with widening upwards; they offer

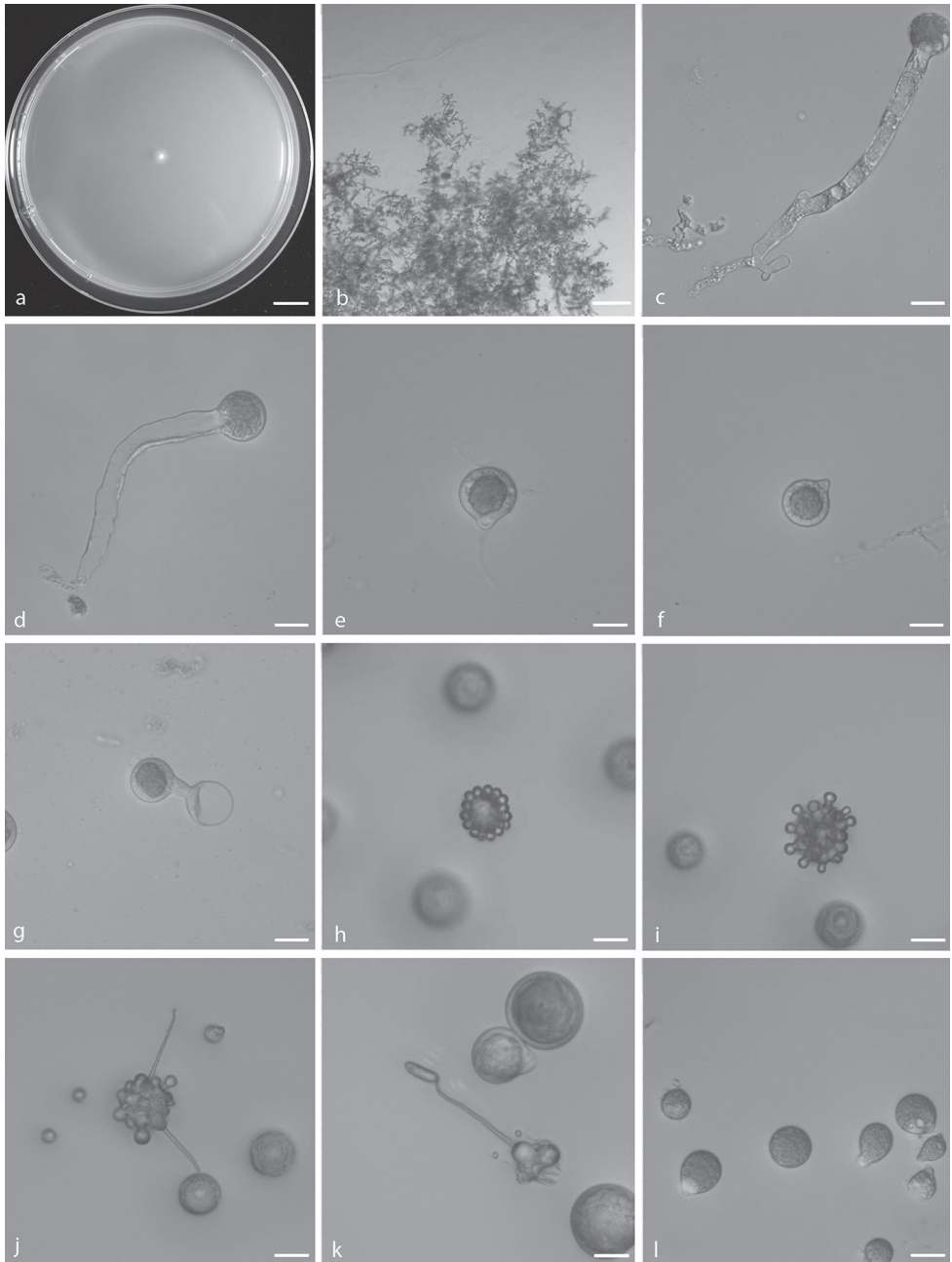


Figure 3. *Capillidium adiaereturum* **a** colony on PDA after 3 d at 25 °C **b** mycelia **c, d** primary conidiophores bearing primary conidia **e, f** primary conidia **g** Production of secondary conidia **h** first stage of forming microconidia **i** second stage of forming microconidia **j, k** ellipsoidal secondary conidia arising from slender conidiophores **l** chlamydospores. Scale bars: 10 mm (**a**); 100 μ m (**b**); 20 μ m (**c–l**).

a pronounced dimensional contrast with the mycelial filaments, extending to a length of 50–210 μm into the air, 3–25 μm wide. Primary conidia forcibly discharged, colourless, globose, measuring 15–45 μm in greatest length and 13–42 μm in total width, including a basal papilla 2–6 μm high and 5–17 μm wide. After discharging on to 2% water-agar, similar and smaller secondary conidia arise from primary conidia, two generations of multiple spherical units forming on the parent globose conidia. Microconidia only formed from the second set, 5–12 \times 9–10 μm . Capilliconidia formed readily from discharged microconidia, 16–24 \times 5–6 μm . Chlamydospores formed within the substratum, colourless, globose to ellipsoidal, 13–40 \times 15–45 μm .

Notes. The species was firstly reported from America (Drechsler 1953a). The ex-type living culture is ATCC 12589 isolated by Drechsler (1953a). It is mainly characterised and differs from other *Capillidium* species by its ability to form both microconidia and capilliconidia (Callaghan et al. 2000). The Chinese specimen CGMCC 3.15888 clusters completely (100/1.00) with an isotype ARSEF 451 (98% sequence similarity in nucLSU) and fits well with its morphological descriptions. It is reported in China for the first time.

***Conidiobolus* Bref., Mykol. Untersuch. 6(2): 35 (1884), emend.**

MycoBank No: MB20144

= *Delacroixia* Sacc. & P. Syd., Syll. fung. (Abellini) 14(1): 457 (1899).

Conidiobolus subgen. *Delacroixia* (Sacc. & P. Syd.) Tyrrell & Macleod, J. Invert. Pathol. 20: 12 (1972).

Type species. *Conidiobolus utriculosus* Bref.

Description. Mycelia colourless. Primary conidiophores simple or branched dichotomously, positively phototropic, bearing a single or 2–4 primary conidia. Primary conidia forcibly discharged, multinucleate, colourless, pyriform, obovoid, globose to subglobose. Secondary conidia usually with shape of primary conidia but smaller, formed singly on short secondary conidiophores. Microspores arising from primary or secondary conidia. Villose appendaged globose conidia and formed villose conidia. Chlamydospores formed intercalarily within assimilative hyphae. Zygosporangia formed in axial alignment with one or two (homothallic or heterothallic) conjugating segments.

Notes. *C. utriculosus*, the type species of the genus *Conidiobolus*, has not been re-collected since Brefeld isolated it in 1884 and most taxonomists working on entomophthoroid fungi now universally recognised it as *C. coronatus* (Gryganskyi et al. 2013). However, the smaller pear-shaped conidia of *C. utriculosus* are different from the larger globose conidia of *C. coronatus* and villose spores in *C. coronatus* are not observed in *C. utriculosus* (Brefeld 1884; King 1977). Consequently, *C. coronatus* is not synonymised with *C. utriculosus* in this study. Instead, this study

agrees with Srinivasan and Thirumalachar (1967) and King (1977) to place *C. minor* in synonymy with *C. utriculosus* because the small conidia of *C. minor* were probably replicative conidia of *C. utriculosus*. Nevertheless, neither *C. utriculosus* nor *C. minor* has available living cultures. Therefore, we have not yet designated an epitype and thus no DNA sequences for explaining this type. Fortunately, we are able to recognise clade III (Fig. 1) as *Conidiobolus* on the basis of its synapomorph, namely microspores.

***Conidiobolus utriculosus* Bref., Mykol. Untersuch. 6(2): 35 (1884)**

MycoBank No: MB144259 (MBT391377)

= *Conidiobolus minor* Bref., Mykol. Untersuch. 6(2): 35, 68 (1884).

Specimens examined. No ex-type.

Description. Refer to Brefeld (1884) and King (1977).

Notes. Due to the lack of ex-type, plates 3, 4, and 5 in Brefeld, Mykol. Untersuch. 6(2): 35 (1884) are designated here as the lectotype for *Conidiobolus utriculosus*.

***Conidiobolus coronatus* (Costantin) A. Batko, Entomophaga, Mémoires hors série 2: 129 (1964)**

MycoBank No: MB283037

Figure 4

Boudierella coronata Costantin, Bull. Soc. mycol. Fr. 13: 40 (1897). Basionym.

Delacroixia coronata (Costantin) Sacc. & P. Syd., Syll. fung. (Abellini) 14(1): 457 (1899).

Entomophthora coronata (Costantin) Kevorkian, J. Agric. Univ. Puerto Rico 21(2): 191 (1937).

= *Conidiobolus villosus* G.W. Martin, Bot. Gaz. 80(3): 317 (1925).

Specimens examined. CHINA, Shandong Province, Plant detritus, 20 Mar 2009, C.F. Wang, RCEF 4518.

Description. Colonies grown on PDA for 3 d at 21 °C, reaching ca. 65 mm in diameter. Mycelia colourless, 8–20 µm wide. Primary conidiophores, positively phototropic, colourless, unbranched and producing a single globose conidium, extending to a length of 53–287 µm into the air, 7.5–20.5 µm wide. Primary conidia forcibly discharged, colourless, globose, measuring 36–52 µm in greatest width and 42–65 µm in total length, including a basal papilla 12–18 µm high and 6.5–14 µm wide. After discharging on to 2% water-agar, similar and smaller secondary conidia arise from primary conidia. Microconidia produced readily from primary conidia, globose or almond-shaped, 13–19 × 11–15 µm. Villose spores formed after 4–5 d, globose, 20–42 µm.

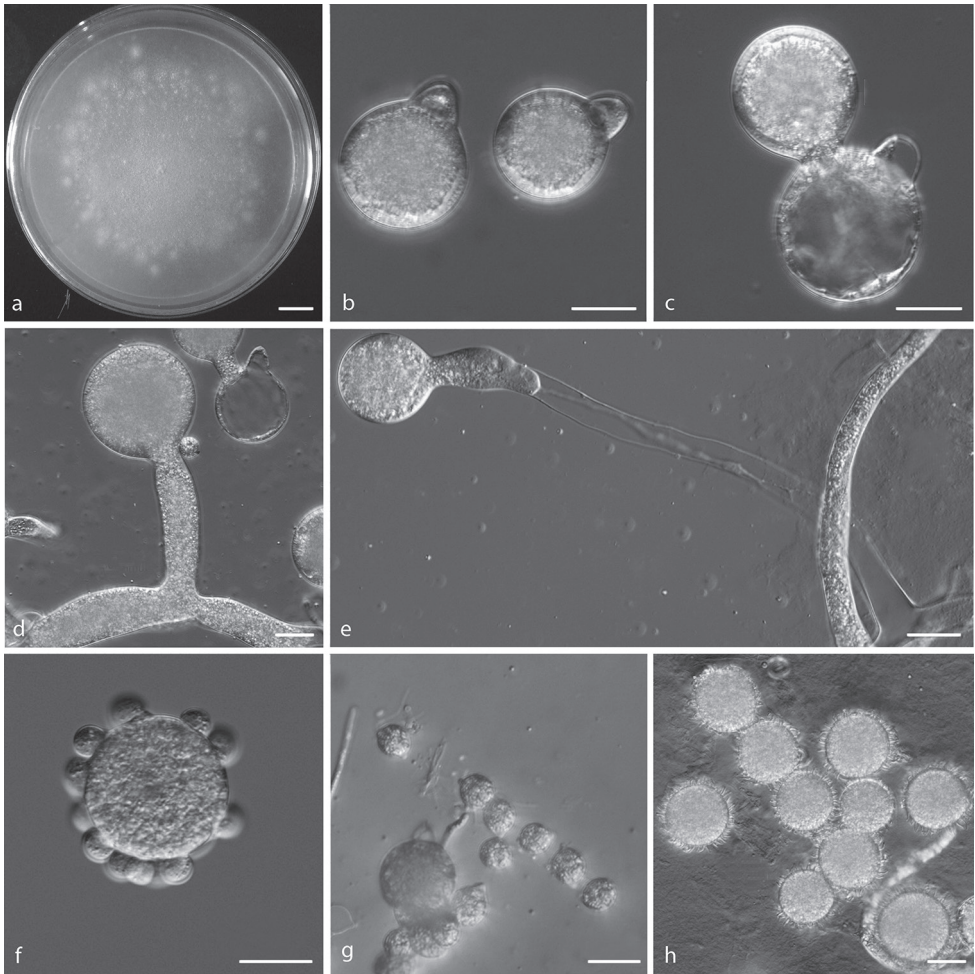


Figure 4. *Conidiobolus coronatus* **a** colony on PDA after 3 d at 21 °C **b** primary conidia **c** production of secondary conidia **d, e** primary conidiophores bearing primary conidia **f, g** microconidia **h** villose spores. Scale bars: 10 mm (**a**); 20 µm (**b–h**).

Notes. The ex-type living culture is ATCC 28691 (United States, Louisiana, Plant detritus, 3 January 1972). Due to the absence of molecular data of ex-type strain ATCC 28691, the molecular data of the authentic strain NRRL 28638, which has been applied in many other phylogenetic analysis (James et al. 2006; Liu and Voigt 2011; Gryganskyi et al. 2012; Tretter et al. 2014; Spatafora et al. 2016), was used in this study instead. The monotypic genus *Delacroixia* was typified by *D. coronata* which was transferred from an ascomycete *Boudierella coronata* Costantin (Costantin 1897; Saccardo and Sydow 1899). After that, it was reclassified as a subgenus of *Conidiobolus*, namely *Conidiobolus* sub. *Delacroixia* (Sacc. & P. Syd.) Tyrrell & MacLeod to define all those *Conidiobolus* species capable of forming microspores and, consequently, *D. coronata* was recombined as *C. coronatus* (Tyrrell and MacLeod 1972; Ben-Ze'ev and Kenneth 1982).

***Conidiobolus iuxtagenitus* S.D. Waters & Callaghan, Mycol. Res. 93(2): 223 (1989)**

MycoBank No: MB135617

Figure 5a–g

Specimens examined. CHINA, Anhui Province, Plant detritus, 8 Nov 2008, *C.F. Wang*, RCEF 4445.

Description. Colonies on PDA at 21 °C after 3 d white, flat, slow-growing, reaching ca. 13 mm in diameter. Mycelia colourless, 5.5–11 µm wide. Primary conidiophores, positively phototropic, arising from hyphal segments, colourless, 28–75 × 7.5–10 µm, unbranched and producing a single globose conidium. Primary conidia forcibly discharged, globose, 27–37 × 21–28 µm, with a basal papilla 6–10 µm wide. Secondary conidia arising from primary conidia, similar to, but smaller than the primary ones, forcibly discharged. Tertiary conidium fusiform arising from primary conidia, 30–45 × 16–22 µm. Zygospores in a position separated by a short beak near a lateral conjugation, globose to subglobose, smooth, 21–25 × 17–24 µm, with a 1–2 µm thick wall.

Notes. The ex-type living culture is ARSEF 6378 (United Kingdom, Staffordshire, Plant detritus, 31 October 1983, M. F. Smith).

***Conidiobolus khandalensis* Sriniv. & Thirum., Mycologia 54(6): 692 (1963) [1962]**

MycoBank No: MB328754

Figure 5h

Specimens examined. INDIA, Khandala, Dec. 1961, *Srinivasan and Thirumalachar*, ATCC 15162.

Description. Refer to Srinivasan and Thirumalachar (1962b). Microconidia produced from global conidia on the 2% water-agar at 16 °C (Fig. 5h).

Notes. According to the original morphological description (Srinivasan and Thirumalachar 1962b) and the re-examination by King (1977), microconidia have not been reported. However, we observed the microconidia produced from global conidia on 2% water-agar at 16 °C. Moreover, this specimen was located in the *Conidiobolus* lineage (Figure 1) which was supported by our morphological analyses.

***Microconidiobolus* B. Huang & Y. Nie, gen. nov.**

MycoBank No: MB831597

Etymology. Referring to small discharged primary conidia.

Type species. *Microconidiobolus paulus* (Drechsler) B. Huang & Y. Nie.

Description. Mycelia colourless. Primary conidiophores simple and short, bearing a single primary conidia. Primary conidia forcibly discharged, multinucleate, colourless, globose to obovoid, usually small, mostly less than 20 µm. Only globose repli-

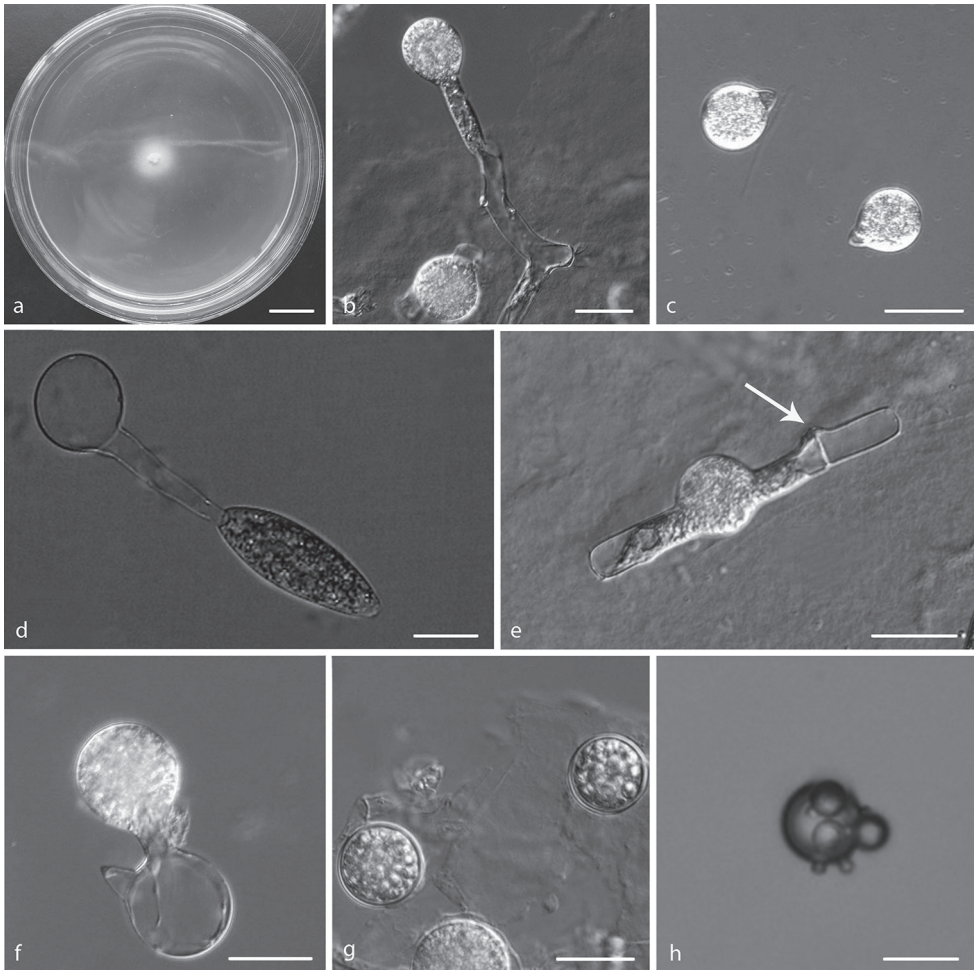


Figure 5. **a–g** *Conidiobolus iuxtagenitus* **h** *Conidiobolus khandalensis* **a** colony on PDA after 3 d at 21 °C **b** primary conidiophores bearing primary conidia **c** primary conidia **d** tertiary fusiform conidium from a globose spore **e** zygospore formation with the beak almost emptied of protoplasm **f** production of secondary conidia **g** zygospores **h** microconidia produced from global conidia. Scale bars: 10 mm (**a**); 20 µm (**b–h**).

cative conidia produced, similar and smaller than primary conidia. Chlamydoconidia globose, formed terminally on hyphae or from globose cells by thickening of the wall. Zygospores formed in axial alignment with two conjugating segments, globose to ellipsoidal, smooth and yellowish.

Notes. This genus includes three species producing smaller primary conidia (mostly less than 20 µm) without microspores or capilliconidia compared to other *Conidiobolus* spp. These three species are *C. nodosus*, *C. paulus* and *C. terrestris*. According to the taxonomic scheme of *Conidiobolus* by King (1977), *C. undulatus* is a synonym of *C. paulus*, which is supported herein by molecular evidence (Figure 1). However, the phylogeny does not support *C. nodosus* and *C. terrestris* as synonyms of *C. lachnodes*, since the former two were located in clade IV and the latter in clade II

(Figure 1). Therefore, we accept the taxonomic status at species level for *C. nodosus* and *C. terrestris*, based on the morphological and phylogenetic analyses.

***Microconidiobolus paulus* (Drechsler) B. Huang & Y. Nie, comb. nov.**

MycoBank No: MB831605

Conidiobolus paulus Drechsler, Bull. Torrey bot. Club. 84: 269 (1957). Basionym.
= *Conidiobolus undulatus* Drechsler, Bull. Torrey bot. Club. 84: 275 (1957).
= *Conidiobolus parvus* Drechsler, Bull. Torrey bot. Club. 89: 233 (1962).

Description. Refer to Drechsler (1957a).

Notes. The ex-type living culture is ATCC 12942 (United States, Wisconsin, 18 November 1954, Drechsler).

***Neoconidiobolus* B. Huang & Y. Nie, gen. nov.**

MycoBank No: MB831598

Etymology. Referring to the subgenus *Conidiobolus* raised to generic rank.

Type species. *Neoconidiobolus thromboides* (Drechsler) B. Huang & Y. Nie.

Description. Mycelia colourless. Primary conidiophores simple, sometimes branched from hyphal knots or differentiated from aerial hyphae, positively phototropic, bearing a single primary conidium. Primary conidia forcibly discharged, multinucleate, colourless, globose, pyriform to obovoid. Replicative conidia similar and smaller than primary conidia. Chlamydospores globose, formed terminally on hyphae or from globose cells by thickening of the wall. Zygospores formed in axial alignment with two conjugating segments, globose to ellipsoidal, smooth, colourless, rarely pale yellowish.

Notes. The genus *Neoconidiobolus* is strikingly similar to the subgenus *Conidiobolus* which produces neither microconidia nor capilliconidia. All members in the clade of *Neoconidiobolus* share the following characteristics: forcibly discharged, colourless, globose, pyriform to obovoid primary conidia. Two kinds of replicative conidia produced. One is discharged, similar and smaller than primary conidia and the other is elongate and forcibly discharged. Two types of resting spores produced: zygospores and chlamydospores.

***Neoconidiobolus thromboides* (Drechsler) B. Huang & Y. Nie, comb. nov.**

MycoBank No: MB831606

Figure 6

Conidiobolus thromboides Drechsler, J. Wash. Acad. Sci. 43: 38 (1953). Basionym.

Specimens examined. CHINA, Anhui Province, Plant detritus, 21 Feb 2009, C.F Wang, RCEF 4492.

Description. Colonies grown on PDA for 3 d at 25 °C, white, reaching ca. 30 mm diameter. Mycelium colourless, filamentous, 5–7.5 µm wide. Primary conidiophores colourless, unbranched and producing a single conidium, 50–122.5 × 6–16.5 µm. Primary conidia forcibly discharged, colourless, globose to subglobose, 20–26.5 µm wide, 26.5–34 µm long, including a basal papilla 6–10 µm wide. Secondary conidia globose, forming from the primary conidia. Zygospores most often formed between segments of separate hyphae. Mature zygospores smooth, globose to subglobose, 25–30 µm in diameter with wall 2–3 µm thick.

Notes. The ex-type living culture is ATCC 12587 (United States, New Hampshire, September 1957, Drechsler).

More new combinations

In addition to previously described taxa, more new combinations were proposed here-in and their descriptions refer to relevant protologues.

***Capillidium bangaloreense* (Sriniv. & Thirum.) B. Huang & Y. Nie, comb. nov.**
MycoBank No: MB831607

Conidiobolus bangalorensis Sriniv. & Thirum., Mycologia 59(4): 702 (1967). Basionym.

***Capillidium denaeosporum* (Drechsler) B. Huang & Y. Nie, comb. nov.**
MycoBank No: MB831608

Conidiobolus denaeosporus Drechsler, J. Wash. Acad. Sci. 47: 309 (1957). Basionym.

***Capillidium lobatum* (Sriniv. & Thirum.) B. Huang & Y. Nie, comb. nov.**
MycoBank No: MB831609

Conidiobolus lobatus Sriniv. & Thirum., J. Elisha Mitchell scient. Soc. 84: 212 (1968).
Basionym.

***Capillidium pumilum* (Drechsler) B. Huang & Y. Nie, comb. nov.**
MycoBank No: MB831610

Conidiobolus pumilus Drechsler, J. Wash. Acad. Sci. 45: 115 (1955). Basionym.
= *Conidiobolus globuliferus* Drechsler, Am. J. Bot. 43: 783 (1957) [1956].
= *Conidiobolus inordinatus* Drechsler, J. Wash. Acad. Sci. 47: 312 (1957).

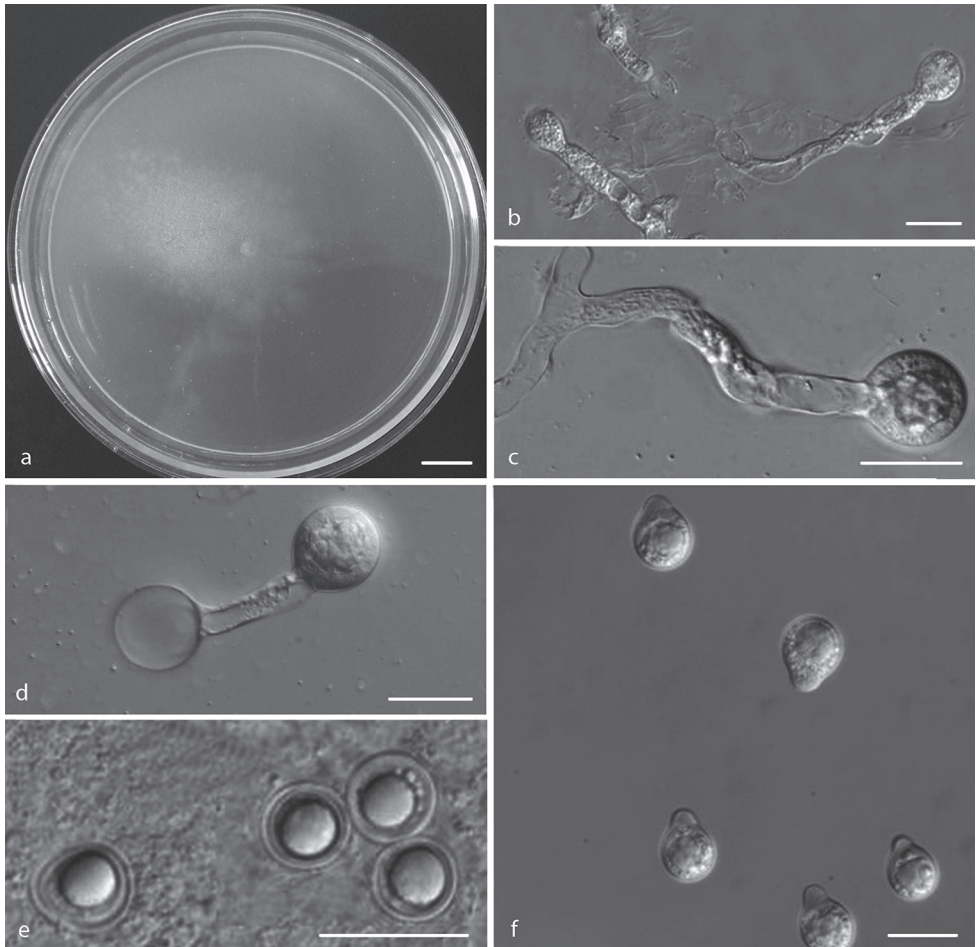


Figure 6. *Neoconidiobolus thromboides* **a** colony on PDA after 3 d at 25 °C **b, c** primary conidiophores bearing primary conidia **d** production of secondary conidia **e** zygospores **f** primary conidia. Scale bars: 10 mm (**a**); 20 μ m (**b–d, f**); 40 μ m (**e**).

Capillidium rhyosporum (Drechsler) B. Huang & Y. Nie, comb. nov.
Mycobank No: MB831611

Conidiobolus rhyosporus Drechsler, Am. J. Bot. 41: 567 (1954). Basionym.

Microconidiobolus nodosus (Sriniv. & Thirum.) B. Huang & Y. Nie, comb. nov.
Mycobank No: MB831624

Conidiobolus nodosus Sriniv. & Thirum., Mycologia 59(4): 705 (1967). Basionym.

***Microconidiobolus terrestris* (Sriniv. & Thirum.) B. Huang & Y. Nie, comb. nov.**
MycoBank No: MB831625

Conidiobolus terrestris Sriniv. & Thirum., Mycopathol. Mycol. appl. 36(3–4): 344 (1968). Basionym.

***Neoconidiobolus couchii* (Sriniv. & Thirum.) B. Huang & Y. Nie, comb. nov.**
MycoBank No: MB831626

Conidiobolus couchii Sriniv. & Thirum., J. Elisha Mitchell scient. Soc. 84: 211 (1968).
Basionym.

***Neoconidiobolus lachnodes* (Drechsler) B. Huang & Y. Nie, comb. nov.**
MycoBank No: MB831627

Conidiobolus lachnodes Drechsler, Am. J. Bot. 42: 442 (1955). Basionym.

***Neoconidiobolus mirabilis* (Y. Nie & B. Huang) B. Huang & Y. Nie, comb. nov.**
MycoBank No: MB831628

Conidiobolus mirabilis Y. Nie & B. Huang, Mycol. Progr. 17(10): 1204 (2018). Basionym.

***Neoconidiobolus osmodes* (Drechsler) B. Huang & Y. Nie, comb. nov.**
MycoBank No: MB831629

Conidiobolus osmodes Drechsler, Am. J. Bot. 41: 571 (1954). Basionym.
= *Conidiobolus antarcticus* S. Tosi, Caretta & Humber, Mycotaxon 90(2): 344 (2004).

***Neoconidiobolus pachyzygosporus* (Y. Nie & B. Huang) B. Huang & Y. Nie, comb. nov.**
MycoBank No: MB831630

Conidiobolus pachyzygosporus Y. Nie & B. Huang, Mycol. Progr. 17(10): 1206 (2018).
Basionym.

***Neoconidiobolus sinensis* (Y. Nie, X.Y. Liu & B. Huang) B. Huang & Y. Nie, comb. nov.**

MycoBank No: MB831631

Conidiobolus sinensis Y. Nie, X.Y. Liu & B. Huang, Mycotaxon 120: 432 (2012). Basionym.

***Neoconidiobolus stilbeus* (Y. Nie & B. Huang) B. Huang & Y. Nie, comb. nov.**

MycoBank No: MB831632

Conidiobolus stilbeus Y. Nie & B. Huang, Mycosphere 7(6): 804 (2016). Basionym.

***Neoconidiobolus stromoideus* (Sriniv. & Thirum.) B. Huang & Y. Nie, comb. nov.**

MycoBank No: MB831633

Conidiobolus stromoideus Sriniv. & Thirum., Sydowia 16(1–6): 65 (1963) [1962].
Basionym.

***Neoconidiobolus vermicola* (J.S. McCulloch) B. Huang & Y. Nie, comb. nov.**

MycoBank No: MB831634

Entomophthora vermicola J.S. McCulloch, Trans. Br. mycol. Soc. 68(2): 173 (1977).
Basionym.

Macrobotophthora vermicola (J.S. McCulloch) B.E. Tucker, Mycotaxon 13(3): 499
(1981).

Discussion

The phylogenetic position of *Basidiobolus* in the Kingdom *Fungi* has been problematic for a long time. Previous phylogenetic analyses of the rDNA (18S, 28S and 5.8S) sequences grouped *Basidiobolus* outside or basal in the *Entomophthorales* (Nagahama et al. 1995; Jensen et al. 1998; White et al. 2006). Combined with the study of other protein-coding molecular markers, *Basidiobolus* was located inside the *Entomophthorales* (James et al. 2006). Recently, according to the phylogeny of much more available molecular data of entomophthoroid fungi in three families, *Basidiobolus* was grouped basal to other entomophthoroid taxa (Gryganskyi et al. 2012) which was also supported by the phylogenomic analyses of zygomycete fungi (Spatafora et al. 2016) and by the multi-gene analyses in this study. Although the morphological characteristics of *Batkoa* were similar to *Conidiobolus*, the *Batkoa* lineage appeared to be most closely related to the other taxa in the *Entomophthoraceae* Clade and should be distinguished

from *Conidiobolus* lineage by its obligate pathogenicity for invertebrates and by staining readily, while most members of *Conidiobolus* are saprobic and non-staining.

The phylogenetic relationship of the genus *Conidiobolus* has been unclear for a long time, because of its high heterology (Gryganskyi et al. 2013). This article used more available ex-type strains to revise this genus, based on phylogeny and morphology. According to Figure 1, four main clades were reconstructed and the results showed that *Conidiobolus* s.l. is not a monophyletic group but paraphyletic with *Macrobotophthora vermicola*. The *M. vermicola* was originally placed in *Entomophthora* (McCulloch 1977) and transferred to *Macrobotophthora*, based on the morphological characters of primary spores, secondary spores and zygospores (Tucker 1981). The paraphyletic relationship between *Macrobotophthora vermicola* and *Conidiobolus* s.l. was also revealed by Gryganskyi et al. (2012). In this paper, we treated it as a new combination and, therefore, proposed a monophyletic group of the new genus *Neoconidiobolus*.

In Clade I of the genus *Capillidium*, seven species grouped in a monophyletic clade with good support (100/1.00) and the synapomorph of producing capilliconidia: *Conidiobolus adiaeretus* (= *Capillidium adiaeretum*), *Co. bangalorensis* (= *Ca. bangalorensis*), *Co. denaeosporus* (= *Ca. denaeosporum*), *Co. heterosporus* (= *Ca. heterosporum*), *Co. lobatus* (= *Ca. lobatum*), *Co. pumilus* (= *Ca. pumilum*) and *Co. rhyso sporus* (= *Ca. rhyso sporum*). As a note, *Co. denaeosporus* was synonymised with *Co. pumilus* (King 1976b), but herein its taxonomic status of species level was accepted according to the phylogeny. *Co. adiaeretus* forms not only capilliconidia but also microspores (Callaghan et al. 2000).

In Clade II of the genus *Neoconidiobolus*, all 14 strains comprising 10 species produce neither microspores nor capilliconidia. Amongst these, *C. antarcticus* was identified as a synonym of *C. osmodes* (Chen and Huang 2018), which was confirmed here as they grouped into a robust clade.

Considering its long history and significant impact, we kept and emended the genus *Conidiobolus* and the original illustrations of the type species *C. utriculosus* (Brefeld 1884) were designated as its lectotype. Thus, we were able to recognise clade III under the genus name *Conidiobolus* on the basis of its synapomorph, namely microspores. In Clade III of the genus *Conidiobolus*, all species definitely produce microspores, except *Conidiobolus dabieshanensis*, *C. iuxtagenitus*, *C. khandalensis* and *C. lichenicolus*. Microspores have never been observed in *C. dabieshanensis* and *C. iuxtagenitus* (King 1977; Waters and Callaghan 1989; Nie et al. 2017), but cases for *C. khandalensis* and *C. lichenicolus* are somewhat different. For *C. khandalensis*, the protologue did not document any microspores (Srinivasan and Thirumalachar 1962b; King 1977), but they can be observed on 2% water-agar at 16 °C (Fig. 5h). Although the microspore of *C. lichenicolus* was not mentioned in the original description, the ability to produce microspores has been exhibited in accordance with original illustrations (Srinivasan and Thirumalachar 1968a). The phylogeny also resulted in the following taxonomic treatments. On the one hand, some previously synonymised taxa recover their specific status, for example, *C. gonimodes*, *C. megalotocus* and *C. mycophagus* should be separated from *C. incongruus*, *C. macrosporus* and *C. mycophilus*, respectively. On the other hand, *C. chlamydosporus* is synonymised with *C. firmipilleus*.

In Clade IV of the genus *Microconidiobolus*, *Conidiobolus undulatus* was identified as a synonym of *C. paulus* (= *M. paulus*) by King (1976b), which is supported by our molecular data. Otherwise, *C. nodosus* (= *M. nodosus*) and *C. terrestris* (= *M. terrestris*) were classified as synonyms of *C. lachnodes* (= *Neoconidiobolus lachnodes*) in the study of King (1976b). Morphologically, *C. lachnodes* bears larger primary conidia (9–25 × 10–27 µm) than *C. nodosus* (13–16 × 17–22 µm) and *C. terrestris* (8–12 µm in width) (Drechsler 1955b; Srinivasan and Thirumalachar 1967, 1968a). Furthermore, *C. lachnodes* was located in Clade II and is distantly related to *C. nodosus* and *C. terrestris*. Therefore, *C. nodosus* and *C. terrestris* are accepted as two distinct species. This clade comprises four ex-type strains, all producing smaller primary conidia (mostly less than 20 µm) and can be morphologically easily distinguished from other *Conidiobolus* species.

Phylogenetically, *Conidiobolus lamprauges* does group with Clade III and received strong bootstrap support (100/1.00). Morphologically, this species produces small primary conidia (12.5–20 × 15–22 µm) without microconidia or capilliconidia and is similar to species within Clade IV. Its taxonomic status remains unclear in the present study.

Acknowledgements

We thank Dr. Z.F. Yu (Yunnan University) for improving the manuscript. We also thank Y. Gao (Jiangxi Agricultural University) for collecting some *Conidiobolus* strains. This project was supported by the National Natural Science Foundation of China (Nos. 31900008, 30770008 and 31670019).

References

- Bałazy S, Wiśniewski J, Kaczmarek S (1987) Some noteworthy fungi occurring on mites. Bulletin of the Polish Academy of Sciences, Biological Sciences 35: 199–224.
- Balazy S (1993) Entomophthorales. Flora of Poland (Flora Polska), Fungi (Mycota) 24: 1–356. Polish Academy of Sciences, W. Szafer Institute of Botany, Kraków, Poland.
- Ben-Ze'ev IS, Kenneth RG (1982) Features-criteria of taxonomic value in the *Entomophthorales*: I. A revision of the *Batkoan* classification. Mycotaxon 14: 393–455.
- Brefeld O (1884) *Conidiobolus utriculosus* und *minor*. Untersuchungen aus der Gesamtgebiete der Mykologie 6(2): 35–78.
- Bruns TD, White TJ, Taylor JW (1991) Fungal molecular systematics. Annual Review of Ecology and Systematics 22: 525–564. <https://doi.org/10.1146/annurev.es.22.110191.002521>
- Callaghan AA, Waters SD, Manning RJ (2000) Alternative repetitional conidia in *Conidiobolus adiaeretus*: development and germination. Mycological Research 104: 1270–1275. <https://doi.org/10.1017/S0953756200003063>
- Chen MJ, Huang B (2018) *Conidiobolus antarcticus*, a synonym of *C. osmodes*. Mycotaxon 133(4): 635–641. <https://doi.org/10.5248/133.635>
- Costantin J (1897) Sur une entomophthorée nouvelle. Bulletin de la Société Mycologique de France 13: 38–43.

- Couch JN (1939) A new *Conidiobolus* with sexual reproduction. *American Journal of Botany* 26: 119–130. <https://doi.org/10.1002/j.1537-2197.1939.tb12878.x>
- DePriest PT (1993) Small subunit rDNA variation in a population of lichen fungi due to optional group I introns. *Gene* 134: 67–74. [https://doi.org/10.1016/0378-1119\(93\)90175-3](https://doi.org/10.1016/0378-1119(93)90175-3)
- Drechsler C (1952) Widespread distribution of *Delacroixia coronata* and other saprophytic *Entomophthoraceae* in plant detritus. *Science* 115: 575–576. <https://doi.org/10.1126/science.115.2995.575>
- Drechsler C (1953a) Three new species of *Conidiobolus* isolated from leaf mold. *Journal of the Washington Academy of Science* 43(2): 29–34.
- Drechsler C (1953b) Two new species of *Conidiobolus* occurring in leaf mold. *American Journal of Botany* 40(3): 104–115. <https://doi.org/10.1002/j.1537-2197.1953.tb06458.x>
- Drechsler C (1954) Two species of *Conidiobolus* with minutely ridged zygospores. *American Journal of Botany* 41: 567–575. <https://doi.org/10.1002/j.1537-2197.1954.tb14380.x>
- Drechsler C (1955a) A small *Conidiobolus* with globose and with elongated secondary conidia. *Journal of Washington Academy of Sciences* 45(4): 114–117.
- Drechsler C (1955b) Three new species of *Conidiobolus* isolated from decaying plant detritus. *American Journal of Botany* 42(5): 437–443. <https://doi.org/10.1002/j.1537-2197.1955.tb11144.x>
- Drechsler C (1955c) Two new species of *Conidiobolus* that produce microconidia. *American Journal of Botany* 42(9): 793–802. <https://doi.org/10.1002/j.1537-2197.1955.tb10424.x>
- Drechsler C (1956) Two new species of *Conidiobolus*. *American Journal of Botany* 43(10): 778–787. <https://doi.org/10.1002/j.1537-2197.1956.tb11168.x>
- Drechsler C (1957a) Two small species of *Conidiobolus* forming lateral zygospores. *Bulletin of the Torrey Botanical Club* 84(4): 268–280. <https://doi.org/10.2307/2482673>
- Drechsler C (1957b) A new species of *Conidiobolus* with distended conidiophores. *Sydowia Annales Mycologici* 9: 189–192.
- Drechsler C (1957c) Two medium-sized species of *Conidiobolus* occurring in Colorado. *Journal of Washington Academy of Sciences* 47: 309–315.
- Drechsler C (1960) Two new species of *Conidiobolus* found in plant detritus. *American Journal of Botany* 47: 368–377. <https://doi.org/10.1002/j.1537-2197.1960.tb07138.x>
- Drechsler C (1961) Two species of *Conidiobolus* often forming zygospores adjacent to antheridium-like distentions. *Mycologia* 53(3): 278–303. <https://doi.org/10.2307/3756275>
- Drechsler C (1962) A small *Conidiobolus* with resting spores that germinate like zygospores. *Bulletin of the Torrey Botanical Club* 89(4): 233–240. <https://doi.org/10.2307/2483199>
- Drechsler C (1965) A robust *Conidiobolus* with zygospores containing granular parietal protoplasm. *Mycologia* 57(6): 913–926. <https://doi.org/10.2307/3756891>
- Edgar RC (2004) MUSCLE: Multiple sequence alignment with high accuracy and high throughput. *Nucleic Acids Research* 32: 1792–1797. <https://doi.org/10.1093/nar/gkh340>
- Gargas A, DePriest PT (1996) A nomenclature for fungal PCR primers with examples from intron-containing SSU rDNA. *Mycologia* 88: 745–748. <https://doi.org/10.2307/3760969>
- Gryganskyi AP, Humber RA, Smith ME, Miadlikovska J, Wu S, Voigt K, Walther G, Anishchenko IM, Vilgalys R (2012) Molecular phylogeny of the *Entomophthoromycota*. *Molecular Phylogenetics and Evolution* 65: 682–694. <https://doi.org/10.1016/j.ympev.2012.07.026>

- Gryganskyi AP, Humber RA, Smith ME, Hodge K, Huang B, Voigt K, Vilgalys R (2013) Phylogenetic lineages in *Entomophthoromycota*. *Persoonia* 30: 94–105. <https://doi.org/10.3767/003158513X666330>
- Hibbett DS, Binder M, Bischo JF, Blackwell M, Cannon PF, Eriksson OE, Huhndorf S, James T, Kirk PM, Lücking R, Lumbsch HT, Lutzoni F, Matheny PB, McLaughlin DJ, Powell MJ, Redhead S, Schoch CL, Spatafora JW, Stalpers JA, Vilgalys R, Aime MC, Aptroot A, Bauer R, Begerow D, Benny GL, Castlebury LA, Crous PW, Dai YC, Gams W, Geiser DM, Grith GW, Gueidan C, Hawksworth DL, Hestmark G, Hosaka K, Humber RA, Hyde KD, Ironside JE, Kõljalg U, Kurtzman CP, Larsson KH, Lichtwardt R, Longcore J, Miadlikowska J, Miller A, Moncalvo JM, Mozley-Standridge S, Oberwinkler F, Parmasto E, Reeb V, Rogers JD, Roux C, Ryvarden L, Sampaio JP, Schüßler A, Sugiyama J, Thorn RG, Tibell L, Untereiner WA, Walker C, Wang Z, Weir A, Weiss M, White MM, Winka K, Yao YJ, Zhang N (2007) A higher-level phylogenetic classification of the Fungi. *Mycological Research* 111: 509–547. <https://doi.org/10.1016/j.mycres.2007.03.004>
- Huang B, Humber RA, Hodge KT (2007) A new species of *Conidiobolus* from Great Smoky Mountains National Park. *Mycotaxon* 100: 227–233.
- Humber RA (1989) Synopsis of a revised classification for the *Entomophthorales* (*Zygomycotina*). *Mycotaxon* 34: 441–460. <https://doi.org/10.1098/rspa.1937.0056>
- Humber RA (1997) Fungi: identification. In: LA Lacey (Ed.) *Manual of Techniques in Insect Pathology*. Academic Press, London. <https://doi.org/10.1016/B978-012432555-5/50011-7>
- James TY, Kau F, Schoch C, Matheny PB, Hofstetter V, Cox CJ, Celio G, Geuidan C, Fraker E, Miadlikowska J, Lumbsch HT, Rauhut A, Reeb V, Arnold AE, Amtoft A, Stajich JE, Hosaka K, Sung GH, Johnson D, O'Rourke B, Crockett M, Binder M, Curtis JM, Slot JC, Wang Z, Wilson AW, Schüßler A, Longcore JE, O'Donnell K, Mozley-Standridge S, Porter D, Letcher PM, Powell MJ, Taylor JW, White MW, Grith GW, Davies DR, Humber RA, Morton JB, Sugiyama J, Rossman A, Rogers JD, Pfister DH, Hewitt D, Hansen K, Hambleton S, Shoemaker RA, Kohlmeyer J, Volkmann-Kohlmeyer B, Spotts RA, Serdani M, Crous PW, Hughes KW, Matsuura K, Langer E, Langer G, Untereiner WA, Lücking R, Büdel B, Geiser DM, Aptroot A, Diederich P, Schmitt I, Schultz M, Yahr R, Hibbett DS, Lutzoni F, McLaughlin DJ, Spatafora JW, Vilgalys R (2006) Reconstructing the early evolution of Fungi using a six-gene phylogeny. *Nature* 443: 818–822. <https://doi.org/10.1038/nature05110>
- Jensen AB, Gargas A, Eilenberg J, Rosendahl S (1998) Relationships of the insect-pathogenic order *Entomophthorales* (*Zygomycota*, *Fungi*) based on phylogenetic analyses of nucleus small subunit ribosomal DNA sequences (SSU rDNA). *Fungal Genetics and Biology* 24(3): 325–334. <https://doi.org/10.1006/fgbi.1998.1063>
- King DS (1976a) Systematics of *Conidiobolus* (*Entomophthorales*) using numerical taxonomy I. Taxonomic considerations. *Canadian Journal of Botany* 54: 45–65. <https://doi.org/10.1139/b76-008>
- King DS (1976b) Systematics of *Conidiobolus* (*Entomophthorales*) using numerical taxonomy II. Taxonomic considerations. *Canadian Journal of Botany* 54: 1285–1296. <https://doi.org/10.1139/b76-141>

- King DS (1977) Systematics of *Conidiobolus* (*Entomophthorales*) using numerical taxonomy III. Descriptions of recognized species. *Canadian Journal of Botany* 55: 718–729. <https://doi.org/10.1139/b77-086>
- Liu M, Rombach MC, Humber RA, Hodge KT (2005) What's in a name? *Aschersonia insperata*: a new pleoanamorphic fungus with characteristics of *Aschersonia* and *Hirsutella*. *Mycologia* 97: 249–256. <https://doi.org/10.3852/mycologia.97.1.246>
- Liu XY, Voigt K (2011) Molecular Characters of Zygomycetous Fungi. In: Gherbawy Y, Voigt K (Eds) *Molecular Identification of Fungi*. Springer-Verlag, Heidelberg, Berlin, 461–488. https://doi.org/10.1007/978-3-642-05042-8_20
- Martin GW (1925) Morphology of *Conidiobolus villosus*. *Botanical Gazette* 80: 311–318. <https://doi.org/10.1086/333540>
- Mcculloch JS (1977) New species of nematophagous fungi from Queensland. *Transactions of the British Mycological Society* 68(2): 173–179. [https://doi.org/10.1016/S0007-1536\(77\)80005-3](https://doi.org/10.1016/S0007-1536(77)80005-3)
- Miller MA, Pfeiffer W, Schwartz T (2010) Creating the CIPRES Science Gateway for Inference of Large Phylogenetic Trees. *Proceedings of the Gateway Computing Environments Workshop (GCE)*, 14 Nov. 2010, New Orleans, 8 pp. <https://doi.org/10.1109/GCE.2010.5676129>
- Nagahama T, Sato H, Shimazu M, Sugiyama J (1995) Phylogenetic divergence of the entomophthoralean fungi: evidence from nuclear 18S ribosomal RNA gene sequences. *Mycologia* 87: 203–209. <https://doi.org/10.2307/3760906>
- Nie Y, Yu CZ, Liu XY, Huang B (2012) A new species of *Conidiobolus* (*Ancylistaceae*) from Anhui, China. *Mycotaxon* 120: 427–435. <https://doi.org/10.5248/120.427>
- Nie Y, Tang XX, Liu XY, Huang B (2016) *Conidiobolus stilbeus*, a new species with mycelial strand and two types of primary conidiophores. *Mycosphere* 7(6): 801–809. <https://doi.org/10.5943/mycosphere/7/6/11>
- Nie Y, Tang XX, Liu XY, Huang B (2017) A new species of *Conidiobolus* with chlamydospores from Dabie Mountains, eastern China. *Mycosphere* 8(7): 809–816. <https://doi.org/10.5943/mycosphere/8/7/1>
- Nie Y, Qin L, Yu DS, Liu XY, Huang B (2018) Two new species of *Conidiobolus* occurring in Anhui, China. *Mycological Progress* 17(10): 1203–1211. <https://doi.org/10.1007/s11557-018-1436-z>
- Nie Y, Wang L, Cai Y, Tao W, Zhang YJ, Huang B (2019) Mitochondrial genome of the entomophthoroid fungus *Conidiobolus heterosporus* provides insights into evolution of basal fungi. *Applied Microbiology and Biotechnology* 103(3): 1379–1391. <https://doi.org/10.1007/s00253-018-9549-5>
- Posada D, Crandall KA (1998) MODELTEST: testing the model of DNA substitution. *Bioinformatics* 14: 817–818. <https://doi.org/10.1093/bioinformatics/14.9.817>
- Rambaut A (2012) FigTree version 1.4.0. <http://tree.bio.ed.ac.uk/software/figtree/>
- Ronquist F, Huelsenbeck JP (2003) MRBAYES 3: Bayesian phylogenetic inference under mixed models. *Bioinformatics* 19: 1572–1574. <https://doi.org/10.1093/bioinformatics/btg180>
- Saccardo PA, Sydow P (1899) *Delacroixia* Sacc. et Syd. *Sylloge Fungorum* 14: 1–457.

- Silvestro D, Michalak I (2012) RaxmlGUI: a graphical front-end for RAxML. *Organisms Diversity & Evolution* 12: 335–337. <https://doi.org/10.1007/s13127-011-0056-0>
- Spatafora JW, Chang Y, Benny GL, Lazarus K, Smith ME, Berbee ML, Bonito G, Corradi N, Grigoriev I, Gryganskyi A, James TY, O'Donnell K, Roberson RW, Taylor TN, Uehling J, Vilgalys R, White MM, Stajich JE (2016) A phylum-level phylogenetic classification of zygomycete fungi based on genome-scale data. *Mycologia* 108(5): 1028–1046. <https://doi.org/10.3852/16-042>
- Srinivasan MC, Thirumalachar MJ (1961) Studies on species of *Conidiobolus* from India-I. *Sydowia, Annales Mycologici* 15: 237–241.
- Srinivasan MC, Thirumalachar MJ (1962a) Studies on species of *Conidiobolus* from India-II. *Sydowia, Annales Mycologici* 16: 60–66.
- Srinivasan MC, Thirumalachar MJ (1962b) Studies on species of *Conidiobolus* from India-III. *Mycologia* 54(6): 685–693. <https://doi.org/10.2307/3756504>
- Srinivasan MC, Thirumalachar MJ (1965) Studies on species of *Conidiobolus* from India-IV. *Sydowia* 19: 86–91.
- Srinivasan MC, Thirumalachar MJ (1967) Evaluation of taxonomic characters in the genus *Conidiobolus* with key to known species. *Mycologia* 59: 698–713. <https://doi.org/10.2307/3757098>
- Srinivasan MC, Thirumalachar MJ (1968a) Studies on species of *Conidiobolus* from India-V. *Mycopathologia et Mycologia Applicata* 36: 341–346. <https://doi.org/10.1007/BF02050380>
- Srinivasan MC, Thirumalachar MJ (1968b) Two new species of *Conidiobolus* from India. *Journal of the Mitchell Society* 84: 211–212.
- Taylor JW, Jacobson DJ, Kroken S, Kasuga T, Geiser DM, Hibbett DS, Fisher MC (2000) Phylogenetic species recognition and species concepts in fungi. *Fungal Genetics and Biology* 31: 21–32. <https://doi.org/10.1006/fgbi.2000.1228>
- Tretter ED, Johnson EM, Benny GL, Lichtwardt RW, Wang Y, Kandel P, Novak SJ, Smith JF, White MM (2014) An eight-gene molecular phylogeny of the *Kickxellomycotina*, including the first phylogenetic placement of *Asellariales*. *Mycologia* 106(5): 912–935. <https://doi.org/10.3852/13-253>
- Tucker BE (1981) A review of the nonentomogenous *Entomophthorales*. *Mycotaxon* 13: 481–505.
- Tyrrell D, MacLeod DM (1972) A taxonomic proposal regarding *Delacroixia coronata* (*Entomophthoraceae*). *Journal of Invertebrate Pathology* 20(1): 11–13. [https://doi.org/10.1016/0022-2011\(72\)90074-2](https://doi.org/10.1016/0022-2011(72)90074-2)
- Vaidya G, Lohman DJ, Meier R (2011) SequenceMatrix: concatenation software for the fast assembly of multi-gene datasets with character set and codon information. *Cladistics* 27(2): 171–180. <https://doi.org/10.1111/j.1096-0031.2010.00329.x>
- Vilgalys R, Hester M (1990) Rapid genetic identification and mapping of enzymatically amplified ribosomal DNA from several *Cryptococcus* species. *Journal of Bacteriology* 172: 4238–4246. <https://doi.org/10.1128/JB.172.8.4238-4246.1990>
- Waingankar VM, Singh SK, Srinivasan MC (2008) A new thermophilic species of *Conidiobolus* from India. *Mycopathologia* 165: 173–177. <https://doi.org/10.1007/s11046-007-9088-6>

- Watanabe M, Lee K, Goto K, Kumagai S, Sugita-Konishi Y, Hara-Kudo Y (2010) Rapid and effective DNA extraction method with bead grinding for a large amount of fungal DNA. *Journal of Food Protection* 73(6): 1077–1084. <https://doi.org/10.4315/0362-028X-73.6.1077>
- Waters SD, Callaghan AA (1989) *Conidiobolus iuxtagenitus*, a new species with discharge elongate repetitional conidia and conjugation tubes. *Mycological Research* 93: 223–226. [https://doi.org/10.1016/S0953-7562\(89\)80121-2](https://doi.org/10.1016/S0953-7562(89)80121-2)
- White MM, James TY, O'Donnell K, Cafaro MJ, Tanabe Y, Sugiyama J (2006) Phylogeny of the *Zygomycota* based on nuclear ribosomal sequence data. *Mycologia* 98: 872–884. <https://doi.org/10.3852/mycologia.98.6.872>
- Zollera S, Scheidegger C, Sperisena C (1999) PCR primers for the amplification of mitochondrial small subunit ribosomal DNA of lichen-forming ascomycetes. *The Lichenologist* 31(5): 511–516. <https://doi.org/10.1006/lich.1999.0220>

Hydnaceous fungi of China 8. Morphological and molecular identification of three new species of *Sarcodon* and a new record from southwest China

Yan-Hong Mu^{1,2}, Ya-Ping Hu³, Yu-Lian Wei¹, Hai-Sheng Yuan¹

1 CAS Key Laboratory of Forest Ecology and Management, Institute of Applied Ecology, Chinese Academy of Sciences, Shenyang 110164, China **2** University of the Chinese Academy of Sciences, Beijing 100049, China **3** Research Center for Nature Conservation and Biodiversity of Nanjing Institute of Environmental Sciences, Ministry of Ecology and Environment/ State Environmental Protection Scientific Observation and Research Station for Ecological Environment of Wuyi Mountains, Nanjing 210042, China

Corresponding author: Hai-Sheng Yuan (hsyuan@iae.ac.cn)

Academic editor: Alfredo Vizzini | Received 7 January 2020 | Accepted 5 March 2020 | Published 3 April 2020

Citation: Mu Y-H, Hu Y-P, Wei Y-L, Yuan H-S (2020) Hydnaceous fungi of China 8. Morphological and molecular identification of three new species of *Sarcodon* and a new record from southwest China. MycoKeys 66: 83–103. <https://doi.org/10.3897/mycokeys.66.49910>

Abstract

Three new stipitate hydroid fungi, *Sarcodon coactus*, *S. grosselepidotus* and *S. lidongensis*, are described and illustrated, based on morphological characteristics and nuc ITS rDNA + nuc LSU rDNA sequence analyses and a new record, *S. leucopus*, from China is reported. *S. coactus* is characterised by ellipsoid to round basidiocarps, reddish-brown to dark brown, felted pileal surface with white and incurved margins, simple-septate and partly short-celled generative hyphae and irregular subglobose, thin-walled, brown basidiospores with tuberculate ornamentation (tuberculi up to 1 µm long). *S. grosselepidotus* is characterised by infundibuliform to round, occasionally deeply fissured pileus, pale orange to dark ruby pileal surface with ascending and coarse scales, simple-septate generative hyphae and irregular ellipsoid to globose, thin-walled, brown basidiospores with tuberculate ornamentation (tuberculi up to 0.7 µm long). *S. lidongensis* is characterised by plano-convex to somewhat depressed and regular orbicular pileus, light brown to dark brown pileal surface with adhering squamose and purplish-brown, incurved and occasionally incised margin, cylindrical or broadened below stipe, simple-septate generative hyphae and irregular ellipsoid to subglobose, thin-walled basidiospores with tuberculate ornamentation (tuberculi up to 1 µm long). The absence of the clamp connection is the common morphological characteristic of these three new species; however, *S. leucopus*, a new record from China, has frequently clamped generative hyphae. Molecular analyses confirm the phylogenetic positions of three new and the new record species. The discriminating characters of these three new species and closely related species are discussed and a key to the species of *Sarcodon* from China is provided.

Keywords

Bankeraceae, ITS and LSU, new species and record, taxonomy, Thelephorales

Introduction

The genus *Sarcodon* Quéél. ex P. Karst. (1881), together with *Bankera* Coker and Beers ex Pouzar (1955), *Hydnellum* P. Karst. (1896) and *Phellodon* P. Karst. (1881), belong to Bankeraceae, Thelephorales of Basidiomycota. They are a group of stipitate hydroid fungi that inhabit the soil (Maas Geesteranus 1975).

Species of Bankeraceae are ectomycorrhizal fungi which associate with many kinds of angiosperm and gymnosperm trees, especially with Pinaceae and Fagaceae, such as *Pinus strobus*, *Picea sitchensis*, *Fagus grandifolia*, *Quercus rubra* and *Castanea sativa* (Maas Geesteranus 1975; Harrison 1984; Baird 1986; Baird et al. 2013) and usually occur in natural and comparatively undisturbed forests (Arnolds 1989). They can obtain energy from and transport nutrients to the host plants and are of great ecological significance in promoting forest vegetation recovery (Gardes and Bruns 1996; Erland and Taylor 1999). These fungi are vulnerable to impact due to changes in the environment, such as habitat loss, nitrogen deposition, decrease of host tree species and subsequently increased ground temperatures (Arnolds 1989; Otto 1992; Vesterholt et al. 2000; Newton et al. 2002; Arnolds 2010; Baird et al. 2013). In Europe, stipitate hydroid fungi have been considered one of the most endangered groups of macrofungi and have been included in Red Data Lists (Hroudá 1999; Walley and Verbeke 2000; Hroudá 2005; Nitare 2006; Senn-Irlet et al. 2007), which have been used as indicators that forests need to be protected (Ainsworth 2005; Nitare 2019).

The genus *Sarcodon* is characterised by solitary to gregarious, stipitate, pileate basidiocarps, hydnoeous hymenophore, the monomitic hyphal system owning inflating or not inflating hyphae, the presence or absence of clamp connections and irregular ellipsoid to globose, tuberculate basidiospores which are brown in mass. Besides, the dry basidiocarps often produce farinaceous to fragrant or acidic odour (Maas Geesteranus 1971; Baird 1986; Arnolds 2003; Baird et al. 2013). In morphology, *Sarcodon* is closely related to *Hydnellum*, but the former usually has soft and fleshy basidiocarps and the latter has hard and corky basidiocarps (Maas Geesteranus 1971; Larsson et al. 2019). The macro-morphology of these two genera often depends on their environmental parameters, such as precipitation, temperature or obstructions. Additionally, the variable growth of basidiocarps makes it difficult to distinguish each other. Therefore, it is essential to support and confirm their identities using molecular sequence data (Baird et al. 2013). Recent molecular phylogenetic analyses reveal that *Sarcodon* and *Hydnellum* form paraphyletic lineage and suggest using the spore length as the delimitation between the two genera. *Hydnellum* species had spore lengths in the range 4.45–6.95 μm , while the corresponding range for *Sarcodon* was 7.4–9 μm (Larsson et al. 2019).

Most species of *Sarcodon* have been reported from the northern temperate hemisphere (Maas Geesteranus 1971, 1975; Baird 1986; Stalpers 1993; Pegler et al. 1997; Dai 2011) and are commonly found in North America (Harrison 1964, 1984; Baird 1985, 1986; Baird et al. 2013), Netherlands (Maas Geesteranus 1956, 1976), Spain (Pérez-De-Gregorio et al. 2011), France (Pieri and Rivoire 1994), Russia (Baird 1985) and Italy (Caclalli and Caroti 2005). Some species have also been recorded from southern hemisphere, such as New Zealand (Maas Geesteranus 1964, 1971, 1975) and Australia (Mleczko et al. 2011; Magnago et al. 2015; Hahn et al. 2018). Around 59 species have been described or transferred to the genus according to Index Fungorum (<http://www.indexfungorum.org/>) and MycoBank, but only five taxa have been reported from China (Dai 2011). In addition, some species of *Sarcodon* have medicinal functions, for instance, lowering cholesterol, antioxidant, antibacterial, anti-tumour, improving immunity etc. (Wu et al. 2019).

Investigations of hydneaceous fungi in China have been carried out in recent decades and many *Sarcodon* specimens have been collected. During the study of these specimens, three undescribed species and a new record species have been identified using morphological characters and phylogenetic analyses of nuc rDNA ITS1-5.8S-ITS2 combined with nuc 28S rDNA sequences. Here, we describe them in this paper.

Materials and methods

Morphological studies

Specimens are deposited at the herbarium of the Institute of Applied Ecology, Chinese Academy of Sciences (IFP). Microscopic procedures follow Mu et al. (2019). Microscopic studies used sections mounted in Cotton Blue (CB): 0.1 mg aniline blue dissolved in 60 g pure lactic acid; CB- = acyanophilous. Amyloid and dextrinoid reactions were tested in Melzer's reagent (IKI): 1.5 g KI (potassium iodide), 0.5 g I (crystalline iodine), 22 g chloral hydrate, 20 ml distilled water; IKI- = neither amyloid nor dextrinoid reaction. Sections were mounted in 5% KOH (potassium hydroxide) and studied at magnifications up to 1000 \times using a Nikon Eclipse E600 microscope (Tokyo, Japan) with phase contrast illumination. Dimensions were estimated subjectively with an accuracy of 0.1 μm . In presenting basidiospore size ranges, 5% of the measurements at each end of the range are given in parentheses. The following abbreviations are used in the text: L_m = mean spore length, W_m = mean spore width, Q = range of length/width ratios for specimens studied and n = total number of basidiospores measured from a given number of specimens. The surface morphology for the basidiospores was observed with a Phenom Prox scanning electron microscope (ESEM, Phenom Prox, FEI, The Netherlands) at an accelerating voltage of 10 kV. A thin layer of gold was coated on the samples to avoid charging. Special colour terms are from Rayner (1970) and Munsell (2015).

Molecular procedures and phylogenetic analyses

Fungal taxa and strains used in this study are listed in Table 1. Phire Plant Direct PCR Kit (Thermo Fisher Scientific) procedures were used to extract total genomic DNA from the basidiocarps. Polymerase chain reactions (PCR) were performed on a Bio-Rad T100 Thermal cycler (Bio-RAD Inc). Amplification reactions were performed in a 30 µl reaction mixture using the following final concentrations or total amounts: 0.9 µl template DNA, 15 µl of 2× Phire Plant PCR buffer, 1.5 µl of each primer, 0.6 µl Phire HS II DNA Polymerase and 10.5 µl ddH₂O (double distilled water). The nuc rDNA ITS1-5.8S-ITS2 region (ITS) was amplified with the primers ITS1-F (5' CTTGGT-CATTTAGAGGAAGTAA 3') and ITS4 (5' TCCTCCGCTTATTGATATGC 3') (Baird et al. 2013; Loizides et al. 2016). The 28S nuclear rDNA region was amplified with the primers LROR (5' ACCCGCTGAACTTAAGC 3') and LR7 (5' TACTAC-CACCAAGATCT 3') (Vizzini et al. 2016). The PCR thermal cycling programme conditions were set as follows: initial denaturation at 98 °C for 5 min, followed by 39 cycles at 98 °C for 30 s, × °C (the annealing temperatures for ITS1-F/ITS4 and LROR/LR7 were 57.2 °C and 47.2 °C, respectively) for 30 s, 72 °C for 30 s and a final extension at 72 °C for 1 min. PCR amplification was confirmed on 1% agarose electrophoresis gels stained with ethidium bromide (Stöger et al. 2006). DNA sequencing was performed at the Beijing Genomics Institute (BGI). All newly generated sequences were submitted to GenBank. Additional ITS rDNA and LSU rDNA sequences in the dataset, used to establish phylogenetic relationships, were downloaded from GenBank (<http://www.ncbi.nlm.nih.gov/genbank>) and UNITE (<https://unite.ut.ee/index.php>) (Table 1).

Nuclear ribosomal RNA genes were used to determine the phylogenetic position of the new species. After PCR amplification, the products were sequenced in both directions and the sequences were assembled using DNAMAN 8.0. DNA sequences were aligned with MUSCLE in MEGA7 (Kumar et al. 2016). Alignments were manually adjusted to allow maximum alignment and minimise gaps. Maximum parsimony and Bayesian analysis were applied to the ITS + LSU dataset. All characters were weighted and gaps were treated as missing data. Maximum parsimony analysis (PAUP* version 4.0b10) was used (Swofford 2002). Trees were inferred using the heuristic search option with tree bisection reconnection (TBR) branch swapping and 1,000 random sequence additions. Max-trees were set to 5000 and no-increase, branches of zero length were collapsed and all parsimonious trees were saved. Clade stability was assessed using a bootstrap (BT) analyses with 1,000 replicates (Gaget et al. 2017). Descriptive tree statistics, tree length (TL), consistency index (CI), retention index (RI), rescaled consistency index (RC) and homoplasy index (HI), were calculated for all trees generated under different optimality criteria. Maximum Likelihood (ML) analysis was performed in RAxML v8.2.4 with GTR+I+G model (Stamatakis 2014). The best tree was obtained by executing 1000 rapid bootstrap inferences and thereafter a thorough search was undertaken for the most likely tree using one distinct model/data partition with joint branch length optimisation (Stamatakis et al. 2008). Bayesian analyses with MrBayes 3.2.4 (Cannatella 2015) implementing the Markov

Table 1. Voucher numbers, geographic origins and GenBank accession numbers for the specimens and included, in boldface, are sequences produced in this study.

Species	Geographic origin	Voucher number	GenBank Accessions	
			ITS	28S
<i>Amaurodon aquicoeruleu</i> Agerer	Australia	Isotype in M	AM490944	AM490944
<i>Hydnellum aurantiacum</i> (Batsch) P. Karst.	Norway	OF29502	MK602713	MK602713
<i>H. aurantiacum</i>	Norway	EBendiksen177-07	MK602712	MK602712
<i>H. auratile</i> (Britzelm.) Maas Geest.	Norway	OF242763	MK602715	MK602715
	Norway	OF294095	MK602714	MK602714
<i>H. caeruleum</i> (Hornem.) P. Karst.	Norway	EBendiksen584-11	MK602719	MK602719
	Norway	EBendiksen575-11	MK602718	MK602718
<i>H. complicatum</i> Banker	USA	REB-329	KC571712	
	USA	REB-71	KC571711	
<i>H. conrescens</i> (Pers.) Banker	Norway	O-F-251488	UDB036247	
<i>H. cristatum</i> (Bres.) Stalpers	USA	REB-88	KC571718	
	USA	REB-169	JN135174	
<i>H. cumulatum</i> K.A. Harrison	Finland	TU115384	UDB011871	UDB011871
	Estonia	TU111191	UDB032402	
<i>H. cyanopodium</i> K.A. Harrison	USA	SEW 85	AY569027	
<i>H. diabolus</i> Banker	Canada	KAH13873	AF351863	
<i>H. dianthifolium</i> Loizides	Italy	ML902162HY	KX619420	
	Cyprus	ML61211HY	KX619419	
<i>H. earlianum</i> Banker	USA	REB-75	KC571724	
	USA	REB-375	JN135179	
<i>H. ferrugineum</i> (Fr.) P. Karst.	Sweden	ELarsson197-14	MK602722	MK602722
	Norway	OF297319	MK602720	MK602720
<i>H. ferrugipes</i> Coker	USA	REB-176	KC571727	
	USA	REB-324	KC571728	
<i>H. geogenium</i> (Fr.) Banker	Norway	OF66379	MK602723	MK602723
	Norway	OF296213	MK602724	MK602724
<i>H. gracilipes</i> (P. Karst.) P. Karst.	Sweden	GB-0113779	MK602727	MK602727
	Sweden	ELarsson219-11	MK602726	MK602726
<i>H. mirabile</i> (Fr.) P. Karst.	Sweden	SLund140912	MK602730	MK602730
	Sweden	ELarsson170-14	MK602729	MK602729
<i>H. peckii</i> Banker	Norway	EBendiksen567-11	MK602733	MK602733
	Sweden	ELarsson174-14	MK602732	MK602732
<i>H. pineticola</i> K.A. Harrison	USA	REB-94	KC571734	
<i>H. piperatum</i> Coker ex Maas Geest.	USA	REB-67	KC571720	
	USA	REB-332	JN135173	
<i>H. regium</i> K.A. Harrison	USA	SEW 93	AY569031	
<i>H. scleropodium</i> K.A. Harrison	USA	REB-352	KC571740	
	USA	REB-3	JN135186	
<i>H. scrobiculatum</i> (Fr.) P. Karst.	USA	REB-78	JN135181	
<i>H. spongiosipes</i> (Peck) Pouzar	USA	REB-52	JN135184	
	UK	RBG Kew K(M)124986	EU784269	
<i>H. suaveolens</i> (Scop.) P. Karst.	Norway	SSvantesson877	MK602736	MK602736
	Sweden	ELarsson8-14	MK602735	MK602735
<i>H. subsuccosum</i> K.A. Harrison	USA	SEW 55	AY569033	
<i>Sarcodon amygdaliolens</i> Rubio Casas	Spain	SC-2011	JN376763	
<i>S. aspratus</i> (Berk.) S. Ito			DQ448877	
			AF335110	
<i>S. coactus</i>	China	Wei 8094	MN846278	MN846287
	China	Shi 181	MN846279	MN846288

Species	Geographic origin	Voucher number	GenBank Accessions	
			ITS	28S
<i>S. fennicus</i> (P. Karst.) P. Karst.	Sweden	SWesterberg110909	MK602739	MK602739
	Norway	OF242833	MK602738	MK602738
<i>S. fuligineoviolaceus</i> (Kalchbr.) Pat.	Sweden	BNylen130918	MK602741	MK602741
	Norway	AMolia160201	MK602742	MK602742
<i>S. fuscoindicus</i> (K.A. Harrison) Maas Geest.	USA	OSC 113641	EU669230	EU669280
	USA	OSC 107844	EU669229	EU669279
<i>S. glaucopus</i> Maas Geest. & Nannf.	Sweden	Edvinson110926	MK602745	MK602745
	Sweden	JNitare060916	MK602744	MK602744
<i>S. grosselepidotus</i>	China	Yuan 1247	MN846273	
	China	Wei 8120	MN846274	MN846283
	China	Wei 8075	MN846276	MN846285
	China	Wei 8128	MN846277	MN846286
	China	Wei 8097	MN846275	MN846284
<i>S. imbricatus</i> (L.) P. Karst.	Norway	SSvantesson355	MK602748	MK602748
	Sweden	ELarsson384-10	MK602747	MK602747
<i>S. joeides</i> (Pass.) Bataille	Sweden	Nitare110829	MK602751	MK602751
<i>S. lepidus</i> Maas Geest.	Sweden	KHjortstam17589	MK602750	MK602750
	Sweden	JNitare110829	MK602754	MK602754
<i>S. leucopus</i> (Pers.) Maas Geest. & Nannf.	Sweden	RGCarlsson10-065	MK602752	MK602752
	Norway	OF296099	MK602755	MK602755
<i>S. leucopus</i>	Sweden	PHedberg080811	MK602757	MK602757
	China	Dai 5686	MN846282	MN846291
<i>S. lidongensis</i>	China	Wei 8365	MN846280	MN846289
	China	Wei 8329	MN846281	MN846290
<i>S. lundellii</i> Maas Geest. & Nannf.	Norway	OF295814	MK602760	MK602760
	Norway	OF242639	MK602759	MK602759
<i>S. martioflavus</i> (Snell, K.A. Harrison & H.A.C. Jacks.) Maas Geest.	Sweden	ADelin110804	MK602763	MK602763
	Norway	OF242435	MK602762	MK602762
<i>S. quercinofibulatus</i> Pérez-De-Greg., Macau & J. Carbó	Italy	JC-20090718.2	JX271818	MK602773
	USA	TENN	MG663244	
<i>S. scabripes</i> (Peck) Banker	Mexico	FCME:23240	EU293829	
	USA	REB-351	JN135191	
<i>S. scabrosus</i> (Fr.) P. Karst.	Norway	OF292320	MK602766	MK602766
	Norway	OF360777	MK602765	MK602765
<i>S. squamosus</i> (Schaeff.) P. Karst.	Norway	OF295554	MK602769	MK602769
	Norway	OF177452	MK602768	MK602768
<i>S. underwoodii</i> Banker	USA	REB-358	JN135189	
	USA	REB-119	KC571782	
<i>S. versipellis</i> (Fr.) Nikol.	Sweden	RGCarlsson11-08	MK602772	MK602772
	Sweden	RGCarlsson13-057	MK602771	MK602771
<i>Sarcodon</i> sp.		SL71	EU627610	
		TPML20130628-34	MF611700	
		SFC20140822-38	MF611702	
	Italy	OTU9	MH681180	
	New Caledonia	CY13_061	KY774274	KY774274
	China	LL_119	KX008981	
	Mexico	GO-2009-415	KC152220	
	New Zealand	PDD:105158	KP191971	KP191774

Chain Monte Carlo (MCMC) technique and parameters predetermined with MrMODELTEST2.3 (Posada and Crandall 1998; Nylander 2004) were performed and the parameters in MrBayes were set as follows: lset nst = 6, rates = invgamma. Four simultaneous Markov chains were run starting from random trees, keeping one tree every 100th generation until the average standard deviation of split frequencies was below 0.01. The value of burn-in was set to discard 25% of trees when calculating the posterior probabilities. Bayesian posterior probabilities were obtained from the 50% majority rule consensus of the trees kept. Then we used the FigTree v1.3.1 or Tree32 to visualise the resulting trees.

Results

Phylogenetic analyses

The combined ITS-LSU dataset represented 97 taxa and 1328 characters long after being trimmed. *Amaurodon aquicoerule* was used as the outgroup. The data matrix comprised 800 constant characters, 81 parsimony uninformative variable characters and 447 parsimony informative positions. Maximum parsimony analysis was performed and a strict consensus tree was obtained (TL = 2351, CI = 0.376, RI = 0.728, RC = 0.273, HI = 0.624). Bayesian analysis ran for 8 million generations and resulted in an average standard deviation of split frequencies of 0.004708. The same dataset and alignment were analysed using the ML method and a similar topology was generated. The ML tree is shown in Figure 1. In the phylogenetic tree, nine sampled specimens formed three single clades with high to full support (100% in ML, 99% or 100% in MP and 1.00 BPP) and clustered in the clade that comprised most species of *Sarcodon*. *S. coactus* and *S. grosselepidotus*, clustered together with moderate support (67% in ML, 67% in MP and 0.99 BPP). *S. lidongensis* clustered with *S. scabrosus* with strong support (96% in ML, 100% in MP and 1.00 BPP). One sampled specimen of *S. leucopus* clustered with two samples (MK602757 and MK602755) from Sweden with full support (100% in ML, 100% in MP and 1.00 BPP). It confirmed a newly recorded species of *S. leucopus* from China.

Taxonomy

***Sarcodon coactus* Y.H. Mu & H.S. Yuan, sp. nov.**

Mycobank No: 833889

Figures 2–4

Diagnoses. Differs from *Sarcodon thwaitesii* by slightly shorter and decurrent spines, olivaceous tissues in KOH, simple-septate hyphae in all parts of basidiocarp, narrower basidia with shorter sterigmata and smaller basidiospores.

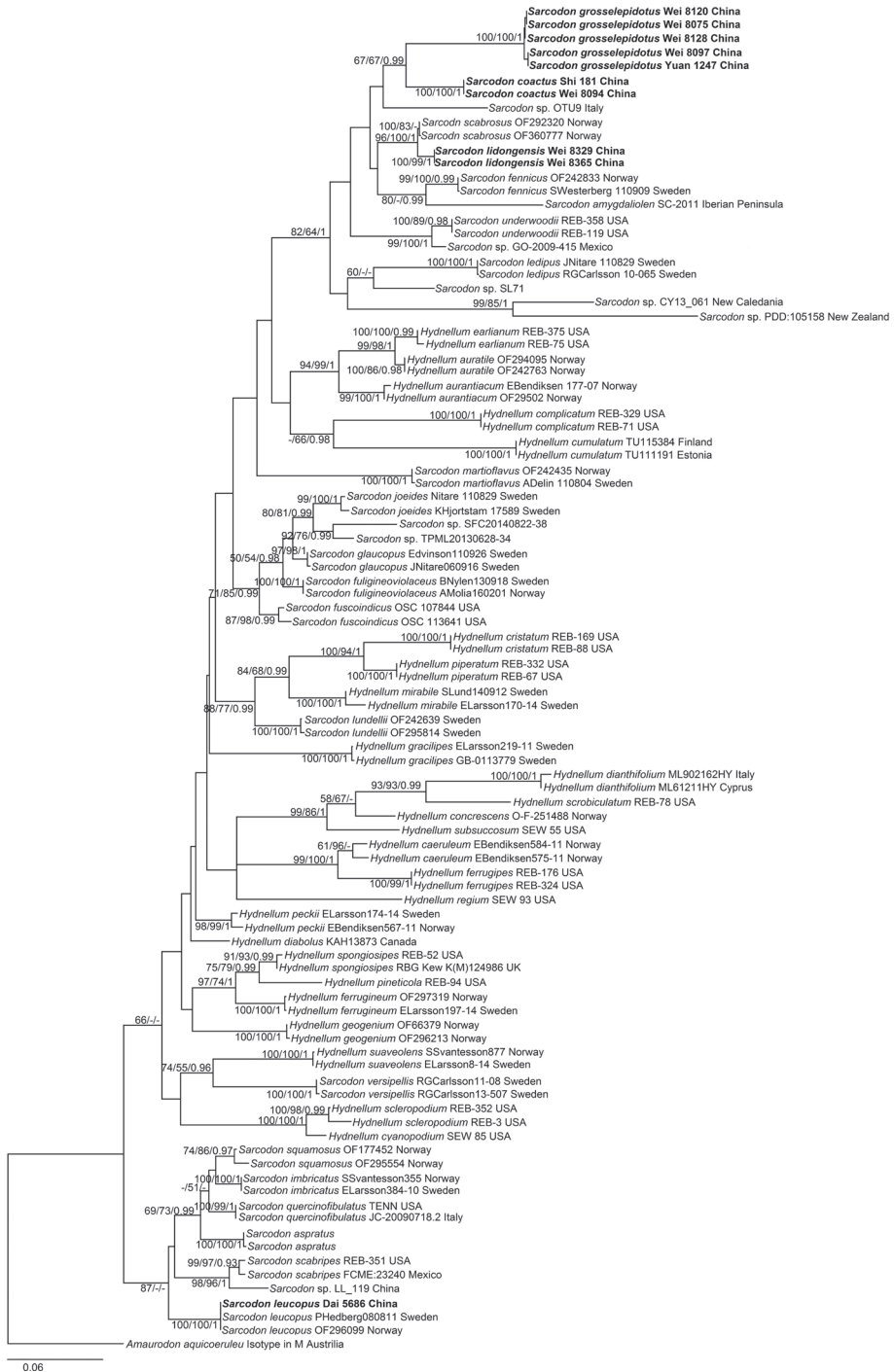


Figure 1. Maximum likelihood tree illustrating the phylogeny of *Sarcodon coactus*, *S. grosselepidotus*, *S. lidongensis*, *S. leucopus* and related taxa based on ITS and LSU sequence datasets. Branches are labelled with maximum likelihood bootstrap support greater than 50%, parsimony bootstrap proportions greater than 50% and Bayesian posterior probabilities greater than 0.95.



Figure 2. A basidiocarp of *Sarcodon coactus* (holotype: IFP 019351).

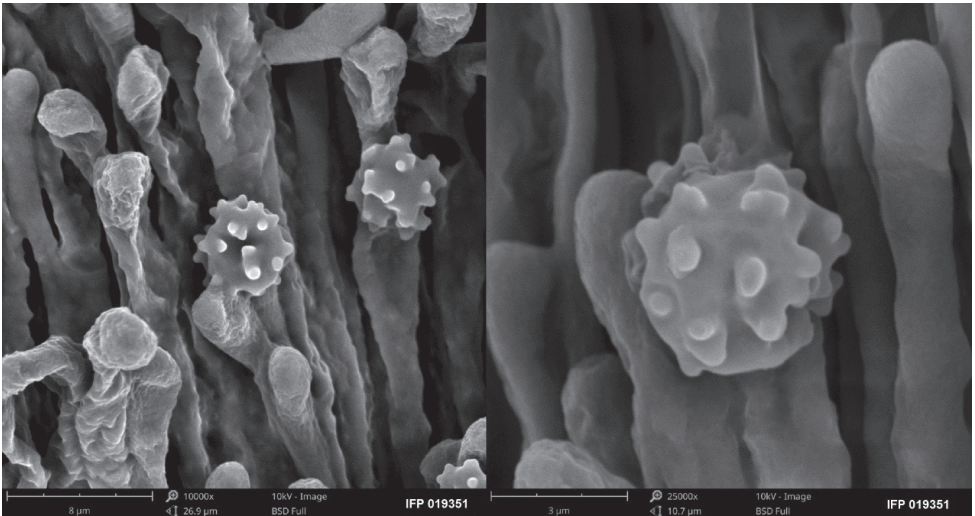


Figure 3. SEM of basidiospores of *Sarcodon coactus* (holotype: IFP 019351).

Type. China. Yunnan Province, Chuxiong, Zixishan Nat. Res., 24°58'28"N, 101°22'13"E, 2000 m alt., solitary to gregarious, on the ground in Fagaceae forest, 19.07.2018, *Wei 8094* (holotype: IFP 019351).

Etymology. *Coactus* (Lat.), refers to the felted pileal surface.

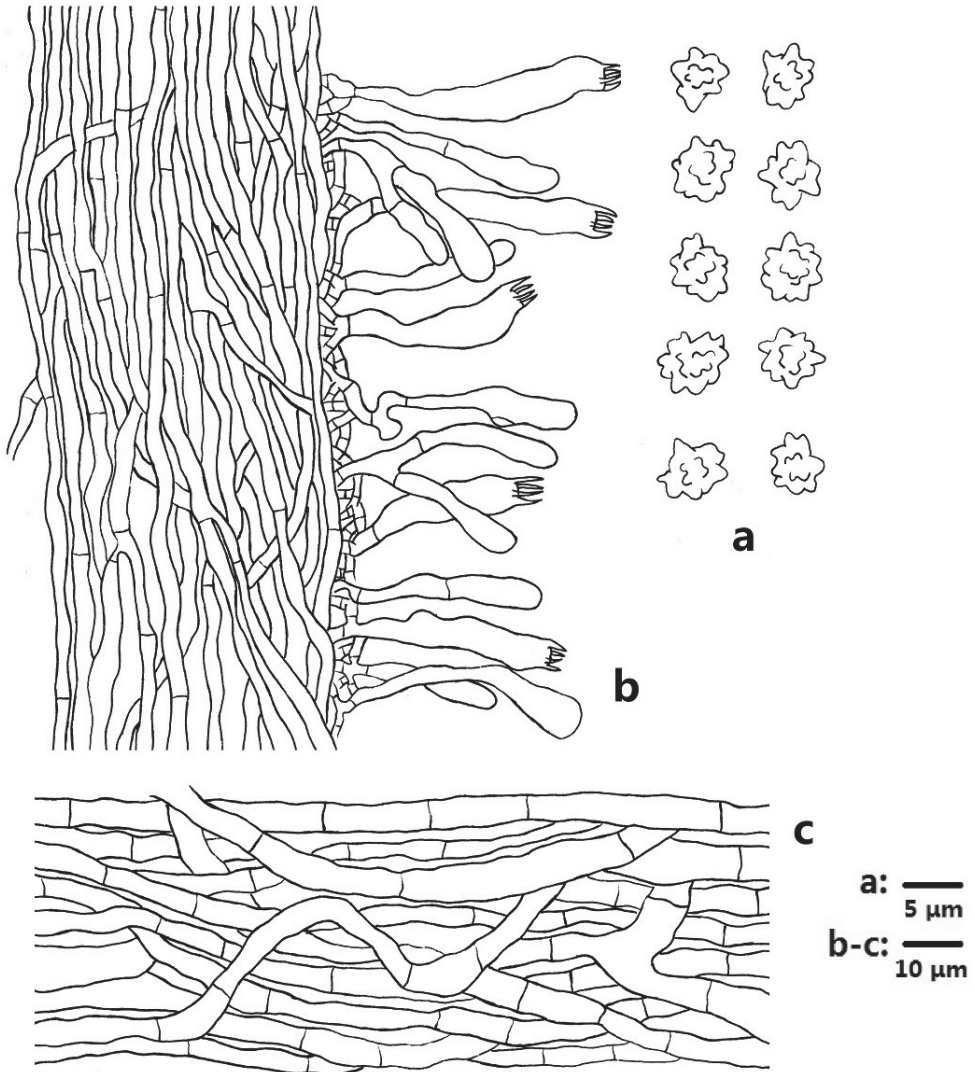


Figure 4. Microscopic structures of *Sarcodon coactus* (drawn from IFP 019351) **a** basidiospores **b** section of hymenophoral trama with basidia **c** hyphae from pileal context.

Description. Basidiocarps annual, solitary to gregarious, soft and fleshy when fresh, becoming firm and light in weight upon drying; taste none, odour farinaceous when dry. Pileus planar, ellipsoid when young, later round with age, up to 35 mm across and 4–8 mm thick at centre. Pileal surface reddish-brown (8D5) to dark brown (8F8), azonate, pubescent, floccose to felted when fresh, becoming smooth, rugose, scrobiculate when dry; margin white (7A1) when fresh, greyish-brown (7D3) with age, incurved, rarely lobed. Spine surface white (4A1) to yellowish-white (4A2) when fresh, brownish-orange (5C5) to yellowish-brown (5F6) when dry; spines up to 2.1 mm long, base up to 0.3 mm diam., conical, 3–5 per mm, decurrent on stipe, without spines at pileus margin,

brittle when dry. Context not duplex, up to 6 mm thick, light brown (5D5), firm; Stipe central, up to 5.5 cm long and 1.3 cm diam., fleshy, greyish-brown (8D3) to violet brown (10F7) when fresh, becoming hollow with age, greyish-orange (5B3) to dark brown (7F7) upon drying, rugose, columniform or attenuate below with bulbous base when old.

Hyphal structure. Hyphal system monomitic; generative hyphae with simple-septa, CB-, IKI-; tissues olivaceous in KOH.

Context. Generative hyphae hyaline, thin-walled, rarely branched, simple-septate, inflated, partly short-celled, interwoven, mostly 4–10 μm diam.

Spines. Tramal hyphae hyaline, thin-walled, frequently branched, more or less parallel along spines, frequently simple-septate, straight, 2–5 μm diam. Cystidia and cystidioles absent. Basidia clavate, thin-walled, with four sterigmata (3.1–5.2 μm long), simple-septate at base, 16.5–50 \times 6.2–9.4 μm ; basidioles similar to basidia.

Basidiospores irregular subglobose, brown, thin-walled, tuberculate, CB-, IKI-, (5.1–)5.7–7(–7.1) \times (4.6–)4.7–5.9(–6) μm , Lm = 6.2 μm , Wm = 5.3 μm , Q = 1.17–1.18 (n = 60/2); tuberculi usually isolated or grouped in 2 or more, bi- to trifurcate-like in shape, up to 1.0 μm long.

Additional specimen examined – China. Yunnan Province, Maguan County, On the way from Dalishu Township to Damagu Village, 23°4'55"N, 104°12'59"E, 1616 m alt., solitary, on the ground in Fagaceae forest, 7.08.2017, *Shi 181* (IFP 019352).

***Sarcodon grosselepidotus* Y.H. Mu & H.S. Yuan, sp. nov.**

Mycobank No: 833890

Figures 5–7

Diagnoses. Differs from *Sarcodon lepidus* in having shorter and slightly wider spines, fragrant odour, narrower hyphae in context, slightly wider basidia with shorter sterigmata and wider basidiospores.

Type. **China.** Yunnan Province, Chuxiong, Zixishan Nat. Res., 24°58'28"N, 101°22'13"E, 2000 m alt., solitary or gregarious, on the ground in Fagaceae forest, 1.08.2005, *Yuan 1247* (holotype: IFP 012529).

Etymology. *Grosselepidotus* (Lat.), from the Latin word *grosse* and *lepidotus*, in reference to the coarsely scaled pileal surface.

Description. Basidiocarps annual, solitary to gregarious, soft and fleshy when fresh, becoming fragile and light in weight upon drying; taste none, odour mildly fragrant when dry. Pileus infundibuliform or circular when young, later planar and ellipsoid to round with age, occasionally deeply fissured, up to 75 mm diam. and 4–8 mm thick at centre. Pileal surface pale orange (6A3) to dark ruby (12F8), azonate, glabrous with ascending, broad and dark brown (9F5) scales when fresh, becoming scabrous, rugose when dry; margin inflexed and wavy, sometimes lobed with age. Spine surface white (4A1) to pale yellow (4A3) when fresh, light brown (6D6) to dark brown (6F8) when dry; spines up to 1.4 mm long, base up to 0.3 mm diam., conical, 4–6 per mm, strongly decurrent on stipe, without spines at pileus margin, brittle when dry. Context not duplex, up to



Figure 5. Basidiocarps of *Sarcodon grosselepidotus* (holotype: IFP 012529).

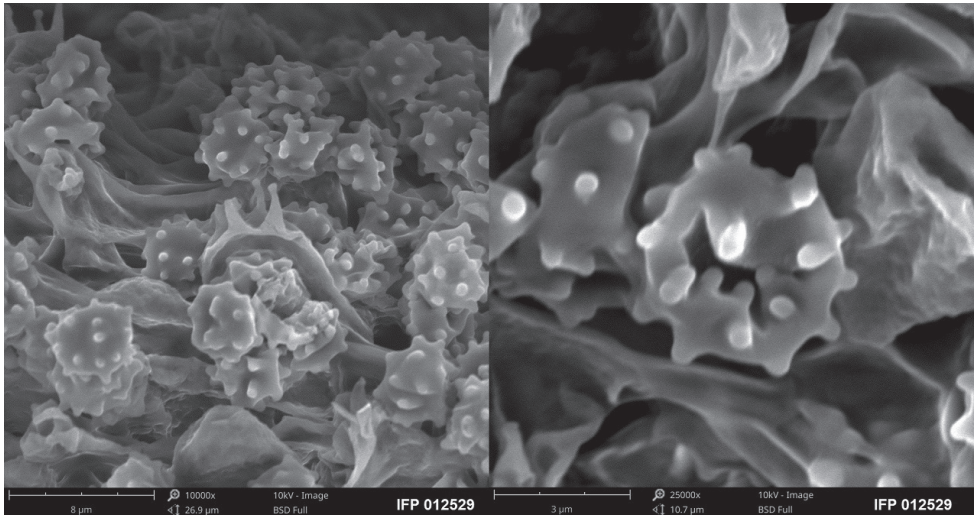


Figure 6. SEM of basidiospores of *Sarcodon grosselepidotus* (holotype: IFP 012529).

5 mm thick, greyish-orange (5B5), firm; Stipe central to lateral, up to 9.5 cm long and 2 cm diam., fleshy when fresh, firm upon drying, brownish-yellow (5C7) to dark brown (7F7), creased, inside solid, cylindrical or attenuate below with bulbous base when old.

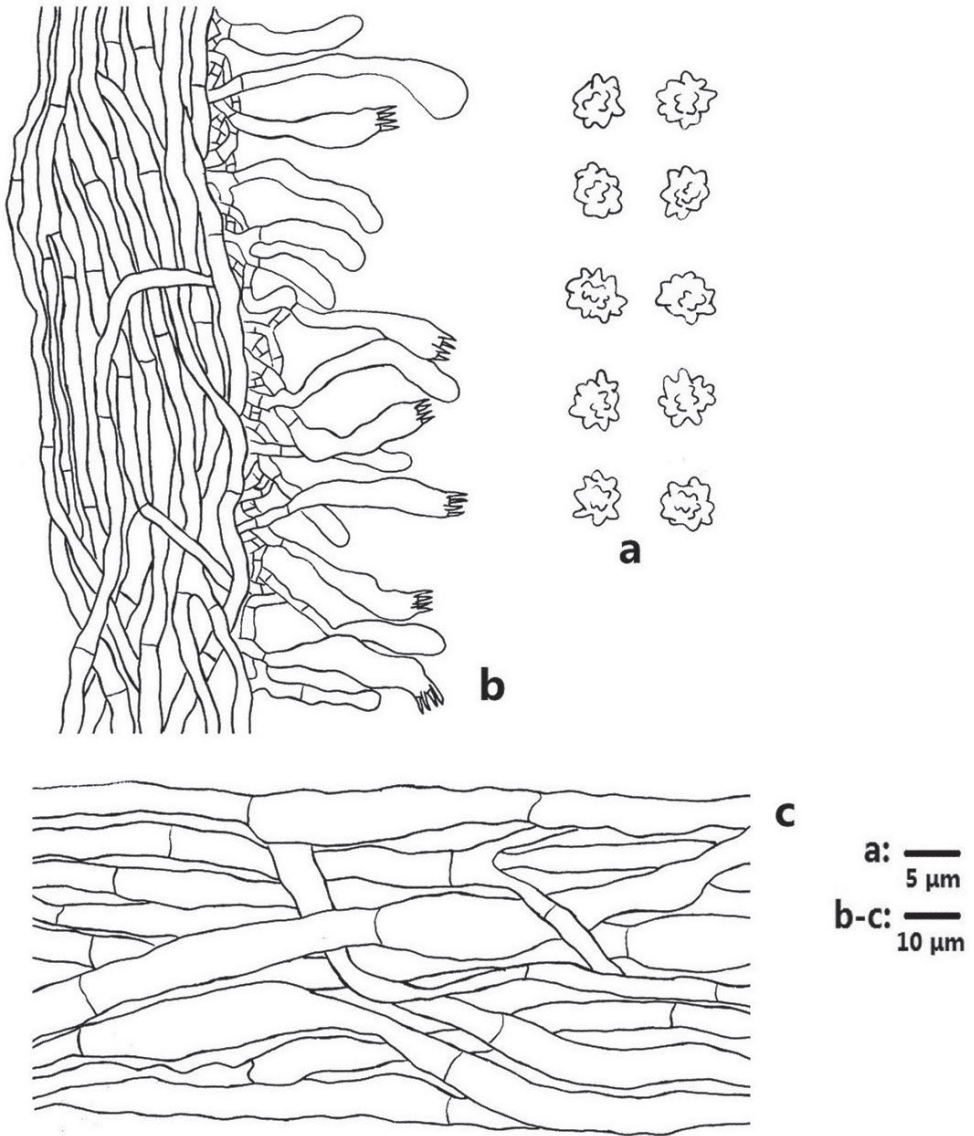


Figure 7. Microscopic structures of *Sarcodon grosselepidotus* (drawn from IFP 012529) **a** basidiospores **b** section of hymenophoral trama with basidia **c** hyphae from pileal context.

Hyphal structure. Hyphal system monomitic; generative hyphae with simple-septa, CB-, IKI-; tissues olivaceous in KOH.

Context. Generative hyphae hyaline, thin-walled, rarely branched, simple-septate, inflated, interwoven, mostly 7–11 µm diam.

Spines. Tramal hyphae hyaline, thin-walled, occasionally branched, more or less parallel along spines, frequently simple-septate, straight, 2–5 µm diam. Cystidia and cystidioles absent. Basidia clavate, thin-walled, with four sterigmata (2.5–5 µm long), simple-septate at base, 23.5–55.5 × 5.3–8.2 µm; basidioles similar to basidia.

Basidiospores irregular ellipsoid to globose, brown, thin-walled, tuberculate, CB–, IKI–, (5–)5.1–6.4(–6.6) × (4–)4.1–5.9(–6) μm, Lm = 5.5 μm, Wm = 4.9 μm, Q = 1.13–1.19 (n = 60/2); tuberculi usually isolated, sometimes grouped in 2 or more, bito trifurcate-like in shape, up to 0.7 μm long.

Additional specimen examined – China. Yunnan Province, Chuxiong, Zixishan Nat. Res., 24°58'28"N, 101°22'13"E, 2000 m alt., solitary to gregarious, on the ground in Fagaceae forest, 19.07.2018, *Wei 8075* (IFP 019353), *Wei 8097* (IFP 019354), *Wei 8120* (IFP 019355) and *Wei 8128* (IFP 019356).

***Sarcodon lidongensis* Y.H. Mu & H.S. Yuan, sp. nov.**

MycoBank No: 833891

Figures 8–10

Diagnoses. Differs from *Sarcodon joeides* in having shorter, more or less decurrent spines, the absence of gloeoplerous hyphae, shorter basidia sterigmata and narrower basidiospores.

Type. China. Yunnan Province, Lidong County, Qunlong Villa, 26°35'28"N, 99°24'16"E, 2400 m alt., solitary to conrescent, on the ground in Fagaceae forest, 24.07.2018, *Wei 8365* (holotype: IFP 019357).

Etymology. *Lidongensis*, refers to Lidong County, where the specimens were collected.

Description. Basidiocarps annual, simple to conrescent, soft and fleshy when fresh, becoming firm and light in weight upon drying; taste bitterish, odour farinaeous when dry. Pileus planar and circular when young, later plano-convex to somewhat depressed and regular orbicular with age, up to 35 mm across and 5–8 mm thick at centre. Pileal surface light brown (6D7) to brown (7E8), azonate, velutinate, then matted, appressed squamose to rimose when fresh, and purplish-brown at the pileal margin, dark brown in centre, becoming scrobiculate and verrucose when dry; margin incurved and occasionally incised with age. Spine surface greyish-orange (6B3) to brown (6E6) when fresh, light brown (6D5) to brown (6E7) when dry; spines up to 1 mm long, base up to 0.2 mm diam., conical, 4–6 per mm, more or less decurrent on stipe, with spines at pileus margin, brittle when dry. Context not duplex, up to 6 mm thick, orange white (5A2) to yellowish-brown (5D6), firm; stipe central, up to 4.5 cm long and 1 cm diam., fleshy when fresh, rigid upon drying, light brown (6D6) to dark brown (6F6), fibrillose, inside solid, cylindrical or broadened below with bulbous base when old.

Hyphal structure. Hyphal system monomitic; generative hyphae with simple-septa, CB–, IKI–; tissues olivaceous in KOH.

Context. Generative hyphae hyaline, thin-walled, occasionally branched, simple-septate, inflated, interwoven, mostly 5–9 μm diam.

Spines. Tramal hyphae hyaline, thin-walled, occasionally branched, more or less parallel along spines, frequently simple-septate, straight, sometimes flexuous and collapsed, 2–4 μm diam. Cystidia and cystidioles absent. Basidia clavate, thin-walled, with



Figure 8. Basidiocarps of *Sarcodon lidongensis* (holotype: IFP 019357).

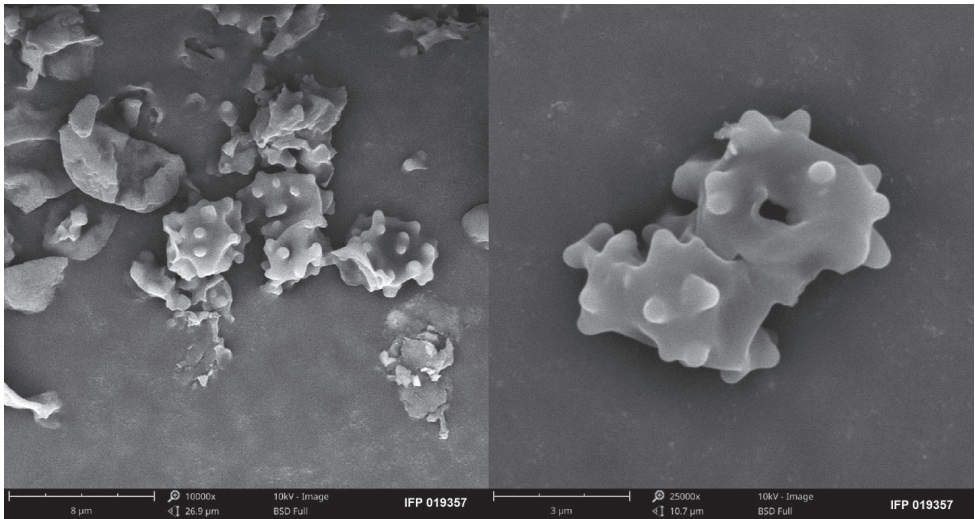


Figure 9. SEM of basidiospores of *Sarcodon lidongensis* (holotype: IFP 019357).

four sterigmata (2.0–3.0 μm long), simple-septate at base, 19.2–39.3 \times 3.0–7.2 μm ; basidioles similar to basidia.

Basidiospores irregular ellipsoid to subglobose, brown, thin-walled, tuberculate, CB–, IKI–, (4–)4.1–6(–6.1) \times (3.9–)4–5(–5.1) μm , Lm = 5.5 μm , Wm = 4.9 μm , Q = 1.15–1.20 (n = 60/2); tuberculi usually isolated or grouped in 2 or more, bi- to trifurcate-like in shape, up to 1.0 μm long.

Additional specimen examined – China. Yunnan Province, Lidong County, Qunlong Villa, 26°35'28"N, 99°24'16"E, 2400 m alt., solitary to conrescent, on the ground in Fagaceae forest, 24.07.2018, Wei 8329 (IFP 019358).

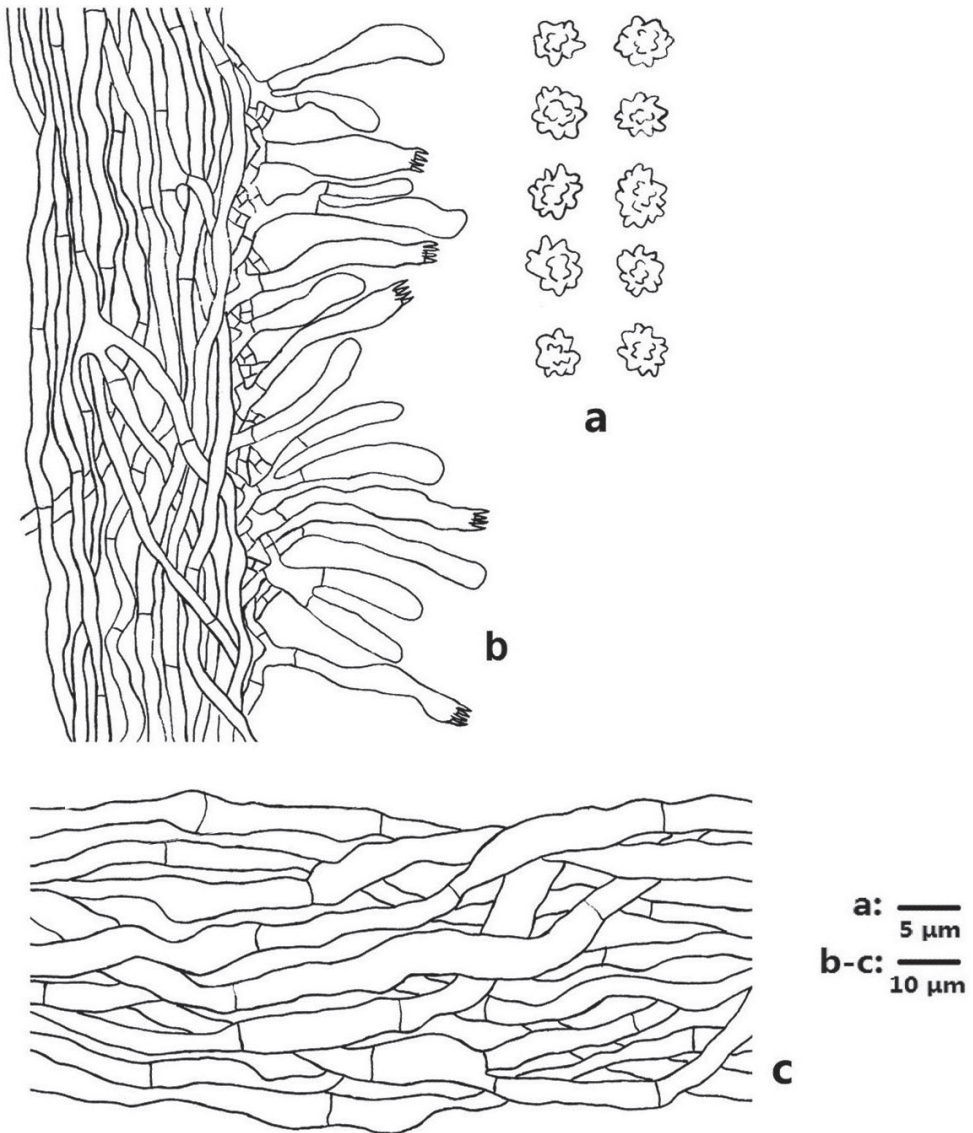


Figure 10. Microscopic structures of *Sarcodon lidongensis* (drawn from IFP 019357) **a** basidiospores **b** section of hymenophoral trama with basidia **c** hyphae from pileal context.

Sarcodon leucopus (Pers.) Maas Geest. & Nannf., *Svensk Botanisk Tidskrift* 63: 415, 1969.

Diagnoses. Morphological and nuc ITS rDNA + nuc LSU rDNA sequences analyses confirmed the new record species, which is described in detail by Mleczko (2011). This species was recorded by several European countries, such as Estonia, Finland, Bulgaria and Sweden and was frequently placed on the Red List (Rassi et al. 2001; Gärdenfors 2005; Gyosheva et al. 2006; Parmasto 2009).

Specimen examined – China. Xizang Auto. Reg., Linzhi, Bayi Town, 92°09'14"E, 26°52'26"N, 3000 m alt., solitary or gregarious, on the ground of alpine *Pinus* forest, 3.08.2004, *Dai 5686* (IFP 010196).

Discussion

Three new species of *Sarcodon* were described, based on the morphological characteristics and molecular data and were the first new species described from China. Phylogenetic analyses of the nuc ITS rDNA + nuc LSU rDNA dataset by ML, MP and Bayes in this study showed a low level of support in the deeper nodes of the topology, but high support at the species level. The result is in keeping with previous reports (Baird et al. 2013; Larsson et al. 2019).

The felted pileal surface is the main feature of *Sarcodon coactus* and this is consistent with *S. repandus* and *S. thwaitesii*. However, *S. repandus* differs from *S. coactus* by a larger pileus (up to 50 mm vs. 35 mm in *S. coactus*) with longer spines (up to 4 mm vs. 2.1 mm in *S. coactus*), clamped hyphae and wider hyphae in the context (up to 25 μm) (Maas Geesteranus 1971). *S. thwaitesii* resembles *S. coactus* in having an azonate pileal surface, central and hollow stipe when old and thin-walled hyphae in trama. However, *S. thwaitesii* differs from *S. coactus* by slightly longer (up to 3 mm vs. 2.1 mm in *S. coactus*) and not decurrent spines, blue-green tissues in KOH, clamped hyphae in all parts of the basidiocarp, wider basidia (10–11 μm vs. 6.2–9 μm in *S. coactus*) with longer sterigmata (5.4–9 μm vs. 3.1–5.2 μm in *S. coactus*) and larger basidiospores (8.1–9.4 \times 5.8–7.2 μm vs. 5.7–7 \times 4.7–5.9 μm in *S. coactus*) (Maas Geesteranus 1971).

Sarcodon grosselepidotus presents a distinct characteristic: pileal surface with ascending and coarse scales, that coincide with that of *S. imbricatus* and *S. lepidus* (Maas Geesteranus 1975; Baird et al. 2013). However, *S. imbricatus* is differentiated from the new species by having longer spines (up to 8 mm vs. 1.4 mm in *S. grosselepidotus*), clamped hyphae in all parts of the basidiocarp, presence of gloeoplerous-like hyphae and larger basidiospores (8–9 \times 7–8 μm vs. 5.1–6.4 \times 4.1–5.9 μm in *S. grosselepidotus*) (Maas Geesteranus 1971; Baird et al. 2013). *S. lepidus* differs from *S. grosselepidotus* by having longer spines (up to 3 mm vs. 1.4 mm in *S. grosselepidotus*), farinaceous odour, wider hyphae in the context and narrower basidiospores (3.6–4.3 μm vs. 4.1–5.9 μm in *S. grosselepidotus*) (Maas Geesteranus 1975).

Sarcodon coactus and *S. grosselepidotus* are closely related in the phylogenetic tree and share similar morphological and anatomical characteristics: solitary to gregarious basidiocarps with round pileus, central and columniform stipe, decurrent spines, context tissue becoming olivaceous in KOH and isolated or grouped tuberculi. However, *S. grosselepidotus* can be differentiated by infundibuliform basidiocarps, fissured pileus, coarse and scaly pileal surface, shorter spines (up to 1.4 mm vs. 2.1 mm in *S. coactus*) and slightly shorter tuberculi (up to 0.7 μm vs. 1 μm in *S. coactus*).

Sarcodon lidongensis and *S. scabrosus* reveal a close phylogenetic relationship according to the phylogenetic tree. In morphology, *S. lidongensis* is similar to *S. scabrosus* in having a single or gregarious basidiocarp with convex to planar or depressed pileus,

brown and scaled pileal surface, central and terete stipe, olivaceous tissues in KOH and basidiospores of similar shape. However, *S. scabrosus* is differentiated by a larger pileus (up to 15 cm across) with longer spines (up to 8 mm vs. 1 mm in *S. lidongensis*), wider basidia (7–9 μm vs. 3.0–7.2 μm in *S. lidongensis*) with longer sterigmata (4–5 μm vs. 2–3 μm in *S. lidongensis*) and larger basidiospores (6–7 \times 5–7 μm vs. 4.1–6 \times 4–5 μm in *S. lidongensis*) (Maas Geesteranus 1971; Baird 1986; Baird et al. 2013).

Sarcodon joeides is similar to *S. lidongensis* in having simple basidiocarps with plano-convex or depressed pileus, mottling or tear-like pileal surface, appressed scales, central and terete stipe, olivaceous tissue in KOH, inflated and interwoven hyphae in the context and tuberculate basidiospores of similar shape. However, it differs from *S. lidongensis* in having longer, decurrent to strongly decurrent spines (up to 3 mm vs. 1 mm in *S. lidongensis*), presence of gloeoplerous-like hyphae, longer basidia sterigmata (4–5 μm vs. 2–3 μm in *S. lidongensis*) and wider basidiospores (5–6 μm vs. 4–5 μm in *S. lidongensis*) (Baird et al. 2013).

The specimens, involved in this study, were collected from the forests dominated by Fagaceae trees such as *Quercus acutissima*, *Lithocarpus dealbatus*, *Castaopsis orthacantha* and a small portion of coniferous trees, for instance, *Pinus armandii*. We speculated that these species may form an ectomycorrhizal association with Fagaceae trees. The new record sample was fully identical with *S. leucopus* described by Mleczko (2011) in morphology and molecular analysis and pine and spruce were primary ectomycorrhizal companions of this fungus.

Key to species of *Sarcodon* from China

- 1 Basidiospores lengths in the range 8–10 μm , hyphae with frequent clamp connections in all parts of basidiocarps ***S. leucopus***
- Basidiospores lengths in the range 4–7 μm , hyphae without clamp connection in any part of basidiocarps **2**
- 2 Pileal surface not scaled, felted when fresh, spines up to 2.1 mm .. ***S. coactus***
- Pileal surface scaled when fresh, spines up to 1.4 mm **3**
- 3 Basidiocarps of occasionally deeply fissured pileus, pileal surface with ascending squama ***S. grosselepidotus***
- Basidiocarps of not deeply fissured pileus, pileal surface with appressed squama ***S. lidongensis***

Acknowledgements

This research was financed by the National Natural Science Foundation of China (Project Nos. 31770028 & 31970017) and the Biodiversity Investigation, Observation and Assessment Program (2019–2023) of the Ministry of Ecology and Environment of China.

References

- Ainsworth AM (2005) BAP Fungi Handbook. English Nature Research Reports 600, English Nature, Peterborough, 115 pp.
- Arnolds E (1989) Former and present distribution of stipitate hydnyaceous fungi (Basidiomycetes) in the Netherlands. *Nova Hedwigia* 48: 107–142.
- Arnolds E (2003) De stekelzwammen en pruikzwammen van Nederland en België. Nederlandse Mycologische Vereniging.
- Arnolds E (2010) The fate of hydnyoid fungi in The Netherlands and Northwestern Europe. *Fungal Ecology* 3: 81–88. <https://doi.org/10.1016/j.funeco.2009.05.005>
- Baird RE (1985) New species of stipitate hydnyums from southeastern United States and Mexico. *Mycotaxon* 23: 297–304.
- Baird RE, Khan SR (1986) The stipitate hydnyums (Thelephoraceae) of Florida. *Brittonia* 38: 171–184. <https://doi.org/10.2307/2807273>
- Baird R, Wallace LE, Baker G, Scruggs M (2013) Stipitate hydnyoid fungi of the temperate southeastern United States. *Fungal Diversity* 62: 41–114. <https://doi.org/10.1007/s13225-013-0261-6>
- Caclalli G, Caroti V (2005) Prodrómo alla flora fungina della provincia di Livorno. –Quad. Mus. Stor. Nat. di Livorno 18 (Suppl. 1): 1–85.
- Cannatella D (2015) Xenopus in space and time: fossils, node calibrations, tip-dating, and paleobiogeography. *Cytogenetic and Genome Research* 145: 283–301. <https://doi.org/10.1159/000438910>
- Dai YC (2011) A revised checklist of corticioid and hydnyoid fungi in China for 2010. *Mycoscience* 52: 69–79. <https://doi.org/10.1007/S10267-010-0068-1>
- Erland S, Taylor AFS (1999) Resupinate ectomycorrhizal fungal genera. In: Cairney JWG, Chambers SM (Eds) Ectomycorrhizal fungi key genera in profile. Berlin and Heidelberg, Springer 347–363. https://doi.org/10.1007/978-3-662-06827-4_15
- Gaget V, Humpage AR, Huang Q, Monis P, Brookes JD (2017) Benthic cyanobacteria: a source of cylindrospermopsin and microcystin in Australian drinking water reservoirs. *Water Research* 124: 454–464. <https://doi.org/10.1016/j.watres.2017.07.073>
- Gärdenfors U (2005) Rödlistade arter i Sverige 2005. The 2005 Red List of Swedish species. ArtDatbanken, SLU, Uppsala.
- Gardes M, Bruns TD (1996) Community structure of ectomycorrhizal fungi in a *Pinus muricata* forest: above- and belowground views. *Canadian Journal of Botany* 74: 1572–1583. <https://doi.org/10.1139/b96-190>
- Gyosheva MM, Denchev CM, Dimitrova EG, Assyov B, Petrova RD, Stoichev GT (2006) Red List of fungi in Bulgaria. *Mycologia Balcanica* 3: 81–87.
- Hahn CJ, Friebe G, Krisai-Greilhuber I (2018) *Sarcodon fennicus*, a boreo-montane stipitate hydnyoid fungus with a remarkable smell. *Austrian Mycological Society* 27: 43–52.
- Harrison KA (1964) New or little known North American stipitate hydnyums. *Canadian Journal of Botany* 42: 1205–1233. <https://doi.org/10.1139/b64-116>
- Harrison KA (1984) New combinations in the genus *Sarcodon*. *The Michigan Botanist* 23: 76–76.

- Hrouda P (1999) Hydneous fungi – changes in their occurrence and possible causes. In: Jankovský L, Krejčíř R, Antonín V (Eds) Houby a les (sborník referátu). MZLU, Brno, 53–56.
- Hrouda P (2005) Bankeraceae in Central Europe. 1. Czech Mycology 57: 57–78. <https://doi.org/10.33585/cmy.57103>
- Kumar S, Stecher G, Tamura K (2016) MEGA7: Molecular evolutionary genetics analysis version 7.0 for bigger datasets. Molecular Biology and Evolution 33: 1870–1874. <https://doi.org/10.1093/molbev/msw054>
- Larsson KH, Svantesson S, Miscovic D, Koljalg U, Larsson E (2019) Reassessment of the generic limits for *Hydnellum* and *Sarcodon* (Thelephorales, Basidiomycota). MycoKeys 54: 31–47. <https://doi.org/10.3897/mycokeys.54.35386>
- Loizides M, Alvarado P, Assyov B, Arnolds EEF, Moreau PA (2016) *Hydnellum dianthifolium* sp. nov. (Basidiomycota, Thelephorales), a new tooth-fungus from southern Europe with notes on *H. concrescens* and *H. scrobiculatum*. Phytotaxa 280: 023–035. <https://doi.org/10.11646/phytotaxa.280.1.2>
- Maas Geesteranus RA (1956) The stipitate hydnums of the Netherlands I. *Sarcodon* P. Karst. Fungus 26: 44–60.
- Maas Geesteranus RA (1964) Notes on hydnums – II. Persoonia 3: 155–192.
- Maas Geesteranus RA (1971) Hydneous fungi of the eastern old world. Verhandelingen Koninklijke Nederlandse Akademie van Wetenschappen Afdeling Natuurkunde 60(3): 1–176.
- Maas Geesteranus RA (1975) Die terrestrischen Stachelpilze Europas. Verhandelingen Koninklijke Nederlandse Akademie van Wetenschappen Afdeling Natuurkunde 65: 1–127.
- Maas Geesteranus RA (1976) Notes on hydnums X. Proceedings van de Koninklijke Nederlandse Akademie van Wetenschappen Section C 79: 273–289.
- Magnago AC, Muller ACN, da Silveira RMB (2015) *Sarcodon atroviridis* (Bankeraceae, Thelephorales): new records for the southern Atlantic Forest, Brazil. Brazilian Journal of Botany 38: 193–197. <https://doi.org/10.1007/s40415-014-0131-9>
- Mleczo P, Zubek S, Kozak M (2011) Description of ectomycorrhiza and a new Central European locality of the rare hydroid species *Sarcodon leucopus* (Pers.) Maas Geest. et Nannf. (Thelephorales, Basidiomycota). Nova Hedwigia 92: 257–272. <https://doi.org/10.1127/0029-5035/2011/0092-0257>
- Mu YH, Wu F, Yuan HS (2019) Hydneous fungi of China 7. Morphological and molecular characterization of *Phellodon subconfluens* sp. nov. from temperate, deciduous forests. Phytotaxa 414: 280–288. <https://doi.org/10.11646/phytotaxa.414.6.2>
- Munsell AH (2015) Munsell soil-color charts with genuine Munsell color chips. Grand Rapids. Munsell Color.
- Newton AC, Holden E, Davy LM, Ward SD, Fleming LV, Watling R (2002) Status and distribution of stipitate hydroid fungi in Scottish coniferous forests. Biological Conservation 107: 181–192. [https://doi.org/10.1016/S0006-3207\(02\)00060-5](https://doi.org/10.1016/S0006-3207(02)00060-5)
- Nitare J (2006) Åtgärdsprogram för bevarande av rödlistade fjälltaggsvampar (*Sarcodon*). Naturvårdsverket, Stockholm, Rapport 5609.
- Nitare J (2019) Skyddsvärd skog. Naturvårdsarter och andra kriterier för naturvärdesbedömning. Skogsstyrelsens förlag, Jönköping.

- Nylander J (2004) MrModeltest v2. Program distributed by the author. Evolutionary Biology Centre, Uppsala University, Uppsala, Sweden.
- Otto P (1992) Verbreitung und Rückgang der terrestrischen Stachelpilze Ostdeutschlands. *Gleditschia* 20: 153–202.
- Parmasto E (2009) Red data list of Estonian fungi 2008. Official Estonian Red List authorized by Minister of the Environment of the Estonian Republic.
- Pegler DN, Roberts PJ, Spooner BM (1997) British chanterelles and tooth fungi. Royal Botanical Gardens KEW, London.
- Pérez-De-Gregorio MA, Macau N, Carbó J (2011) *Sarcodon quercinofibulatum*, una nueva especie del género con hifas fibulíferas. *Revista Catalana de Micologia*. 33: 25–30.
- Pieri M, Rivoire B (1994) Contribution à l'inventaire des Aphyllophoromycetidae et Heterobasidiomycetes de la Corse-II. – Bulletin Semestriel de la Fédération des Associations Mycologiques Méditerranéennes 5: 15–19.
- Posada D, Crandall KA (1998) MODELTEST: testing the model of DNA substitution. *Bioinformatics* 14: 817–818. <https://doi.org/10.1093/bioinformatics/14.9.817>
- Rassi P, Alanen A, Kanerva T, Mannerkoski I (2001) The Red List of Finnish species. Ministry of the Environment & Finnish Environment Institute, Helsinki.
- Rayner RW (1970) A mycological colour chart. Kew: Commonwealth Mycological Institute and British Mycological Society.
- Senn-Irlet B, Bieri G, Egli S (2007) Lista Rossa dei macromiceti minacciati in Svizzera. Ed. Ufficio federale dell'ambiente, Bernae WSL, Birmensdorf. Pratica ambientale n. 0718.
- Stalpers JA (1993) The Aphyllophoraceous fungi I: keys to the species of the Thelephorales. *Studies in Mycology* 35: 1–168.
- Stamatakis A, Hoover P, Rougemont J (2008) A rapid bootstrap algorithm for the RAxML web-servers. *Systematic Biology* 75: 758–771. <https://doi.org/10.1080/10635150802429642>
- Stamatakis A (2014) RAxML version 8: a tool for phylogenetic analysis and post-analysis of large phylogenies. *Bioinformatics* 30: 1312–1313. <https://doi.org/10.1093/bioinformatics/btu033>
- Stöger A, Schaffer J, Ruppitsch W (2006) A rapid and sensitive method for direct detection of *Erwinia amylovora* in symptomatic and asymptomatic plant tissues by polymerase chain reaction. *Journal of Phytopathology* 154: 469–473. <https://doi.org/10.1111/j.1439-0434.2006.01130.x>
- Swofford DL (2002) PAUP*: Phylogenetic analysis using parsimony (*and other methods). Version 4.0b10. Sunderland, Massachusetts: Sinauer Associates.
- Vesterholt J, Asman W, Christensen M (2000) Nitrogen deposition and decline of fungi on poor and sandy soils. *Svampe* 42: 53–60.
- Vizzini A, Angelini C, Losi C, Ercole E (2016) *Thelephora dominicana* (Basidiomycota, Thelephorales), a new species from the Dominican Republic, and preliminary notes on thelephoroid genera. *Phytotaxa* 265: 27–38. <https://doi.org/10.11646/phytotaxa.265.1.2>
- Walley R, Verbeke A (2000) Een gedocumenteerde Rode Lijst van enkele groepen paddestoelen (macrofungi) in Vlaanderen. Instituut voor Natuurbehoud, Brussel.
- Wu F, Zhou LW, Yang ZL, Bau T, Li TH, Dai YC (2019) Resource diversity of Chinese macrofungi: edible, medicinal and poisonous species. *Fungal Diversity* 98: 1–76. <https://doi.org/10.1007/s13225-019-00432-7>

Discovery of a new species of the *Hypoxylon rubiginosum* complex from Iran and antagonistic activities of *Hypoxylon* spp. against the Ash Dieback pathogen, *Hymenoscyphus fraxineus*, in dual culture

Mohammad Javad Pourmoghaddam^{1,2,3}, Christopher Lambert³, Frank Surup³,
Seyed Akbar Khodaparast¹, Irmgard Krisai-Greilhuber²,
Hermann Voglmayr^{2,4}, Marc Stadler³

1 Department of Plant Protection, Faculty of Agricultural Sciences, University of Guilan, Rasht, Iran **2** Department of Botany and Biodiversity Research, University of Vienna, Rennweg 14, 1030, Wien, Austria **3** Helmholtz-Zentrum für Infektionsforschung GmbH, Dept. Microbial Drugs, Inhoffenstrasse 7, 38124, Braunschweig, Germany **4** Institute of Forest Entomology, Forest Pathology and Forest Protection, Department of Forest and Soil Sciences, BOKU-University of Natural Resources and Life Sciences, Franz-Schwackhöfer-Haus, Peter-Jordan-Straße 82/I, 1190, Vienna, Austria

Corresponding author: Marc Stadler (Marc.Stadler@helmholtz-hzi.de)

Academic editor: T. Lumbsch | Received 17 February 2020 | Accepted 17 March 2020 | Published 24 April 2020

Citation: Pourmoghaddam MJ, Lambert C, Surup F, Khodaparast SA, Krisai-Greilhuber I, Voglmayr H, Stadler M (2020) Discovery of a new species of the *Hypoxylon rubiginosum* complex from Iran and antagonistic activities of *Hypoxylon* spp. against the Ash Dieback pathogen, *Hymenoscyphus fraxineus*, in dual culture. MycoKeys 66: 105–133. <https://doi.org/10.3897/mycokeys.66.50946>

Abstract

During a survey of xylarialean fungi in Northern Iran, several specimens that showed affinities to the *Hypoxylon rubiginosum* complex were collected and cultured. A comparison of their morphological characters, combined with a chemotaxonomic study based on high performance liquid chromatography, coupled with diode array detection and mass spectrometry (HPLC-DAD/MS) and a multi-locus phylogeny based on ITS, LSU, *rbp2* and *tub2* DNA sequences, revealed a new species here described as *Hypoxylon guilanense*. In addition, *Hypoxylon rubiginosum sensu stricto* was also encountered. Concurrently, an endophytic isolate of the latter species showed strong antagonistic activities against the Ash Dieback pathogen, *Hymenoscyphus fraxineus*, in a dual culture assay in our laboratory. Therefore, we decided to test the new Iranian fungi for antagonistic activities against the pathogen, along with several cultures of other *Hypoxylon* species that are related to *H. rubiginosum*. Our results suggest that the antagonistic effects of *Hypoxylon* spp. against *Hym. fraxineus* are widespread and that they are due to the production of antifungal phomopsidin derivatives in the presence of the pathogen.

Keywords

Ascomycota, Chemotaxonomy, Chemical ecology, Hypoxylaceae, Natural Products, Taxonomy, one new species

Introduction

Hypoxylon Bull., 1791 is one of the largest genera of the Xylariales and comprises more than 200 species, which are mainly associated with angiosperm trees as saprotrophs and endophytes and are predominant in all forest ecosystems of the world (Daranagama et al. 2018; Helaly et al. 2018).

It traditionally belonged to the Xylariaceae until a recent phylogenetic study has resulted in a re-arrangement of the genera of stromatic Xylariales and the resurrection of the family Hypoxylaceae (Wendt et al. 2018). In this study and during the follow-up work by Lambert et al. (2019), genera like *Hypomontagnella* and *Pyrenopolyporus* were segregated from *Hypoxylon*, but the genus remained paraphyletic, indicating that further taxonomic segregation will eventually become necessary.

While the type species of *Hypoxylon*, *H. fragiforme*, belongs to a relatively small clade in the phylogeny of Wendt et al. (2018), the largest clades were comprised of the species of the “*Hypoxylon rubiginosum* complex” sensu Ju and Rogers (1996). Of these species, many had been lumped in *H. rubiginosum*, according to the broad concept established in the first monograph of the genus by Miller (1961). Miller’s concept was mainly based on teleomorph morphology. In their revision of *Hypoxylon*, Ju and Rogers (1996) later recognised that anamorph characters, stromatal pigments and the micromorphology of ascospores and asci (in particular the apical apparatus) constitute valuable diagnostic characters. Modern concepts of the genus combine holomorph morphology with molecular phylogenetic data (Hsieh et al. 2005; Kuhnert et al. 2014). Moreover, secondary metabolite profiles generated by high performance liquid chromatography coupled to diode array detection and mass spectrometry (HPLC-DAD/MS) not only proved highly useful for segregation of species, but even led to the discovery of numerous novel natural products with prominent biological activities (see overviews by Stadler and Hellwig 2005a and Helaly et al. 2018).

Hypoxylon rubiginosum and related taxa have been studied rather well on their stromatal secondary metabolites and, in many cases, morphologically similar species may contain entirely different pigments and other compounds (Stadler et al. 2004, 2008; Fournier et al. 2010). Interestingly, several species of the *H. rubiginosum* complex are known to frequently colonise *Fraxinus* species in the temperate Northern hemisphere. In some cases (e.g. *H. cercidicola*, *H. fraxinophilum* and *H. petriniae*), stromata are even almost exclusively found on dead wood of ash trees. They have also been frequently reported as endophytes of the same trees where they produce their stromata (Petrini and Petrini 1985) and are widespread endophytes of other host plants on which their stromata do not even occur (U’Ren et al. 2016). Therefore, the

modern concepts of the taxonomy of the Hypoxylaceae take this fact into account and are based on the One Fungus-One Name concept. Some species have even been recognised on the basis of their anamorphic traits (Pažoutová et al. 2013) or their life cycle has been elucidated, based on a polythetic approach, i.e., by comparison of morphological, chemotaxonomic and molecular data of ascospore-derived cultures with endophytic isolates (see Bills et al. 2012 for *H. pulicicidum* and Kuhnert et al. 2014 for *H. griseobrunneum*).

The Ash Dieback disease caused by the introduced apothecial ascomycete *Hym. fraxineus* (Leotiomyces) has become one of the greatest problems in European forestry and the majority of common ash trees have succumbed to the fungal pathogen. We have recently studied the secondary metabolism of *Hym. fraxineus* (previously also known under the synonyms, *Hym. pseudoalbidus* or *Chalara fraxinea*) and its non-pathogenic domestic relative, *Hym. albidus*, for secondary metabolite production (Halecker et al. 2014, 2018; Surup et al. 2018a). In parallel, we have also isolated endophytic fungi from apparently resistant ash trees in order to find natural antagonists that may be able to combat the devastating disease. One of the best candidates was identified as *H. rubiginosum* and, as reported recently (Halecker et al. 2020), it was found to produce the anti-fungal beta-tubulin inhibitor phomopsidin in dual culture with virulent strains of the pathogen. This compound was first reported from a marine-derived fungus that was originally assigned to the genus *Phomopsis* (Kobayashi et al. 2003). However, it has since then been found in other, terrestrial strains of the same genus, which should now be referred to as *Diaporthe* (Chepkirui and Stadler 2017), a large genus of the order Diaporthales. Interestingly, phomopsidin derivatives have never been reported from cultures of Xylariales before Halecker et al. (2020) found the compound in dual antagonist assays in agar cultures as described above. Moreover, they do not constitute major detectable metabolites of *H. rubiginosum* in the culture media that were used to study the chemotaxonomy of the genus before (cf. Bitzer et al. 2008).

Concurrently, we were about to study the taxonomy of new collections of *Hypoxylon* species originating from Iran that also belong to the *Hypoxylon rubiginosum* complex. Since mycelial cultures of these fungi had just become available, it appeared practical to combine the description of their taxonomy with an evaluation of their antagonistic potential to combat *Hym. fraxineus*. We have also included a number of other *Hypoxylon* species that colonise *Fraxinus* in Europe. The current study therefore provides new evidence on both, the taxonomy and chemical ecology of *Hypoxylon*.

Materials and methods

Sample sources

Samples were collected from Guilan and Mazandaran provinces (Northern Iran) during 2015–2017. Parts of corticated branches and trunks bearing Hypoxylaceae stro-

mata were transferred to the laboratory. Details of the specimens used for morphological investigations are listed in the Taxonomy section under the respective descriptions. Specimens have been deposited in the fungarium of the Department of Plant Protection, Faculty of Agricultural Science, University of Guilan, Guilan, Iran (GUM). Living cultures have been deposited in MUCL (Louvain, Belgium).

Morphological characterisation

Microscopic characters of the teleomorph were observed in distilled water and 10% potassium hydroxide (KOH). Melzer's reagent was used for staining of the apical ascus apparatus. The numbers of perithecia, ascospores, asci, conidia and conidiophores that were measured for size in the descriptions are 10, 30, 10, 30 and 5, respectively. Specimens were cultured from single ascospore isolates, using 2 % malt extract agar (MEA). For examination of culture macro-morphology, the strains were grown on Difco Oatmeal Agar (OA), following the protocols by Ju and Rogers (1996). Pigment colours were determined as described in the latter monograph, with colour codes following Rayner (1970). Macrophotographs were obtained with a Keyence VHX-6000 microscope. Light microscopy with Nomarski differential interference contrast (DIC) was done using a Zeiss Axio Imager A1 compound microscope, equipped with a Zeiss Axiocam 506 colour digital camera. SEM of ascospores were recorded using a field-emission scanning electron microscope (FE-SEM Merlin, Zeiss, Germany), in a similar fashion as reported previously (Kuhnert et al. 2017).

DNA extraction, PCR and sequencing

DNA extraction of fresh cultures and amplification of the ITS (nuc rDNA internal transcribed spacer region containing ITS1-5.8S-ITS2), LSU (5' 1200 bp of the large subunit nuc 28S rDNA), *rpb2* (partial second largest subunit of the DNA-directed RNA polymerase II) and *tub2* (partial β -tubulin) loci were performed as described by Wendt et al. (2018). Sequences were generated by an in-house Sanger capillary sequencing solution on campus. Sequences were processed with Geneious 7.1.9 (<http://www.geneious.com>).

Molecular phylogenetic analyses

The newly generated sequences were aligned with selected sequences from Wendt et al. (2018) and a combined matrix of the four loci (ITS, LSU, *rpb2* and *tub2*) was concatenated for phylogenetic analyses, with four species (*Biscogniauxia nummularia*, *Graphostroma platystomum*, *Xylaria arbuscula* and *Xylaria hypoxylon*) added as the out-group. The GenBank accession numbers of sequences are listed in Table 1. Sequences

were aligned with the server version of MAFFT (<http://mafft.cbrc.jp/alignment/server/>, Katoh et al. 2019), checked and refined using BioEdit v. 7.2.6 (Hall 1999). After exclusion of ambiguously aligned regions and long insertions, the final combined data matrix contained 4369 characters, i.e. 578 nucleotides of ITS, 1301 nucleotides of LSU, 1017 nucleotides of *rpb2*, and 1473 nucleotides of *tub2*.

Maximum Parsimony (MP) analyses were performed with PAUP v. 4.0a165 (Swofford 2002). All molecular characters were unordered and given equal weight; analyses were performed with gaps treated as missing data; the COLLAPSE command was set to MINBRELEN. MP analysis of the combined multilocus matrix was done using 1000 replicates of heuristic search with random addition of sequences and subsequent TBR branch swapping (MULTREES option in effect, steepest descent option not in effect). Bootstrap analyses with 1000 replicates were performed in the same way but using 10 rounds of random sequence addition and subsequent branch swapping during each bootstrap replicate.

Maximum Likelihood (ML) analyses were performed with RAxML (Stamatakis 2006) as implemented in raxmlGUI 1.3 (Silvestro and Michalak 2012), using the ML + rapid bootstrap setting and the GTRGAMMA substitution model with 1000 bootstrap replicates. The matrix was partitioned for the different gene regions. In the Results and Discussion, bootstrap values $\leq 70\%$ are considered low, between 70–90% intermediate and $\geq 90\%$ high.

HPLC profiling

Stromata of *Hypoxylon* specimens were extracted as described by Kuhnert et al. (2017) and subsequently analysed by high performance liquid chromatography, coupled with diode array and electrospray mass spectrometric detection (HPLC/DAD-ESIMS) instrument settings as described by Halecker et al. (2020). The resulting UV/Vis and mass spectra were compared with an internal database (cf. Bitzer et al. 2008), comprising standards of known Hypoxylaceae.

Dual culture experiments

Dual cultures of *Hypoxylon* spp. and *Hym. fraxineus* (STMA 18166) were co-incubated on barley-malt agar by inoculation at opposite sites on 9 cm Petri dishes (cf. Halecker et al. 2020) with *Hym. fraxineus* being inoculated one week prior the beginning of the dual culturing due to its slow growth. Axenic cultures, containing only one fungus, were inoculated in parallel as a control group. Growth was documented and observed weekly after incubation in the dark for a maximum of four weeks. Thereafter, the agar plates were extracted with acetone following the method described by Halecker et al. (2020), except that the entire agar plate was extracted instead of the fungal interaction zone.

Table 1. Isolates and accession numbers of sequences used in the phylogenetic analyses. Type specimens are labelled with HT (holotype) ET (epitype) and PT (paratype). Isolates/sequences in bold were isolated/sequenced in the present study.

Species	Strain number	Origin	Status	GenBank accession numbers			Reference
				ITS	LSU	rp62	
<i>Annulohyphylon annulatum</i>	CBS 140775	Texas	ET	KY610418	KY610418	KX376353	Kuhnert et al. (2017), Wendt et al. (2018)
<i>Annulohyphylon moriforme</i>	CBS 123579	Martinique	ET	KX376321	KY624263	KX271261	Kuhnert et al. (2017), Wendt et al. (2018)
<i>Annulohyphylon truncatum</i>	CBS 140778	Texas	ET	KY610419	KY624277	KX376352	Kuhnert et al. (2017), Wendt et al. (2018)
<i>Biscognitansia nannulidaria</i>	MUCL 51395	France	ET	KY610382	KY610427	KY624236	Wendt et al. (2018)
<i>Daldinia caldarium</i>	MUCL 49211	France	ET	AM749934	KY610433	KC977282	Bitzer et al. (2008), Kuhnert et al. (2014), Wendt et al. (2018)
<i>Daldinia concentrica</i>	CBS 113277	Germany	HT	AY616683	KY610434	KY624243	Triebel et al. (2005), Kuhnert et al. (2014), Wendt et al. (2018)
<i>Daldinia demissii</i>	CBS 114741	Australia	HT	JX658477	KY610435	KY624244	Stadler et al. (2014), Kuhnert et al. (2014), Wendt et al. (2018)
<i>Daldinia petriinae</i>	MUCL 49214	Austria	ET	AM749937	KY610439	KY624248	Bitzer et al. (2008), Kuhnert et al. (2014), Wendt et al. (2018)
<i>Daldinia placunififormis</i>	MUCL 47603	Mexico	PT	AM749921	KY610440	KC977278	Stadler et al. (2014), Kuhnert et al. (2014), Wendt et al. (2018)
<i>Daldinia theissenii</i>	CBS 113044	Argentina	ET	KY610388	KY610441	KY624251	Bitzer et al. (2008), Kuhnert et al. (2014), Wendt et al. (2018)
<i>Daldinia vernicosa</i>	CBS 119316	Germany	ET	KY610395	KY610442	KY624252	Bitzer et al. (2008), Kuhnert et al. (2014), Wendt et al. (2018)
<i>Enonema liquescens</i>	ATCC 46302	USA	ET	KY610389	KY610443	KY624253	Wendt et al. (2018)
<i>Graphostroma platystomum</i>	CBS 270.87	France	HT	JX658535	DQ836906	KY624296	Kuhnert et al. (2014), Wendt et al. (2018)
<i>Hypomontagnella barboensis</i>	STMA 14081	Argentina	HT	MK131720	MK131718	MK135891	Zhang et al. (2006), Stadler et al. (2014), Koukol et al. (2015), Wendt et al. (2018)
<i>Hypomontagnella monticulosa</i>	MUCL 54604	French Guiana	ET	KY610404	KY610487	KY624305	Lambert et al. (2019)
<i>Hypomontagnella submonticulosa</i>	CBS 115280	France	ET	KC968923	KY610457	KY624226	Wendt et al. (2018)
<i>Hyphylon carneum</i>	MUCL 54177	France	ET	KY610400	KY610480	KY624297	Wendt et al. (2018)
<i>Hyphylon terradicola</i>	CBS 119009	France	ET	KC968908	KY610444	KY624254	Kuhnert et al. (2014), Wendt et al. (2018)
<i>Hyphylon crocophellum</i>	CBS 119004	France	ET	KC968907	KY610445	KY624255	Kuhnert et al. (2014), Wendt et al. (2018)
<i>Hyphylon fenuliferi</i>	MUCL 54792	France	ET	KF234421	KY610481	KY624298	Kuhnert et al. (2014), Wendt et al. (2018)
<i>Hyphylon fragiforme</i>	MUCL 51264	France	ET	KC477229	KM186295	KM186296	Stadler et al. (2013), Daranagama et al. (2015), Wendt et al. (2018)
<i>Hyphylon fuscum</i>	CBS 113049	France	ET	KY610401	KY610482	KY624299	Wendt et al. (2018)
<i>Hyphylon griseobrunneum</i>	CBS 331.73	India	HT	KY610402	KY610483	KY624300	Kuhnert et al. (2014), Wendt et al. (2018)
<i>Hyphylon guilanesse</i>	MUCL 57726	Iran	HT	MT214997	MT214992	MT212235	This study
<i>Hyphylon haematostroma</i>	MUCL 53301	Martinique	ET	KC968911	KY610484	KY624301	Kuhnert et al. (2014), Wendt et al. (2018)
<i>Hyphylon howeanum</i>	MUCL 47599	Germany	ET	AM749928	KY610448	KY624258	Bitzer et al. (2008), Kuhnert et al. (2014), Wendt et al. (2018)
<i>Hyphylon hypnium</i>	MUCL 51845	Guadeloupe	ET	KY610403	KY610449	KY624302	Wendt et al. (2018)
<i>Hyphylon investiens</i>	CBS 118183	Malaysia	ET	KC968925	KY610450	KY624259	Kuhnert et al. (2014), Wendt et al. (2018)
<i>Hyphylon lateripigmentum</i>	MUCL 53304	Martinique	HT	KC968933	KY610486	KY624304	Kuhnert et al. (2014), Wendt et al. (2018)
<i>Hyphylon lenormandii</i>	CBS 119003	Ecuador	ET	KC968943	KY610452	KY624261	Kuhnert et al. (2014), Wendt et al. (2018)
<i>Hyphylon muscum</i>	MUCL 53765	Guadeloupe	ET	KC968926	KY610488	KY624306	Bitzer et al. (2008), Kuhnert et al. (2014), Wendt et al. (2018)
<i>Hyphylon olivaceopigmentum</i>	DSM 107924	USA	HT	MK287530	MK287542	MK287558	Sir et al. (2019)
<i>Hyphylon papillatum</i>	ATCC 58729	USA	HT	KC968919	KY610454	KY624223	Bitzer et al. (2008), Kuhnert et al. (2014), Wendt et al. (2018)
<i>Hyphylon perforatum</i>	CBS 115281	France	ET	KY610391	KY610455	KY624224	Wendt et al. (2018)

Species	Strain number	Origin	Status	GenBank accession numbers			Reference	
				ITS	LSU	<i>rpb2</i>		
<i>Hypoxylon peritriac</i>	CBS 114746	France	HT	KY610405	KY610491	KY624279	Bitzer et al. (2008), Kuhnert et al. (2014), Wendt et al. (2018)	
<i>Hypoxylon pilgerianum</i>	STMA 13455	Martinique		KY610412	KY624308	KX271274	Wendt et al. (2018)	
<i>Hypoxylon pophyreum</i>	CBS 119022	France		KY610456	KY624225	KC977264	Bitzer et al. (2008), Kuhnert et al. (2014), Wendt et al. (2018)	
<i>Hypoxylon pulchricidum</i>	CBS 122622	Martinique	HT	JX183075	KY610492	KY624280	Bills et al. (2012), Wendt et al. (2018)	
<i>Hypoxylon rickii</i>	MUCL 53309	Martinique	ET	KC968932	KY610416	KY624281	KC977288	Kuhnert et al. (2014), Wendt et al. (2018)
<i>Hypoxylon rubiginosum</i>	MUCL 52887	Germany	ET	KC477232	KY610469	KY624266	Stadler et al. (2013), Wendt et al. (2018)	
<i>Hypoxylon rubiginosum</i>	MUCL 57727	Iran		MT214998	MT214993	MT212236	This study	
<i>Hypoxylon aff. rubiginosum</i>	MUCL 57724	Iran		MT214999	MT214994	MT212237	This study	
<i>Hypoxylon aff. rubiginosum</i>	MUCL 57725	Iran		MT215000	MT214995	MT212238	This study	
<i>Hypoxylon samuelii</i>	MUCL 51843	Guadeloupe	ET	KC968916	KY610466	KY624269	Kuhnert et al. (2014), Wendt et al. (2018)	
<i>Hypoxylon texense</i>	DSM 107933	USA	HT	MK287536	MK287548	MK287561	Sir et al. (2019)	
<i>Hypoxylon ticinense</i>	CBS 115271	France		JQ009317	KY610471	KY624272	AY951757	Hsieh et al. (2005), Wendt et al. (2018)
<i>Hypoxylon tringoides</i>	MUCL 54794	Sri Lanka	ET	KF234422	KY610493	KY624282	KF300548	Kuhnert et al. (2014), Wendt et al. (2018)
<i>Hypoxylon vogesiacum</i>	CBS 115273	France		KC968920	KY610417	KY624283	KX271275	Kuhnert et al. (2014), Kuhnert et al. (2017), Wendt et al. (2018)
<i>Jackogasterella colhaerens</i>	CBS 119126	Germany		KY610396	KY610497	KY624270	KY624314	Wendt et al. (2018)
<i>Jackogasterella minutella</i>	CBS 119015	Portugal		KY610381	KY610424	KY624235	KX271240	Kuhnert et al. (2017), Wendt et al. (2018)
<i>Jackogasterella multifornis</i>	CBS 119016	Germany	ET	KC477234	KY610473	KY624290	KX271262	Kuhnert et al. (2014), Kuhnert et al. (2017), Wendt et al. (2018)
<i>Pyrenopezizomyces hunteri</i>	MUCL 52673	Ivory Coast	ET	KY610421	KY610472	KY624309	KU159530	Kuhnert et al. (2017), Wendt et al. (2018)
<i>Pyrenopezizomyces laminosus</i>	MUCL 53305	Martinique	HT	KC968934	KY610485	KY624303	KC977292	Kuhnert et al. (2014), Wendt et al. (2018)
<i>Pyrenopezizomyces nicaraguaensis</i>	CBS 117739	Burkina_Faso		AM749922	KY610489	KY624307	KC977272	Bitzer et al. (2008), Kuhnert et al. (2014), Wendt et al. (2018)
<i>Rhopalosiroma angolense</i>	CBS 126414	Ivory Coast		KY610420	KY610459	KY624228	KX271277	Wendt et al. (2018)
<i>Ruenzoraria pseudanmudata</i>	MUCL 51394	D. R. Congo	HT	KY610406	KY610494	KY624286	KX271278	Stadler et al. (2010), Wendt et al. (2018)
<i>Thamnomycetes dendroides</i>	CBS 123578	French Guiana	HT	FN428831	KY610467	KY624232	KY624313	Fournier et al. (2011), Wendt et al. (2018)
<i>Xylaria arbuscula</i>	CBS 126415	Germany	ET	KY610394	KY610463	KY624287	KX271257	Sir et al. (2016), Wendt et al. (2018)
<i>Xylaria hypoxylon</i>	CBS 122620	Sweden	ET	KY610407	KY610495	KY624231	KX271279	Sir et al. (2016), Wendt et al. (2018)

Results

Phylogenetic analyses

Of the 4369 nucleotide characters of the combined matrix, 1618 are parsimony informative (298 of ITS, 156 of LSU, 487 of *rpb2* and 677 of *tub2*). Fig. 1 shows a phylogram of the best ML tree (lnL = -63870.651550) obtained by RAxML. Maximum parsimony analyses revealed one MP tree comprising 14,014 steps (data not shown). All major groups and deeper, highly supported nodes were consistent between the ML and MP analyses, but topologies of deeper unsupported nodes differed in the MP tree; as these differences are not relevant within the context of our new species, they are not further considered here. The phylogenies reveal a paraphyly of *Hypoxylon*, with the genera *Annulohypoxylon*, *Daldinia*, *Entonaema*, *Jackrogersella*, *Hypomontagnella*, *Pyrenopolyporus*, *Rhopalostroma*, *Ruwenzoria* and *Thamnomycetes* embedded within the former. All of the latter genera appeared monophyletic except for *Daldinia* (Fig. 1). All of our new Iranian species and records described below are contained within the highly supported *Hypoxylon* clade **H5**. The new species *H. guilanense* clustered together with *H. texense* with 100% BS support, while sequences of two additional strains (*Hypoxylon* aff. *rubiginosum* MUCL 57724) and (*Hypoxylon* aff. *rubiginosum* MUCL 57725) formed a highly supported (100% BS support) clade that is the sister group of *H. rubiginosum* (Fig. 1). The sequences of the Iranian collection of *H. rubiginosum* (MUCL 57727) are almost identical to those of the ex-epitype culture (MUCL 52887) and they clustered together with maximum support. As in previous studies, the position of *H. griseobrunneum* and *H. trugodes* could not be resolved within the family. The remaining clades are in accordance with previous results of Wendt et al. (2018).

Taxonomy

Hypoxylon guilanense Pourmoghaddam & C. Lambert, sp. nov.

MycoBank No: 834521

Fig. 2

Holotype. Iran, Guilan Province, Rasht County, Saravan forest, 37°04'26"N, 49°38'13"E, 183 m elev., on fallen branch of *Quercus castaneifolia*, 9 Apr 2015, M.J. Pourmoghaddam. (GUM 989; ex-holotype culture MUCL 57726).

Etymology. *Guilanense*, refers to its origin in Guilan province, Iran.

Teleomorph. Stromata superficial, hemispherical to pulvinate, up to 2 cm long × 0.1–0.7 cm wide, with conspicuous perithecial mounds, surface Sienna (8), Umber (9) to Buff (45); Scarlet (5) to Orange (7) granules beneath the surface and between the perithecia, with Orange (7) KOH-extractable pigments. Perithecia spherical to obo-

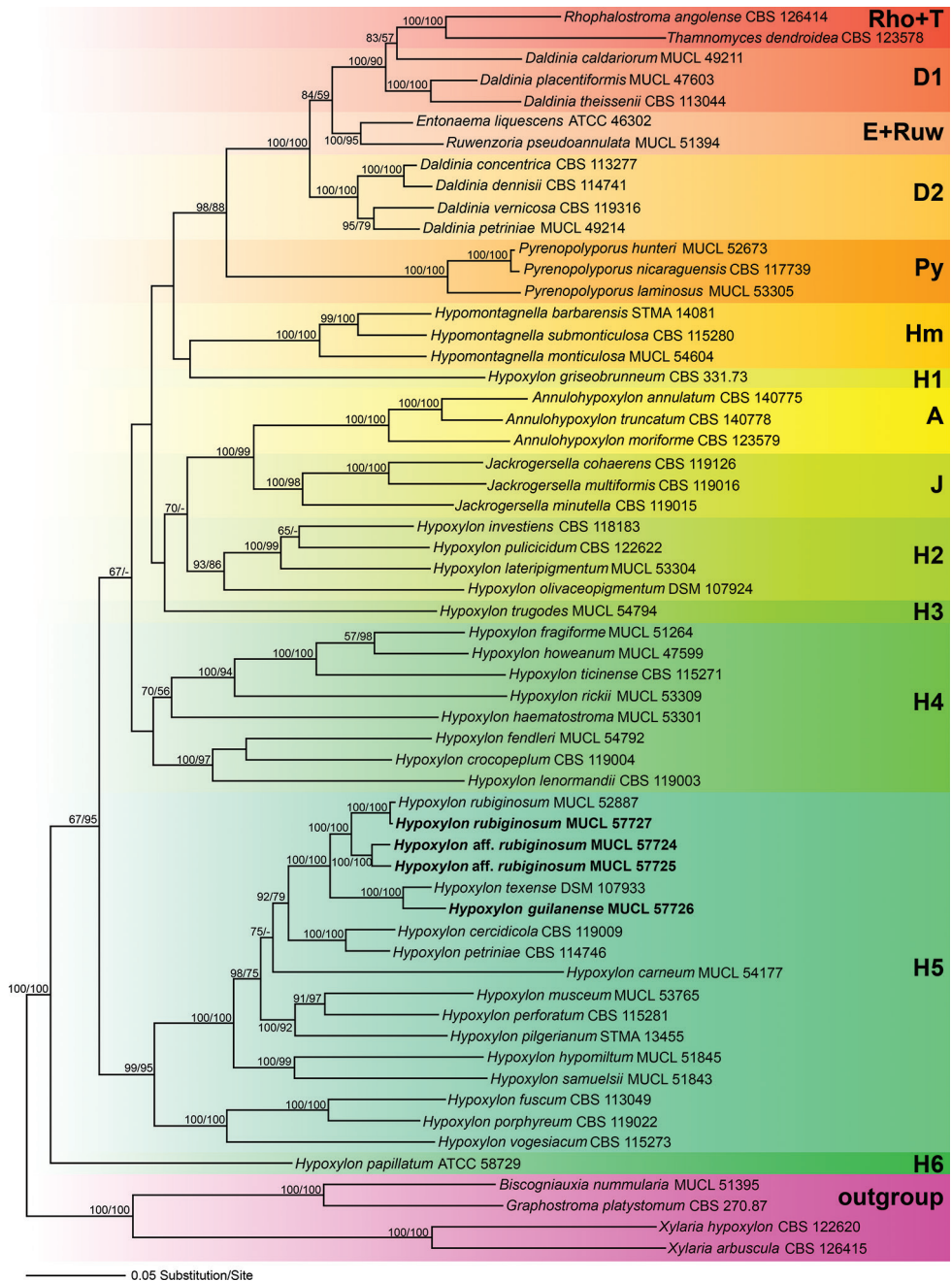


Figure 1. Phylogram of the best ML trees (lnL = -63870.651550) revealed by RAxML from an analysis of the combined ITS-LSU-*rpb2*-*tub2* matrix of selected Xylariales. Strains in bold were sequenced in the current study. ML and MP bootstrap support above 50% are given at the first and second positions, respectively, above or below the branches.

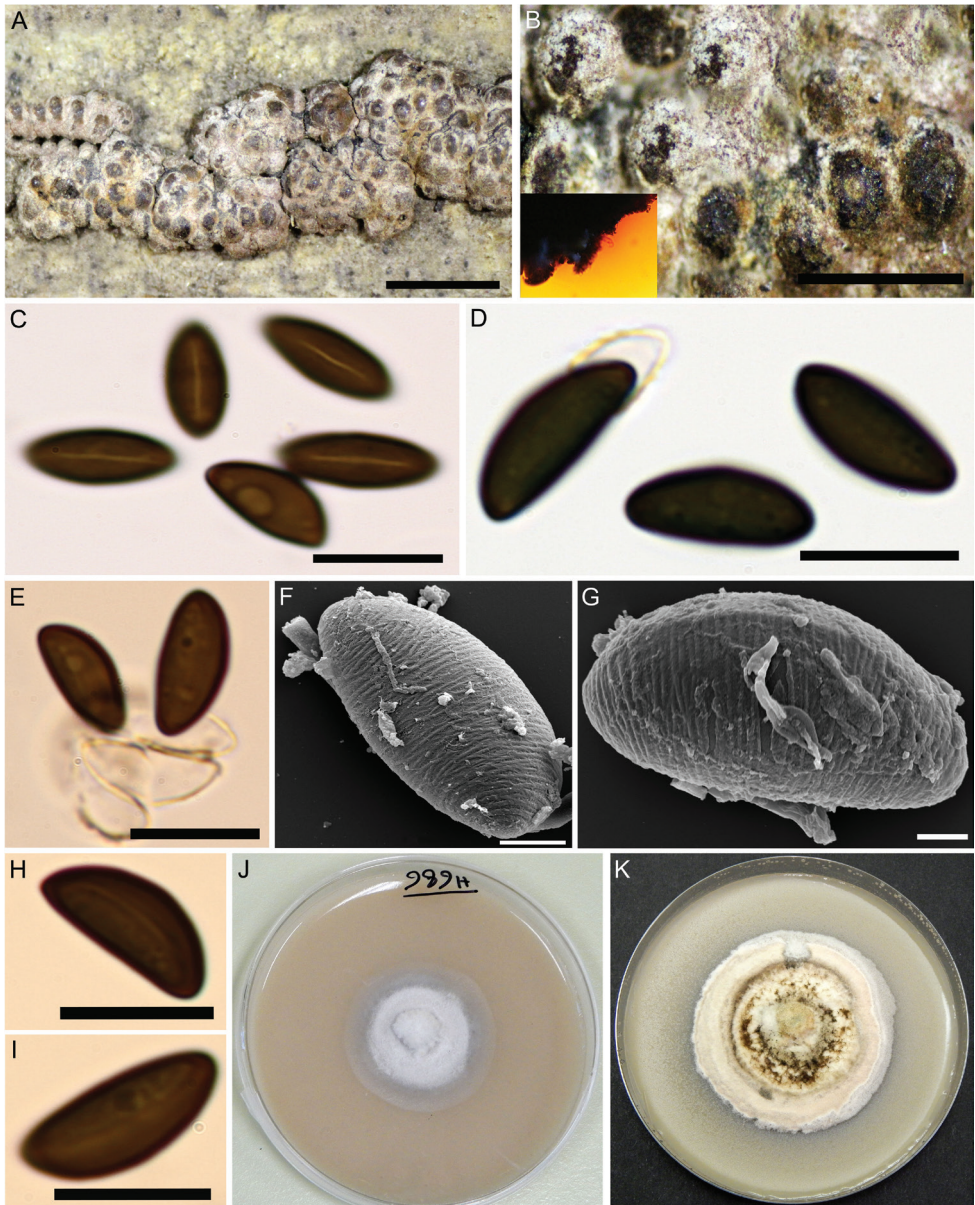


Figure 2. *Hypoxylon guilanense* (Holotype GUM 989) **A** stromatal habit **B** close-up view of stromatal surface, with stromatal pigments in 10% KOH **C, H, I** ascospores in water, with germ-slits **D, E** ascospores in 10% KOH with dehiscent perispore **F, G** ascospore under SEM **J, K** culture on 9 cm OA plates after 1 and 3 wk of incubation (left to right). Scale bars: 2.5 mm (**A**), 1 mm (**B**); 10 μ m (**C–E**); 2 μ m (**F, G**); 10 μ m (**H, I**).

void, 0.33–0.66 high \times 0.3–0.55 mm wide. Ostioles umbilicate, inconspicuous. Asci not seen. Ascospores smooth, unicellular, brown to dark brown, ellipsoid, inequilateral with narrowly rounded ends, 12–15 \times 5–6 μ m, with straight germ slit spore-length on

convex side; perispore dehiscent in 10% KOH, conspicuous coil-like ornamentation in SEM; episore smooth.

Cultures and anamorph. Colonies on OA covering a 9 cm Petri dish in 4 wk, at first white, becoming Buff (45), cottony, slightly zonate with diffuse margins; finally, becoming Honey (64). Anamorph not produced in culture.

Secondary metabolites. Orsellinic acid, rubiginosin A and an unknown isomer thereof, as well as mitorubrinol acetate as prevailing stromatal components; cultures produce yet unidentified compounds on barley-malt agar.

Notes. The description of this taxon is based on a single specimen, which shows the salient features of the teleomorph and can be discriminated easily from all previously described species of the *H. rubiginosum* complex. The stromata of the holotype specimen differ from *H. texense* (i.e. the closest relative in the phylogeny), in having stromata with hemispherical to pulvinate shape, Orange (7) KOH-extractable pigments and larger ascospores [$12\text{--}15 \times 5\text{--}6$ vs. $9.1\text{--}10.8$ (-11.5) \times (4.0--) $4.5\text{--}5.4$ (-5.7) μm with straight germ slit.

Hypoxylon guilanense can also be easily differentiated from *H. rubiginosum sensu stricto* and *H. petriniae* in the peculiar stromatal shape and it also has larger ascospores. *H. cercidicola* differs from *H. guilanense* in having erumpent stromata with discoid shape and smaller ascospores [$(9\text{--}) 9.5\text{--}12 \times 5\text{--}6 \mu\text{m}$] with straight to slightly sigmoid germ slit. Table 2 compares morphological characters of some other taxa that may be confused with *H. guilanense*.

Hypoxylon rubiginosum (Pers.) Fr., *Summa Veg. Scand.* II, p. 384. (1849).

Fig. 3

Teleomorph. Stromata superficial, effused-pulvinate, up to 8 cm long \times 0.3–0.2 cm wide; with inconspicuous to conspicuous perithecial mounds, surface Red (2) to Brick (59); Scarlet (5) to Orange (7) granules beneath the surface and between the perithecia, with Orange (7) to Scarlet (5) KOH-extractable pigments. Perithecia spherical to obovoid, 0.2–0.5 high \times 0.15–0.45 mm wide. Ostioles umbilicate, inconspicuous. Asci 8-spored, cylindrical, with amyloid, discoid apical apparatus, 0.5–1 μm high \times 1.5–2.5 μm wide, stipe up to 180 μm long and spore-bearing portion 40–80 \times 6.5–10 μm . Ascospores smooth, unicellular, brown to dark brown, ellipsoid, inequilateral with narrowly rounded ends, 9–12 (-13) \times 4–6 μm , with straight germ slit spore-length on convex side; perispore dehiscent in 10% KOH; episore smooth.

Cultures and anamorph. Colonies on OA covering a 9 cm Petri dish in 3 wk, at first white, becoming Smoke Grey (105), felty, azonate with diffuse margins; finally becoming Pale Luteous (11) to Straw (46). Asexual morph not produced in culture.

Secondary metabolites. Rubiginosin A and an unknown compound of the mitorubrin / rubiginosin azaphilone family prevalent; cultures produce phomopsidin and unidentified compounds on barley-malt agar.

Specimens examined. Iran, Guilan Province, Siahkal County, Deilaman forest, 36°57'25"N, 49°51'54"E, 1100 m elev., on fallen branch of *Quercus castaneifolia*,

Table 2. Diagnostic characters of *Hypoxylon rubiginosum* sensu stricto and closely related species.

Taxon	Stromatal shape	Stromatal surface	KOH-extractable pigments	Ascospores (µm)	Germ slit	Host	Known distribution	Anamorph	Secondary metabolites*
<i>Hypoxylon canariense</i>	effused to effused-pulvinate	Fulvous, Dark Brick, Dark Vinaceous	Orange to Stemma	9.5–11.5 × 4.5–5	straight	<i>Erica</i> , <i>Oxycas</i> , <i>Laurus</i> , <i>Persea</i>	Spain (Canary Islands)	vigariella-like	Rubiginosins A–C, mitorubrinol acetate
<i>Hypoxylon carneum</i>	Effused-pulvinate	Dark purple, Dark vinaceous	Livid violet, absent in old stromata	(7.5–)8–11.5 × 4.5–5	straight	Various angiosperm hosts including <i>Fraxinus</i>	probably cosmopolitan but rare	sporothrix-like	Carneic acids A and B, BNT
<i>Hypoxylon verrucicola</i>	discoid	Dark brick to Sepia	Orange	(9–)9.5–12 × 5–6	straight to slightly sigmoid	<i>Fraxinus</i>	Europe and North America	unknown	Mitorubrin, rubiginosin A and C
<i>Hypoxylon guilense</i>	hemispherical to pulvinate	Sienna, Umber to Buff	Orange	12–15 × 5–6	straight	<i>Quercus</i>	Iran	unknown	Rubiginosin A, mitorubrinol acetate
<i>Hypoxylon lucitanicum</i>	effused	Brown Vinaceous	Sienna	11–13.5 × 5–7	straight	<i>Rhamnus</i>	Portugal	unknown	Rubiginosins A and C, rutilin A
<i>Hypoxylon petriniiae</i>	irregularly effused	Lilac, Vinaceous to Brown Vinaceous	Orange to Rust	8–11.5(–13) × 4.8–6	straight	<i>Fraxinus</i> (mostly), <i>Acer</i> , <i>Salicaceae</i>	Western and Central Europe	vigariella-like	Rubiginosin A, BNT
<i>Hypoxylon retpela</i>	effused-pulvinate	Livid Vinaceous, Brown Vinaceous, Dark Brick, Brown Vinaceous	Orange or Scarlet	(9–)9.5–12 × 4.5–5	straight or slightly sigmoid	unknown	Southeast and East Asia, New Guinea	nodulisporium-like	Mitorubrinol acetate, unknown rubiginosins
<i>Hypoxylon rubiginosum</i>	effused-pulvinate	Dark Brick, Brown Vinaceous	Orange	9–13 × 4–5.5	straight	Various angiosperm hosts including <i>Fraxinus</i>	Europe, North America	nodulisporium-like	Mitorubrin, rubiginosin A–C, rubiginosic acid, daldinin C
<i>Hypoxylon</i> aff. <i>rubiginosum</i> (GUM 1587)	pulvinate to effused-pulvinate	Luteous, Orange to Ochraceous	Orange	8–10 (–11) × (3–)4–4.5 (–5)	straight to slightly sigmoid	<i>Quercus</i>	Iran	vigariella-like	like <i>H. rubiginosum</i>
<i>Hypoxylon</i> aff. <i>rubiginosum</i> (GUM 1588)	pulvinate	Orange to Apricot	Orange	10–15 × 5–6.5	straight to slightly sigmoid	unknown	Iran	not observed-	like <i>H. rubiginosum</i>
<i>Hypoxylon salicicola</i>	effused	Dark rust to Sepia, Brown Vinaceous	Fulvous to Rust	7.2–9.6 × 3–4.2	straight	<i>Salix</i> , rarely on <i>Fraxinus</i> and <i>Prunus</i>	Northern Europe, USA	nodulisporium-like	Mitorubrinol acetate
<i>Hypoxylon texense</i>	effused to effused-pulvinate	Livid Vinaceous to Brown Vinaceous	Rust to Dark Brick	9.1–10.8(–11.5) × (4.0–)4.5–5.4(–5.7)	straight or slightly sigmoid	unknown	USA	nodulisporium to vigariella-like	Rubiginosin A, mitorubrinol acetate, unknown rubiginosins
<i>Hypoxylon urrtiesii</i>	effused	Dark Brick	Orange	11–14.5 × 5–6	straight or slightly sigmoid	unknown	Spain (Canary Islands)	unknown	Mitorubrinol acetate, rubiginosin A



Figure 3. *Hypoxylon rubiginosum* (GUM 1586) **A, B** stromatal habit **C** close-up view of stromatal surface **D** close-up view of stromatal surface, with stromatal pigments in 10% KOH **E** ascospores in 10% KOH with dehiscent perispore **F** mature and immature asci in water **G** immature ascus in water **H** mature ascus in water **I** ascus in Melzer's reagent **J** ascospores in water **K** ascus tip in Melzer's reagent. Scale bars: 2 cm (**A**); 1 cm (**B**); 4 mm (**C**); 2 mm (**D**); 10 μ m (**E**); 20 μ m (**F-I**), 10 μ m (**J, K**).

6 Oct 2017 (GUM 1586; culture MUCL 57727); Guilan Province, Shaft County, 36°59'08"N, 49°18'43"E, 594 m elev., on fallen trunk of *Pterocarya fraxinifolia*, 15 Sep 2015 (GUM 1583); Guilan Province, Langaroud County, Liseroud forest, 37°7'44"N,

50°8'41"E, 28 m elev., on fallen branch of *Quercus castaneifolia*, 10 Sep 2016 (GUM 1584); Guilan Province, Talesh County, Gisoum forest, 37°37'30"N, 48°58'15"E, 477 m elev., on fallen branch of *Populus* sp., 20 Oct 2016 (GUM 1585). All specimens collected by M.J. Pourmoghaddam.

Notes. *H. rubiginosum sensu stricto* is a very common fungus in the temperate Northern hemisphere (Stadler et al. 2008) and may occur in subtropical areas, such as Florida, USA (Ju and Rogers 1996). Most of the characters of the Iranian specimens are in accordance with previous descriptions (Stadler et al. 2004), aside from insignificant variations in the size of ascospores.

Additional potentially new species of the *H. rubiginosum* complex

Below, we describe two collections that may eventually be recognised to represent new species. They appear phylogenetically different from the type specimen, as well as from Iranian records of *H. rubiginosum*, but share salient features with the latter species. It is explained in the Notes why we hesitate to describe them as new taxa in this complicated species complex.

Hypoxylon sp. (aff. *rubiginosum*) GUM 1587

Figs 4, 5

Teleomorph. Stromata superficial, pulvinate to effused-pulvinate, up to 5 cm long × 0.6–2 cm wide, with inconspicuous to conspicuous perithecial mounds; surface Luteous (12), Orange (7) to Ochreous (44); Orange (7) granules beneath the surface, Orange (7) and Leaden Black (126) granules between the perithecia, with KOH-extractable pigments Orange (7). Perithecia obovoid, compressed-obovoid to spherical, 0.27–0.50 high × 0.23–0.35 mm wide. Ostioles umbilicate, inconspicuous, usually overlain with conspicuous white substance. Asci 8-spored, cylindrical, with amyloid, discoid apical apparatus, 0.5–1 µm high × 2–2.5 µm wide, stipe up to 180 µm long; spore-bearing portion 80–100 × 5.5–7 µm. Ascospores smooth, unicellular, brown to dark brown, ellipsoid, inequilateral with narrowly rounded ends, 8–10 (–11) × (3–) 4–4.5 (–5) µm, with straight to slightly sigmoid germ slit spore-length on convex side; perispore dehiscent in 10% KOH, conspicuous coil-like ornamentation in SEM; epispore smooth.

Cultures and anamorph. Colonies on OA covering a 9 cm Petri dish in 3 wk, at first white, becoming Luteous (12) from outwards, cottony, slightly zonate with diffuse margins; finally, attaining a variety of different colours. Conidiogenous structure branching virgariella-like as defined by Ju and Rogers (1996), (Fig. 5C–G). Conidiophores hyaline, smooth to finely roughened. Conidiogenous cells hyaline, smooth to finely roughened, 15–30 × 2–3 µm. Conidia hyaline, smooth to ellipsoid, 4–6 × 2–3 µm.

Specimen examined. Iran, Guilan Province, Astaneh-Ashrafieh County, Safra-Basteh forest, 37°20'19"N, 49°58'26"E, 14 m elev., on fallen branch of *Quercus castaneifolia*, 4 Oct 2016, M.J. Pourmoghaddam (GUM 1587; culture MUCL 57724).

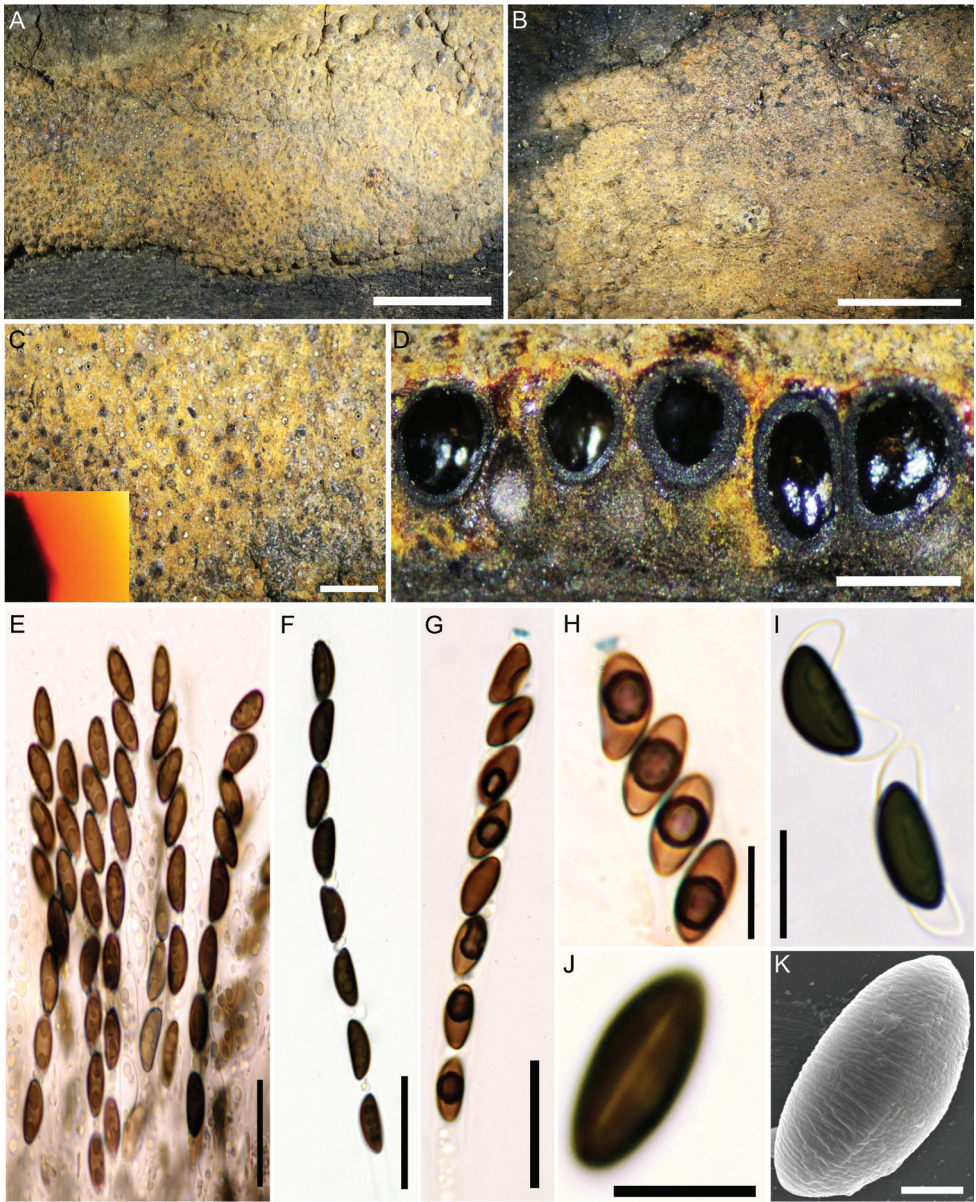


Figure 4. *Hypoxylon* aff. *rubiginosum* (GUM 1587) **A, B** stromatal habit **C** close-up view of stromatal surface, with stromatal pigments in 10% KOH **D** stroma in section showing perithecia and ostioles **E** mature and immature asci in water **F** ascus in water **G** ascus in Melzer's reagent **H** ascus tip in Melzer's reagent **I** ascospores in 10% KOH with dehiscent perispore **J** ascospore in water, with germ-slit **K** ascospore under SEM. Scale bars: 5 mm (**A, B**); 1 mm (**C**); 0.5 mm (**D**); 20 μ m (**E–G**); 10 μ m (**H–J**); 2 μ m (**K**).

Notes. This specimen resembles *H. rubiginosum* in many respects. However, it has slightly smaller ascospores [8–10 (–11) \times (3–) 4–4.5 (–5) vs. 9–13 \times 4–5.5 μ m] and the germ slit of the ascospores is often slightly sigmoid. The most significant differences

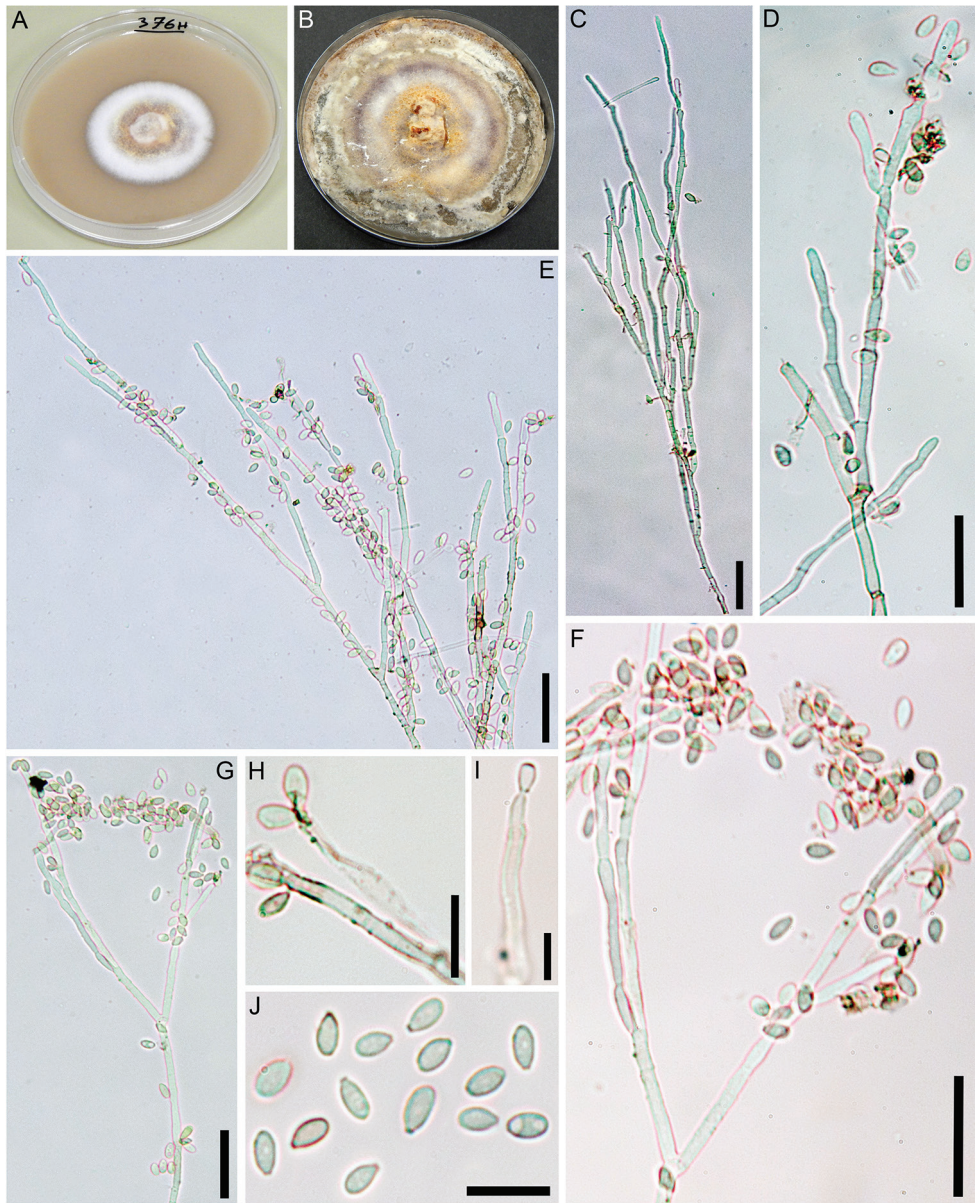


Figure 5. Culture and anamorphic structures of *Hypoxylon* aff. *rubiginosum* (GUM 1587) on OA **A, B** surface of colony after 1 and 8 wk of incubation (respectively, left to right) **C–G** general view of anamorph structure with virgariella-like branching patterns **H, I** conidiogenous cells and immature conidia **J** mature conidia. Scale bars: 20 μ m (**C–G**); 10 μ m (**H–J**).

were noted in the anamorphic structures with virgariella-like branching patterns. This anamorph actually resembles that of *H. petriniae*. However, this species is normally associated with *Fraxinus* and differs from *Hypoxylon* aff. *rubiginosum* GUM 1587 in having Lilac (54), Vinaceous (57) to Brown Vinaceous (84) stromatal surface colours

(owing to the presence of BNT, which was not found in the Iranian specimen). It also differs in having more elongate to irregularly effused stromata with black margins and its ascospores are larger ($8\text{--}11.5$ (-13) \times $4.8\text{--}6$ μm) and have a straight germ slit.

Hypoxylon sp. (aff. *rubiginosum*) GUM 1588

Fig. 6

Teleomorph. Stromata superficial, pulvinate, up to 1 cm long \times 0.2–0.5 cm wide, with inconspicuous to conspicuous perithecial mounds; surface Orange (7) to Apricot (42); Orange (7) granules beneath the surface and Laeden Black (126) granules between the perithecia, with Orange (7) KOH-extractable pigments. Perithecia obovoid to compressed-obovoid, 0.35–0.65 high \times 0.3–0.45 mm wide. Ostioles umbilicate, inconspicuous. Asci with amyloid, discoid apical apparatus, 1–1.5 μm high \times 2–3 μm wide, stipe up to 160 μm and spore-bearing portion 70–100 \times 6–8 μm long. Ascospores smooth, unicellular, brown to dark brown, ellipsoid, inequilateral with narrowly-rounded ends, 10–15 \times 5–6.5 μm , with straight to slightly sigmoid germ slit spore-length on convex side; perispore dehiscent in 10% KOH; episporium smooth.

Cultures and anamorph. Colonies on OA covering a 9 cm Petri dish in 3 wk, at first white, becoming whitish, cottony, azonate with entire margins; remaining mainly uncoloured with Pale Luteous tinges. Anamorph not produced in culture.

Specimen examined. Iran, Mazandaran Province, Tonekabon County, Do-hezar forest, 36°42'30"N, 50°49'43"E, 456 m elev., on dead branches (host unknown), 28 Oct 2016, M.J. Pourmoghaddam (GUM 1588; culture MUCL 57725).

Notes. This specimen is morphologically similar to *Hypoxylon* aff. *rubiginosum* GUM 1587, but it can be distinguished by its larger ascospores [10–15 \times 5–6.5 vs. 8–10 (-11) \times (3–) 4–4.5 (-5) μm]. *H. rubiginosum sensu stricto* differs from this specimen in having smaller ascospores [(8–) 9–12 \times 4–5.5 vs. 10–15 \times 5–6.5 μm]. In addition, the stromatal secondary metabolite profile is similar to that of *H. rubiginosum* with two unknown azaphilone compounds of the mitorubrin / rubiginosin family (UC 2, retention time = 8.7 min, 442 Dalton and UC 3, RT = 10.6 min, 884 Da) and rubiginosin A. *H. guilanense* differs from *Hypoxylon* aff. *rubiginosum* GUM 1588 in having stromata with hemispherical to pulvinate shape and difference in average ascospores sizes (12–15 \times 5–6 vs. 10–15 \times 5–6.5 μm) with straight germ slit. *H. texense* differs from *Hypoxylon* aff. *rubiginosum* GUM 1588 in having Rust (39) to Dark Brick (86) KOH-extractable pigments and much smaller ascospores [9.1–10.8 (-11.5) \times (4.0–) 4.5–5.4 (-5.7) vs. 10–15 \times 5–6.5 μm].

HPLC profiling of stromata

Amongst the four studied Iranian *Hypoxylon* spp., five major metabolites could be identified. Beneath common secondary metabolites of the *H. rubiginosum* complex like orsellinic acid (**1**, Stadler et al. 2008), mitorubrin acetate (**2**, Steglich et al. 1974;

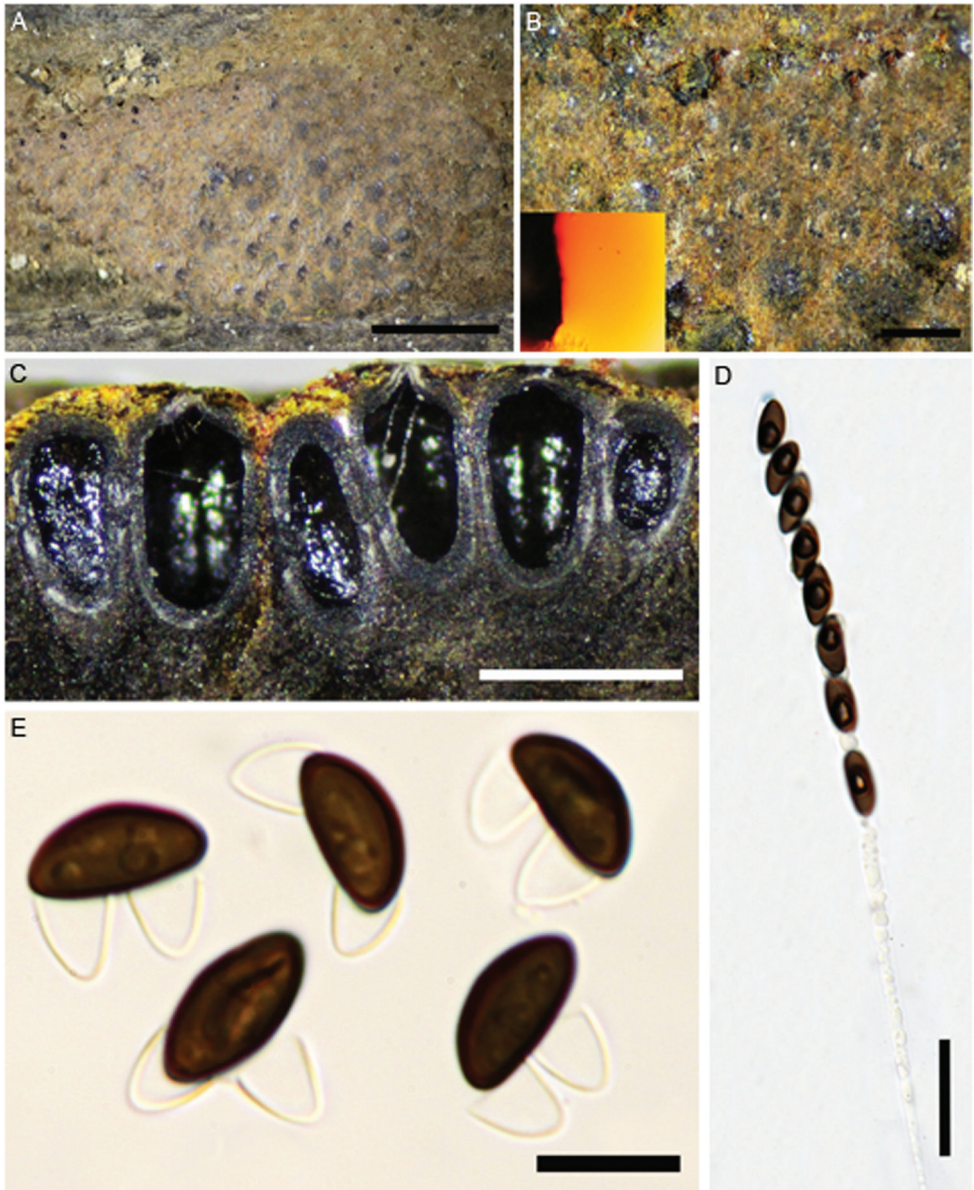


Figure 6. *Hypoxylon* aff. *rubiginosum* (GUM 1588) **A** stromatal habit **B** close-up view of stromatal surface, with stromatal pigments in 10% KOH **C** section of stroma showing perithecia and ostioles **D** ascus in Melzer's reagent **E** ascospores in 10% KOH with dehiscent perispore. Scale bars: 2.5 mm (**A**); 0.5 mm (**B**, **C**); 20 µm (**D**); 10 µm (**E**).

Stadler et al. 2001) and rubiginosin A (**3**, Quang et al. 2004), three more non-assignable compounds were detected. UV/Vis data of these metabolites tentatively suggested affinities to the rubiginosin azaphilone family (Fig. 9, **UC 2** and **3**) with one unknown

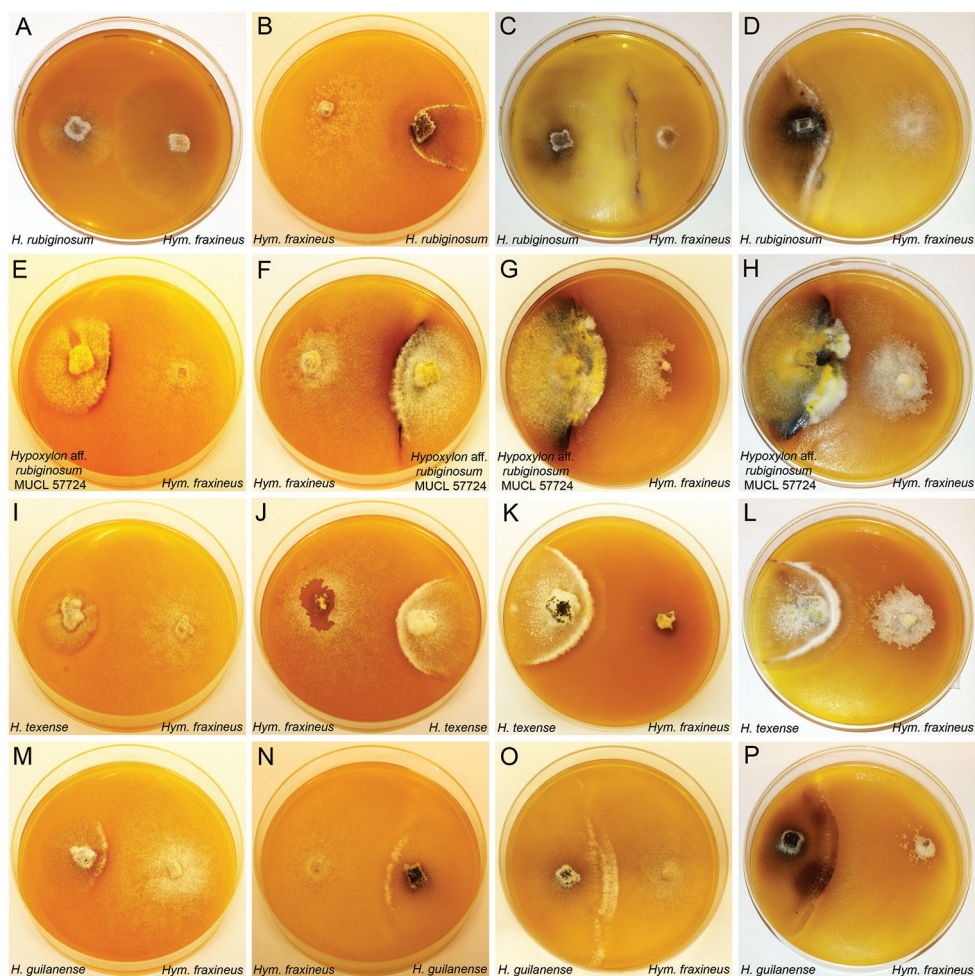


Figure 7. Illustration of antagonist test by dual culture technique of *Hypoxylon* spp. and *Hymenoscyphus fraxineus* on barley-malt agar in 9-cm diam. plates **A** dual culture of *H. rubiginosum* (MUCL 47152) against *Hym. fraxineus* (STMA 18166) after 1 wk of incubation **B** dual culture of *H. rubiginosum* (MUCL 47152) against *Hym. fraxineus* (STMA 18166) after 2 wk of incubation **C** dual culture of *H. rubiginosum* (MUCL 47152) against *Hym. fraxineus* (STMA 18166) after 3 wk of incubation **D** dual culture of *H. rubiginosum* (MUCL 47152) against *Hym. fraxineus* (STMA 18166) after 4 wk of incubation **E–H** (*Hypoxylon* aff. *rubiginosum* MUCL 57724) against *Hym. fraxineus* after 1, 2, 3, 4 wk **I–L** *H. texense* (DSM 107933) against *Hym. fraxineus* after 1, 2, 3, 4 wk **M–P** *H. guilainense* (MUCL 57726) against *Hym. fraxineus* after 1, 2, 3, 4 wk.

compound sharing the same mass and UV/Vis maxima of mitorubrinol (**4**), which could possibly constitute a yet undescribed isomer (**URg**). Compounds **URg** and **UC 2** have been reported from *H. texense*, which was recently discovered in Texas, USA, as another species of the *H. rubiginosum* complex (Sir et al. 2019). These findings are further reflected in the taxonomic part of this paper.

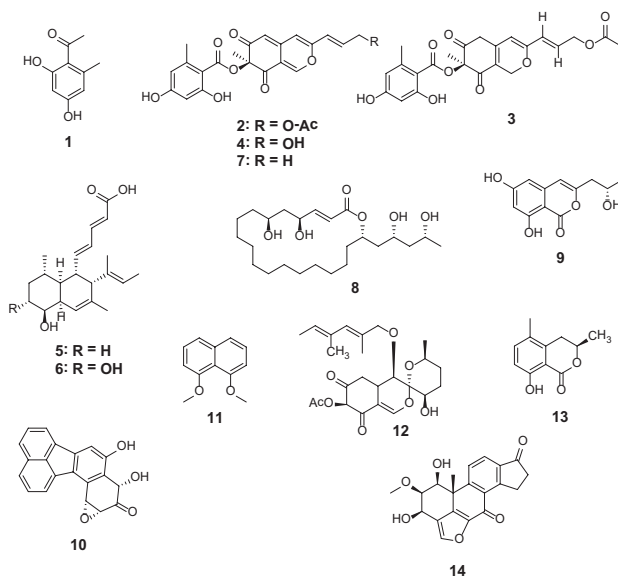


Figure 8. Chemical structures of discussed secondary metabolites. Orsellinic acid (**1**); mitorubrinol acetate (**2**); rubiginosin A (**3**); mitorubrinol (**4**); phomopsidin (**5**); 10-hydroxyphomopsidin (**6**); mitorubrin (**7**); ricklial A (**8**); orthosporin (**9**); daldinone B (**10**); 1,8-dimethoxynaphthalene (**11**); daldinin F (**12**); 5-methyl mellein (**13**); viridial (**14**).

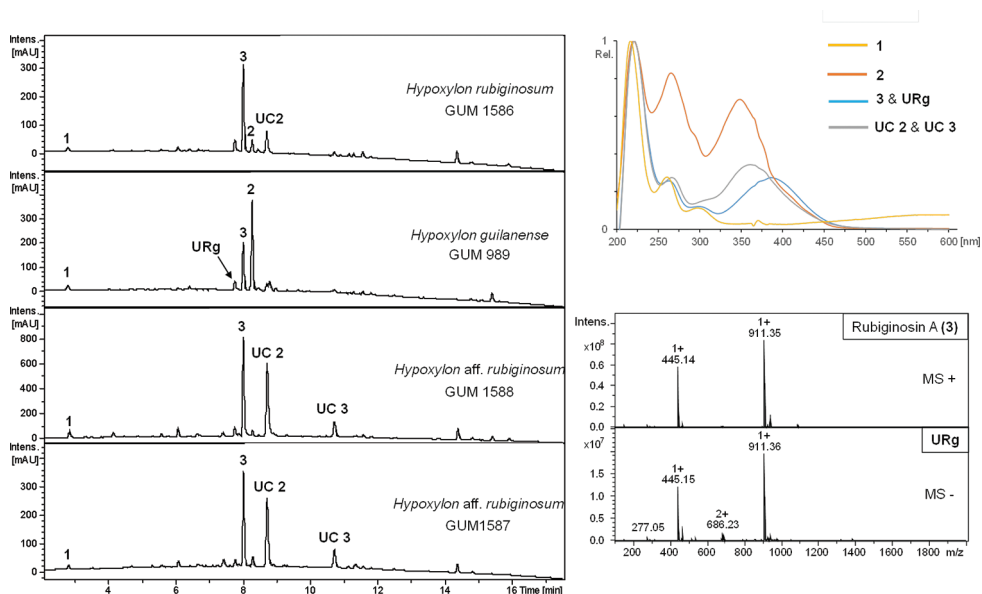


Figure 9. HPLC-UV profiles at 210 nm derived from stromal extracts of strains *H. rubiginosum* (GUM 1586), *H. guilanaense* (from holotype) and *Hypoxylon* aff. *rubiginosum* GUM 1587 and GUM 1588. UV/Vis spectra are shown for orsellinic acid (**1**), mitorubrinol acetate (**2**), rubiginosin A (**3**), an unknown rubiginosin A – like derivative (**URg**) and rubiginosin – like derivatives (**UC 2** and **UC 3**). ESI mass spectra are shown for compounds **URg** and **2**.

HPLC profiling of extracts from single and dual culture experiments (Figs 10, 11)

In total, 32 different *Hypoxyton* strains were screened for production of phomopsidin (**5**, Kobayashi et al. 2003) and 10-hydroxyphomopsidin (**6**, Halecker et al. 2020). Due to the availability of well-studied strains of *H. rubiginosum*, *H. perforatum* and *H. petriniae* in public culture collections, a pre-screening was conducted to confirm production of **5** and **6** (with 13, 7 and 4 strains each, respectively (cf. Table 3, Fig. 11H). Out of these 24 strains, 16 emerged as producers of compound **5** and partially **6** (12 strains). Compound **6** was not detected in the absence of **5**. Out of those, two strains of *H. rubiginosum* (MUCL 47152 and MUCL 47970), one representative of *H. perforatum* (MUCL 47187) and one culture of *H. petriniae* (MUCL 53756) were selected for further testing against *Hym. fraxineus*. The results are illustrated, based on four examples in Fig. 7, showing the dual cultures after 1–4 weeks of incubation. The chemical structures are shown in Fig. 8 and selected chromatographic data are depicted in Figs 10, 11.

Strikingly, during evaluation and comparison of the HPLC UV/Vis chromatograms with our internal database, the mitorubrin derivatives **2**, **4** and **7** were identified by direct comparison of chromatograms derived from extracts of stromata and cultures of the ex-type strain and the holotype of *H. texense* (Sir et al. 2019; Figs 7 I–L, 11B, D).

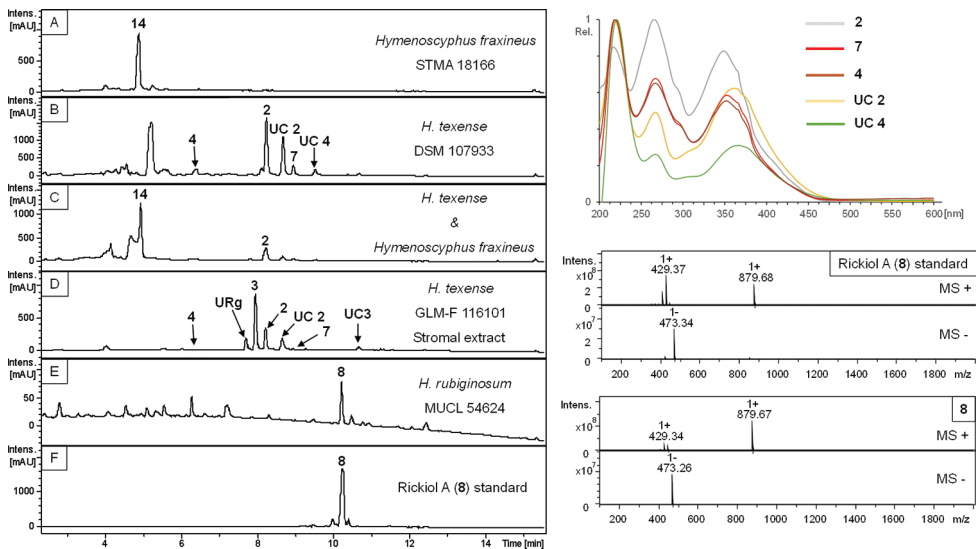


Figure 10. HPLC-UV profiles at 210 nm derived from barley-malt agar (**A–C, E**) and stromal (**E**) extracts and compound standard (**F**). UV/Vis spectra are shown for identified compounds in mono- and dual culture (**C**) experiments of STMA 18166 (*Hym. fraxineus*, **A**) and DSM 107933 (*H. texense*, **B**; UC **2, 4** – unknown compounds); stromal metabolites (**4** – mitorubrinol; **URg** – unknown rubiginosin A derivative; **3** – rubiginosin A; **2** – mitorubrinol acetate; **7** – mitorubrin; **UC 2** – Unknown compound 2 of GLM-F116101 (*H. texense*, **D**), and ... ESI mass spectra of **8** in positive and negative modes... of **8** (rickioli A, **F**) identified in the mono culture extract of MUCL 54624 (*H. rubiginosum*, **E**).

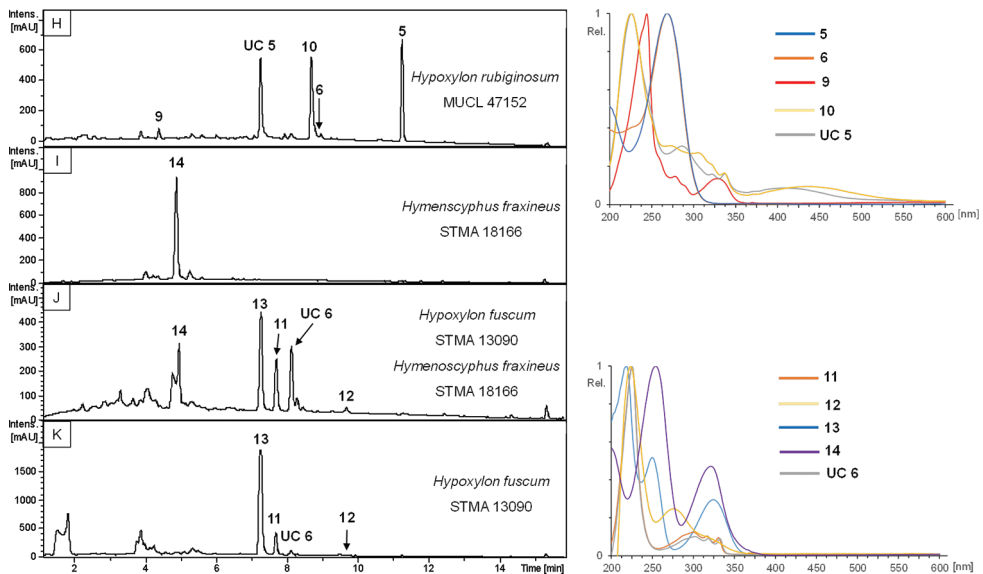


Figure 11. HPLC-UV chromatograms at 210 nm from mono cultural barley-malt agar extracts of MUCL 47152 (*H. rubiginosum*), STMA 18166 (*Hym. fraxineus*), STMA 13090 (*H. fuscum*) and one dual culture experiment thereof. UV/Vis spectra are shown for phomopsidin (**5**), 10-hydroxyphomopsidin (**6**), orthosporin (**9**), daldinone B (**10**), 1,8-dimethoxynaphthalene (**11**), daldinin F (**12**), 5-methylmellein (**13**), viridiol (**14**) and an unidentifiable compound (UC **6**) after comparison of data with internal databases. The UV signal of UC **6** was enhanced in the dual culture extract.

Beneath the aforementioned UC **2**, another yet undescribed compound was revealed (UC **4**). The main metabolite of the mono cultural extract of MUCL 54624 was identified by comparison of UV/Vis and MS data as rickiol A (**8**; Fig. 11E–F), previously described from *H. rickii* (Surup et al. 2018b). Orthosporin (**9**; Quang et al. 2002), daldinone B (**10**; Stadler et al. 2008) was identified by comparison with an internal database in several strains of *H. rubiginosum*, *H. perforatum* and *H. petriniae* (cf. Tables 3, 4, Fig. 11H). The mono cultural extract of *H. fuscum* (STMA 13090) revealed 1,8 dimethoxynaphthalene (**11**; Chang et al. 2014) and another unidentified peak (UC **6**, Fig. 11J, K) with an identical UV/Vis spectrum as **11**, as well as traces of Daldinin F (**12**; Quang et al. 2004) and 5- methylmellein (**13**; Stadler et al. 2005b) as the main product. Interestingly, the UV signal of UC **7** was visibly enhanced in the chromatogram derived from the dual culture extract. The phytotoxic compound viridiol (**14**; Figs 10A, 11I–K) was found in both mono and dual culture extracts of *Hym. fraxineus* (Andersson et al. 2010; Halecker et al. 2020).

Discussion

The present study dealt with the identification of *Hypoxylon* species from Northern Iran based on morphological, chemotaxonomic and phylogenetic data, focusing on

Table 3. Identified secondary metabolites in axenic cultures on barley-malt medium of the surveyed strains. Strains in **bold** have been used concurrently against STMA 18166 (*Hymenoscyphus fraxineus*) in an antagonism assay. Identified compounds: **5**: phomopsidin; **6**: 10-hydroxyphomopsidin; **8**: rickiol A; **9**: orthosporin **10**: daldinone B; **11**: 1,8-dimethoxynaphthalene; **13**: 5-methyl-mellein. Identified stromal azaphilone groups detected in culture: MI = Mitorubrin type; NA = Naphthalene type; DA =Daldinin type. For chemical structures, see Fig. 8.

Organism	Strain	Culture metabolites			Stromal metabolites		
		5	6	Others	MI	NA	DA
<i>Hypoxyylon guilanense</i>	MUCL 57726	–	–	–	–	–	–
<i>Hypoxyylon</i> aff. <i>rubiginosum</i>	MUCL 57724	+	+	–	+	–	–
<i>Hypoxyylon rubiginosum</i>	MUCL 57727	+	–	–	–	–	–
<i>Hypoxyylon</i> aff. <i>rubiginosum</i>	MUCL 57725	+	+	–	–	–	–
<i>Hypoxyylon perforatum</i>	MUCL 57728	–	–	10	–	–	–
<i>Hypoxyylon perforatum</i>	CBS 119011	–	–	10	–	–	–
<i>Hypoxyylon perforatum</i>	MUCL 47187	+	+	–	–	–	–
<i>Hypoxyylon perforatum</i>	MUCL 54798	–	–	10	–	–	–
<i>Hypoxyylon perforatum</i>	STMA 13041	+	+	–	–	–	–
<i>Hypoxyylon perforatum</i>	STMA 14051	–	–	10	–	–	–
<i>Hypoxyylon perforatum</i>	CBS 140779	–	–	10	–	–	–
<i>Hypoxyylon petriniae</i>	MUCL 53756	+	+	–	–	–	–
<i>Hypoxyylon petriniae</i>	STMA 12020	–	–	–	–	–	–
<i>Hypoxyylon petriniae</i>	STMA 13303	–	–	–	–	–	–
<i>Hypoxyylon petriniae</i>	STMA 13313	–	–	10	–	–	–
<i>Hypoxyylon rubiginosum</i>	MUCL 2354	–	–	–	–	–	–
<i>Hypoxyylon rubiginosum</i>	MUCL 47152	+	+	9, 10	–	+	–
<i>Hypoxyylon rubiginosum</i>	MUCL 47970	+	+	9, 10	–	+	–
<i>Hypoxyylon rubiginosum</i>	MUCL 47150	+	–	–	+	–	–
<i>Hypoxyylon rubiginosum</i>	MUCL 52672	+	+	–	+	–	–
<i>Hypoxyylon rubiginosum</i>	MUCL 54624	–	–	8	–	–	–
<i>Hypoxyylon rubiginosum</i>	MUCL 2709	–	–	–	–	–	–
<i>Hypoxyylon rubiginosum</i>	MUCL 34183	+	+	13	–	–	–
<i>Hypoxyylon rubiginosum</i>	MUCL 47147	+	–	–	+	–	–
<i>Hypoxyylon rubiginosum</i>	STMA 04040	+	+	–	+	–	–
<i>Hypoxyylon rubiginosum</i>	STMA 07027	+	+	–	–	–	–
<i>Hypoxyylon rubiginosum</i>	STMA 13346	+	+	–	–	–	–
<i>Hypoxyylon rubiginosum</i>	STMA 17058	+	+	–	–	–	–
<i>Hypoxyylon cercidicola</i>	MUCL 54180	+	–	13	–	–	–
<i>Hypoxyylon fuscum</i>	STMA 13090	–	–	11, 13	–	+	+
<i>Hypoxyylon texense</i>	DSM 107933	–	–	–	+	–	–
<i>Hypoxyylon croceoplum</i>	CBS 119004	–	–	–	+	–	–
<i>Hypoxyylon carneum</i>	MUCL 54177	–	–	10	–	–	–

the *H. rubiginosum* complex. The specimens encountered appeared morphologically and chemotaxonomically related to *H. rubiginosum sensu stricto*, as revealed from their morphology and secondary metabolite profiles. While the majority of specimens were assigned to typical *H. rubiginosum*, we have encountered a new taxon that significantly deviates from the complex in both stromatal and ascospore morphology and appears most closely related to a species that was so far only reported from the southern USA (Sir et al. 2019). Furthermore, we found two specimens that slightly differed in one or two characters from typical *H. rubiginosum* and also showed deviating positions in the phylogenetic trees, but are so far only known from single collections. Attempts should be made to encounter additional specimens of these fungi, which may eventually lead to their recognition as new species. The recent study on intragenomic polymorphisms

Table 4. Identified secondary metabolites in dual culture (barley-malt medium with *Hymenoscyphus fraxineus*) of the surveyed strains listed in Table 3. Identified compounds: **5**: phomopsidin; **6**: 10-hydroxyphomopsidin; **8**: rickiol A; **9**: orthosporin; **10**: daldinone B; **11**: 1,8-dimethoxynaphthalene; **13**: 5-methyl-mellein. Identified stromal azaphilone groups detected in culture: **MI** = Mitourbrin type; **NA** = Naphthalene type; **DA** = Daldinin type. For chemical structures, see Fig. 8.

Organism	Strain	Culture metabolites			Stromal metabolites	
		5	6	Others	MI	NA
<i>Hypoxyylon cercidicola</i>	MUCL 54180	+	–	13	–	–
<i>Hypoxyylon fuscum</i>	STMA 13090	–	–	11, 13	–	+
<i>Hypoxyylon texense</i>	DSM 107933	–	–	–	+	–
<i>Hypoxyylon crocopleplum</i>	CBS 119004	–	–	–	+	–
<i>Hypoxyylon perforatum</i>	MUCL 47187	+	–	–	+	–
<i>Hypoxyylon petriniae</i>	MUCL 53756	+	–	–	–	–
<i>Hypoxyylon</i> aff. <i>rubiginosum</i>	MUCL 57724	+	+	–	+	–
<i>Hypoxyylon rubiginosum</i>	MUCL 47152	+	–	9, 10	–	+
<i>Hypoxyylon rubiginosum</i>	MUCL 47970	+	–	9, 10	–	+
<i>Hypoxyylon guilanense</i>	MUCL 57726	–	–	–	–	–
<i>Hypoxyylon carneum</i>	MUCL 54177	–	–	10	–	–

in Hypoxylaceae has suggested that molecular data alone may be misleading in this family and new taxa should be based on multiple records sharing the same genotypic and phenotypic features (Stadler et al. 2020). Hsieh et al. (2005) have already established that protein-coding genes provide a better resolution in the Hypoxylaceae than ITS and finally even omitted this locus from the phylogeny and rather decided to focus on *tub2* and alpha-actin sequences. Kuhnert et al. (2014) also found *tub2* to be more suitable than ITS in their phylogeny, based on material from the Caribbean.

Our phylogenetic analyses confirmed previous results (Wendt et al. 2018; Lambert et al. 2019; Sir et al. 2019), suggesting that the genus *Hypoxyylon* appears paraphyletic in Hypoxylaceae, with a relatively small clade comprising the type species *H. fragiforme* as “core group” to which members of the *Hypoxyylon rubiginosum* complex form a sister clade. The genus will eventually need to be further subdivided, but molecular data for the majority of known species remain incomplete and such a task should only commence as the phylogenetic data matrix has increased. Our study further contributed to this monumental task by adding some data on representatives from the Middle East, a geographic area that has certainly not been as well explored as Western Europe and other parts of the world.

A main objective of this work was to assess the antagonistic potential of the newly isolated cultures and some strains of related species against an important pathogen, following the recent discovery that an endophytic isolate of *H. rubiginosum* from a resistant ash tree inhibited the growth of the alien pathogen, *Hym. fraxineus* (Halecker et al. 2020). Assessment of axenic cultures of the *Hypoxyylon* species in a single medium (barley-malt) led to the detection of phomopsidin in one out of five strains of *H. petriniae*, two out of seven strains of *H. perforatum* and ten out of 13 strains of *H. rubiginosum*. The stromata of these three taxa have been frequently reported from *Fraxinus* and it is plausible that they all occur as endophytes in this host and only form the stromata on dead host tissues. On the other hand, phomopsidin was not detected in other related, but apparently rare species like *H. texense*, *H. crocopleplum* and *H. carneum*. Only the

two latter species, however, were represented in our study by cultures that were isolated from stromata growing on *Fraxinus* wood. In addition, our results need to be further validated because we cannot exclude that some of the strains, which have been kept in culture collections for many years, may have degenerated. In any case, our results suggest that phomopsidin is not a specific marker for the species complex or for *H. rubiginosum sensu stricto*. As the compound is preferentially observed in dual cultures, its biosynthesis may be under control of epigenetic effectors. Therefore, in the future, it would be useful to evaluate a broader range of ascospore-derived cultures of *Hypoxylon* for their potential as biocontrol agents against the ash dieback pathogen and to define the genetic mechanisms encoding phomopsidin biosynthesis.

Last but not least, the current study also revealed some interesting aspects for potential follow-up projects. For instance, the examination of *H. fuscum* (a species that has never been isolated from *Fraxinus*, but is actually associated with *Corylus* and other Betulaceae) in the antagonism assay, revealed the production of several hitherto unknown compounds whose production was significantly enhanced in the presence of *Hym. fraxineus*. This observation suggests that it will be worthwhile to further study the secondary metabolism of *Hypoxylon* species in other scenarios using the dual culture approach. The first step would be to scale-up the production of the unknown molecules, isolating enough for structure elucidation and biological studies. This should not be expected to be a trivial task, but it appears doable using the methodology that is presently available.

The production of known and yet unidentified azaphilones (i.e. a compound class that is normally found in high concentrations in the stromata of various Hypoxylaceae, but was rarely observed in their mycelial cultures) in *H. rubiginosum* and allies, is another interesting observation relating to the differential expression of biosynthetic genes encoding secondary metabolites. It should be rewarding to evaluate the regulation mechanisms that lead to the production of the pigments, aided by genomic and transcriptomic studies.

Acknowledgements

This study was partially financed by the Ministry of Science, Research and Technology (MSRT) of Iran. Mohammad Javad wants to express his appreciation to all colleagues in the labs of Irmgard Krisai-Greilhuber (Vienna) and Marc Stadler (Braunschweig) for their support, especially Kathrin Wittstein and Silke Reinecke and to all colleagues in the University of Guilan. The authors want to express their gratitude to Manfred Rohde for recording the SEM pictures.

References

- Andersson PF, Johansson SBK, Stenlid J, Broberg A (2010) Isolation, identification and necrotic activity of viridiol from *Chalara fraxinea*, the fungus responsible for dieback of ash. *Forest Pathology* 40: 43–46. <https://doi.org/10.1111/j.1439-0329.2009.00605.x>

- Bills GF, Gonzalez-Menendez V, Platas G, Fournier J, Persoh D, Stadler M (2012) *Hypoxylon pulicicidum* sp. nov. (Ascomycota, Xylariales), a pantropical insecticide-producing endophyte. PLoS ONE 7: e46687. <https://doi.org/10.1371/journal.pone.0046687>
- Bitzer J, Læssøe T, Fournier J, Kummer V, Decock C, Tichy HV, Piepenbring M, Peršoh D, Stadler M (2008) Affinities of *Phylacia* and the daldinoid Xylariaceae, inferred from chemotypes of cultures and ribosomal DNA sequences. Mycological Research 112: 251–270. <https://doi.org/10.1016/j.mycres.2007.07.004>
- Chang CW, Chang HS, Cheng MJ, Liu TW, Hsieh SY, Yuan GF, Chen IS (2014) Inhibitory effects of constituents of an endophytic fungus *Hypoxylon investiens* on nitric oxide and interleukin-6 production in RAW264.7 macrophages. Chemistry & Biodiversity 11(6): 949–961. <https://doi.org/10.1002/cbdv.201300364>
- Chepkirui C, Stadler M (2017) The genus *Diaporthe*: a rich source of diverse and bioactive metabolites. Mycological Progress 16:477–494. <https://doi.org/10.1007/s11557-017-1288-y>
- Daranagama DA, Camporesi E, Tian Q, Liu X, Chamyuang S, Stadler M, Hyde KD (2015) *Anthostomella* is polyphyletic comprising several genera in Xylariaceae. Fungal Diversity 73: 203–238. <https://doi.org/10.1007/s13225-015-0329-6>
- Daranagama DA, Hyde KD, Sir EB, Thambugala KM, Tian Q, Samarakoon MC, McKenzie EHC, Jayasiri SC, Tibpromma S, Bhat JD, Liu XZ, Stadler M (2018) Towards a natural classification and backbone tree for Graphostromataceae, Hypoxylaceae, Lopadostomataceae and Xylariaceae. Fungal Diversity 88: 1–165. <https://doi.org/10.1007/s13225-017-0388-y>
- Fournier J, Köpcke B, Stadler M (2010) New species of *Hypoxylon* from western Europe and Ethiopia. Mycotaxon 113: 209–235. <https://doi.org/10.5248/113.209>
- Fournier J, Flessa F, Peršoh D, Stadler M (2011) Three new *Xylaria* species from southwestern Europe. Mycological Progress 10: 33–52. <https://doi.org/10.5248/113.209>
- Halecker S, Surup F, Kuhnert E, Mohr KI, Brock NL, Dickschat JS, Junker C, Schulz B, Stadler M (2014) Hymenoseitin, a 3-decalynoyl tetramic acid antibiotic from cultures of the ash dieback pathogen, *Hymenoscyphus pseudoalbidus*. Phytochemistry 100: 86–91. <https://doi.org/10.1016/j.phytochem.2014.01.018>
- Halecker S, Surup F, Solheim H, Stadler M (2018) Albiducins A and B, salicylaldehyde antibiotics from the ash tree-associated saprotrophic fungus *Hymenoscyphus albidus*. Journal of Antibiotics (Tokyo) 71: 339–341. <https://doi.org/10.1038/ja.2017.66>
- Halecker S, Wennrich JP, Rodrigo S, Andrée N, Rabsch L, Baschien C, Steinert M, Stadler M, Surup F, Schulz B (2020) Fungal endophytes for biocontrol of ash dieback: The antagonistic potential of *Hypoxylon rubiginosum*. Fungal Ecology 45 (in press). <https://doi.org/10.1016/j.funeco.2020.100918>
- Hall TA (1999) BioEdit: a user-friendly biological sequence alignment editor and analysis program for Windows 95/98/NT. Nucleic Acids Symposium Series 41: 95–98.
- Helaly SE, Thongbai B, Stadler M (2018) Diversity of biologically active secondary metabolites from endophytic and saprotrophic fungi of the ascomycete order Xylariales. Natural Products Report 35: 992–1014. <https://doi.org/10.1039/C8NP00010G>
- Hsieh HM, Ju YM, Rogers JD (2005) Molecular phylogeny of *Hypoxylon* and closely related genera. Mycologia 97: 844–865. <https://doi.org/10.1080/15572536.2006.11832776>

- Ju YM, Rogers JD (1996) A revision of the genus *Hypoxylon*. Mycologia Memoir n° 20. APS Press, St. Paul, 365 pp.
- Katoh K, Rozewicki J, Yamada KD (2019) MAFFT online service: multiple sequence alignment, interactive sequence choice and visualization. Briefings in Bioinformatics, 20(4): 1160–1166. <https://doi.org/10.1093/bib/bbx108>
- Kobayashi H, Meguro S, Yoshimoto T, Namikoshi M (2003) Absolute structure, biosynthesis, and anti-microtubule activity of phomopsidin, isolated from a marine-derived fungus *Phomopsis* sp. Tetrahedron 59: 455–459. [https://doi.org/10.1016/S0040-4020\(02\)01566-1](https://doi.org/10.1016/S0040-4020(02)01566-1)
- Koukol O, Kelnarová I, Černý K (2015) Recent observations of sooty bark disease of sycamore maple in Prague (Czech Republic) and the phylogenetic placement of *Cryptostroma corticale*. Forest Pathology 45: 21–27. <https://doi.org/10.1111/efp.12129>
- Kuhnert E, Fournier J, Peršoh D, Luangsa-ard JJD, Stadler M (2014) New *Hypoxylon* species from Martinique and new evidence on the molecular phylogeny of *Hypoxylon* based on ITS rDNA and β -tubulin data. Fungal Diversity 64: 181–203. <https://doi.org/10.1007/s13225-013-0264-3>
- Kuhnert E, Sir EB, Lambert C, Hyde KD, Hladki AI, Romero AI, Rohde M, Stadler M (2017) Phylogenetic and chemotaxonomic resolution of the genus *Annulohypoxylon* (Xylariaceae) including four new species. Fungal Diversity 85: 1–43. <https://doi.org/10.1007/s13225-016-0377-6>
- Lambert C, Wendt L, Hladki AI, Romero AI, Stadler M, Sir EB (2019) *Hypomontagnella* (Hypoxyloaceae): a new genus segregated from *Hypoxylon* by a polyphasic taxonomic approach. Mycological Progress 18: 187–201. <https://doi.org/10.1007/s11557-018-1452-z>
- Miller JH (1961) A Monograph of the World Species of *Hypoxylon*. A Monograph of the World Species of *Hypoxylon*. University of Georgia Press, Athens.
- Pažoutová S, Follert S, Bitzer J, Keck M, Surup F, Šrůtka P, Holuša J, Stadler M (2013) A new endophytic insect-associated *Daldinia* species, recognised from a comparison of secondary metabolite profiles and molecular phylogeny. Fungal Diversity 60: 107–123. <https://doi.org/10.1007/s13225-013-0238-5>
- Petrini LE, Petrini O (1985) Xylariaceous fungi as endophytes. Sydowia 38: 216–234. https://www.zobodat.at/pdf/Sydowia_38_0216-0234.pdf
- Quang DN, Hashimoto T, Tanaka M, Baumgartner M, Stadler M, Asakawa Y (2002) Chemical constituents of the Ascomycete *Daldinia concentrica*. Journal of Natural Products, 65:1869–1874. <https://doi.org/10.1021/np020301h>
- Quang DN, Hashimoto T, Tanaka M, Stadler M, Asakawa Y (2004) Cyclic azaphilones daldinins E and F from the ascomycete fungus *Hypoxylon fuscum* (Xylariaceae). Phytochemistry, 65(4): 469–473. <https://doi.org/10.1016/j.phytochem.2003.09.022>
- Rayner RW (1970) A Mycological Colour Chart. Commonwealth Mycological Institute, Kew and British Mycological Society.
- Silvestro D, Michalak I (2012) raxmlGUI: a graphical front-end for RAxML. Organisms Diversity & Evolution 12: 335–337. <https://doi.org/10.1007/s13127-011-0056-0>
- Sir EB, Kuhnert E, Lambert C, Hladki AI, Romero AI, Stadler M (2016) New species and reports of *Hypoxylon* from Argentina recognized by a polyphasic approach. Mycological Progress 15: 1–42. <https://doi.org/10.1007/s11557-016-1182-z>

- Sir EB, Becker K, Lambert C, Bills FG, Kuhnert E (2019) Observations on Texas hypoxylons, including two new *Hypoxylon* species and widespread environmental isolates of the *H. croceum* complex identified by a polyphasic approach. *Mycologia* 111: 832–856. <https://doi.org/10.1080/00275514.2019.1637705>
- Stadler M, Wollweber H, Mühlbauer A, Asakawa Y, Hashimoto T, Rogers JD, Ju YM, Wetzstein HG, Tichy HV (2001) Molecular chemotaxonomy of *Daldinia* and other Xylariaceae. *Mycological Research* 105: 1191–1205. [https://doi.org/10.1016/S0953-7562\(08\)61990-5](https://doi.org/10.1016/S0953-7562(08)61990-5)
- Stadler M, Wollweber H, Fournier J (2004) A host-specific species of *Hypoxylon* from France, and notes on the chemotaxonomy of the “*Hypoxylon rubiginosum* complex”. *Mycotaxon* 90: 187–211.
- Stadler M, Hellwig V (2005a) Chemotaxonomy of the Xylariaceae and remarkable bioactive compounds from Xylariales and their associated asexual stages. *Recent Research Developments in Phytochemistry* 9: 41–93.
- Stadler M, Laessoe T, Vasilyeva L (2005b) The genus *Pyrenomyxa* and its affinities to other cleistocarpous Hypoxyloideae as inferred from morphological and chemical traits. *Mycologia* 97: 1129–1139. <https://doi.org/10.1080/15572536.2006.11832761>
- Stadler M, Fournier J, Granmo A, Beltrán-Tejera E (2008) The “red Hypoxylons” of the temperate and subtropical Northern Hemisphere. *North American Fungi* 3: 1–73. <https://doi.org/10.2509/naf2008.003.0075>
- Stadler M, Fournier J, Læssøe T, Chlebicki A, Lechat C, Flessa F, Rambold G, Peršoh D (2010) Chemotaxonomic and phylogenetic studies of *Thamnomycetes* (Xylariaceae). *Mycoscience* 51: 189–207. <https://doi.org/10.1007/S10267-009-0028-9>
- Stadler M, Kuhnert E, Peršoh D, Fournier J (2013) The Xylariaceae as model example for a unified nomenclature following the “one fungus-one name” (1F1N) concept. *Mycology* 4: 5–21. <https://doi.org/10.3114/sim0016>
- Stadler M, Læssøe T, Fournier J, Decock C, Schmieschek B, Tichy HV, Peršoh D (2014) A polyphasic taxonomy of *Daldinia* (Xylariaceae). *Studies in Mycology* 77: 1–143. <https://doi.org/10.3114/sim0016>
- Stadler M, Lambert C, Wibberg D, Kalinowski J, Cox RJ, Kolarik M, Kuhnert E (2020) Intra-genomic polymorphisms in the ITS region of high quality genomes of the Hypoxylaceae (Xylariales, Ascomycota). *Mycological Progress*, 19: 235–245. <https://doi.org/10.1007/s11557-019-01552-9>
- Stamatakis A (2006) RAxML-VI-HPC: maximum likelihood-based phylogenetic analyses with thousands of taxa and mixed models. *Bioinformatics* 22: 2688–2690. <https://doi.org/10.1093/bioinformatics/btl446>
- Steglich W, Klaar M, Furtner W (1974) Mitorubrin derivatives from *Hypoxylon fragiforme*. *Phytochemistry* 13: 2874–2875. [https://doi.org/10.1016/0031-9422\(74\)80262-1](https://doi.org/10.1016/0031-9422(74)80262-1)
- Surup F, Halecker S, Nimtz M, Rodrigo S, Schulz B, Steinert M, Stadler M (2018a) Hyfraxins A and B, cytotoxic ergostane-type steroid and lanostane triterpenoid glycosides from the invasive ash dieback ascomycete *Hymenoscyphus fraxineus*. *Steroids* 135: 92–97. <https://doi.org/10.1016/j.steroids.2018.03.007>
- Surup F, Kuhnert E, Böhm A, Pendzialek T, Solga D, Wiebach V, Engler H, Berkessel A, Stadler M, Kalesse M (2018b) The Rickiols: 20-, 22-, and 24-membered macrolides from the

- ascomycete *Hypoxylon rickii*. Chemistry-an European Journal 24: 2200–2213. <https://doi.org/10.1002/chem.201704928>
- Swofford DL (2002) PAUP* 4.0b10: phylogenetic analysis using parsimony (*and other methods). Sinauer Associates, Sunderland.
- Triebel D, Peršoh D, Wollweber H, Stadler M (2005) Phylogenetic relationships among *Daldinia*, *Entonaema* and *Hypoxylon* as inferred from ITS nrDNA sequences. Nova Hedwigia 80: 25–43. <https://doi.org/10.1127/0029-5035/2005/0080-0025>
- U'Ren JM, Miadlikowska J, Zimmerman NB, Lutzoni F, Stajich JE, Arnold AE (2016) Contributions of North American endophytes to the phylogeny, ecology, and taxonomy of Xylariaceae (Sordariomycetes, Ascomycota). Molecular Phylogenetics and Evolution 98: 210–232. <https://doi.org/10.1016/j.ympev.2016.02.010>
- Wendt L, Sir EB, Kuhnert E, Heitkämper S, Lambert C, Hladki AI, Romero AI, Luangsa-ard JJ, Srikitikulchai P, Peršoh D, Stadler M (2018) Resurrection and emendation of the Hypoxylaceae, recognized from a multigene phylogeny of the Xylariales. Mycological Progress 17: 115–154. <https://doi.org/10.1007/s11557-017-1311-3>
- Zhang N, Castlebury LA, Miller AN, Huhndorf SM, Schoch CL, Seifert KA, Rossman AY, Rogers JD, Kohlmeyer J, Volkmann-Kohlmeyer B, Sung GH (2006) An overview of the systematics of the Sordariomycetes based on a four-gene phylogeny. Mycologia 98: 1076–1087. <https://doi.org/10.1080/15572536.2006.11832635>

Supplementary material I

Discovery of a new species of the *Hypoxylon rubiginosum* complex from Iran and antagonistic activities of *Hypoxylon* spp. against the Ash Dieback pathogen, *Hymenoscyphus fraxineus*, in dual culture

Authors: Mohammad Javad Pourmoghaddam, Christopher Lambert, Frank Surup, Seyed Akbar Khodaparast, Irmgard Krisai-Greilhuber, Hermann Voglmayr, Marc Stadler
Data type: Multimedia.

Copyright notice: This dataset is made available under the Open Database License (<http://opendatacommons.org/licenses/odbl/1.0/>). The Open Database License (ODbL) is a license agreement intended to allow users to freely share, modify, and use this Dataset while maintaining this same freedom for others, provided that the original source and author(s) are credited.

Link: <https://doi.org/10.3897/mycokeys.66.50946.suppl1>

Squamarina (lichenised fungi) species described from China belong to at least three unrelated genera

Yan-Yun Zhang^{1,2}, Xin-Yu Wang¹, Li-Juan Li^{1,2}, Christian Printzen³, Einar Timdal⁴, Dong-Ling Niu⁵, An-Cheng Yin¹, Shi-Qiong Wang¹, Li-Song Wang¹

1 CAS Key Laboratory for Plant Diversity and Biogeography of East Asia, Kunming Institute of Botany, Chinese Academy of Sciences, Kunming, Yunnan 650201, China **2** University of Chinese Academy of Sciences, Beijing 100049, China **3** Department of Botany and Molecular Evolution, Senckenberg Research Institute, 60325 Frankfurt am Main, Germany **4** Natural History Museum, University of Oslo, P.O. Box 1172, Blindern, N-0318 Oslo, Norway **5** Department of Life Science, Ningxia University, Yinchuan, Ningxia 750021, China

Corresponding author: Li-Song Wang (wanglisong@mail.kib.ac.cn)

Academic editor: E. Gaya | Received 13 August 2019 | Accepted 23 March 2020 | Published 24 April 2020

Citation: Zhang Y-Y, Wang X-Y, Li L-J, Printzen C, Timdal E, Niu D-L, Yin A-C, Wang S-Q, Wang L-S (2020) *Squamarina* (lichenised fungi) species described from China belong to at least three unrelated genera. MycoKeys 66: 135–157. <https://doi.org/10.3897/mycokeys.66.39057>

Abstract

New collections of six *Squamarina* species from type localities in China were studied. The comparison of morphological characteristics and secondary metabolites with those of the type specimens and phylogenetic analyses suggest that *S. callichroa* and *S. pachyphylla* belong to *Rhizoplaca*, *S. semisterilis* belongs to *Lobothallia* and *S. chondroderma* should be retained in *Lecanora* temporarily. Only two species, *S. kansuensis* and *S. oleosa*, remain in *Squamarina*. The new combinations *Lobothallia semisterilis* (H. Magn.) Y. Y. Zhang, *Rhizoplaca callichroa* (Zahlbr.) Y. Y. Zhang and *R. pachyphylla* (H. Magn.) Y. Y. Zhang are proposed. Detailed descriptions to aid the identification of these species, distributions and phylogenetic trees, based on multiple collections, are presented. The generic concept of *Squamarina* is recircumscribed in this study.

Keywords

Squamarinaceae, *Petroplaca*, *Rhizoplaca*, *Lobothallia*, *Lecanora*, type study

Introduction

The genus *Squamarina* Poelt was first erected by Poelt (1958) and is characterised by thick squamules, large apothecia and a “*Squamarina*-type” thallus, consisting of a well-separated and more or less equally high upper cortex, algal layer and medulla. Two sections, *S. sect. Squamarina* and *S. sect. Petroplaca*, were distinguished by Poelt (1958), based on the former having a larger thallus and larger apothecia, and the latter smaller thallus and apothecia. Hafellner (1984) accommodated the genus in a new family, Squamarinaceae, based on asci with an evenly amyloid tholus without any axial body. However, the circumscription of *Squamarina* or Squamarinaceae has been disputed for a long time and molecular studies for this genus are largely lacking (Hafellner 1984; Haugan and Timdal 1992; Hertel and Rambold 1988; Poelt 1958). Recent studies showed that the species of the sect. *Squamarina* have asci with an amyloid tube in the tholus, resembling those of Porpidiaceae and that the ascus structure of sect. *Petroplaca* resembles that of *Protoparmeliopsis muralis* (Schreb.) Rabenh. (Haugan and Timdal 1992; Hertel and Rambold 1988). Hence, the detailed circumscription of the genus *Squamarina* is urgently needed and it was also one of the aims of this study.

Nine species of *Squamarina* have so far been reported from China (Wei 1991), of which six were originally collected in China by Birger Bohlin and Heinrich Frh. von Handel-Mazzetti: *S. callichroa* (Zahlbr.) Poelt, *S. chondroderma* (Zahlbr.) Wei, *S. kansuensis* (H. Magn.) Poelt, *S. oleosa* (Zahlbr.) Poelt, *S. pachyphylla* (H. Magn.) Wei and *S. semisterilis* (H. Magn.) Wei. Although these species were published about 100 years ago (Magnusson 1940; Zahlbruckner 1930), no more collections have, however, been reported since then, except for *S. chondroderma* and molecular data are not available for any of them in GenBank. Therefore, studies on the identification, distribution and phylogeny of these species are necessary. We have undertaken several field trips along the collection routes of Birger Bohlin (1930–1932) and Handel-Mazzetti (1914–1915) in the past few years and collected fresh material of the six species from the type localities for the molecular study presented here.

Methods

Morphological and chemical studies

Type specimens were loaned from the Museum of Natural History Vienna (W) and the Swedish Museum of Natural History (S). The fresh material collected for this study is deposited in Kunming Institute of Botany, Chinese Academy of Sciences (KUN-L). Morphological features were studied under a dissecting microscope (Nikon SMZ745T). Apothecia and thalli were sectioned with an S-30 microtome with a KS-34 cryostat (Zeiss, Jena) and microscopic traits were observed and measured using a microscope (Leica 020-518.500). Secondary metabolites were analysed by spot reactions and thin-layer chromatography (TLC) in solvents A, B and C (Orange et al. 2001).

DNA extraction, PCR and sequencing

Total DNA was extracted from dry or fresh specimens using the DNeasy Plant Mini Kit (Qiagen, Germany), according to the manufacturer's instructions. Amplifications were performed in a 25 μ l volume containing 12.5 μ l 2 \times MasterMix (TaqDNA Polymerase [0.1 units/ μ l], 0.4 mM MgCl₂, 0.4 nM dNTPs) (Aidlab Biotechnologies Co. Ltd.), 0.5 μ l of each primer, 10 μ l ddH₂O and 1 μ l of DNA. The PCR settings and the primers of nrITS (ITS1-5.8S-ITS2), nrLSU, RPB1, RPB2 and mtSSU follow Zhao et al. (2015). All PCR reactions were sequenced by TsingKe Biological Technology (Kunming, China) using the amplification primers.

Phylogenetic analyses

Sequences were assembled and edited using SeqMan 7.1 (DNASTAR packages). An nrITS matrix of *Lobothallia* (Clauzade & Cl. Roux) Hafellner, an nrLSU matrix of *Squamarina* and a 5-locus (nrITS, nrLSU, RPB1, RPB2 and mtSSU) concatenated matrix of *Rhizoplaca* Zopf and related genera were generated using Geneious R8. Single-gene analyses were conducted, based on the Maximum Likelihood (ML) method to assess the conflict amongst individual genes and no significant incongruence was detected. Matrices were aligned with MAFFT, using the web service (<http://mafft.cbrc.jp/alignment/server/index.html>). Ambiguous positions were removed, using the web service of Guidance (<http://guidance.tau.ac.il/ver2/>). MrModeltest2.3 (Nylander 2004), based on Akaike Information Criterion (AIC), was used to estimate the best-fitting substitution model for each dataset for Maximum Likelihood (ML) and Bayesian Inference (BI). The selected model for nrITS-*Lobothallia* was HKY+I and, for the other matrices, GTR+I+G. Bayesian reconstructions of phylogenies were performed with MrBayes 3.1.2 (Huelsenbeck and Ronquist 2001), using four Markov chains running for 2 million generations for single locus matrices and 10 million generations for the concatenated dataset. Trees were sampled every 100 generations. ML analyses were performed with RaxmlHPC, using the General Time Reversible model of nucleotide substitution with the gamma model of rate heterogeneity (GTRGAMMA). Support values were inferred from the 70% majority-rule tree of all saved trees obtained from 1000 non-parametric bootstrap replicates. Trees were visualised in FigTree v1.4.0 (Rambaut 2012).

Results and discussions

A total of 84 sequences of the nrITS, nrLSU, RPB1, RPB2 and mtSSU were newly generated for the species *Squamarina chondroderma*, *S. semisterilis*, *S. callichroa*, *S. pachyphylla*, *S. gypsacea* (Sm.) Poelt, *S. kansuensis* and *S. oleosa* in this study (Table 1). The BLAST results showed that these species belong to at least three unrelated genera,

Table 1. Specimens and DNA sequences for nrITS, nrLSU, RPB1, RPB2 and mtSSU used in this study, with the corresponding voucher information from GenBank indicated. Sequences, newly obtained in this study, are indicated in boldface.

Species	Locality*	Voucher specimens	Accession number*				
			nrITS	nrLSU	RPB1	RPB2	mtSSU
<i>Aspicilia cinerea</i>	Sweden	Nordin 6213 (UPS)	JF703115	–	–	–	–
<i>A. epiglypta</i>	Sweden	Nordin 6105 (UPS)	HQ259262	–	–	–	–
<i>Cladia aggregata</i>	Australia	HTL 19970f (F)	–	GQ500969	–	–	–
<i>C. deformis</i>	Australia	HTL 19994d (F)	–	GQ500967	–	–	–
<i>Cladonia digitata</i>	na	Ekman 3424 (BG)	–	AY756319	–	–	–
<i>C. stipitata</i>	na	AFTOL-ID 1657 (DUKE)	–	DQ973026	–	–	–
<i>C. sulcata</i>	Australia	HTL 19975i (F)	–	GQ500959	–	–	–
<i>Herteliana schuyleriana</i>	USA: North Carolina	1885671	–	MH887488	–	–	–
<i>H. taylorii</i>	na	Hertel 39599 (UPS)	–	AY756351	–	–	–
<i>Heterodea muelleri</i>	Australia	Elix 39643 (CANB)	–	GQ500962	–	–	–
<i>Lecanora achroa</i>	Thailand	Papong 6458 (F)	JN943714	na	JN987926	KT453937	JQ782663
<i>L. caesiurubella</i>	Australia	Lumsch 19974k (F)	JN943728	JN939508	JN987920	na	na
<i>L. chondroderma</i> 1	China: Yunnan	16-54907 (KUN-L)	MK778053	MK778013	MK766421	MK766441	na
<i>L. chondroderma</i> 2	China: Xizang	16-52925 (KUN-L)	MK778052	MK778012	MK766420	MK766440	MN192155
<i>L. chondroderma</i> 3	China: Xizang	16-53527 (KUN-L)	MK778056	MK778016	MK766423	MK766443	MN192156
<i>L. chondroderma</i> 4	China: Yunnan	17-55591 (KUN-L)	MK778057	MK778017	MK766424	MK766444	na
<i>L. conizaeoides</i>	na	K. Molnar U0505/M (DUKE)	na	na	KJ766862	KJ766956	KJ766418
<i>L. contractula</i>	na	AFTOL-ID 877 (DUKE)	HQ650604	DQ986746	DQ986817	DQ992428	DQ986898
<i>L. dispersa</i>	USA: Illinois	Leavitt 12-002	KT453733	na	KT453888	KT453921	na
<i>L. farinacea</i>	Australia	Lumsch 20003 (F)	JN943725	JN939513	JN987924	na	JQ782672
<i>L. flavopallida</i>	Australia	Lumsch 19972d (F)	JN943723	JN939516	JN987925	KT453938	JQ782673
<i>L. formosa</i>	China: Xinjiang	ZX 20129045-2 (SDNU)	KT453771	KT453773	na	KT453978	KT453819
<i>L. hybocarpa</i>	na	Lumsch s.n. (F)	EF105412	EF105421	EF105430	na	EF105417
<i>L. intricata</i>	na	U166 (GZU)	AF070022	DQ787345	na	na	DQ787346
<i>L. novomexicana</i>	USA	55026 (BRY-C)	HM577257	na	KU935390	KU935136	na
<i>L. polytropa</i>	na	AFTOL-ID 1798 (DUKE)	HQ650643	DQ986792	na	DQ992418	DQ986807
<i>L. saligna</i>	USA	Leavitt 5702 (BRY-C)	KU934539	na	KU935293	KU935036	na
<i>L. tropica</i>	Kenya	Lumsch 19573a (F)	JN943718	JN939537	JN987936	na	na
<i>Lecidella carpathica</i>	China: Xinjiang	ZX 20140367-2 (SDNU)	KT453741	KT453784	KT453905	KT453944	KT453831
<i>L. stigmatea</i>	China: Xinjiang	ZX 20140838 (SDNU)	KT453766	KT453803	KT453918	KT453971	KT453849
<i>L. tumidula</i>	China: Xinjiang	ZX XL0009 (SDNU)	–	KT453810	–	–	–
<i>Leparia bergensis</i>	na	Tonsberg 28875 (BG)	–	AY756324	–	–	–
<i>L. incana</i>	na	AFTOL-ID 1792 (DUKE)	–	DQ986795	–	–	–

Species	Locality*	Voucher specimens	Accession number*				
			nrITS	nrLSU	RPB1	RPB2	mtSSU
<i>Lobothallia alphoplaca</i>	China	20117616 (SDNU)	JX499233	–	–	–	–
<i>L. alphoplaca</i>	China	20117646 (SDNU)	JX476025	–	–	–	–
<i>L. crassimarginata</i>	China	20122565 (SDNU)	JX476026	–	–	–	–
<i>L. crassimarginata</i>	China	20122583 (SDNU)	KC007439	–	–	–	–
<i>L. helanensis</i>	China	20122517 (SDNU)	JX476030	–	–	–	–
<i>L. helanensis</i>	China	20122791 (SDNU)	JX476031	–	–	–	–
<i>L. melanaspis</i>	Sweden	Nordin 6622 (UPS)	HQ259272	–	–	–	–
<i>L. melanaspis</i>	Norway	Owe-Larsson 8943a (UPS)	JF825524	–	–	–	–
<i>L. praeradiosa</i>	China	20126314 (SDNU)	JX499232	–	–	–	–
<i>L. praeradiosa</i>	China	20126613 (SDNU)	JX499234	–	–	–	–
<i>L. pruinosa</i>	China	20123278 (SDNU)	JX476028	–	–	–	–
<i>L. pruinosa</i>	China	20123630 (SDNU)	JX476027	–	–	–	–
<i>L. radiosa</i>	Sweden	Nordin 5889 (UPS)	JF703124	–	–	–	–
<i>L. recedens</i>	Sweden	Nordin 6035 (UPS)	HQ406807	–	–	–	–
<i>L. semisterilis</i>	China: Qinghai	18-59262 (KUN-L)	MK778040	MK778009	na	na	na
<i>L. semisterilis</i>	China: Qinghai	18-59322 (KUN-L)	MK778039	MK778008	MK766413	na	na
<i>L. semisterilis</i>	China: Qinghai	18-59345 (KUN-L)	MK778042	MK778011	MK766415	na	na
<i>L. semisterilis</i>	China: Gansu	18-59596 (KUN-L)	MK778041	MK778010	MK766414	na	na
<i>Metus conglomeratus</i>	Australia	HTL 19982b (F)	–	GQ500958	–	–	–
<i>Miriquidica complanata</i>	Poland: Karkonosze Mts	Szczepanska 935 (herb. Szczepanska)	KF562187	KF562179	KF601233	na	KR995349
<i>M. garovaglii</i>	Slovakia: Karpaty Mts	Szczepanska 538 (herb. Szczepanska)	KF562188	na	KF601234	na	na
<i>Mycoblastus affinis</i>	na	AFTOL-ID 1047 (DUKE)	na	KJ766601	na	KJ766958	na
<i>M. sanguinarius</i>	na	AFTOL-ID 196 (DUKE)	DQ782842	DQ912333	na	DQ782867	DQ912276
<i>Paralecia pratorum</i>	Italy	M-0045925 (M)	–	KP224503	–	–	–
<i>Pilophorus cereolus</i>	na	na	–	AY340559	–	–	–
<i>P. strumaticus</i>	na	na	–	AY340560	–	–	–
<i>Protoparmeliopsis achariana</i>	na	U525	na	DQ787341	DQ973051	DQ973088	DQ972976
<i>P. garovaglii</i>	USA	Leavitt 106 (BRY-C)	KU934546	na	KU935300	KU935043	na
<i>P. muralis</i>	na	K. Molnar U0501/AO (EGR)	na	KJ766634	KJ766830	KJ766943	KJ766466
<i>P. peltata</i>	Iran	MS014622	KT453723	na	KT453892	KT453927	na
<i>P. zareii</i>	Iran	SK 480	KP059049	na	na	na	KP059055
<i>Ramboldia gowardiana</i>	na	Bjork 9447 (UBC)	na	KJ766649	KJ766889	na	KJ766483
<i>R. sanguinolenta</i>	Australia: Queensland	Elix 28835 (F)	EU075548	EU075523	KT453920	na	EU075534
<i>Rhizoplaca callichroa</i> 1	China: Sichuan	14-43348 (KUN-L)	MK778045	na	na	na	na
<i>R. callichroa</i> 2	China: Sichuan	14-43357 (KUN-L)	MK778046	na	na	na	na
<i>R. callichroa</i> 3	China: Sichuan	14-43359 (KUN-L)	MK778043	na	na	na	na
<i>R. callichroa</i> 4	China: Yunnan	14-43308 (KUN-L)	MK778044	na	na	na	na
<i>R. chrysoleuca</i> 1	USA	55000 (BRY-C)	HM577233	KT453812	KU935335	KU935084	KT453856
<i>R. chrysoleuca</i> 2	Iran	MS014636	KT453731	na	KT453898	KT453934	na

Species	Locality*	Voucher specimens	Accession number*				
			nrITS	nrLSU	RPB1	RPB2	mtSSU
<i>R. huashanensis</i>	China	Wei 18357 (HAMS)	AY530885	AY648104	na	na	na
<i>R. marginalis</i> 1	USA: California	Leavitt 739 (BRY-C)	KT453732	na	KT453901	KT453936	na
<i>R. marginalis</i> 2	USA	0020826b (BRY-L)	KU934655	na	KU935370	KU935123	na
<i>R. melanophthalma</i>	Iran	MS014628 (H)	JX948271	na	JX948317	JX948355	na
<i>R. pachyphylla</i> 1	China: Gansu	18-59466 (KUN-L)	MK778048	na	MK766417	MK766436	MN192152
<i>R. pachyphylla</i> 2	China: Gansu	18-59446 (KUN-L)	MK778047	na	MK766416	MK766435	MN192151
<i>R. pachyphylla</i> 3	China: Gansu	18-59482 (KUN-L)	MK778049	na	MK766416	MK766437	MN192153
<i>R. pachyphylla</i> 4	China: Gansu	18-59561 (KUN-L)	MK778050	na	MK766419	MK766438	MN192154
<i>R. polymorpha</i>	USA	55095 (BRY-C)	HM577326	na	KU935411	KU935159	na
<i>R. porterii</i>	USA	55149 (BRY-C)	HM577380	na	JX948341	JX948380	na
<i>R. shushanii</i>	USA	55065 (BRY-C)	HM577286	na	JX948334	JX948372	na
<i>R. subdiscrepans</i>	Russia	Vondrak 9408 (PRA)	KU934898	na	KU935435	KU935187	na
<i>Squamarina cartilaginea</i>	na	AFTOL-ID 1281	–	DQ986763	–	–	–
<i>S. gypsacea</i>	Greece	O-L-196249 (O)	na	MK778021	na	na	na
<i>S. gypsacea</i>	Greece	O-L-196255 (O)	na	MK778020	na	na	na
<i>S. gypsacea</i>	Greece	O-L-59266 (O)	na	MK778019	na	na	na
<i>S. gypsacea</i>	Spain	O-L-16444 (O)	na	MK778022	na	na	na
<i>S. kansuensis</i>	China: Xizang	16-54052 (KUN-L)	MK778059	MK778023	MK766425	MK766446	na
<i>S. kansuensis</i>	China: Ningxia	14-09-1429 (NXAC)	MK778060	MK778024	MK766426	MK766447	na
<i>S. kansuensis</i>	China: Xinjiang	20139103 (XJU)	MK778061	MK778025	MK766427	MK766448	na
<i>S. kansuensis</i>	China: Qinghai	18-59260 (KUN-L)	MK778062	MK778026	MK766428	MK766449	na
<i>S. kansuensis</i>	China: Gansu	18-59601 (KUN-L)	na	MK778031	na	na	na
<i>S. lentigera</i>	na	Haugan & Timdal 4801 (O)	–	AY756363	–	–	–
<i>S. oleosa</i>	China: Yunnan	19-66398 (KUN-L)	MN904892	MN904896	na	MN923191	MN915135
<i>S. oleosa</i>	China: Yunnan	19-66399 (KUN-L)	MN904893	MN904897	MN923189	MN923192	MN911318
<i>S. oleosa</i>	China: Yunnan	19-66401 (KUN-L)	MN904894	MN904898	MN923190	MN923193	MN915136
<i>Stereocaulon alpinum</i>	Austria	AT1194 (HBG)	–	JN941201	–	–	–
<i>S. sasakii</i>	Japan	AT1187 (TUR)	–	JN941206	–	–	–
<i>S. tomentosum</i>	Finland	AT1084 (TUR)	–	JN941203	–	–	–

*na = not available; *– = not used in this study

Lobothallia, *Squamarina* and *Rhizoplaca*, respectively. Given the large evolutionary divergence of these species, we reconstructed three separate phylogenies focusing on the three genera, based on nrITS, nrLSU and a 5-locus (nrITS, nrLSU, RPB1, RPB2 and mtSSU) concatenated matrix, respectively (Figs 2, 4, 6), to clarify the phylogenetic position of the six species. The results showed that *Squamarina semisterilis* is nested within the genus *Lobothallia*, which is closely related to the species *L. alphoplaca* (Wahlenb.)

Hafellner, *L. melanaspis* (Ach.) Hafellner and *L. praeradiosa* (Nyl.) Hafellner, but differs in having a pruinose thallus and grows on soil. The *Aspicilia*-type ascus and bacilliform conidia clearly distinguish this species from the genus *Squamarina*. *Squamarina callichroa* and *S. pachyphylla* were nested within the *Rhizoplaca chrysoleuca* (Sm.) Zopf group. The exclusion of the two species from *Squamarina* is also supported by their *Lecanora*-type ascus and the orange or black apothecia. Therefore, the new combinations *Lobothallia semisterilis* (H. Magn.) Y. Y. Zhang, *Rhizoplaca callichroa* (Zahlbr.) Y. Y. Zhang and *R. pachyphylla* (H. Magn.) Y. Y. Zhang are proposed here.

Lecanora chondroderma (= *Squamarina chondroderma*) is sister to the genus *Rhizoplaca*, but differs in growing on moss and meadow and the presence of numerous rhizinose strands that are never present in its related genera. It is also distinct from the genus *Squamarina* by the *Lecanora*-type ascus and the strongly gelatinised lower cortex. This species could belong to a genus separate from *Lecanora* s. str. and closely related to the genera *Rhizoplaca* and *Protoparmeliopsis*, but as only one species from this group was included here, further exploration is needed in the future and we prefer to retain this species in *Lecanora* here. The remaining two species, *Squamarina kansuensis* and *S. oleosa*, proved to belong in *Squamarina*. *Squamarina kansuensis* is sister to *S. lentigera*, but differs in the larger thallus and the presence of psoromic and 2'-O-demethylpsoromic acids. *Squamarina oleosa* is a basal clade of the genus, which is close to the species *S. cartilaginea* (With.) P. James and *S. gypsacea*.

We revised the previously reported ascus structure for the two sections of *Squamarina* (Haugan and Timdal 1992; Hertel and Rambold 1988) and verified that the species in sect. *Squamarina* display a *Porpidia*-type ascus and the species in sect. *Petroplaca* form a *Lecanora*-type ascus. Our phylogenetic analyses, containing the type species of the two sections, *S. callichroa* and *S. gypsacea*, were in accordance with the ascus type: the sect. *Squamarina* is close to the genus *Stereocaulon* (Schreb.) Schrad., which also has a *Porpidia*-type ascus (Högnabba 2006); section *Petroplaca* is nested within the genus *Rhizoplaca* having a *Lecanora*-type ascus. Therefore, we suggest excluding the section *Petroplaca* from the genus *Squamarina* and recircumscribe this genus as follows: thallus saxicolous or terricolous, squamulose, placodioid or subfoliose, squamules or lobes dispersed, continuous to irregularly overlapping, very thick, usually with a white, thickened and slightly upturned marginal rim; upper surface white, yellowish-green, grey green to olive green, smooth to strongly cracked and wrinkled; lower surface white, pale brown to blackish-brown, well defined but without cortex; thallus section with well-differentiated upper cortex, algae layer and medulla; upper cortex with pale brown granules, turning colourless in potassium hydroxide (KOH); algal layer continuous; medulla very thick, filled with grey calcium oxalate crystals that become needle shaped after treatment with 25% sulphuric acid (H₂SO₄); apothecia lecanorine type, algal layer usually absent from the margin and only present under hypothecium, rarely biatorine type because of the strong convex disc; disc light yellow, yellow, pale brown to reddish-brown, pruinose or not; ascus narrowly clavate, *Porpidia*-type, 8-spored; ascospores colourless, ellipsoid to subfusiform, non-septate; pycnidia yellowish-brown, conidia filiform, curved; usnic acid always present and psoromic acid also present in most species.

Taxonomy

Lobothallia semisterilis (H. Magn.) Y. Y. Zhang, comb. nov.

MycoBank No: 832199

Fig. 1A–E

Lecanora semisterilis H. Magn., Lichens from Central Asia 1: 123–124 (1940) (Basionym). \equiv *Squamarina semisterilis* (H. Magn.) J.C. Wei, Enumeration of Lichens in China: 232 (1991). Type: CHINA, Gansu Province, 2450–2600 m elev., on soil, 1931, Birger Bohlin 38L (S–Holotype!).

Description. Thallus to 5 cm across, areolate centrally, with irregularly elongate lobes at the margin, closely to loosely attached to soil; areoles angular, plane to slightly convex, continuous to crowded, ca. 1 mm across; marginal lobes ca. 1 mm wide and 2–3 mm long; upper surface white to grey, pruinose, the pruina on the marginal lobes becoming granular; lower surface white, attached to soil directly with medullary hyphae. Upper cortex colourless with pale brown upper part, 22–55 μm high; epinecral layer colourless, 10–20 μm high; algal layer ca. 95 μm high, not continuous, the interval between different groups of algae 16–32 μm wide; medulla filled with grey granules, lower cortex lacking.

Apothecia rounded, sessile, constricted at the base, up to 2 mm in diam.; disc plane to slightly convex, blackish-brown, non-pruinose; thalline margin entire, concolourous with thallus; hymenium colourless, ca. 60 μm high; subhymenium and hypothecium colourless, I + blue; epihymenium consisting of brown granules, ca. 15 μm high; paraphyses simple, slightly thickened at the apex, ca. 3 μm in diam.; asci *Aspicilia*-type, 8-spored; ascospores colourless, ellipsoid, 9–13 \times 5–9 μm .

Pycnidia prominent, sometimes protruding from the thallus-like apothecia, with blackish-brown ostioles, numerous, 0.1–0.4 mm across; conidia bacilliform, 5.5–6.5 \times ca. 1 μm .

Chemistry. Upper cortex K + red, C-, P-, medulla K + red, C-, P + yellow; norstictic acid.

Ecology and distribution. Growing on soil in very dry habitats at elevations of 1760–3151 m. This species was previously only known from Gansu Prov. and is reported here as new to Qinghai Prov., China.

Notes. The holotype consists of numerous fragments on soil, without apothecia but numerous pycnidia. This species was originally described as a *Lecanora* by Magnusson (1940) and transferred to *Squamarina* by Wei (1991). We initially treated our materials as “*S. semisterilis*” since their morphology was identical with the holotype, which is characterised by the pruinose and lobate thallus containing norstictic acid, terricolous habit, pycnidia resembling apothecia and bacilliform conidia. We transfer this species to the genus *Lobothallia*, based on the phylogenetic reconstruction. Its position within this genus is supported by the lobate and slightly convex thallus, the *Aspicilia*-type ascus, the bacilliform conidia and the absence of usnic acid.

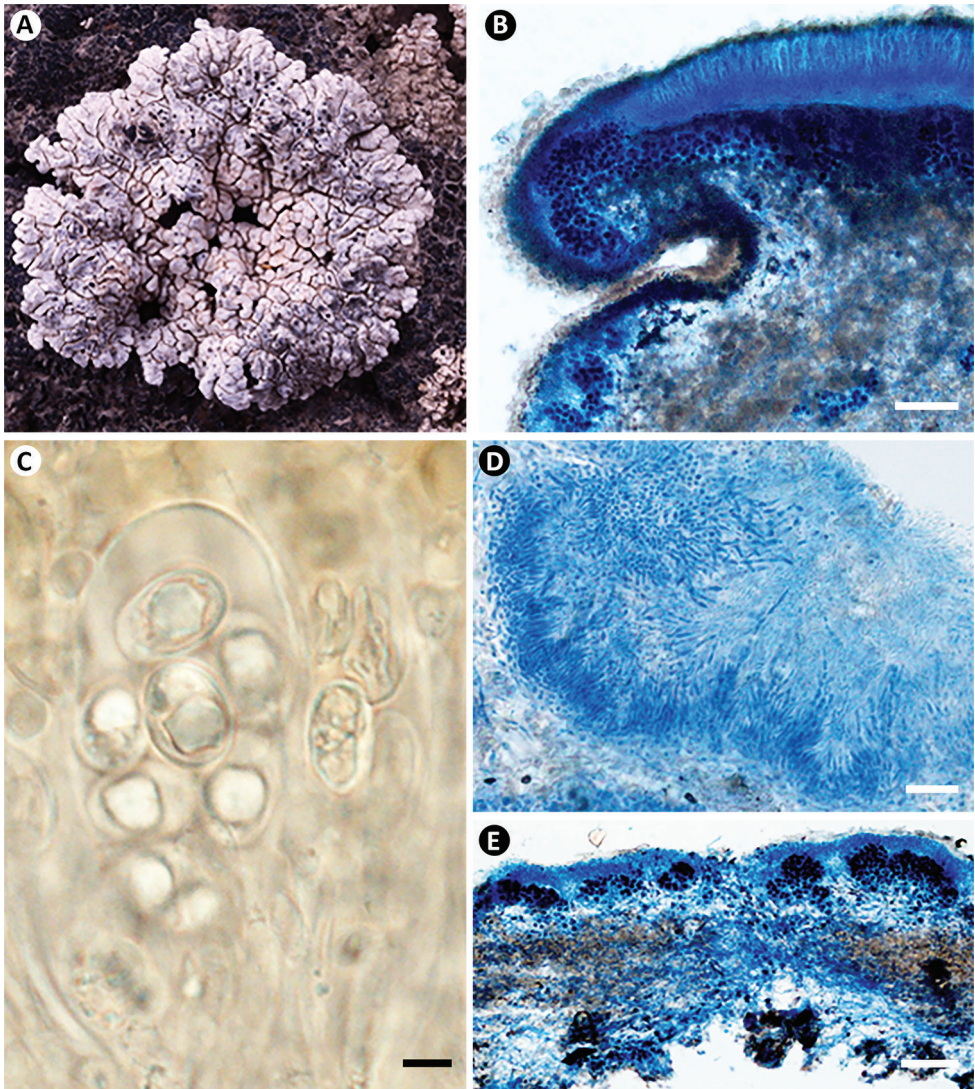


Figure 1. *Lobothallia semisterilis* (KUN-L 18-59656). **A** Habit **B** apothecial anatomy (LCB) **C** ascus and spores (Lugol's) **D** section of pycnidia (LCB) **E** section of thallus (LCB). Scale bars: 100 μm (**B**, **E**); 5 μm (**C**); 20 μm (**D**).

The genus *Lobothallia* is a small genus mainly growing on rocks, containing twelve species (Kou et al. 2013; Lüicking et al. 2017). We added eight of these species as intergroups to assess the phylogenetic position of *Lobothallia semisterilis* in the genus. The results show that *Lobothallia semisterilis* is close to *L. alphoplaca*, *L. melanaspis* and *L. praevalida* in the phylogeny (Fig. 2). However, *L. alphoplaca* differs in the epruinose thallus and the presence of constrictic and stictic acids, *L. melanaspis* differs in the saxicolous habit and the distinctly rosette-forming thallus. *L. praevalida* can be distinguished by the epruinose and green grey to orange brown thallus (Galloway and

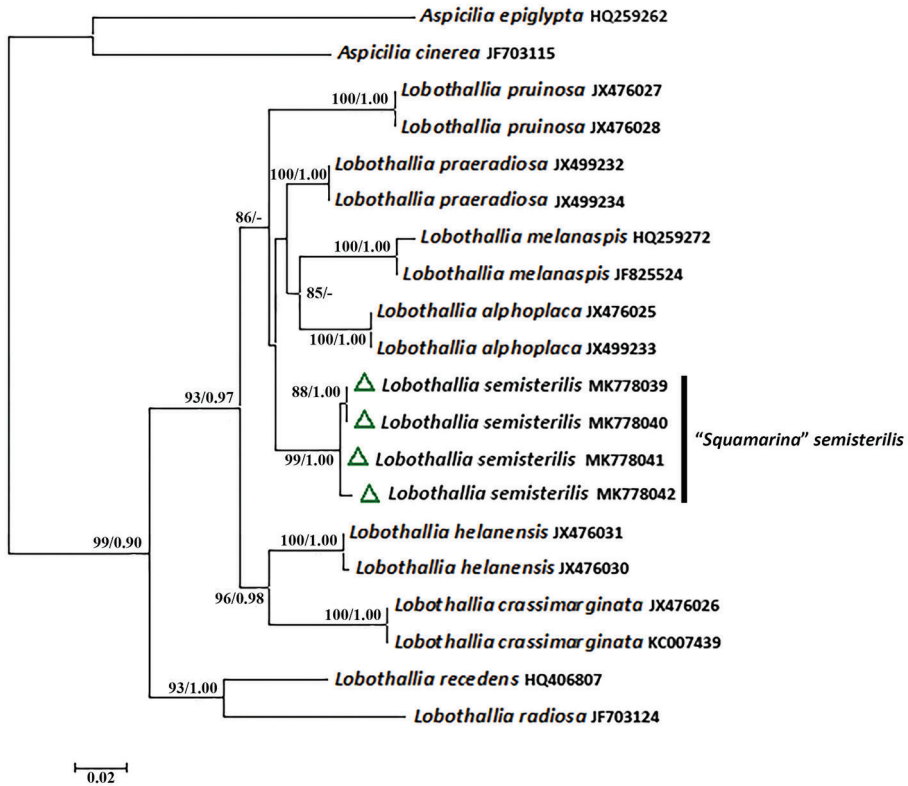


Figure 2. Maximum Likelihood phylogeny of the genus *Lobothallia*, based on nrITS. ML bootstrap value $\geq 70\%$ and posterior probabilities ≥ 0.95 from the Bayesian analysis are given adjacent to nodes.

Ledingham 2012; Kou et al. 2013). *Lobothallia pruinoso* Kou & Q. Ren is similar to *L. semisterilis* in having a pruinose upper surface, but differs in the saxicolous habit and the presence of constictic acid (Kou et al. 2013).

***Rhizoplaca callichroa* (Zahlbr.) Y. Y. Zhang, comb. nov.**

Mycobank No: 832200

Fig. 3A–D

Lecanora callichroa Zahlbr., in Handel-Mazzetti, Symb. Sinic. 3: 172–173 (1930) (Basionym) \equiv *Squamarina callichroa* (Zahlbr.) Poelt, Mitt. Bot. Staatssamml., München 1–20: 527 (1958). Type: CHINA, Yunnan Province, 2100 m elev., on rock, 1914, Heinrich Frh. von Handel-Mazzetti 35 (W–Isotype!)

Description. Thallus saxicolous, to 4 cm across, squamulose to placodioid; squamules pruinose on the edges, more or less umbilicate when young; central squamules

scattered to continuous, closely attached to the substrate, 1–2 mm across; marginal squamules larger than those in the centre, 2–4 mm across, with 1–2 mm free margin; upper surface yellowish-brown, smooth, plane to slightly convex; lower surface pale to pale brown, without rhizinose strands. Upper cortex filled with yellowish-brown granules dissolving in KOH, ca. 32 μm high; epinecral layer also filled with yellowish-brown granules, ca. 15 μm ; algal layer continuous, 64–80 μm high; medulla thick, filled with grey to pale brown granules; lower cortex of free margin poorly developed, non-gelatinised, ca. 30 μm .

Apothecia lecanorine, laminal, dispersed, sessile, becoming slightly constricted at the base, round to irregular, 0.5–1.5 mm; disc orange, covered with pale pruina, plane to slightly convex; thalline margin entire and thick when young, becoming thin and occasionally flexuose with age; hymenium with scattered orange granules, 1+ blue, ca. 80 μm high; thalline margin with evenly thick cortex, ca. 26 μm thick; epihymenium yellowish-brown, ca. 10 μm high; subhymenium and hypothecium colourless; ascus *Lecanora*-type, 8-spored; paraphyses slightly branched, without anastomoses; ascospores subfusiform to ellipsoid, 9.5–13.5 \times 6–9 μm . Pycnidia immersed in the thallus, with pale brown ostioles; conidia filiform, straight to slightly curved, 19–26 \times ca. 0.7 μm .

Chemistry. Upper cortex K-, C-, P-, medulla K + yellow, C-, P-; usnic and placodiolic acids.

Ecology and distribution. Growing on rock in arid environments at elevations of 984–2100 m. Previously only known from Yunnan Prov., here reported as new to Sichuan Prov., China.

Notes. The isotype grows on quartzitic rock ca. 2 cm across, containing several intact apothecia. The spore size of "*Squamarina callichroa*", given in the protologue, is 15–20 \times 8–9 μm (Zahlbruckner 1930); however, Poelt (1958) measured the spore size of the type material as 11–12 \times 8–9 μm . Our measurements of the freshly collected materials, 9.5–13.5 \times 6–9 μm , are in accordance with Poelt's results and the other characteristics, elevation and locality of our collections are more or less identical with the isotype. We did not find any specimens around the type locality having those long ascospores as in the description of the protologue. Therefore, we treat our specimens as "*Squamarina callichroa*". This species was originally described as a *Lecanora* by Zahlbruckner (1930) and transferred to *Squamarina* as the type species of the section *Petroplaca* by Poelt (1958). We transfer this species to the genus *Rhizoplaca*, primarily based on its nested position within the *R. chrysoleuca* group in the phylogeny (Fig. 4) and also based on the orange apothecia, the *Lecanora*-type ascus and the presence of usnic and placodiolic acids. The genus *Rhizoplaca* is a small genus containing eleven species (Lücking 2017). We added nine of these species as intergroups to assess the phylogenetic position of *R. callichroa* in the genus. The results show that *R. callichroa* is sister to *R. chrysoleuca* and *R. huashanensis* J.C. Wei, which differ by the umbilicate thallus, narrower ascospores, (7)8.5–12 \times 3.5–6 μm and the monophyllus thallus and black apothecia, respectively (Nash et al. 2002; Wei 1984). *Rhizoplaca subdiscrepans* (Nyl.) R. Sant. is similar to *R. callichroa* in the squamulose thallus and orange apothecia, but differs in the very convex and smaller (0.3–1 mm) squamules and the narrower ascospores 7–12 \times 3.5–5 μm .

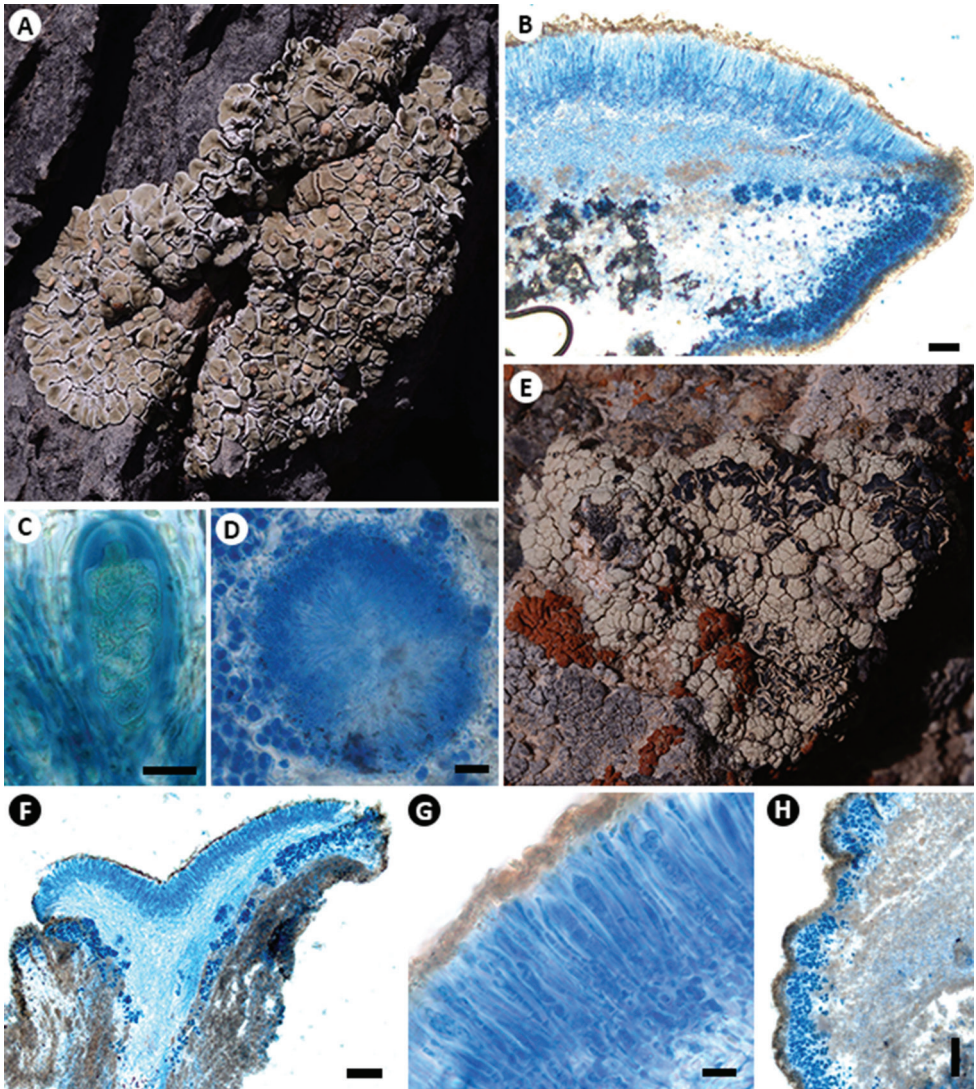


Figure 3. *Rhizoplaca callichroa* (A–D KUN-L 19-62900): **A** habit **B** apothecial anatomy (LCB) **C** ascus and spores (Lugol's) **D** section of pycnidia (LCB). *R. pachyphylla* (E–H KUN-L 18-59446): **E** habit **F** section of apothecia **G** ascus and spores (LCB) **H** section of thallus (LCB). Scale bars: 100 µm (B, F, H); 10 µm (C, G); 20 µm (D).

Specimens examined (KUN-L). CHINA: Sichuan Province: Huili Co., beside Jiaopingdu bridge, near to the Jinsha river, 1550 m elev., 26°18'N, 102°22'E, on rock, 2014, Li-Song Wang et al. 14-43348, 14-43357, 14-43359; Yunnan Province: Luquan Co., beside Jiaopingdu bridge, 984 m elev., 26°18'N, 102°22'E, on rock, 2014, Li-Song Wang et al. 14-43308.

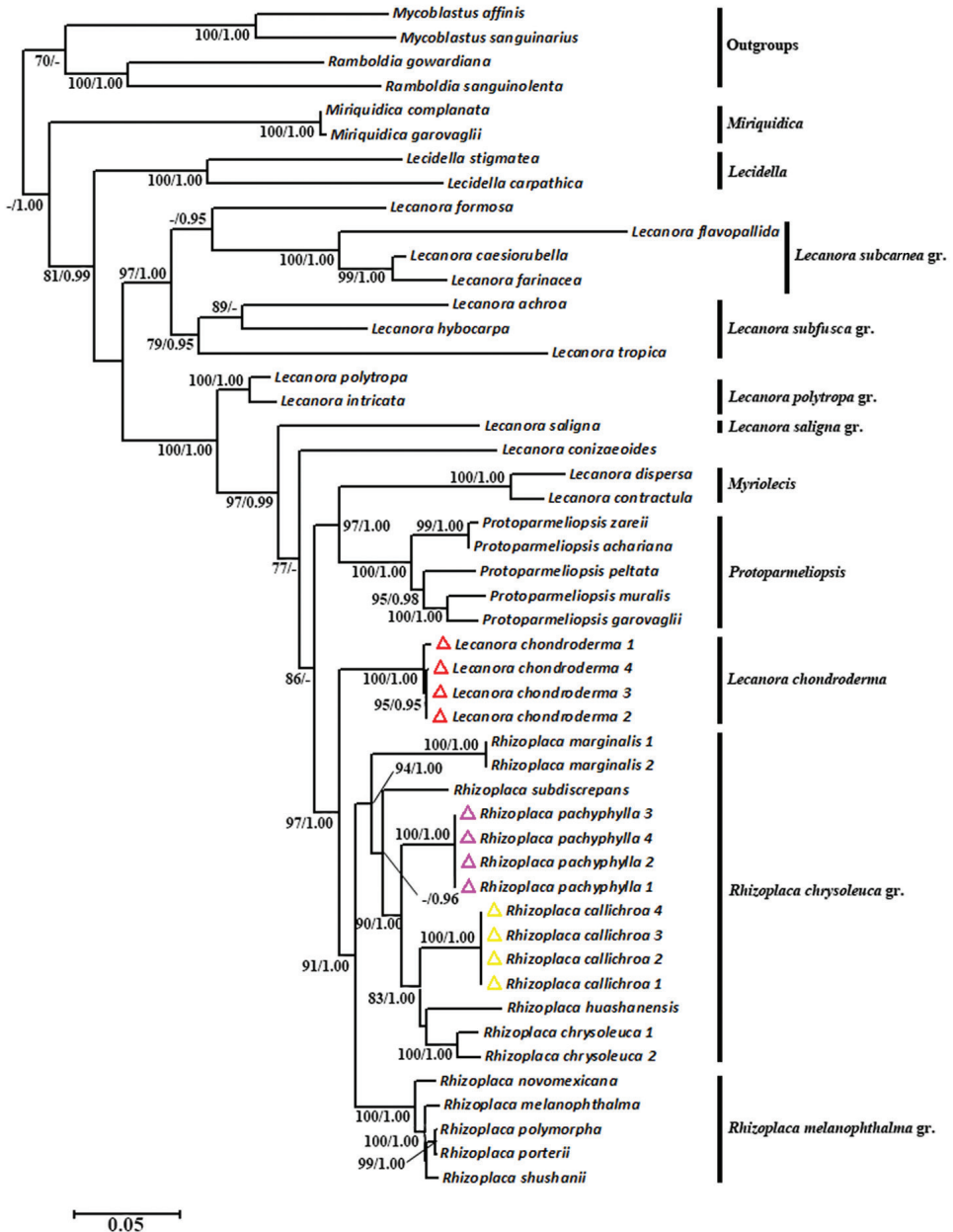


Figure 4. Maximum Likelihood phylogeny of the genus *Rhizoplaca* and related genera of Lecanoraceae, based on combined nrITS, nrLSU, RPB1, RPB2 and mtSSU. ML bootstrap value $\geq 70\%$ and posterior probabilities ≥ 0.95 from the Bayesian analysis are given adjacent to nodes.

***Rhizoplaca pachyphylla* (H. Magn.) Y. Y. Zhang, comb. nov.**

MycoBank No: 832201

Fig. 3E–H

Lecanora pachyphylla H. Magn., Lichens from Central Asia 1: 120–121 (1940) (Basionym) \equiv *Squamarina pachyphylla* (H. Magn.) J.C. Wei, Enumeration of Lichens in China: 232 (1991). Type: CHINA, Gansu Province, 3800–3850 m elev., on rock, 1932, Birger Bohlin (S–Holotype!).

Description. Thallus saxicolous, areolate without lobate margin, to 4 cm across, to 5 mm thick; areoles continuous, plane to slightly convex, 1–2 mm across; upper surface yellow, densely shallow rimose; lower side with thick, grey to white hypothallus. Upper cortex uneven, filled with yellowish-brown granules dissolving in KOH, 32–48 μm thick, algal layer continuous, variable in height, 80–128 μm ; medulla very thick, filled with grey to pale brown granules; lower cortex lacking.

Apothecia common, usually densely grouped, irregular in shape, up to 5 mm in diam.; disc black, pruinose at the centre, plane when young, strongly concave with age; thalline margin thin and crenate, strongly bending towards inside with age; hymenium colourless, I+ blue, ca. 50 μm high; epihymenium containing yellowish-brown granules, ca. 9.5 μm high; subhymenium and hypothecium colourless; paraphyses evenly septate, simple, 2–3 μm in diam., apex more or less swollen and bluish-green, ca. 4.5 μm in diam.; ascus *Lecanora*-type, 8-spored; ascospores regular in shape, ellipsoid, colourless, 5.8–8 \times 3–4.5 μm .

Chemistry. Upper cortex K-, C-, P-, medulla K-, C-, P-; usnic acid and traces of unknown substances.

Ecology and distribution. Growing on rock at elevations of 3291–3909 m. Only known from Gansu Prov., China.

Notes. The holotype grows on rock with *Lecidea tessellata* Flörke, *Lecanora asiatica* H. Magn. and *Xanthoria elegans* (Link) Th. Fr. and contains numerous apothecia.

This species was originally described as a *Lecanora* by Magnusson (1940) and transferred to *Squamarina* by Wei (1991). It is characterised by the yellowish, areolate and very thick thallus, the black lecanorine apothecia and the very small ascospores. We transfer this species to *Rhizoplaca*, primarily based on the phylogenetic results (Fig. 4) and also based on the yellow thallus, the large, concave apothecia with margins bending towards the inside and the *Lecanora*-type ascus. *Rhizoplaca pachyphylla* is phylogenetically closely related to *R. callichroa*, *R. chrysoleuca* and *R. huashanensis*, but differs in the very thick and areolate thallus without lobate margin and the very small ascospores, 5.8–8 \times 3–4.5 μm . *Rhizoplaca subdiscrepans* is similar to *R. pachyphylla* in the squamulose thallus, but differs in the orange apothecia, longer ascospores, 7–12 \times 3.5–4.5 μm , and the presence of pseudoplacodiolic or placodiolic acids. *Rhizoplaca melanophthalma* (DC.) Leuckert is also similar to the species in having black apothecia, but differs in the umbilicate thallus and the larger ascospores, 6.5–12 \times 4–7 μm .

Specimens examined (KUN-L). CHINA: Gansu Province: Shubei Co., Mengke Glacier, 3942 m elev., 39°12'N, 95°23'E, on rock, 2018, Li-Song Wang et al. 18-59446, 18-59466, 3785 m elev., on rock, 2018, Li-Song Wang et al. 18-59482; Yumen Ci., Yuerhong Vi., 3291 m elev., 39°50'N, 96°45'E, on rock, 2018, Li-Song Wang et al. 18-59560, 18-59561.

***Lecanora chondroderma* Zahlbr., in Handel-Mazzetti, Symb. Sinic. 3: 174 (1930).**
Fig. 5A, B

≡ *Squamarina chondroderma* (Zahlbr.) J.C. Wei, Enumeration of Lichens in China: 231 (1991). Type: CHINA, Sichuan Province, 3600–3900 m elev., 1914, Heinrich Frh. von Handel-Mazzetti 497 (W-holotype!)

Description. Thallus to 6 cm across, squamulose or lobate, growing on moss over rock or on the meadow; squamules 0.5–2 mm across, convex, continuous to slightly overlapped; marginal lobes branched, convex, 0.5–2 mm wide, 2–4 mm long; the apex of squamules and lobes rounded, bent downwards; upper surface smooth, pale green to straw, covered by white pruina; lower surface pale to dark brown in the centre and white to pale brown at the margin; rhizinose strands blackish-brown. Upper cortex very thin, ca. 16 µm, filled with yellowish-brown granules dissolving in KOH; algal layer continuous, 48–60 µm thick, medulla filled with grey to pale brown granules, 129–161 µm high, medullary hyphae very loose, more or less hollow in centre; lower cortex well separated from medulla, evenly thick with strongly gelatinised and anticlinally arranged hyphae, ca. 80 µm thick, colourless, hyphae at lower part brown. Apothecia lecanorine, sessile, with constricted base, rounded, scattered or in small groups, up to 3 mm in diam.; disc pruinose, reddish to dark brown, slightly concave when young, slightly convex with age; thalline margin concolorous with thallus, entire to flexuose, forming a well-delimited cortex consisting of strongly gelatinised and anticlinally arranged hyphae; hymenium colourless, 58–80 µm; epihymenium filled with yellowish-brown granules, 10–15 µm; paraphyses simple, evenly septate; ascus *Lecanora*-type, 8-spored; ascospores colourless, ellipsoid to slightly ovoid, 7–13 × 6.5–9 µm.

Chemistry. Upper cortex K-, C-, P + yellow, medulla K+ yellow, C-, P-; usnic acid and zeorin present in each sample, placodiolic and isousnic acids also present in most samples.

Ecology and distribution. Growing on moss over rock or in meadow at 3600–4968 m elevation in the alpine zone. Worldwide distribution: China, India and Nepal. China: Sichuan Prov., reported here as new to Yunnan and Xizang provinces.

Notes. The holotype of *Lecanora chondroderma* consists of several fragments, containing numerous apothecia.

Lecanora chondroderma was originally described by Zahlbruckner (1930) and transferred to *Squamarina* by Wei (1991). We transfer this species back to *Lecanora* temporarily because of its *Lecanora*-type ascus and phylogenetic position being closely related to

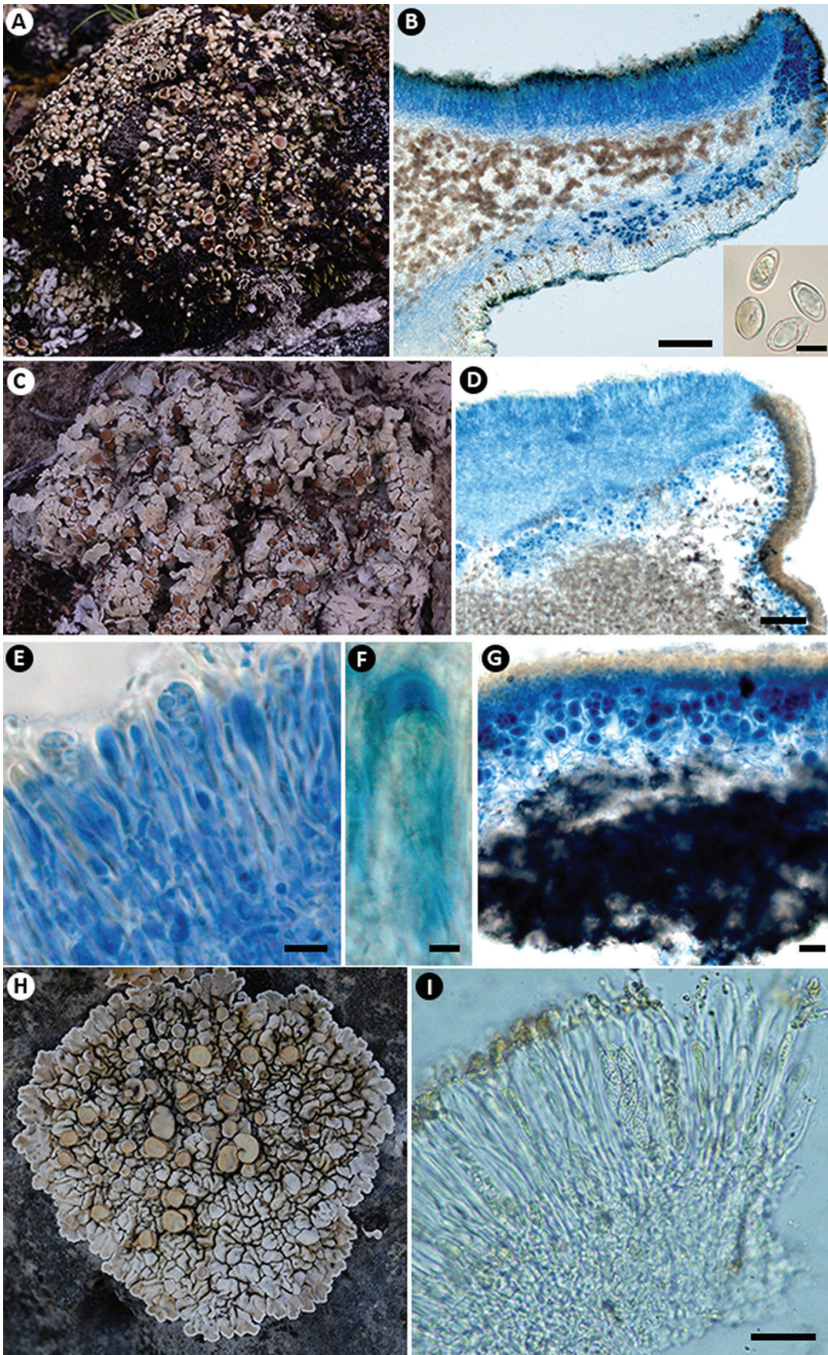


Figure 5. *Lecanora chondroderma* (A, B KUN-L 18-60317): A habit B apothecial anatomy (LCB) and ascospores (water). *Squamarina kansuensis* (C–G KUN-L 18-59601): C habit D apothecial anatomy (LCB) E ascus and ascospores (LCB) F apical structure of ascus (Lugol's) G section of thallus (LCB). *S. oleosa* (H, I KUN-L 09–30043): H habit I ascus and ascospores (water). Scale bars: 100 μm (B-apothecia, D); 5 μm (B-ascospores, F); 10 μm (E); 20 μm (G); 25 μm (I).

the genera *Rhizoplaca* and *Protoparmeliopsis* (Fig. 4). Although *Lecanora chondroderma* is highly supported as a basal clade of the genus *Rhizoplaca* in our topology, it differs in dwelling on moss and meadow and having numerous rhizino-se strands. Given that there are still many taxa of *Lecanora* which have not been included in our analyses and the phylogenetic relationships between *Rhizoplaca* and its related genera have still not been thoroughly resolved, we prefer to retain this species in *Lecanora* temporarily, rather than treat it as *Rhizoplaca*. *Lecanora chondroderma* is only known from the Himalayan region at elevations between 3600–4968 m. The morphology of the species varies amongst localities, with samples growing on moss over rock in Yunnan and Sichuan provinces, having broad (1–2 mm) and pale green lobes and samples from meadows at higher altitudes in Xizang Prov. developing narrower (0.5–1 mm) and more branched lobes with a yellowish appearance. These populations, however, share a pruinose thallus, convex lobes with rounded and downwards bent apices, a loose medulla, a well-delimited cortex of the thalline margin and lower cortex and the presence of usnic acid and zeorin.

Lecanora geophila (Th. Fr.) Poelt is similar to *L. chondroderma* in morphology, chemistry and habitat, whereas the former forms a yellowish crustose, squamulose to placodioid thallus with loboid projections or phyllidia or terete lobes and epruinose, pale, flat to convex apothecia, including usnic acid, zeorin and methylplacodiolic acid (Brodo 1981; Obermayer and Kantvilas 2003); the latter presents a totally pruinose, squamulose to lobate thallus that never forms phyllidia and terete lobes, pruinose, reddish-brown to black apothecia, numerous rhizino-se strands and absence of methylplacodiolic acid.

Specimens examined (all in KUN-L unless otherwise noted). CHINA: Sichuan Province: 4650 m elev., 1915, Heinr. Frh. & Handel-Mazzetti 1353 (W). Yunnan Province: Shangri-La Co., Mt. Hong Shan, 4470 m elev., 28°07'N, 99°54'E, on soil, 2018, Li-Song Wang et al. 18-60317; Luquan Co., Mt. Jiaozi Snow, 4000 m elev., 26°05'N, 102°51'E, on moss over rock, 2016, Li-Song Wang et al. 16-54907; Lijiang Co., Mt. Laojunshan, 4036 m elev., 26°37'N, 99°44'E, on rock, 2017, Li-Song Wang et al. 17-55591. Xizang Province: Linzhou Co., Mt. Qiala, 4830 m elev., 30°06'N, 91°16'E, on the meadow, 2016, Li-Song Wang et al. 16-53527; Zuogong Co., on the way from Rumei to Zuogong, 4968 m elev., 29°43'N, 98°01'E, on the meadow, 2016, Li-Song Wang et al. 16-52925, 16-53079, on the meadow, 2016, Li-Song Wang et al. 16-52931.

Squamarina kansuensis (H. Magn.) Poelt

Fig. 5C–G

Lecanora kansuensis H. Magn., Lichens from Central Asia 1: 116–117 (1940). Type:

CHINA, Gansu Province, 1500–1700 m elev., on soil, 1930, Birger Bohlin 20₂ (S–Holotype!) (Basionym)

Description. Thallus terricolous, loosely to tightly adnate on soil, irregular to radiate in outline and with elongate marginal lobes, up to 10 cm in diam.; lobes 2–4(5) mm long,

1–2(3) mm wide, 0.2–0.4 mm thick, with white, thickened and slightly upturned edges, more or less overlapping; upper surface greenish to straw, pruinose and strongly cracked at least in the centre of the thallus; lower surface well delimited, milk-white to pale, without rhizines, margins usually containing sparse white tomentum. Upper cortex filled with yellowish-brown granules, turning colourless in KOH, 26–32 μm thick; epinecral layer grey to brown, 5–15 μm thick; algal layer continuous, well delimited, ca. 50 μm high; medulla grey, filled with calcium oxalate crystals; lower cortex lacking.

Apothecia frequent, rounded, single or in small groups, usually less than 2 mm in diam. Disc pale brown to reddish-brown, slightly concave to flat when young, usually becoming strongly convex with age. Thalline margin distinctive when young and disappearing with age. Hymenium colourless, I + blue, ca. 65 μm high; epihymenium yellowish-brown turning colourless in KOH, ca. 12.5 μm high; thalline margin with evenly thick cortex filled with grey granules; paraphyses septate, ca. 2.5 μm in diam.; hypothecium colourless, 75–87 μm high; algal layer below hypothecium continuous, 62–87 μm high; ascus *Porpidia*-type, 8-spored; ascospores colourless, ellipsoid to slightly fusiform, variable in size and shape even within one ascus, 7.5–15 \times 5–7.5 μm .

Chemistry. Upper cortex K-, C-, P-, medulla K-, C-, P+ yellow; isousnic, usnic, psoromic and 2'-O-demethylpsoromic acids.

Ecology and distribution. Growing on soil at 1310–4730 m of elevation. Previously only known from Gansu Prov. and reported here as new to Neimenggu, Ningxia, Sichuan, Xizang, Xinjiang and Yunnan provinces, China.

Notes. The holotype consists of several small fragments on soil, bearing a single small apothecium. This species was originally described as a *Lecanora* by Magnusson (1940) and transferred to *Squamarina* by Poelt (1958). It is characterised by the pruinose, greenish- to straw-coloured thallus, lobes with white, thickened and slightly upturned edges, exposing a milk-white to pale lower surface, without rhizines and the presence of psoromic and 2'-O-demethylpsoromic acids. This species is very common in the deserts and alpine zones of China. In desert regions, the thallus is usually irregular in outline with wider lobes and becomes rosette-like with narrower lobes when growing in the alpine zone.

The genus *Squamarina* (= *S.* sect. *Squamarina*) includes eleven species (Poelt 1958) and there are three species with sequences in GenBank. We integrated the data from GenBank with the newly-produced data here to reconstruct the phylogeny of the genus *Squamarina* to assess the phylogenetic position of the species *S. kansuensis* (Fig. 6). The results show that *S. kansuensis* is a sister species to *S. lentigera* which, in turn, is also very similar in morphology, but differs in the larger thallus and by containing psoromic and 2'-O-demethylpsoromic acids. *Squamarina nivalis* Frey & Poelt and *S. provincialis* Clauzade & Poelt are similar to *S. kansuensis* in having a strongly white pruinose thallus; however, *S. nivalis* differs in the smaller thallus, ca. 2 cm, not cracked upper surface, the apices of lobes bent downwards and the absence of psoromic acid; *S. provincialis* differs in the continuous but never overlapped lobes, the absence of the white thickened edges of lobes and the presence of atranorin. So far, the two species, *S. nivalis* and *S. provincialis*, are only known from very restricted places from Europe.

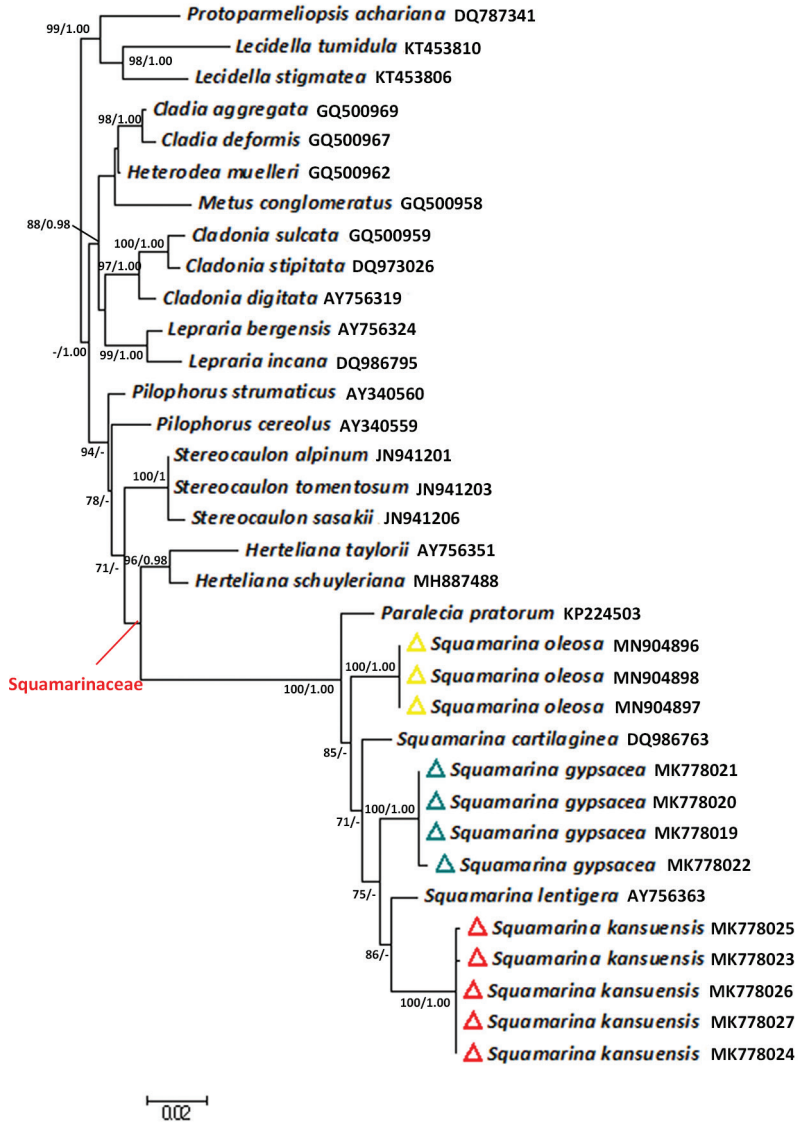


Figure 6. Maximum Likelihood phylogeny of the genus *Squamarina* and related genera, based on nrLSU. ML bootstrap value $\geq 70\%$ and posterior probabilities ≥ 0.95 from the Bayesian analysis are given adjacent to nodes.

Specimens examined (all in KUN-L unless otherwise noted). CHINA: Gansu Province: Jiayuguan, 1500 m–1700 m elev., 1930, Briger Bohlin, S-L60805 (S); Yumen Ci., Moshan National Geological Park, 1760 m elev., 39°57'N, 97°14'E, on soil, 2018, Li-Song Wang et al. 18-59601; Sunan Co., Binggou Danxia landform Park, 1970 m elev., 38°56'N, 99°50'E, on soil, 2018, Li-Song Wang et al. 18-59658; Ningx-

ia Province: Mt. Helanshan, 38°40'N, 1310 m elev., 105°46'E, on soil, 2014, Dong-Ling Niu et al. 14-09-1429 (NXAC); Qinghai Province: Wulan Co., Gobi desert along the way from Chaka to Wulan, 3151 m elev., 36°52'N, 98°55'E, on soil, 2018, Li-Song Wang et al. 18-59260, along the way from Wulan to Delingha, 3039 m elev., 36°59'N, 98°12'E, on soil, 2018, Li-Song Wang et al. 18-59274, 18-59306; Delingha Ci., Chayegou Station, 2974 m elev., 37°23'N, 96°37'E, on soil, 2018, Li-Song Wang et al. 18-59344, 18-59343. Sichuan Province: Derong Co., 1960 m elev., 28°12'N, 99°20'E, on soil, 2009, Li-Song Wang & Wang Jue 09-31112, 09-31118; Xizang Province: Linzhou Co., 3780 m elev., 29°54'N, 91°14'E, on soil, 2016, Li-Song Wang et al. 16-54052; Xinjiang Province: A-ke-tao Co., Oytagh observation zone, 2850 m elev., 38°54'N, 75°14'E, on soil, 2013, Hurnisa Shahidin et al. 20139103; Yunnan Province: Deqin Co., 2110 m elev., 28°13'N, 99°19'E, on soil, 2012, Li-Song Wang et al. 12-34756. Neimenggu Province: Beli-miao, 41°30'N, 110°10'E, on soil, 1929, Briger Bohlin, S-F304837 (S).

Squamarina oleosa (Zahlbr.) Poelt

Fig. 5H, I

Lecanora oleosa Zahlbr., in Handel-Mazzetti, *Symb. Sinic.* 3: 175 (1930) (Basionym)

Type: CHINA, Yunnan Province, Lijiang Co., Mt. Yulongxueshan, on rock, 1914, Heinrich Frh. von Handel-Mazetti 3576 (W–holotype!)

Description. Thallus placodioid to subfoliose, rather closely attached to calcareous rocks, olive-green turning to yellowish-brown in the herbarium, up to 8 cm across and 5 mm high in the centre; lobes 2–4 mm long, 1.5–2.5 mm wide, ca. 1 mm thick, apices usually detached from the substrate with a white thickened edge; upper surface pruinose at least on the margins, matt to somewhat shiny, centrally cracked and faveolate-wrinkled, strongly convex, giving the thallus centre a bullate appearance, the base of the bullae carbonised, black; lower surface covered with pale brown to blackish-brown pulvinate hyphae, with sparse to numerous rhizinose strands; rhizinose strands brown to black, irregularly branched, up to 5 mm long. Upper cortex filled with yellowish-brown granules, turning colourless in KOH, 62–75 µm high, without epinecral; algal layer continuous, 65–70 µm thick; medulla filled with grey crystals of calcium oxalate and brick-red hyphae in lower part; lower cortex lacking.

Apothecia common but not abundant, laminal, scattered to slightly grouped, up to 4 mm in diam.; disc concave, plane to convex, light yellow, covered by yellowish pruina; thalline margin pruinose or not, darker than thallus, shiny, entire and distinctive when young, excluded with age. Hymenium 75–85 µm high, hyaline, I+ blue; epihymenium filled with yellowish-brown granules, not disperse into hymenium, turning colourless in KOH, 5–12.5 µm high; thalline margin without algae in the upper part, cortex filled with yellowish-brown granules, 112–125 µm thick; paraphyses septate, tips not swollen; hypothecium colourless, 100–162 µm thick, with pale

brown granules forming a narrow line; algal layer below hypothecium continuous, 50–75 μm thick; ascus *Porpidia*-type, 8-spored. Ascospores ellipsoid to subfusiform, 15–20 \times 5–7 μm . Pycnidia rare and small, ostioles yellow to yellowish-brown, conidia colourless, filiform, curved, 15–22.5 \times ca. 0.7 μm .

Chemistry. Upper cortex K-, C-, P-, medulla K-, C-, P+ yellow; usnic, psoromic and 2'-O-demethylpsoromic acids.

Ecology and distribution. Growing on rock at elevations of 2623–3440 m. Only known from Yunnan Prov., China.

Notes. The holotype grows on calcareous rock and bears only one apothecium.

This species was originally described as a *Lecanora* by Zahbruckner (1930) and transferred to *Squamarina* by Poelt (1958). It is characterised by the thick, olive-green, placodioid to subfoliose thallus, yellowish apothecia covered with yellow pruina, the ellipsoid to subfusiform ascospores and the filiform, curved conidia. This species is the most basal clade in our reconstruction of the genus and it is close to *S. cartilaginea* and *S. gypsacea* (Fig. 6); however, *S. cartilaginea* differs in the non-pruinose, yellowish- to reddish-brown apothecia, smaller ascospores 10–14 \times 4–6 μm and *S. gypsacea* differs in the yellowish-green, squamulose thallus, the very large and thick squamules that adnate to the substratum only by the central part and the larger apothecia (up to 1 cm). *Squamarina kansuensis* and *S. lentigera* can be distinguished from this species by the strongly white pruinose thallus, thinner lobes (< 0.5 mm) and smaller (< 2 mm) apothecia with non-pruinose and reddish-brown disc.

Specimens examined (all in KUN-L unless otherwise noted). CHINA: Yunnan Province: Lijiang Co., 3440 m elev., on rock, 2009, Li-Song Wang & Wang Jue 09-30034, Yulong Snow Mt., 26°56'N, 100°12'E, 2623 m elev., on calcareous rock, 2019, Li-Song Wang & Yan-yun Zhang 19-66398, 19-66399, 19-66401, 19-66402, 19-66404.

***Squamarina gypsacea* (O).** GREECE: Corfu, hill above Troumpetas, 420 m elev., 39°74'N, 19°86'E, on exposed limestone outcrops, 2014, Rui, S. & Timdal, E., O-L-196249, Sokrati – Zigos road, 370 m elev., 39°72'N, 19°80'E, on rather shady limestone boulders in olive groove, 2014, Rui, S. & Timdal, E., O-L-196255; Kavalla, Thassos, along dirt road from Maries to Theologos, near Vatos, 590 m elev., 40°70'N, 24°66'E, on E-facing limestone wall in/above steep pine forest, 2000, Rui, S. & Timdal, E., O-L-59266. SPAIN: Alicante, between Callosa de Ensarria and Confrides, 260 m elev., 38°68'N, -0°21'E, 1985, Timdal, E., O-L-16444.

Acknowledgements

We would like to express our deep thanks to Dr. Arne Anderberg from the Swedish Museum of Natural History (S) and the curator of the Vienna Museum of Natural History (W) for the loan of specimens. This study was supported by grants from the National Natural Science Foundation of China (Nos. 31660007, 31970022, 31670028), Flora Lichenum Sinicorum (31750001), Youth Innovation Promotion Association CAS, Biological Resources Programme, Chinese Academy of Sciences (KFJ-BRP-017-23) and

China Scholarship Council. This work benefitted from the sharing of expertise within the DFG priority programme SPP 1991 “Taxon-Omics” and support from DFG grant PR567/19-1 to CP.

References

- Brodo IM (1981) *Lecanora luteovernalis*, a new species of the *L. symmetrica* complex from the Canadian arctic. *The Bryologist* 84: 521–526. <https://doi.org/10.2307/3242560>
- Galloway DJ, Ledingham J (2012) Additional lichen records from New Zealand 48. *Australasian Lichenology* 70: 14–25.
- Hafellner J (1984) Studien in Richtung einer natürlicheren Gliederung der Sammelfamilien Lecanoraceae und Lecideaceae. *Nova Hedwigia*, Beiheft 79: 1–371.
- Haugan R, Timdal E (1992) *Squamarina scopulorum* (Lecanoraceae), a new lichen species from Norway. *Nordic Journal of Botany* 12: 357–360. <https://doi.org/10.1111/j.1756-1051.1992.tb01314.x>
- Hertel H, Rambold G (1988) Cephalodiate Arten der Gattung *Lecidea* sensu lato (Ascomycetes lichenisati). *Plant Systematics and Evolution* 158: 289–312. <https://doi.org/10.1007/BF00936352>
- Högnabba F (2006) Molecular phylogeny of the genus *Stereocaulon* (Stereocaulaceae, lichenized ascomycetes). *Mycological Research* 110: 1080–1092. <https://doi.org/10.1016/j.mycres.2006.04.013>
- Huelsenbeck JP, Ronquist F (2001) MRBAYES: Bayesian inference of phylogenetic trees. *Bioinformatics* 17: 754–755. <https://doi.org/10.1093/bioinformatics/17.8.754>
- Kou XR, Li SX, Ren Q (2013) Three new species and one new record of *Lobothallia* from China. *Mycotaxon* 123: 241–249. <https://doi.org/10.5248/123.241>
- Lücking R, Hodkinson BP, Leavitt SD (2017) The 2016 classification of lichenized fungi in the Ascomycota and Basidiomycota – Approaching one thousand genera. *The Bryologist* 119: 361–416. <https://doi.org/10.1639/0007-2745-119.4.361>
- Magnusson AH (1940) Lichens from Central Asia. Stockholm, 5–167.
- Nash III TH, Ryan BD, Gries C, Bungartz F (2002) Lichen flora of the greater Sonoran Desert region, volume I. Lichen Unlimited, Arizona State University.
- Nylander JAA (2004) MrModeltest 2.3. Program distributed by the author. Evolutionary Biology Centre, Uppsala University.
- Obermayer W, Kantvilas G (2003) The identity of the lichens *Siphula himalayensis* and *Lecanora teretiuscula*. *Herzogia* 16: 27–34.
- Orange A, James PW, White FJ (2001) Microchemical methods for the identification of lichens. London: British Lichen Society.
- Poelt J (1958) Die lobaten Arten der Flechtengattung *Lecanora* Ach. sensu ampl. in der Holarktis. *Mitteilungen der Botanischen Staatssammlung München* 2 (19–20): 411–589.
- Rambaut A (2012) FigTree, v. 1.4.0. Institute of Evolutionary Biology, University of Edinburgh. <http://tree.bio.ed.ac.uk/software/figtree/>

- Wei JC (1984) A preliminary study of the lichen genus *Rhizoplaca* from China. *Acta Mycologica Sinica* 3: 207–213.
- Wei JC (1991) *An Enumeration of Lichens in China*. International Academic Publishers, Beijing, 218 pp.
- Zahlbruckner A (1930) Lichenes. In: Handel-Mazzetti H (Ed.) *Symbolae Sinicae* 3. J. Springer, Vienna, 254 pp. https://doi.org/10.1007/978-3-7091-4178-6_1
- Zhao X, Zhang LL, Zhao ZT, Wang WC, Leavitt SD, Lumbsch HTA (2015) Molecular phylogeny of the lichen genus *Lecidella* focusing on species from mainland China. *PloS ONE* 10(9): e0139405. <https://doi.org/10.1371/journal.pone.0139405>

